Autoreceptor and glutamatergic regulation of serotonin release from the suprachiasmatic nuclei

Garabette, M. L.

Award date:
1998

Awarding institution:
University of Bath

AUTORECEPTOR AND GLUTAMATERGIC REGULATION OF SEROTONIN RELEASE FROM THE SUPRACHIASMATIC NUCLEI

Submitted by Martine L. Garabette

for the degree of Ph.D.

of the University of Bath

1998

ProQuest LLC
789 East Eisenhower Parkway
P.O. Box 1346
Ann Arbor, MI 48106-1346

ABSTRACT

Scientific research investigating the generation and regulation of circadian rhythms has become more popular over the last few years. Chronopharmaceutics and identifying that the timing of drug delivery is important are valuable steps toward the global recognition of this topic. Clinical depression is one example of what is considered a 'disorder of time keeping' i.e. a disruption in the internal body clock. Although the intricate mechanisms behind both depression and the workings of the body clock are, at best, moderately understood, the pivotal involvement of serotonin (5-HT) in both depression and in the regulation of circadian rhythms justifies further investigation. The aims of this thesis were to further the knowledge of the normally functioning circadian pacemaker (the suprachiasmatic nuclei; SCN) with the view that studies of abnormalities in clock function such as depressive illness and jet-lag, might be better understood.

The *in vivo* sampling technique of microdialysis was utilised in the rat to examine the function of the 5-HT_{1B} auto- and hetero- receptors in the SCN, the 5-HT_{1A} autoreceptor in the midbrain raphe nuclei regulating 5-HT release in the SCN , and the relationship between the serotonergic and glutmatergic systems in the SCN and midbrain raphe was also examined.

The 5-HT_{1B} autoreceptor in the SCN was shown to exhibit a marked diurnal variation in function, as examined at six time points across the light:dark cycle, whereas the function of the 5-HT_{1B} heteroreceptor was not significantly different at the two time points examined. Reverse-transcriptase polymerase chain reaction (RT-PCR) was used to examine 5-HT_{1B} auto-, hetero- and postsynaptic receptor mRNA, and to identify potential diurnal rhythms in message levels. Postsynaptic 5-HT_{1B} receptor and 5-HT_{1B} heteroceptor mRNA levels varied significantly over eight equally spaced time points. The 5-HT_{1B} autoreceptor mRNA levels on the other hand, did not display a circadian variation. It is therefore unlikely that the functional variation in the 5-HT_{1B} autoreceptor is a result of an underlying rhythm in mRNA expression. Thus, the amount of 5-HT_{1B} receptor protein present in the SCN was examined. Immunocytochemical detection of the 5-HT_{1B} receptor in brain tissue proved unsuccessful, and Western blotting was chosen to detect possible changes in protein levels over eight time points across the

light:dark cycle. Using this method the 5-HT_{1B} receptor levels did not appear to display a diurnal variation. Therefore, the mechanism(s) behind the functional variation in 5-HT_{1B} autoreceptor function has yet to be elucidated. The somatodendritic 5-HT_{1A} autoreceptor did not display a diurnal variation in function as measured at two time points utilising a dual probe paradigm.

5-HT release in the SCN was shown to be regulated by both ionotropic and metabotropic glutamate receptors. The effect of NMDA was concentration-dependent and displayed a circadian variation, which was in part due to stimulation of α_2-adrenoceptors by endogenously released agonist. The effect of metabotropic glutamate receptor stimulation also displayed a diurnal variation, whereas the effect of kainate did not exhibit variation, and AMPA receptor stimulation was without effect on 5-HT release.

NMDA receptor stimulation in the midbrain raphe nuclei also regulated SCN 5-HT release as measured by the dual probe paradigm, which was in part mediated by a stimulation of somatodendritic 5-HT_{1A} autoreceptors. This provides functional evidence for the presence of a retino-raphe-hypothalamic tract in the rat, although it probably involves stimulation of interneurones in the raphe nuclei.

Together, the data collected in this thesis provide a better understanding of the regulation of 5-HT release in the circadian pacemaker by autoreceptor and glutamatergic receptor stimulation. The data might be useful to further the understanding of abnormalities in clock function.

ACKNOWLEDGMENTS

I would like to thank my supervisor at Bath, Professor Peter Redfern, and my supervisor at Knoll Pharmaceuticals, Professor Keith Martin, for their encouragement and their reassurance that one day it would be all over! I know that often I am not the easiest person to knock sense into, but I am grateful that they kept trying.

Enormous thanks must go to Dr. David Marshall for guiding me in those early days and for the all the fun we had in the dungeons! Big thank you's also to Dr. Sue Aspley and Dr. AnneMarie Simpson at Knoll pharmaceuticals for having the patience to teach me the microdialysis and RT-PCR techniques respectively, and also to Elaine Ann Orchiston for not losing her temper with me (except once - that Gilson will never be the same again!) whilst teaching me how to Western blot at Bath.

The help and support of Lesley, Ewan, Mark, Keith, Charlie and Lionel was very much appreciated in addition to the great laughs we had. Without them I am sure that I would have lost my sanity. Also thanks to all the technical staff, without whom I am sure I would still be asking 'where's my methanol...?'. Thank you also to Malcolm Holley - the histology 'expert' - for the advice, rushed orders and the use of his office as a great source of gossip!

I would also like to thank Dr. John, Em, Regal, Elaine and Dave for making my time at Bath, well, I suppose, memorable!

Finally, the financial support of mum and dad and Mike was very much appreciated, as well as their faith in my ability - Thank you!

For mum and dad

CONTENTS

Title page i
Abstract ii
Acknowledgments iv
Dedication v
Contents vi
List of Abbreviations x

CHAPTER 1: General Introduction

1.1 The suprachiasmatic nuclei (SCN) 1
1.2 SCN afferents 3
1.2.1 The retinohypothalamic tract (RHT) 3
1.2.2 The raphe-hypothalamic tract (RaHT) 7
1.2.3 The geniculohypothalamic tract (GHT) 10
1.3 SCN efferents 11
1.4 Aims of thesis 11

CHAPTER 2: General microdialysis and HPLC-ED parameters

2.1 Microdialysis 12
2.1.1 Principles of microdialysis 12
2.2 High performance liquid chromatography with electrochemical detection (HPLC-ED) 15
2.2.1 Principles of chromatography 15
2.2.2 Basic HPLC-ED apparatus set up 15
2.2.3 Detection of 5-HT by 'ion-pairing' HPLC 16
2.2.4 Detection of glutamate by pre-column derivatisation HPLC 16
2.3 Methods 19
2.3.1 Probe construction 19
2.3.2 *In vitro* probe recovery 19
2.3.3 Probe implantation 20
2.3.4 Dialysis set up 20
2.3.5 Separation and detection of 5-HT in dialysate 21
2.3.6 Separation and detection of glutamate in dialysate 21

2.4 Results and Discussion 25
2.4.1 General HPLC parameters 25
2.4.2 General microdialysis parameters 25

CHAPTER 3: The 5-HT_{1B} terminal auto- and hetero- receptors

3.1 Introduction 32
3.2 Protocol 34
3.2.1 Animals 34
3.2.2 Microdialysis 34
3.2.3 Drugs 35
3.2.4 Statistics 35
3.3 Results 36
3.3.1 The 5-HT_{1B} autoreceptor 36
3.3.1.1 Pharmacological controls 36
3.3.1.2 Effect of local infusion of RU24969 into the SCN 36
3.3.1.3 Effect of WAY100635 on the RU24969 infusion at ZT 6 37
3.3.1.4 Effect of a local infusion of RU24969 into the hippocampus at ZT 6 and 18 37
3.3.2 The 5-HT_{1B} heteroceptor 47
3.3.2.1 Pharmacological controls 47
3.3.2.2 Effect of RU24969 into the SCN 47
3.4 Discussion 50
3.4.1 The 5-HT_{1B} autoreceptor 50
3.4.2 The 5-HT_{1B} heteroceptor 57
3.5 Conclusions 60

CHAPTER 4: 5-HT_{1B} auto-, hetero- and postsynaptic receptor mRNA and 5-HT_{1B} receptor expression in the SCN

4.1 Introduction 61
4.2 Methods 64
4.2.1 Reverse-transcriptase polymerase chain reaction (RT-PCR) 64
4.2.1.1 Preparation of tissue samples 64
4.2.1.2 Isolation of total RNA 65
4.2.1.3 Isolation of mRNA 67

4.2.1.4 Reverse-transcriptase reaction (RT) 68
4.2.1.5 cDNA amplification 68
4.2.1.6 Visualization of RT-PCR product 69
4.2.1.7 Statistics 69
4.2.2 Immunocytochemistry 70
4.2.2.1 Cymotrypsin treatment 71
4.2.2.2 Heat treatment 71
4.2.3 Western blotting 72
4.2.3.1 Preparation of tissue samples 72
4.2.3.2 Bradford protein assay 72
4.2.3.3 Electrophoresis 72
4.2.3.4 Immunoblotting 73
4.3 Results 74
4.3.1 Reverse transcriptase polymerase chain reaction 74
4.3.1.1 Total RNA extraction from SCN tissue 74
4.3.1.2 RT-PCR reaction 74
4.3.1.3 mRNA extraction from SCN, retinal and raphe samples 76
4.3.1.4 RT-PCR reaction 76
4.3.2 Immunocytochemistry 86
4.3.3 Western blotting 89
4.3.3.1 Determination of tissue protein concentration 89
4.3.3.2 Optimization of conditions for immunoblotting 89
4.4 Discussion 96
4.4.1 5-HT_{1B} receptor mRNA levels in SCN, raphe and retina 96
4.4.2 5-HT_{1B} receptor protein in the SCN 100
4.5 Conclusions 102

CHAPTER 5: Glutamatergic receptor agonist regulation of 5-HT release in the SCN

5.1 Introduction 104
5.2 Protocol 106
5.2.1 Animals 106
5.2.2 Microdialysis 106
5.2.3 Drugs 106

5.2.4 Statistics..... 107
5.3 Results..... 108
5.3.1 Effect of local infusion of AMPA into the SCN..... 108
5.3.2 Effect of local infusion of kainate into the SCN..... 108
5.3.3 Effect of local infusion of NMDA into the SCN..... 108
5.3.4 Effect of local infusion of ACPD into the SCN..... 110
5.4 Discussion.....123
5.5 Conclusions..... 129

CHAPTER 6: The raphe 5-HT_{1A} somatodendritic autoreceptor and NMDA receptor regulation of SCN 5-HT release

6.1 Introduction..... 130
6.2 Protocol..... 132
6.2.1 Animals..... 132
6.2.2 Microdialysis..... 132
6.2.3 Drugs..... 132
6.2.4 Statistics..... 133
6.3 Results..... 134
6.3.1 Effect of local infusion of 8-OH-DPAT in the midbrain raphe nuclei on 5-HT overflow in the raphe and SCN..... 134
6.3.2 Effect of local infusion of NMDA in the midbrain raphe nuclei on 5-HT overflow in the raphe and SCN..... 135
6.4 Discussion..... 144
6.5 Conclusions..... 155

CHAPTER 7: General discussion

7.1 Summary of thesis..... 157
7.2 Discussion..... 160
7.3 Future work..... 163

Publications..... 175
References..... 176
Appendix..... 199

ABBREVIATIONS

ACPD	(1S,3R)-1-aminocyclopentane-1,3-dicarboxylic acid
aCSF	artificial cerebrospinal fluid
AMPA	α-amino-3-hydroxy-5-methyl-4-isoxazoleproprionic acid
ANOVA	analysis of variance
AP	anterioposterior
AP5	(±)-2-amino-5-phosphonopentanoic acid
AVP	arginine vasopressin
cDNA	complimentary DNA
CTS	circadian timing system
DAB	diaminobenzidine
DD	constant dark
DM-SCN	dorsomedial SCN
DV	dorsoventral
E4CPG	(RS)-α-ethyl-4-carboxyphenylglycine
EDTA	ethylenediaminetetraacetic acid
EPSP	excitatory post synaptic potential
fmol	femtomols
GABA	γ-amino butyrate
GAD	glutamate decarboxylase
GHT	geniculohypothalamic tract
Glu	glutamate
GRP	gastrin-releasing peptide
HPLC-ED	high performance liquid chromatography with electrochemical detection
5-HIAA	5-hydroxyindoleacetic acid
HRP	horseradish peroxidase
5-HT	5-hydroxytryptamine, serotonin
ID	internal diameter
IGL	intergeniculate leaflet
LD	light:dark cycle
LL	constant light
M	molecular weight marker

MA	metamphetamine
MK801	(5R,10S)-(+)-5-methyl-10,11-dihydro-5H-dibenzo[a,d]cyclohepten-5,10-imine, dizocilpine
ML	mediolateral
MPC	magnetic particle concentrator
mRNA	messenger RNA
NMDA	*N*-Methyl-D-aspartate
nNOS	neuronal NOS
NO	nitric oide
NOS	nitric oxide synthase
NRS	normal rabbit serum
OD	outer diameter
OPA	*o*-phthalaldehyde
OSA	octane sulphonis acid
PBS	phosphate buffered saline
PRC	phase response curve
RaHT	raphehypothalamic tract
RAP	raphe
RET	retinal
RHT	retinohypothalamic tract
RT-PCR	reverse transcriptase-polymerase chain reaction
RU24969	5-methoxy-3(1,2,3,6-tetrahydro-4-pyridinyl)-1H-indole
SCN	suprachiasmatic nuclei
SDS	sodium dodecyl sulphate
SOM	somatostatin
SSRI	selective serotonin reuptake inhibitor
TBS	Tris buffered saline
VIP	vasointestinal peptide
VL-SCN	ventrolateral SCN
WAY100635	N-[2-[4-(2-methoxyphenyl0-1-piperazinyl]ethyl]-N-(2-pyridinyl)cyclo-hexanecarboxamide trihydrochloride
WB	whole brain
ZT	zeitgeber time

CHAPTER 1

GENERAL INTRODUCTION

The mammalian circadian timing system (CTS) is a set of neural structures that have evolved uniquely to synchronise an organism's biochemical, physiological and behavioural processes to its environment. The factors that bring about synchronisation, or entrainment, are called zeitgebers ('zeit' time, 'geber' to give) and the principle zeitgeber is the light:dark cycle. Circadian rhythms are those rhythms that can persist in the absence of environmental cues and 'free run' with a periodicity of approximately twenty four hours, hence 'circa', about; 'diem', one day. This persistence of circadian rhythms provides powerful evidence for the existence of an internal, self sustaining clock.

The components of the mammalian CTS are thus:

(1) Photoreceptors and projections of retinal ganglion cells that form entrainment pathways

(2) A circadian pacemaker or pacemakers

(3) Efferent pathways that couple the pacemaker to effector systems displaying circadian function.

1.1 THE SUPRACHIASMATIC NUCLEI (SCN)

Experimental evidence has shown the suprachiasmatic nuclei (SCN) of the hypothalamus to generate, control and express circadian rhythmicity in vertebrates. Stephan and Zucker (1972) demonstrated that nocturnal and free running circadian rhythms of drinking and locomotor activity were severely disrupted by relatively discrete lesions in the area of the SCN. Since this time, many fascinating and well performed experiments have been carried out implanting donor SCN tissue into a host animal that has become arrhythmic after its pacemaker has been destroyed by selective lesions (for review see Ralph and Lehman, 1991). In general, animals are maintained under constant environmental lighting conditions, and the rhythm in either locomotor activity or drinking activity, or another parameter of circadian rhythmicity monitored. After a period of time when the animal exhibits free running rhythms, a surgical destruction of the SCN is undertaken. The animal is again monitored for a period of time, and successful lesions are those that destroy rhythmicity. Foetal SCN tissue is then prepared and implanted into the third ventricle near to the site of the destroyed host SCN. A period of approximately four weeks is needed before circadian rhythmicity is

restored. Subsequent experiments using *tau* mutant hamsters that present with a free running period shorter than that of wild type animals, identified that the restoration of circadian rhythmicity was attributable to that of the donor animal (Ralph *et al.*, 1991). Successful transplants were those situated close to the site of the original SCN, and were thought to involve neuronal contacts containing vasopressin and vasointestinal polypeptide from the donor SCN with the host brain into the periventricular and subparaventricular zones (DeCoursey and Buggy, 1989; Griffioen *et al.*, 1993; Lehman *et al.*, 1987). However, a humoral agent is also considered important in the restoration of circadian rhythmicity. Experiments in which donor tissue was encapsulated in a semipermeable polymeric membrane prior to implantation into the host brain, prevented neural outgrowth of foetal SCN whilst maintaining diffusion of humoral signals. Hamsters that had been made arrhythmic by SCN lesions and implanted with the encapsulated donor tissue, had their locomotor activity rhythm restored after approximately 21 days (Silver *et al.*, 1996).

The SCN are small paired nuclei situated in the midline on the ventral surface of the brain above ('supra') the optic chiasm ('chiasmatic'). In all mammalian species looked at to date, the SCN are readily compartmentalised into a ventrolateral (VL) and dorsomedial (DM) segment with respect to immunostaining of perykarya, cell size, neuropil extent, neurotransmitter content and afferent projections to the nucleus. Comprehensive early studies, utilising immunological staining techniques, attempted to locate neurotransmitters to the nucleus (Card and Moore, 1984; van den Pol and Tsujimoto, 1985). Many immunoreactive fibres for arginine vasopressin (AVP), bombesin, γ-amino butyrate (GABA), glutamate decarboxylase (GAD), gastrin-releasing peptide (GRP), neurophysin, serotonin (5-hydroxytryptamine, 5-HT), somatostatin (SOM) and vasointestinal peptide (VIP) were found in the nuclei with VIP, GRP and bombesin concentrated in the VL-SCN and AVP, SOM concentrated in the DM-SCN. In addition to these early studies, glutamate, aspartate (van den Pol, 1991; van den Pol and Tsujimoto, 1985) and substance-P (Takatsuji *et al.*, 1991) have been located in the VL-SCN and neuropeptide-Y (NPY) to the DM-SCN (Shinohara et al., 1993).

A great number of fibres cross the midline between the left and right SCN suggesting that the two nuclei do not function as separate entities, but rather as a single body (van den Pol and Tsujimoto, 1985). An interesting aspect of the hamster SCN, unique to this

rodent species, is that the DM-SCN join in the midline and present as a single nucleus (Card and Moore, 1984). An important aspect of pacemaker function is the co-ordinated relay of messages to the nuclei and the efficient output of signals to the effector regions.

A number of factors can shift (advance or delay) or reset the phase of the circadian clock, as measured by *in vitro* preparations of SCN slices, or *in vivo* behavioural rhythms. Presumably these phase shifting responses are the result of an altered balance between transmitter substances of input pathways to the central pacemaker. Often the ability of a chemical agent or physical manipulation of an animal to produce a phase shift is presented as a phase response curve (PRC). The PRC is a record of the relative phase change versus the zeitgeber time at which the manipulation was carried out. The zeitgeber time (ZT) is a measurement of circadian time relative to either the light:dark cycle or, in animals allowed to free run, the ZT is related to the onset of locomotor activity: ZT 12 is designated as the time of lights off in an entrained animal or as the onset of activity in a free running animal.

1.2 SCN AFFERENTS

The afferent fibres collectively entrain the circadian pacemaker to environmental cues. The principle afferent fibres originate from the retina (retinohypothalamic tract and geniculohypothalamic tract) and from the midbrain raphe nuclei (raphe-hypothalamic tract) although the SCN do receive fibres from the infralimbic cortex, septal nuclei, substantia innominata and the ventral subiculum (Pickard, 1982; Moore, 1996).

1.2.1 THE RETINOHYPOTHALAMIC TRACT (RHT)

The first convincing evidence demonstrating a mammalian retinal projection to the SCN was in 1972 when tritiated amino acids were injected into the posterior chamber of the eye, anterogradely transported and detected by autoradiography of hypothalamic brain slices (Moore and Lenn, 1972). These authors demonstrated that the retinal projection terminated solely in the SCN of the hypothalamus. However, subsequent studies have demonstrated RHT terminals to be more widespread; in the anterior hypothalamic area, the retrochiasmatic area and the lateral hypothalamic area (Johnson *et al.*, 1988a; Moore *et al.*, 1995). The pathway originates from a small population of small to medium sized

retinal ganglion cells that are randomly scattered throughout the retina (Pickard *et al*, 1982; Moore *et al*, 1995), and conveys information via the optic nerve fibres to the retinorecipient areas. Sectioning of the RHT in hamsters eliminates the normal retinal innervation of the SCN whilst sparing projections to other visual centres, and even when exposed to a light:dark cycle these animals present with a free running rhythm, characteristic of constant environmental lighting conditions, indicating the RHT is necessary for entrainment (Johnson *et al.*, 1988a). Optic nerve stimulation in *in vitro* preparations of hypothalamic slices evokes excitatory post synaptic potentials (EPSPs) in the neurons of the SCN (Cahill and Menaker, 1989; Kim and Dudek, 1991), and electrical stimulation of the optic nerves *in vivo* mimics the phase dependent shifts of hamster wheel running induced by light pulses in constant dark (de Vries *et al.*, 1994).

The transmitter of the RHT has been the focus of much speculation since the demonstration of the pathway. There is mounting evidence implicating the excitatory amino acid glutamate as the putative neurotransmitter of the RHT, exerting its actions through a combination of NMDA (*N*-methyl-D-aspartate), non-NMDA (kainate and α-amino-3-hydroxy-5-methyl-4-isoxazoleproprionic acid [AMPA]) and metabotropic glutamate receptors. Glutamate has been detected immunocytochemically in the rat hypothalamus in presynaptic neurones of the retinohypothalamic tract (van den Pol, 1991; de Vries *et al.*, 1993), providing ultrastructural evidence that glutamate is the transmitter of the RHT. Additionally, NMDA, AMPA, Kainate and metebotropic glutamate receptor mRNA have all been detected in the retinorecipient region of the SCN of rodents by means of *in situ* hybridization or Northern analysis (van den Pol, 1994; Mick *et al.*, 1995; O'Hara *et al.*, 1995; van den Pol *et al.*, 1995; Ghosh *et al.*, 1997), and many *in vitro* (Cahill and Menaker, 1989; Kim and Dudek, 1991; Shibata *et al.*, 1994) and *in vivo* (Amir, 1992; Ohi *et al.*, 1991; de Vries *et al.*, 1994) experiments have demonstrated their importance in the regulation of circadian rhythms.

In slices of rat hypothalamus preloaded with tritiated glutamate and aspartate, optic nerve stimulation increases the release of both amino acids (Liou *et al.*, 1986) strongly suggesting excitatory amino acid involvement in RHT transmission. Excitatory responses of SCN neurons *in vitro* to applied glutamate do not show day-night variation (Shirakawa and Moore, 1994a). Topically applied glutamate in similar preparations can phase shift neuronal firing when applied during the early (delay) or late (advance)

subjective night but not when applied during the subjective day (Shirakawa and Moore, 1994b). This phenomenon of phase delay in the early subjective night versus phase advance in the late subjective night is in keeping with glutamate mimicking light pulse stimulation in experiments monitoring activity records of animals allowed to free run in constant darkness. However, N-acetylaspartylglutamate (Moffett *et al.*, 1990), aspartate (van den Pol, 1991) and substance-P (Takatsuji *et al.*, 1991) have also all been detected immunocytochemically in presynaptic neurones of the SCN, suggesting there may be additional transmitters of the RHT. Indeed, substance-P has been shown to potentiate glutamate-evoked excitatory responses in an *in vitro* rat SCN slice preparation (Shirakawa and Moore, 1994a) and to increase the uptake of 2-deoxyglucose in the SCN during the subjective night when light is known to affect the clock. Substance-P also exhibits a PRC in rat SCN slices similar to that of light (Shibata *et al.*, 1992a). This data strengthens the hypothesis that substance-P is involved in entrainment of circadian rhythms, although the degree of interaction between this system and the glutaminergic system is unknown.

NMDA can mimic the suppressive effects of light pulse on pineal melatonin production. In addition, a specific NMDA receptor antagonist can inhibit light-suppressed melatonin production (Ohi *et al.*, 1991). Light-induced increases in rat heart rate are also blocked by prior infusion into the SCN with a competitive NMDA antagonist (Amir, 1992). *In vitro* SCN brain slice preparations can be a very useful tool for identifying potential phase shifting agents. Topical application of NMDA to SCN slice induces phase shifts very similar to those seen with glutamate (Ding *et al.*, 1994; Shibata *et al.*, 1994; Watanabe *et al.*, 1994), and the non-competitive NMDA antagonist MK-801 can attenuate phase delays in hamster wheel running induced by electrical stimulation of the optic nerves in the early subjective night (de Vries *et al.*, 1994). AMPA receptor stimulation when applied topically to SCN brain slices can also phase delay neuronal firing when applied during the early subjective night (Watanabe *et al.*, 1994). EPSPs evoked in the SCN by electrical stimulation of the optic nerve are blocked by application of a non-selective antagonist of amino acid receptors and kainate also reduces the amplitude of the postsynaptic response (Cahill and Menaker, 1989). Somewhat surprisingly, a competitive NMDA receptor antagonist was without effect both under the same conditions (Cahill and Menaker, 1989), and in another slice preparation (Kim and Dudek, 1991). 1S,3R-ACPD, an agonist at metabotropic

glutamate receptors, can also activate SCN cells as shown in an *in vitro* slice preparation (Scott and Rusak, 1996).

Nitric oxide, a highly reactive messenger molecule produced from the conversion of L-arginine to L-citrulline by the enzyme nitric oxide synthase (NOS), is released upon stimulation of NMDA receptors (Knowles *et al.*, 1989) and has been implicated in the regulation of circadian rhythms (Amir, 1992; Ding *et al.*, 1994; Watanabe *et al.*, 1994, 1995; Weber *et al.*, 1995a). Light-induced phase shifts of circadian rhythm wheel running activity are attenuated by systemic (Watanabe *et al.*, 1995) or intracerebroventricular (Weber *et al.*, 1995a) injection of the NOS inhibitor L-NAME, and in *in vitro* slice preparations of the SCN, L-NAME can block the phase delay produced by NMDA receptor stimulation during the early subjective night (Watanabe *et al.*, 1994). These data suggest that the NMDA- or light- induced phase shifts are mediated by nitric oxide.

Light induced phase shifts also involve the induction of a number of immediate early genes (c-fos, egr-1, NGF1-A, NGF1-B) (Ebling *et al.*, 1991; Sutin and Kilduff, 1992) in the subjective night, the most commonly studied being c-fos and its protein product Fos. Light induced Fos protein is induced in the retinorecipient region of the VL-SCN only during periods in which light can phase shift the circadian pacemaker (Rea, 1989). A greater amount of Fos has been detected after a light pulse that will phase advance the clock (late subjective night) than will delay the clock (early subjective night) (Romijn *et al.*, 1996). Light induced Fos protein in the rat is blocked by prior administration of the NDMA receptor channel blocker MK801 (Ebling *et al.*, 1991; Park *et al.*, 1993) and NMDA infusion intracerebroventricularly can induce c-fos (Ebling *et al.*, 1991), implicating NMDA receptor stimulation in the production of the immediate early gene. Phosporylation of the cyclic AMP response element binding protein (CREB) produces pCREB which can activate a number of immediate early genes (Sheng and Greenberg, 1990). Light can induce the production of pCREB in the rat *in vivo* during the subjective night and in an *in vitro* preparation of rat SCN slices glutamate can also induce pCREB production in the SCN (Ding *et al.*, 1997). This induction of pCREB involves the stimulation of NMDA receptors and the production of nitric oxide, as both an NMDA receptor competitive antagonist and an inhibitor of NOS can attenuate the photic/glutamate induction of pCREB. In addition, a NO-generator can induce a similar

induction of pCREB. The cascade of events leading to photic phase shifting therefore appears to involve release of glutamate from the RHT, stimulation of NMDA receptors, release of nitric oxide, stimulation of phosphorylation of CREB and induction of immediate early genes. However, an inhibitor of NOS injected intracerebroventricularly in free running hamsters fails to block the induction of light induced Fos expression during either the early or late subjective night (Weber *et al.*, 1995a) which would suggest that the involvement of nitric oxide was after induction of Fos. The difference between these experiments may reflect differences in species (rat versus hamster) or photoperiod. The production of pCREB was inducable in animals maintained on a 12:12 LD cycle, whereas in the experiments where inhibition of NOS failed to prevent light induced Fos expression the hamsters were maintained in constant darkness.

It therefore appears that the retinal hypothalamic tract releases glutamate at its terminals to act upon postsynaptic NMDA and non-NMDA glutamate receptors to phase shift the circadian clock during the subjective night. The phase shift produced by the stimulation of NMDA receptors is mediated by nitric oxide and involves the induction of immediate early genes.

1.2.2 THE RAPHE-HYPOTHALAMIC TRACT (RaHT)

The serotonergic innervation of the SCN originates in the midbrain raphe nuclei (Moore *et al.*, 1978; Azmitia and Segal, 1978). This serotonergic projection from the raphe nuclei also innervates the intergeniculate leaflet (IGL) of the thalamus (Moore and Card, 1994). Many attempts have been made to establish a role for 5-HT in the circadian timing system, and the general consensus is that 5-HT serves to modulate photic inputs rather than to have a direct effect upon the clock itself.

A large majority of the studies performed to elucidate the role of serotonin in the regulation of circadian rhythms have been carried out in hamsters. Depleting the serotonergic input to the hamster SCN by administration of the selective neurotoxin 5,7-dihydroxytryptamine (DHT) throws up some confusing data regarding phase changes in either constant light (LL) or constant dark (DD). Under light:dark (LD) conditions DHT treatment induces the rapid appearance of advanced activity onset (Smale *et al.*, 1990; Morin and Blanchard, 1991; Penev *et al.*, 1993), delayed offset and longer duration of

the nocturnal activity phase, whereas in LL normal circadian rhythmicity was rapidly lost in DHT-treated animals. Although in DD there was no effect on circadian period, there was an overall change in the temporal properties of the phase response curve to light (Morin and Blanchard, 1991). 5-HT depletion potentiates light induced phase delays in the mid subjective night and potentiates Fos induction in mice (Bradbury *et al.*, 1997) indicating that 5-HT modulates the magnitude of the photic response. This action of 5-HT may be via stimulation of 5-HT_{1A} receptors as in hamsters maintained under constant dark conditions (DD), systemic administration of the 5-HT_{1A} antagonist NAN-190 potentiated light-induced phase shifts in wheel running activity (Rea *et al.*, 1995).

Metamphetamine (MA) when infused into the SCN increases extracellular 5-HT concentration (Ozaki *et al.*, 1991). In rat SCN slices, application of MA significantly attenuated optic nerve stimulated-evoked field potentials (Moriya *et al.*, 1996), which is abolished by pre-treatment with the 5-HT_{1A} receptor antagonist NAN-190, suggesting that the inhibition is mediated via the action of a 5-HT_{1A}-like receptor. Indeed, 5-HT_{1A} agonists reportedly attenuate optic nerve stimulation-evoked field potentials in the SCN (Liou *et al.*, 1986) and cause a dose dependent inhibition of both spontaneous activity and photic responses in SCN cells (Ying and Rusak, 1994). Light-induced Fos expression in hamsters is reduced by the serotonergic agonist, quipazine (Selim *et al.*, 1993) or the systemic administration of MA. The effect is selectively attenuated by NAN-190 applied in addition to MA, thus indicating the actions of MA to be via a 5-HT_{1A}-like receptor (Moriya *et al.*, 1996). In the rat, however, blockade of the 5-HT_{1A} receptor with NAN-190 partially blocks the photic induction of Fos in the SCN, although the 5-HT_{1A} agonist 8-OH-DPAT also reduces Fos induction (Recio *et al.*, 1996) and quipazine can induce c-fos in the VL-SCN in a manner similar to that of a light pulse in the rat (Moyer *et al.*, 1997). The serotonergic regulation of photically induced Fos in rats therefore appears to be opposite to the serotonergic regulation in the hamster. Thus, species differences must be taken into account when interpreting drug actions.

This modulation of photic responses by 5-HT might be due to a direct retinal projection to the raphe nuclei thereby acting upon the serotonergic neurones projecting to the SCN. In the cat (Foote *et al.*, 1978) and rat (Villar *et al.*, 1987; Shen and Semba, 1994;

Kawano *et al.*, 1996) a retinal projection to the raphe nuclei has been identified. This opens up the possibilty that the RaHT constitutes an indirect retinal pathway from the retina to the SCN.

In addition to modulating photic inputs to the SCN, stimulation of the serotonergic system can also induce phase shifts *in vitro* an *in vivo*. In preparations of rat brain slices, the serotonergic agonist quipazine or 5-HT itself, produces phase shifts in the electrical activity rhythm (Prosser *et al.*, 1990; Medanic and Gillette, 1992). Quipazine can also induce c-fos in the SCN during the subjective day in rat SCN slices maintained *in vitro* (Prosser *et al.*, 1994a) and during the light phase of rats maintained on a 12:12 LD cycle (Moyer *et al.*, 1997). This pattern of Fos protein induction incorporates both the VL-SCN and the DM-SCN, whereas light-induced Fos expression is present only in the VL-SCN. The presence of Fos in the DM-SCN is similar to that induced after *in vivo* electrical stimulation of the IGL (Abe and Rusak, 1992). Thus, the action of quipazine in these circumstances might incorporate the IGL, which itself receives innervation from the serotonergic midbrain raphe. The effects on electrical activity rhythm in SCN slices by quipazine is mimicked by application of the 5-HT_{1A} agonist 8-OH-DPAT (Starkey, 1996; Prosser *et al.*, 1994a; Shibata *et al.*, 1992b), and phase shifting of wheel running activity in hamsters after 8-OH-DPAT administration has also been reported (Cutera *et al.*, 1994, 1997; Tominger *et al.*, 1992). The phase advancing ability of 8-OH-DPAT when applied during the mid subjective day involves nitric oxide production, activation of cAMP dependent protein kinase A (PKA) and the opening of potassium channels: an inhibitor of NOS can block the 8-OH-DPAT induced phase advance in firing, whilst an NO donor can mimic the effect of the agonist (Starkey, 1996), and inhibitors of PKA and a variety of potassium channel blockers can block 8-OH-DPAT induced phase advances in rat SCN slices (Prosser *et al.*, 1994b).

The actions of 5-HT agonists during the subjective day are thought to mediate non-photic phase shift of the circadian clock. Animal handling, cage change and general arousal of the animal during the light phase has the ability to phase shift the circadian pacemaker. The firing rate of the midbrain raphe serotonergic neurones, releasing 5-HT at their terminals, is correlated to the activity state of the animal. The more aroused the animal is the more the serotonergic neurones fire, and the greater the terminal release of 5-HT. It is reasonable to predict that the actions of exogenously applied 5-HT agonists

are mimicking the actions of an increase in raphe neuron firing. In 5-HT depleted animals a 3 hour bout of activity induced by exposure to a new running wheel fails to evoke a phase advance of the clock rhythm during the light period (Bobrzynska et al., 1996a). This in itself is evidence for 5-HT involvement in the ability of a non-photic cue (novelty wheel running) to phase shift the rhythm. However, this mediation of non-photic phase shifting by 5-HT is thought to be via an action through the IGL.

1.2.3 THE GENICULOHYPOTHALAMIC TRACT (GHT)

A second retinal pathway to the SCN is an indirect pathway via the geniculohypothalamic tract (GHT). Retinal fibres project afferent fibres to the IGL before relaying axons to the SCN (Moore and Card, 1990). The IGL contain a population of neuropeptide-Y (NPY) neurones (Harrington *et al.*, 1987) that project bilaterally to the VL-SCN (Morin *et al.*, 1992) and these neurones also colocalise with GABA. Each IGL also sends met-enkephalin and GABA fibres to the contralateral IGL. Since the IGL receive photic information, it was the general consensus that these nuclei must relay photic information to the SCN. However, evidence is accumulating that this structure may also convey non-photic information. A non-photic stimulus that can phase shift the circadian clock in hamsters, dependent upon the time of application, is the systemic administration of the benzodiazepine triazolam. Destruction of the lateral geniculate nuclei with a selective neurotoxin prevented the triazolam-induced phase advances in hamster wheel running activity, suggesting that an intact IGL was required for the phase shifting ability of the benzodiazepine (Johnson *et al.*, 1988c; Janik and Mrosovsky,1994). The effect of triazolam on the pacemaker has a very similar effect on activity as that of dark pulses presented during a period of constant light (Bobrzynska *et al.*, 1996b). Both of these non-photic manipulations are thought to mediate their effects by an increase in activity of the animals. Indeed, the phase advancing or delaying effects of trialozam or dark pulses can be completely suppressed by immobilisation of the animals during treatment (Van Reeth and Turek, 1989). Another non-photic stimulus capable of phase shifting circadian rhythms is that of novel wheel running. Lesions of the IGL completely block the activity-induced phase shift (Janik and Mrosovsky, 1994; Wickland and Turek, 1994) suggesting the common pathway of all non-photic phase shifting is via the IGL and involves an increase in animal activity for the phase shift to result. As stated in the preceding section (1.2.2) the mediator of the

non-photic phase shifts is considered to be 5-HT released at afferent terminals originating from the midbrain raphe nuclei. The serotonergic involvement in the control and regulation of circadian rhythms is thus complicated and can both modulate photic input to the pacemaker directly to the SCN and convey non-photic information indirectly via the IGL.

1.3 SCN EFFERENTS

The most dense projection of neurones from the SCN ends in an area with a relatively low density of cells dorsal to the SCN, in a region known as the subparaventricular zone, centred between the anterior hypothalamic area and the periventricular nucleus. A small number of fibres continue through the paraventricular nucleus of the hypothalamus to end in the midline thalamic nucleus, and a number of fibres continue caudally to end in the dorsomedial nucleus and the dorsal part of the ventromedial shell and the posterior hypothalamic area. A small number of neurones end in the region ventral and lateral to the ventromedial nucleus. A modest terminal field is in the paratenial nucleus and rostral part of the paraventricular thalamic nucleus, and only a few fibres can be found in the ventromedial parts of the pre-optic region, the intermediate lateral septal nucleus and the ventral lateral geniculate nucleus (Watts and Swanson, 1987; Watts *et al*, 1987).

These efferent projections of the SCN shed precious little light on the functioning of the nuclei and how they can influence all manner of circadian responses. It may be that circadian patterns of neuronal activity generated in the SCN are relayed to effector circuitry in the subparaventricular zone, which serves as an amplification stage thereby increasing the influence of the SCN.

1.4 AIMS OF THESIS

The aims of this thesis as a whole were to further the understanding of the mechanisms controlling SCN function in the rat. In particular, the regulation of 5-HT release by autoreceptor and glutamatergic agonists in the SCN was investigated in the freely moving conscious animal using microdialysis. Specific aims of the thesis are outlined in each of the following Chapters.

CHAPTER 2

GENERAL MICRODIALYSIS AND HPLC-ED PARAMETERS

2.1 MICRODIALYSIS

There is a need for more accurate and detailed information concerning the complex and biochemical reactions in the normal and abnormal brain. An ideal method must provide an instantaneous and reliable concentration measurement of a wide variety of interstitial substances in discrete brain areas, and be as non-invasive as possible. The microdialysis technique is an important breakthrough in the neurobiological sciences as it has provided much needed information on the *in vivo* neurochemistry of the intact brain.

2.1.1 Principles of microdialysis

In vivo brain microdialysis involves the stereotaxic implantation of a dialysis probe into a given area of the brain. The membrane at the tip of the probe allows free diffusion of water and solutes between the brain interstitial space and a solution of artificial cerebrospinal fluid (aCSF) which is continually being renewed and sampled for dialysis. Due to the 'macro' size of the probes (outer diameter 290 μm) in relation to the size of the nerve terminals, brain dialysis cannot be expected to measure neurotransmitter release at synaptic sites, but rather neurotransmitter diffused into the extracellular space after its release. The brain is well suited for microdialysis because of the presence of the blood brain barrier which rapidly closes over the implantation site about 30 min after implantation (Dykstra *et al.*, 1992), thus avoiding contamination from the systemic circulation (Beneviste, 1989).

Microdialysis has advantages over other methods of sampling from neuronal tissues. What was once a solitary sample from a whole *post mortem* brain can now be several samples from a freely moving conscious animal. The procedure of microdialysis is continually being improved, and is streets ahead of the method of push-pull cannula which preceded it. Push-pull cannula (Gaddum, 1961) involved the implantation of two stainless steel tubes into the brain, and the extracellular fluid perfused with aCSF. Neurotransmitters and metabolites would thus diffuse into the perfusion fluid, but the 'open' design of the system created many problems including excessive tissue damage, relatively low recoveries from the extracellular medium and the necessity to 'clean up' the perfusate before analysis by high performance liquid chromatography (HPLC). Being a 'closed' system, microdialysis can avoid these problems. It does not pump fluid into the brain tissue (a study by Dykstra *et al.*, 1992 confirmed this by measuring flow

rate of the dialysate leaving the probe compared to that entering the probe, and found no loss of fluid due to bulk flow across the membrane), thereby limiting tissue damage, and there is no need for 'clean up' of dialysate samples due to the molecular weight cut-off of the membrane. Although the implantation of a dialysis probe produces inevitable damage to surrounding brain tissue, tissue levels of neurotransmitters elevated by nerve damage equilibrate within 90 minutes and sampling can begin. Long term sampling from microdialysis probes reduces the efficiency of the membrane and its ability to recover solutes from the interstitial space. This is due to hypertrophy of astrocytes encompassing the probe, and layers of cell products surrounding the dialysis membrane (Benveniste and Diemer, 1987). Thus, guide cannulae are often employed during long term sampling through which microdialysis probes can be inserted and removed at various times over the experimental period, avoiding clogging of the membrane.

In addition to monitoring neurotransmitters in different brain areas and in different behavioural states, drugs can be administered locally into a brain region via the probe (dissolved in aCSF), and immediate effects upon transmitters detected. However, it is important to recognise that the concentration of drug infused via the probe will not reflect the concentration profile of the drug diffused into the interstitial space. Many factors will determine the amount of drug passing through the dialysis membrane into the interstitial space (see Beneviste, 1989) including: diffusion coefficients of the drug, drug concentration and drug interaction with the membrane. Once present in the interstitial space, the availability of the drug is dependent upon the uptake of the drug in intracellular and vascular compartments and binding of the receptor to other membrane proteins i.e. the *in vivo* performance of a microdialysis probe depends primarily on the behaviour of the solute in the tissue. The concentration of drug outside the membrane therefore, cannot be expected to reach that in the aCSF, and it is important to bear in mind this fact when interpreting results of drug infusions down the probe.

The distance a drug will diffuse through the tissue from the probe is only very limited and is dependent upon the duration the drug is present in the perfusing aCSF. Dykstra *et al.* (1992) perfused radiolabelled sucrose via the probe for 14 and 61.5 min, and examined autoradiograms of histological sections cut perpendicular to the site of implantation. After 14 min radiolabelled probe was visible surrounding the probe tract in a radius of 1 mm, whereas after 61.5 min, the label had diffused to approximately 2

mm radially. This demonstrates the importance of stereotaxis during probe implantation for accurate implantation, and also the need for histological examination of brain tissue following microdialysis experiments to ensure correct probe positioning.

The most important characteristic of a dialysis probe is its ability to recover compounds of interest from the extracellular space, since this is a major factor determining the limit of detection of the system. Therefore, prior to each experiment the *in vitro* probe recovery must be tested to ensure that the recovery of 5HT across the dialysis membrane is high enough to detect the low interstitial concentrations. The probe is continuously perfused at a constant flow rate and inserted into an aqueous solution of the substance to be detected, at a known concentration. Other than the substance to be measured, the perfusion fluid and the medium outside the probe should be identical. The probe is perfused for 30 minutes and the dialysate collected. Recovery is expressed as a percentage of the 5HT in the recovered dialysate as compared to that in the medium outside.

Factors affecting the recovery of compounds via the probes include the molecular weight cut-off of the membrane, dialysis membrane area and the perfusion flow rate. Each membrane has a different molecular weight cut-off value for different molecules, and recovery depends on the size of the pores in relation to the size of the molecule. The appropriate membrane is therefore chosen with regard to the size of the molecule of interest. Obviously, the greater the surface area of the membrane, the larger the surface for free diffusion (Sandberg and Lindstrom, 1983) and hence a higher rate of recovery. Conversely, recovery of solutes are inversely proportional to perfusion flow rate. The slower the perfusion flow rate, the higher the rate of recovery across the membrane (see Result and Discussion section this Chapter). An obvious consideration is whether a given probe can detect what are effectively minute changes in concentration of substances in the interstitial fluid. Fortunately, recovery is independent of changes in the concentration outside the membrane (Johnson and Justice, 1983). Therefore, when the outer substance concentration is suddenly increased or decreased, the gradient across the dialysis membrane changes accordingly, thus keeping recovery constant.

2.2 HIGH PERFORMANCE LIQUID CHROMATOGRAPHY WITH ELECTRO-CHEMICAL DETECTION (HPLC-ED)

The successful application of high performance liquid chromatography (HPLC) to biomedical analysis often depends upon good sample preparation. Fortunately, due to the nature of the 'closed' microdialysis sampling system, there is no need for 'clean up' of the samples. The microdialysis samples can therefore be injected directly into the HPLC system.

2.2.1 Principles of chromatography

Reversed-phase chromatography is the most versatile and widely used HPLC method. Injected analytes are partitioned between a hydrophobic stationary phase (the HPLC column) and an aqueous (polar) mobile phase. The HPLC column is packed with a very uniform micro-particulate silica (3-10 μm), chemically bonded with an octadecylsilyl (ODS) group to give a non-polar surface. The mobile phase used for elution is usually water mixed with methanol, or another water-miscible organic solvent. Separation of substances is dependent on their molecular charge, and elution is in order of increasing hydrophobicty (or decreased polarity). Although HPLC is a very efficient system for sample identification it can be further improved by using additives, such as ion-pairing agents added to the mobile phase to aid separation of amines (5-HT; see section 2.3.5), or by pre-column derivatisation for example for the detection and quantification of amino acids (glutamate; see section 2.3.6).

2.2.2 Basic HPLC-ED apparatus set up

Analysis by HPLC requires five basic components: (1) a pump, (2) an injection system, (3) a column, (4) a detector, in this case an electrochemical detector (ED), and (5) a recording system to measure the output from the detector. The basic set up of the HPLC-ED is shown in figure 2.1. EC detection involves the oxidation and/or the reduction of compounds passing over an electrode, across which a given potential is maintained with respect to a reference electrode. The resultant flow of electrons is then measured by the working electrode, and subsequently amplified and measured on a suitable recording device.

2.2.3 Detection of 5-HT by 'ion-pairing' HPLC

Catacholamines are readily broken down by oxidation at the ring hydroxyl groups producing an orthoquinone derivative and two electrons. Whilst a problem to scientists involved in the amine field, the electrochemist has used this to their advantage. Carrying out the oxidation at the surface of an electrode by applying a positive potential, results in a current produced directly proportional to the number of molecules oxidised.

It is worth considering the reasons for the inclusion of certain components of the mobile phase. Amines are known to become unstable in alkaline conditions and therefore an acidic pH is required, achieved by the inclusion of citric acid. Methanol is included to providing a less polar environment for the passing elutes, and at the same time shortening retention times of all compounds. However, under acidic conditions, the amino groups of monoamines tend to be more protonated and are therefore even less hydrophobic than if they were uncharged. For that reason, passing through a hydrophobic column, their separation, at best, would be poor. It is thus advisable to use 'ion-pairing'. This introduces a polar element to the otherwise hydrophobic surface chemistry of the column that can interact with the positively charged species and hence retard elution of molecules from the column. The fine balance between methanol concentration and octane sulphonic acid (OSA) concentration determine the elution time of the compounds and the separation of the compounds within the dialysate.

2.2.4 Detection of glutamate by pre-column derivatisation HPLC

Amino acid side chains rarely have physical characteristics which would permit direct estimation in solution. Therefore, to aid detection, derivatisation of the amino acids at the N-terminus is carried out with agents such as *o*-phthalaldehyde (OPA). The reaction of the OPA reagent with an amino acid produces a new heterocyclic species, responsible for the electrochemical activity of the OPA-amino acid derivatisation. In general, phosphate buffers are utilised with methanol present as an organic modifier. An important factor for adequate separation of amino acids present in biological samples is the pH of the mobile phase. Gentle manipulation of the pH will differentially modulate the retention time of different amino acids, thereby ensuring sufficient separation. Again, not unlike the system for separating 5-HT, it is a fine balance between methanol concentration and the pH of the mobile phase that determines retention time and adequate separation.

Ethylenediaminetetraacetic acid (EDTA), present in the mobile phase of both systems, has the ability to chelate divalent cations. This is beneficial because divalent cations promote auto-oxidation of catechol-containing moieties, and stripping of divalent cations from the inner surface of the HPLC systems' plumbing can lead to undesirable detection of 'noise'.

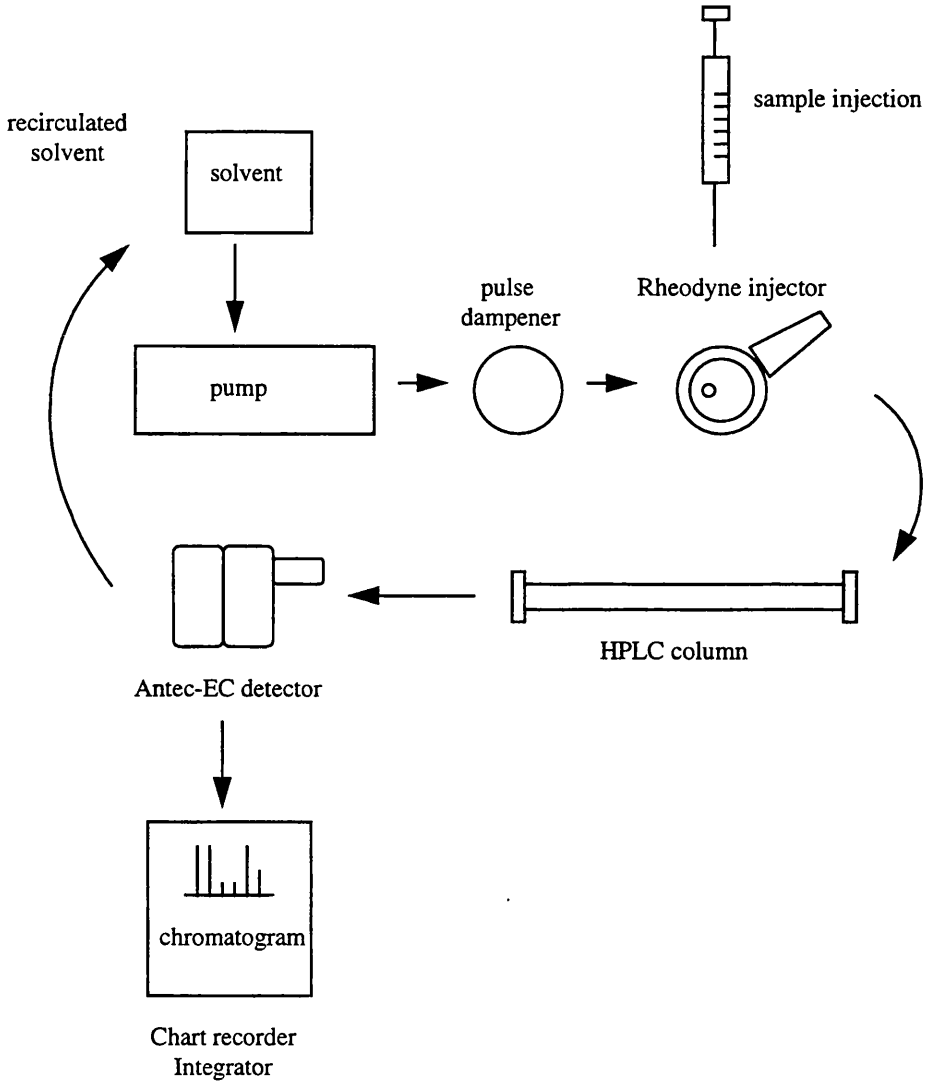

Figure 2.1. Diagrammatic representation of the HPLC-ED system employed for the separation of both 5-HT and glutamate in microdialysate samples. The mobile phase is driven through the entire system by the pump and, in the case of 5-HT separation, recirculated. Pump 'noise' is eliminated by the presence of a pulse dampener. Samples are injected into the system with a Hamilton syringe, via a Rheodyne injection port, and expelled onto the column. The use of a guard column is employed when separating amino acids. Samples are detected electrochemically, and a record of the chromatogram is either printed on a chart recorder or displayed on a programmed integrator.

2.3 METHODS

2.3.1 Probe construction

Construction of concentric microdialysis probes was achieved using the following raw materials: 20 mm and 10 mm lengths of 24 gauge stainless steel cannulae (inner diameter (ID) 0.3 mm; Coopers Needle Works, Birmingham), 25 mm lengths of silica glass tubing (outer diameter (OD) 0.17 mm / ID 0.12 mM, Scientific Glass Engineering), 10 mm lengths of vinyl tubing (OD 0.8 mm / ID 0.5 mm; Elkay Laboratory products), lengths of Gambro membrane (OD 290 μm / ID 240 μm; 6000 Kda cut-off; Gambro), and super glue (Cyanoacrylic, Loctite 454 gel, RS Components).

One end of a 20 mm length cannula was inserted into the end of the vinyl tubing. Into the other end of the vinyl tubing was inserted a 10 mm cannula, leaving approximately a 4 mm gap in the centre of vinyl tubing between the 20 and 10 mm tubes. A small hole was then made in the centre of the vinyl tubing through which a length of silica glass tubing was threaded to emerge at the free end of the 20 mm cannula such that it extended approximately 1.5 mm out the end of the cannula. At this free end a short length of membrane (approx. 10 mm) was threaded over the silica tubing, and inserted a short way up the cannula, and affixed in position with a small quantity of super glue. Using a binocular dissection microscope the membrane was cut to a length of 2 mm ('SCN-probes') or 4 mm ('hippocampal- and raphe-probes') plus 0.5 mm to allow for plugging the end with glue. All join sites were sealed with glue, and a second 10 mm cannula positioned over the exposed end of silica tubing. Figure 2.2 shows a diagram of the completed concentric probe assembly.

2.3.2 In vitro probe recovery

In vitro recoveries of all probes were tested prior to implantation. The dialysis probes were suspended into an artificial CSF solution (see *'dialysis set-up'* section 2.3.4) containing a known concentration of 5-HT (1 μM) or glutamate (1 nM), and continuously perfused with the artificial CSF solution minus the 5-HT/glutamate, at a flow rate to be used in the experiment (1.2 μl/min). The probes were perfused for thirty minutes and the dialysates collected into an Eppendorf (containing 5 μl of 0.5 M perchloric acid for probes being tested for recovery of 5-HT). Recovery was expressed

as a percentage of the 5-HT/glutamate in the recovered dialysate as compared to that in the recovery medium. Individual probe recovery was between 10-20 %. Probes with recoveries below 10 % were discarded. *In situ*, the recovery of solutes from the interstitial space through the probe is dependent upon many factors and the relationship between *in vitro* and *in vivo* recovery is complex (Benveniste and Huttemeier, 1990). Therefore, the *in vitro* recovery of the probe is mearly an indication of how the probe will function *in vivo* and the interstitial concentratin of solute cannot simply be extrapolated from the *in vitro* recovery. It was therefore decided not to correct each dialysate sample for the *in vitro* recovery and to express the data simply as a percentage value.

2.3.3 Probe implantation

Eighteen hours prior to the start of an experiment, rats were anaesthatised with equithesin (0.3 ml / 100 g body weight, i.p.), and placed in a stereotaxic frame with the incisor bar set at -3.3 mm, to maintain the head in a level position. Animals maintained under reverse light:dark cycle conditions had their eyes covered with black tape (PVC electrical insulation tape) during surgery to exclude light. The top of the head was shaved and a 1.5 cm incision made along the midline. The fascia was removed from the surface of the skull and the incision site kept open by use of artery clips. Once the skull surface was allowed to dry thoroughly, Bregma was clearly visible. The probe implantation site was calculated using Bregma as a reference. Three (for single probe implantation) or four (double probe implantation) burr holes were created in the skull using a dental drill (Claudius Ash Steel Burr; model number GLC0183); one (or two) hole(s) directly above the site of implantation, and two further holes. The dura mater was punctured using a sharp needle, and the probe(s) lowered slowly into the brain, to establish a final position on the lateral border of the SCN (co-ordinates, according to Paxinos and Watson, 1982; 6° angle, 1.5 mm medio-lateral (ML), -1.3 mm anterio-posterior (AP), 9.7 mm dorso-ventral (DV)), the hippocampus (4.6 mm ML, -6.0 mm AP, 8.5 mm DV) or the midbrain raphe nuclei (14° angle, 1.5 mm ML, -7.8 mm AP, 9.5 mm DV). The probes were anchored to the skull using two stainless steel screws (2 mm diameter, Semat Technology UK Ltd.) inserted into the two additional burr holes, and cemented into place with dental cement (Dentsply Ltd.).

2.3.4 Dialysis set up

Animals were placed individually into experimental cages which consisted of a round plastic cage (diameter 30 cm; depth 30 cm) and a liquid swivel switch (Biotech Instruments Ltd.) suspended by a retort stand above the centre of the cage (see figure 2.3). The dialysis solution (aCSF; composition in mM: NaCl 147; KCL 4; $CaCl_2$ 4), containing 1μM of the selective serotonin reuptake inhibitor (SSRI), citalopram, except where indicated, was continuously perfused through the probes with a Harvard Apparatus compact infusion pump (Model 22, Harvard Apparatus), set at a flow rate of 1.2 μl/min. Sample collection did not involve contact with the experimental animal and, therefore, any changes in collected 5HT were not due to excessive handling of the animal. The total volume of the inlet and outlet tubing was 45 μl and thus the time taken for the aCSF to pass through the entire dialysis system was 37.5 minutes. Dialysis collection was every ten (glutamate) or fifteen minutes (5-HT), into 500 μl eppendorf tubes. The collection vials for analysis of dialysate 5-HT contained 5 μl 0.5 M perchloric acid to prevent amine oxidation.

2.3.5 Separation and detection of 5-HT in dialysate

The analysis of 5-HT was accomplished via a reverse phase HPLC-ED using an amperometric detector (Antec Electrochemical detector, Antec Leyden B.V., The Netherlands). 5-HT content was analysed by injecting a 22 μl volume of dialysate via a Hamilton syringe into a Rheodyne Syringe Loading Sample Injector port (model 7125; Rheodyne Incorporated, California, USA) holding a 100 μl loop. This off-loads the sample directly into the HPLC equipped with a 10 cm long, 4.6 mm bore, 3 μl 3ODS2 reverse phase column (Spherisorb, Jones Chromatography). The 5-HT was subsequently oxidised on the working electrode at +0.75 volts relative to a Ag/AgCl reference electrode. The current resultant from this oxidation of solute reaching the working electrode was amplified and converted to a voltage (I/E converter). The detector signal was detected on a programmable integrator (Hewlett Packard). Separation at 5.4 mins was achieved with a mobile phase consisting of 82.7 mM citric acid monohydrate, 43.4 mM anhydrous di-sodium hydrogen phosphate, 1.02 mM di-sodium EDTA, 214 μM OSA and 20 % methanol, pumped around the system using a Gynotek duel piston pump (model M300, Severn Analytical, Cheshire, UK; flow rate 0.7 ml/min). The mobile phase was filtered prior to use through 0.2 μm filters

(Millipore) and continually purged with helium to degas the solution. Concentration of 5-HT was determined by the ratio of sample to standard peak height stored in the memory of the programmed integrator, and the results expressed as femtomols.

2.3.6 Separation and detection of glutamate in dialysate

Detection of glutamate in the dialysate samples was achieved using pre-column derivatisation of amino acids with an amperometric detector (Antec E-C detector). The derivitising agent consisted of 11 mg of OPA dissolved in 0.25 ml ethanol (HPLC grade), 0.25 ml 1 M sodium sulphite and 4.5 ml 0.1 M sodium tetraborate (pH 9.5). This OPA-reagent was stored in a brown bottle to protect it from light and maintained at room temperature for a period of up to 5 days. Derivitisation of amino acids was accomplished by diluting 10 µl of dialysate to a total volume of 50 µl with Milli-Q water and adding 1 µl of OPA-reagent. The reaction proceeded for 15 min at room temperature before samples were injected (50 µl) into the HPLC system.

The mobile phase, filtered through 0.2 µm filters and continually degassed with helium, consisted of 0.1 M sodium phosphate, 5 mM EDTA and 10 % methanol (pH 5.2) pumped around the system at a flow rate of 1.0 ml/min using a Jasco (PU-980) pump. During sample analysis the system was operated as an open loop circuit, but when not in use, the mobile phase was recycled. Fifty microlitres of derivitised sample was injected into a Rheodyne Syringe Loading Sample Injector port (model 7125) holding a 100 µl loop. The HPLC system consisted of a C_{18}, 25 cm, 5 µm reverse phase column (Rainin Dynamax) protected by a guard column (Rainin Dynamax). The working electrode was set at +0.85 volts relative to a Ag/AgCl reference electrode. The chromatogram was printed onto a chart recorder (JJ Instruments) and glutamate was identified from the retention time of an injected standard solution and quantified by comparison of the achieved peak height with that of the injected standard. Results were expressed as picomols.

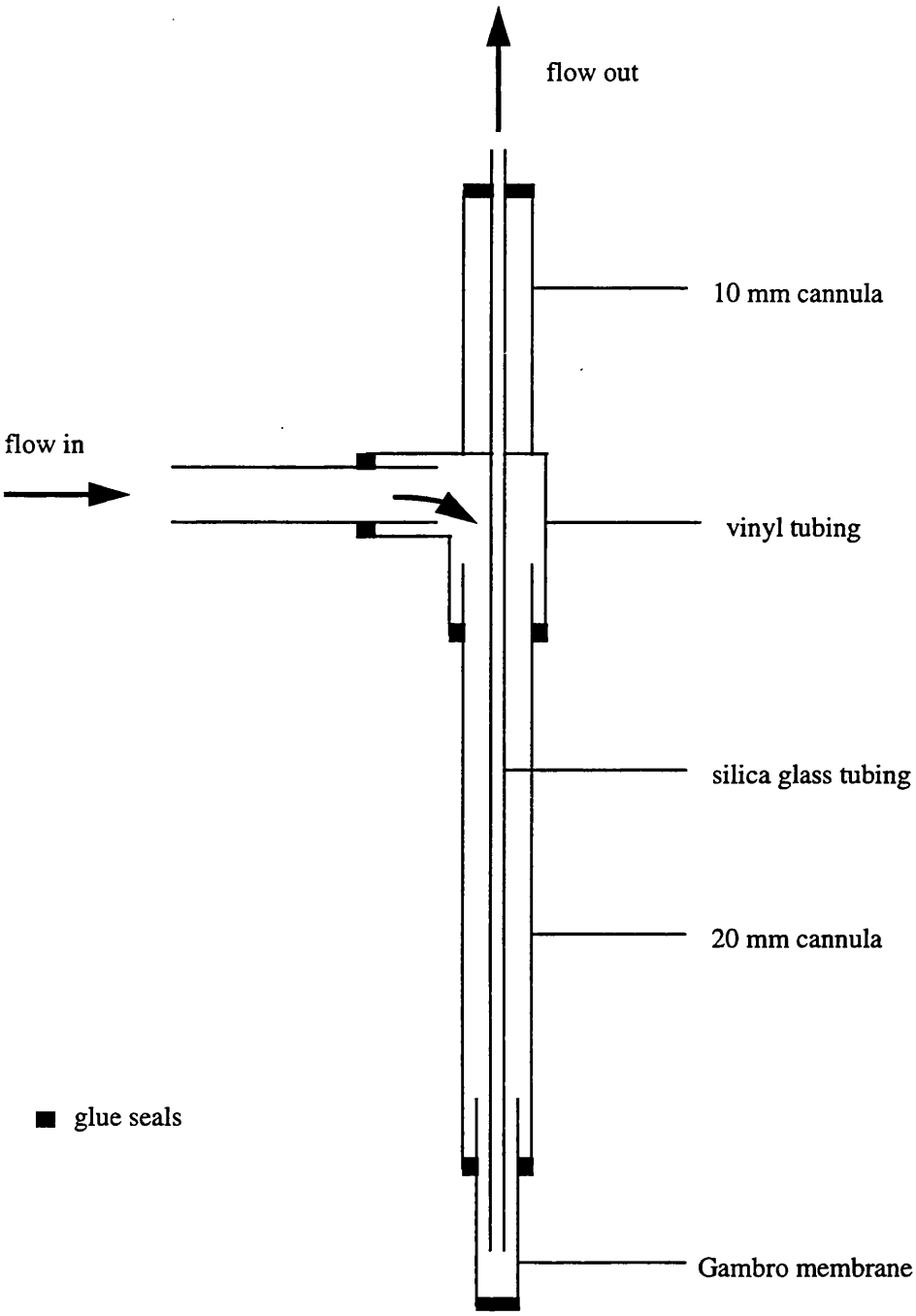

Figure 2.2. Complete concentric probe assembly as constructed in the laboratory. For details of assembly, see text.

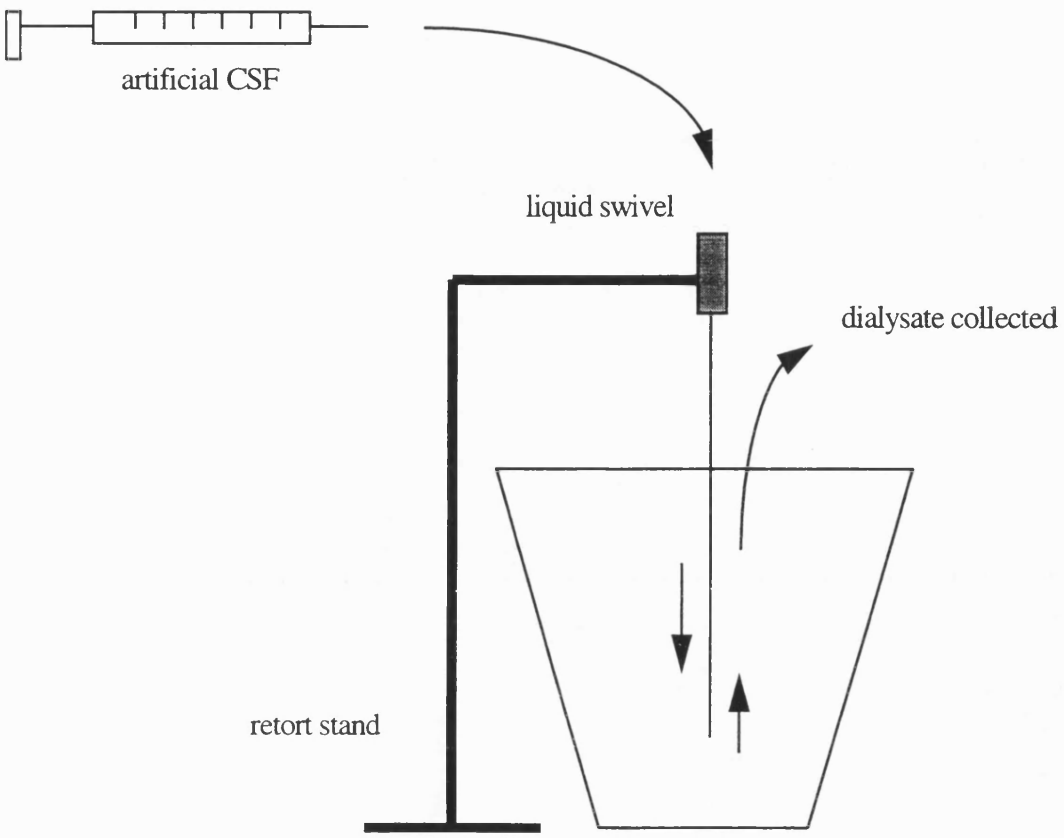

Figure 2.3. Microdialysis experimental set up. The animals were placed in a round experimental cage (diameter 30 cm; depth 30 cm) equipped with a liquid swivel suspended above the cage with a retort stand. The aCSF supplied via a 1 ml syringe, was continuously perfused through the system. Dialysate collection involved no contact with the animal.

2.4 RESULTS and DISCUSSION

2.4.1 General HPLC parameters

During the experimental period a number of HPLC columns and mobile phases of differing compositions were tested for their ability to separate 5-HT or glutamate in dialysate samples. Optimal conditions were those described in the preceding section. HPLC columns when used continuously had a shelf life of about 4-6 months. After this time separation of substances was incomplete, the pressure on the HPLC column increased or a double peak was produced on the chromatogram. When this occurs, the programmed integrator could not recognise the peak of interest and produces false readings. In these situations, the column was first reversed and generally pressure levels dropped to suitable levels and the double peak often disappeared. Alternatively, the column was washed through with a series of graded methanol concentrations (25, 50, 75, 100, 75, 50, 25 %) for a period of 15-30 min each. Often a new column was needed to obtain optimal separation. However, each column had slight differences from the preceding one, and the mobile phase has to be slightly modified to achieve adequate separation. Representative HPLC traces are shown for 5-HT and glutamate in figures 2.4 and 2.5 respectively.

2.4.2 General microdialysis parameters

Although the *in vitro* recovery of each individual probe is not a true reflection of its ability to recover transmitters *in vivo* (Benveniste and Huttemeier, 1990), it is a valuable estimate of how the membrane is likely to function under different conditions. For example, although an increase in perfusion flow rate will increase the flux across the membrane (the amount of fluid passing over the membrane per unit of time), and increase the volume of the dialysate over the collection period, the amount of transmitter recovered is lowered with a higher perfusion rate. Figure 2.6 shows the effect of flow rate on *in vitro* probe recovery. Three dialysis probes were perfused in a solution of 1μM 5-HT at different rates of flow between 1 and 4 μl/min, for a fixed period of 30 min. The data were grouped together, and a linear regression value calculated. There was a very strong inverse correlation between flow rate and amount recovered (R = -0.917). From this preliminary experiment, a flow rate of 1.2 μl/min was chosen and used in all subsequent dialysis experiments.

It was my aim to measure 5-HT and glutamate released from the circadian pacemaker, the SCN. However, due to its size and positioning within the mammalian brain, the SCN poses many problems for the neuroscientist. The SCN lie on the ventral surface of the brain in the midline. The probe is implanted from the dorsal surface of the brain and lowered into position using stereotaxis. Unfortunately due to excessive bleeding from the superior sagital sinus running throughout the midline, the probe could not be lowered vertically into the brain. Many preliminary experiments were performed to verify the best coordinates for implantation, and an angle of 6° yielded the best results. Approximately 70% of all implantated probes were accurately implanted as verified *post mortem*. The SCN are paired nuclei (see Introduction) and each nucleus is 950 μm long, 420 μm wide and 400 μm in depth in the rodent. Lowering the probe (outer diameter 290 μm) directly into the nucleus would therefore ablate the nucleus on the side of implantation. Thus, the probe is implanted so that its medial side lies adjacent to the lateral border of the nucleus. In this position it is expected that most of the 5-HT measured in the dialysate is of SCN origin, as the serotonergic innervation of the hypothalamus from the midbrain raphe culminates in the SCN (Moore *et al.*, 1978). Additionally, a study (S. Barassin, personal communication) verified that the majority of 5-HT collected from the dialysate of rats implanted with dialysis probes in similar positions (lying next to, rather than in, the SCN) did indeed originate from the SCN. The lateral border of the probes were blocked using glue, exposing only the medial side of the probe tip, lying adjacent to the SCN. The amount of 5-HT collected from such probes and intact probes with the whole membrane surface exposed, did not differ significantly. Regarding the collection of dialysate glutamate, one cannot be as positive that the glutamate has originated from the SCN. Although retinal afferents to the SCN release glutamate at their terminals (see Introduction), glutamate immunoreactivity in the whole hypothalamus is high (van den Pol, 1991). However, microdialysis has been successfully employed to measure glutamate from the SCN, and drugs acting thereupon (Selim *et al.*, 1993; Srkalovic *et al.*, 1994).

Regarding the implantation of probes into the midbrain raphe nuclei, the same problem of bleeding from the superior sagital sinus was evident, because of their midline positioning. The probes were therefore implanted at an angle of 14°.

It was deemed necessary to include the SSRI citalopram (1 μM) in the aCSF of all dialysis experiments involving perfusion of the SCN with subsequent 5-HT collection. Preliminary experiments carried out during the light phase measured basal levels of 5-HT collected from dialysate samples not containing citalopram, of between 0 and 5 femtomols (fmol). Upon addition of citalopram the basal 5-HT level increased four-fold (figure 2.7A). The limit of detection of the HPLC was between 0 and 5 fmol and therefore, with addition of drugs postulated to decrease neuronal 5-HT (e.g. RU24969), it was necessary to have higher basal levels of 5-HT in order to observe the expected decrease.

Citalopram was excluded from the aCSF perfusing the midbrain raphe nuclei during the double probe experiments. During these experiments drugs were infused via probes implanted into the midbrain raphe, and the effects on raphe and SCN 5-HT concentration measured. Citalopram in the aCSF perfusing the raphe would increase synaptic 5-HT, thereby increasing the stimulation of 5-HT_{1A} somatodendritic autoreceptors, decreasing serotonergic neuronal firing (Sprouse and Aghajanian, 1987) and decreasing terminal 5-HT release (Davidson and Stamford, 1995). The levels of 5-HT in the SCN dialysate would therefore be decreased, and any further decrease expected after infusion of drugs into the raphe nuclei during these experiments would be more difficult to detect (Romero *et al.*, 1994).

The experimental setup using the round cages equipped with a liquid swivel was such that it avoided excess contact with the animal, thereby ensuring that any fluctuations in 5-HT overflow were not due to excessive handling of the animal. Figure 2.7B shows the effect of handling an animal (n=2) for a short period on 5-HT in the collected dialysate from the midbrain raphe at mid light. A three-fold increase in 5-HT was observed.

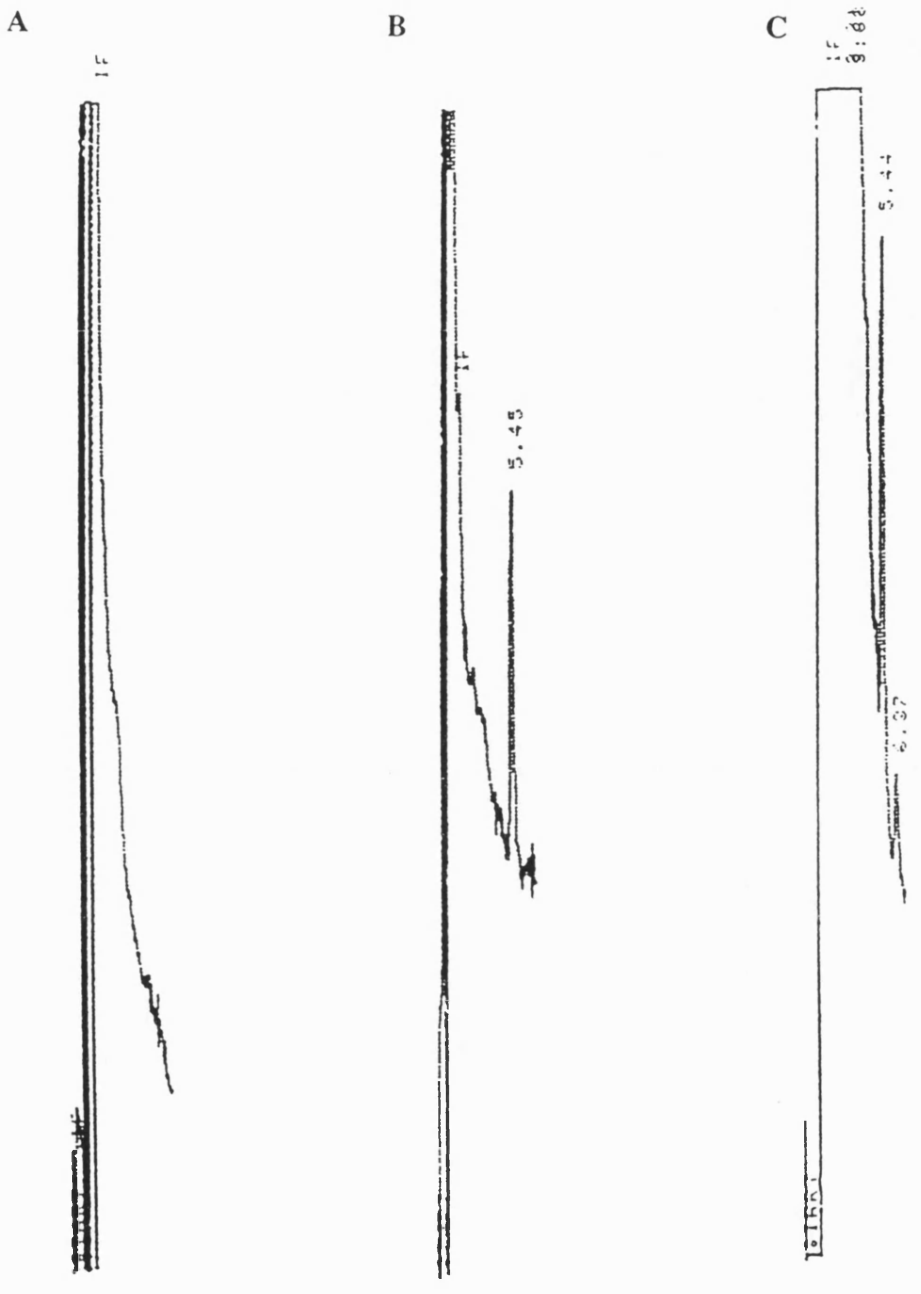

Figure 2.4. Typical HPLC traces for the separation of 5-HT in dialysate samples as recorded by the programmed integrator. (**A**) 20 µl aCSF; (**B**) 20 µl 10^{-9} M 5-HT(20 fmol); (C) 22 µl dialysate sample. Note the separation of the 5-HT peak from the remaining components in the dialysate sample. 5-HT elution time 5.45 min; run time 6.5 min.

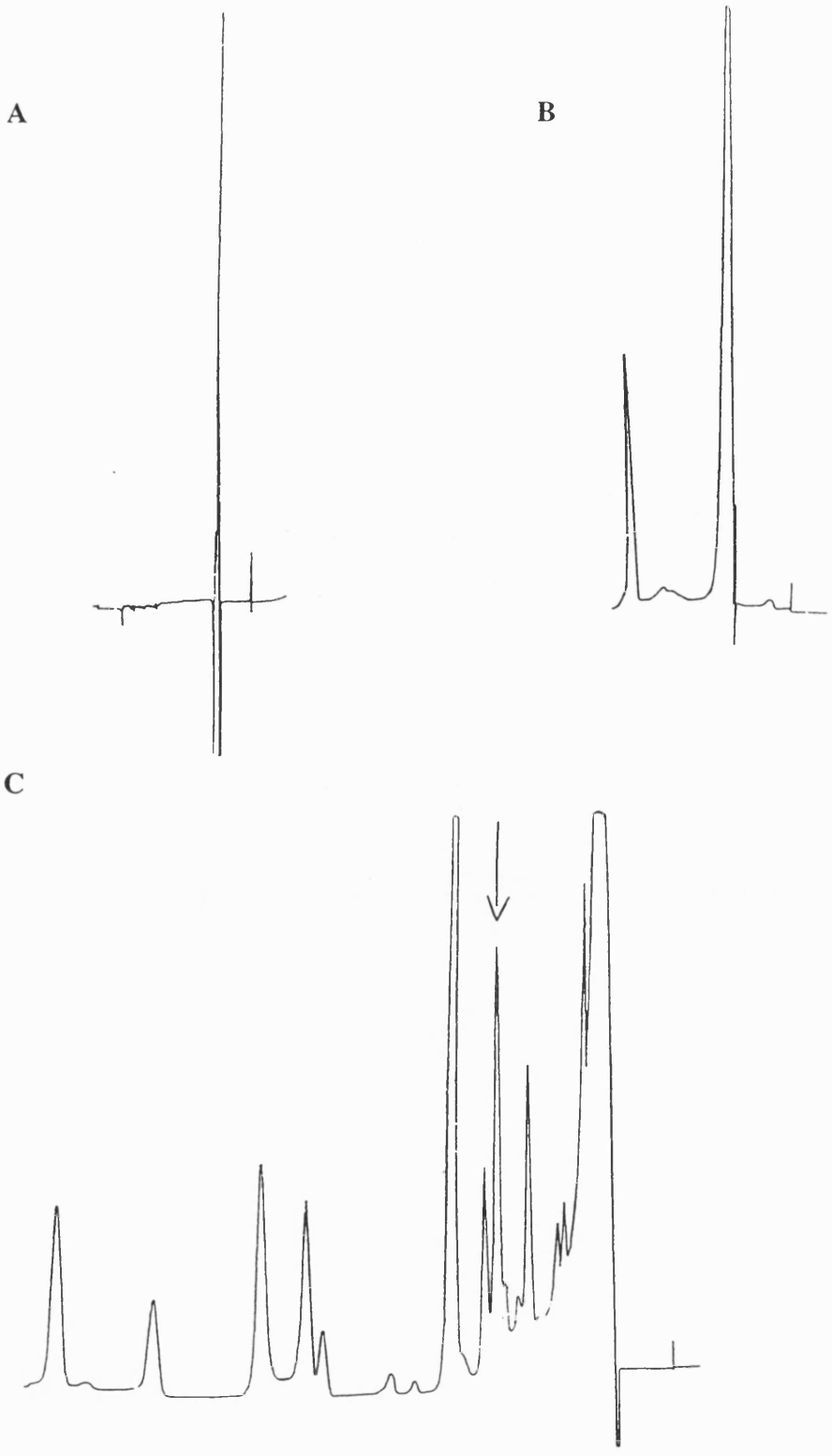

Figure 2.5. Typical HPLC traces for the separation of glutamate in dialysate samples as displayed by the chart recorder. (**A**) 1 pmol glutamate no derivatising agent (10 µl); (**B**) 1 pmol glutamate with derivatising agent (10 µl); (**C**) dialysate sample with derivatising agent (50 µl). Note the separation of the glutamate peak from the remaining components in the dialysate sample indicated by the arrow. Glutamate elution time 7.0 min; run time 25 min.

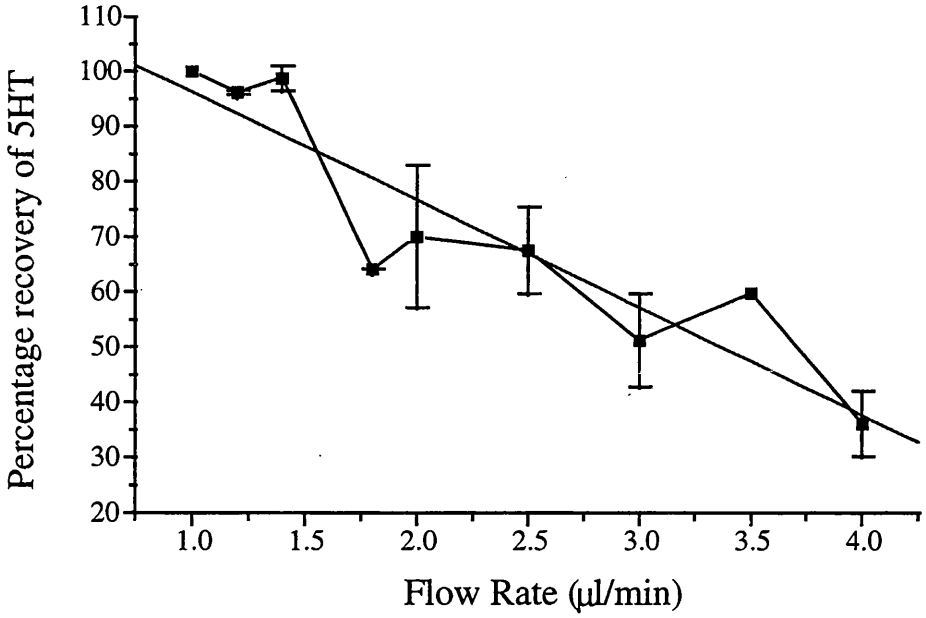

Figure 2.6. Effect of flow rate of perfusing aCSF on the amount of 5-HT collected from a typical dialysis probe, measured by *in vitro* recovery in a solution of 1 µM 5-HT. Flow rate (µl/min) is plotted versus the percent of recovered 5-HT relative to the amount recovered at 1µl/min i.e. amount of 5-HT recovered at a flow rate of 1 µl/min is equal to 100 % on the Y-axis. The line of best fit represents the linear regression (R = -0.917; n=3).

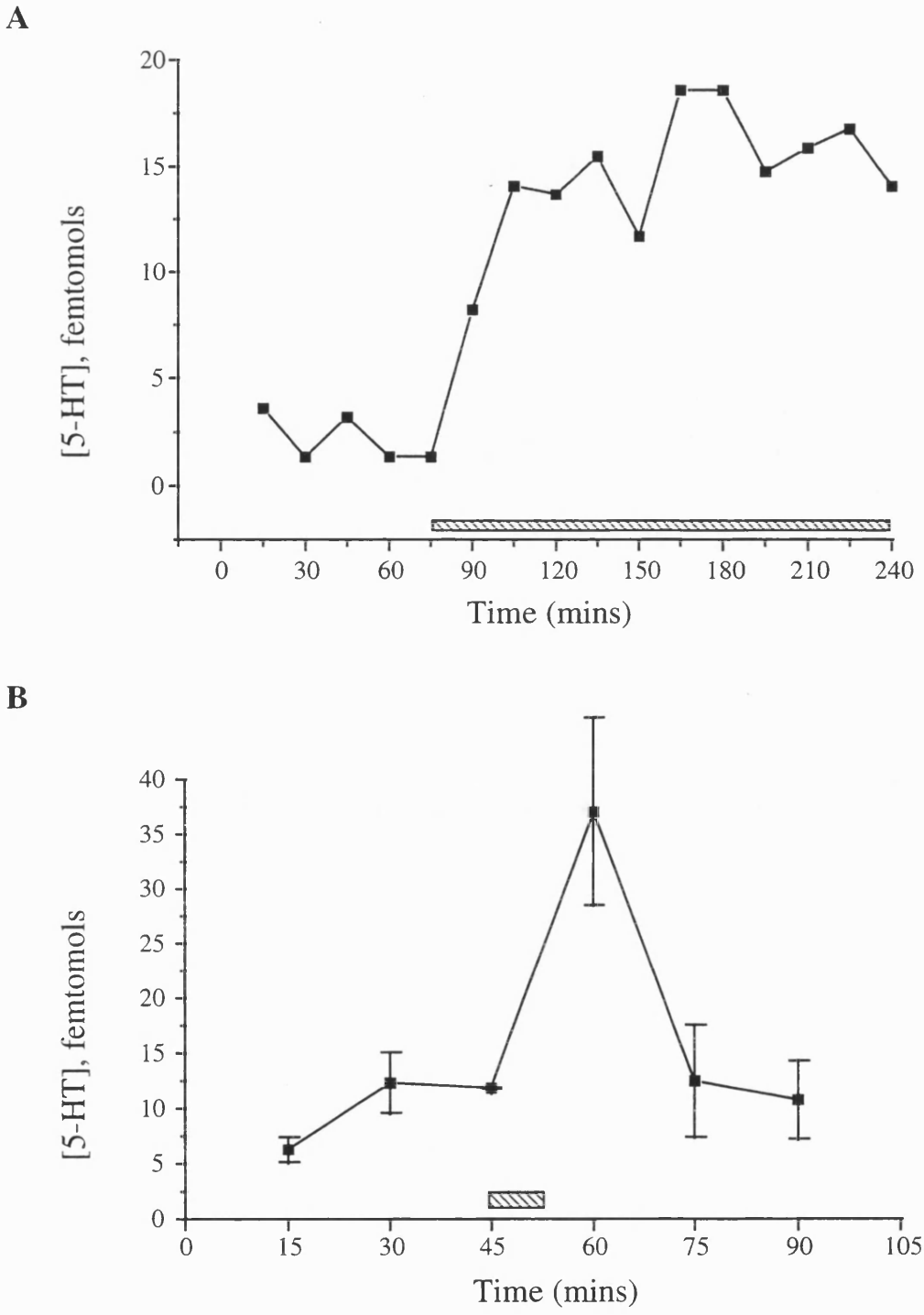

Figure 2.7. Parameters affecting 5-HT overflow as measured from the dialysate. **A:** Effect of addition of the SSRI citalopram (1 μM) to the perfusing aCSF, on 5-HT overflow from the SCN. An immediate increase in measurable 5-HT is observed during the period of citalopram inclusion, denoted by the hatched bar. **B:** Effect of handling the animal during the dialysate collection period (n=2). The animals were handled gently for a period of 5 min, denoted by the hatched bar. An immediate increase in dialysate 5-HT concentration in the raphe was observed.

CHAPTER 3

THE FUNCTION OF THE TERMINAL 5-HT_{1B} AUTO- AND HETERO- RECEPTORS IN THE SCN

3.1 INTRODUCTION

Diurnal variation in brain serotonin concentration first became evident after mouse brains were removed at various time points during the day and night, crushed, and the extract analysed spectrophotometrically for 5-HT. At four hourly intervals measurements of total brain 5-HT levels were obtained, with a peak demonstrated during the light phase at ZT 6, and a nadir at the end of the light phase at ZT 11 (Albrecht et al., 1956). This study was unsophisticated compared to what is possible today, and examined whole brain 5-HT content rather than individual brain regions; nonetheless, the authors did recognise that "drastic changes in certain parts of the brain, like the hypothalamus, may be obscured if other parts of the brain do not vary at the same time and in the same direction". It was not until 1968 that rhythms in 5-HT content were identified in hypothalamic tissue in rats over 24 hours (Quay, 1968). 5-HT levels peaked in hypothalamic tissue during the mid- to end-light period, and were low during the hours of darkness.

Since this time, many investigators have identified rhythms in 5-HT concentration in hypothalamic tissue with higher tissue levels being associated with the light phase (Ferraro and Steger, 1990; Cagampang and Inouye, 1994). The amplitude of the rhythm has been shown to be greatest in the SCN (Martin and Marsden, 1985). This rhythm in 5-HT levels is thought to be generated by an endogenous pacemaker, but influenced by the photic cycle (Cagampang and Inouye, 1994).

Many factors may contribute to the circadian rhythm in serotonergic neuronal level including the activity of the rate limiting enzyme tryptophan-5-hydroxylase or the 5-HT breakdown enzyme monoamine oxidase, the availability of the 5-HT precursor tryptophan and the neuronal uptake of tryptophan. A review of each of these processes is beyond the scope of this thesis but the interested reader is directed to a recent review by Martin and Redfern (1997).

It is now well established that the synthesis and release of 5-HT is influenced by inhibitory autoreceptors. Somatodendritic autoreceptors have been identified as 5-HT_{1A} autoreceptors, stimulation of which reduces firing of serotonergic neurones (Sprouse and Aghajanian, 1987) and predictably results in a reduction of terminal 5-HT release.

Terminal autoreceptors in the rat are classed as 5-HT_{1B} receptors (Engel *et al.*, 1986; Limberger *et al.*, 1991; Trillat *et al.*, 1997) and are negatively coupled to adenylate cyclase (Bouhelal *et al.*, 1988). Stimulation of these receptors reduces terminal 5-HT release, and 5-HT_{1B} receptor binding sites have been identified in high densities in rodent SCN (Pickard *et al.*, 1996). It is possible that a variation in the function of the 5-HT_{1B} autoreceptor contributes to variation in 5-HT synthesis and release, thereby indirectly influencing clock mechanisms within the SCN. In addition to regulating 5-HT release, 5-HT_{1B} receptors can act as presynaptic heteroceptors regulating the release of transmitters other than 5-HT for example acetylcholine (Bolanos-Jimenez *et al.*, 1995; Maura and Raiteri, 1986) and dopamine (Hallbus *et al.*, 1997). Included in the high density of 5-HT_{1B} binding sites recorded in the SCN are 5-HT_{1B} heteroceptors on retinal afferents (Pickard *et al.*, 1996). Bilateral orbital enucleation decreases the density of 5-HT_{1B} binding sites, indicative of a retinal terminal location. These heteroceptors are thought to play a key role in modulating retinal transmission to the SCN as systemic or local administration of a 5-HT_{1B} agonist can inhibit light induced phase shifts and decrease light induced Fos expression in the mouse SCN (Pickard *et al.*, 1996; Pickard and Rea, 1997).

The aim of this Chapter was to firstly perform pharmacological controls to establish that the measured 5-HT/Glutamate in the dialysate was of neuronal origin and secondly to examine the function of the terminal 5-HT_{1B} auto- and hetero- receptors in the SCN and compare the function of the 5-HT_{1B} autoreceptor in the SCN with that present in the hippocampus. I therefore investigated the function of the terminal 5-HT_{1B} autoreceptor using the 5-$HT_{1A/1B}$ agonist RU24969 which has high affinity for the 5-HT_{1B} receptor. Experiments were performed at six time points over the 12:12 hour light:dark cycle in the SCN region of the conscious rat using *in vivo* microdialysis in order to determine whether there was any diurnal variation in the function of the receptor. In a comparative study, the function of the 5-HT_{1B} autoreceptor was examined at mid-light versus mid-dark in another serotonergic rich area, the hippocampus (Moore and Halaris, 1975). The function of the 5-HT_{1B} heteroreceptor in the SCN was also investigated using RU24969 at mid-light versus mid-dark.

3.2 PROTOCOL

3.2.1 Animals

Male Wistar rats (University of Bath strain; 260-320 g) were maintained under a 12:12 light:dark cycle regime (lights on 07:00 "normal" light:dark cycle; lights on 19:00 "reverse" light:dark cycle; temperature 22 ± 2°C). The animals were housed in groups of six prior to experimentation, with food and water available *ad libitum*.

3.2.2 Microdialysis

1) The 5-HT_{1B} autoreceptor

Each animal was implanted with a microdialysis probe as described in the preceding chapter section 2.3.3, directed at either the SCN or the hippocampus, and introduced to the experimental cage. The probe was continuously perfused with aCSF (1.2 µl/min) containing 1 µM of the SSRI citalopram. Six 15 min control samples were collected, and the three samples immediately before drug infusion served as pre-intervention controls. Drugs were infused via the probe and dialysate samples were collected every 15 min over a period of 3 hours post-drug infusion. Dialysate 5-HT content was analysed by HPLC-ED as described in Chapter 2 section 2.3.5.

2) The 5-HT_{1B} heteroceptor

The animals were implanted with a microdialysis probe directed at the SCN. The probe was continuously perfused with aCSF (1.2 µl/min) containing no citalopram. Two to four 10 min control samples were collected which served as pre-intervention control samples. Drugs were infused via the probe and dialysate samples collected over a 60 min experimental period. Dialysate glutamate concentration was analysed by HPLC-ED as described in Chapter 2 section 2.3.6.

Samples not analysed immediately were snap frozen and maintained on dry ice until analysis. At the end of the experiment the animal was killed by CO_2 asphyxiation and the brain removed and frozen onto dry ice. Slicing freehand with a sharp razor blade, the probe tract was clearly visible as a fine line through the brain tissue. With the aid of a stereotaxic atlas (Paxinos and Watson, 1982) the position of the probe tract within the hypothalamus and hippocampus was established. The animals whose probe tracts were not in the target area were discarded for analysis.

3.2.3 Drugs

RU24969 [5-Methoxy-3(1,2,3,6-tetrahydro-4-pyridinyl)-1H-indole] was provided by Roussel-Uclaf and citalopram hydrobromide by Lundbeck (Copenhagen-Valby). WAY100635 (N-[2-[4-(2-methoxyphenyl)-1-piperazinyl]ethyl]-N-(2-pyridinyl) cyclohexanecarboxamide trihydrochloride) was donated by P.J.Mitchell from the University of Bath.

3.2.4 Statistics

5-HT or glutamate concentration in the dialysate samples (uncorrected for probe recovery) were expressed as a percentage of the mean of the pre-intervention controls samples. The sampes collected immediately prior to drug infusion were averaged and each value and subsequent value was expressed as a percentage of this mean value. Values post-drug treatment were analysed by one-way analysis of variance (ANOVA) with repeated measures with Student Newman Keuls *post hoc* test to detect differences between pre-intervention controls samples. Basal 5-HT and glutamate concentration were expressed as fmol or pmol, respectively, and analysed by one way ANOVA with Tukeys *post hoc* test to detect differences between time points. $p < 0.05$ was considered statistically significant.

3.3 RESULTS

3.3.1 The 5-HT_{1B} autoreceptor

Basal 5-HT levels varied significantly across the light dark cycle. 5-HT concentration in SCN dialysate samples were 28.7 ± 2.89, 32.7 ± 7.05, 41.7 ± 5.18, 17.6 ± 3.90, 20.4 ± 4.03 and 15.7 ± 1.56 mean ± s.e.m. fmol for zeitgeber times 3, 6, 9, 15, 18 and 21 respectively (figure 3.1). As a general trend, the 5-HT in the SCN dialysate during the light phase was higher than that collected during the dark phase. Highest levels were measured at ZT 9, and the levels at ZT 15, 18 and 21 were significantly lower than those at ZT 9 ($p < 0.05$). In the absence of drug infusion the 5-HT overflow from the SCN did not vary significantly over the three hour collection period at any of the six time points.

3.3.1.1 Pharmacological controls

Perfusion for 60 min with calcium free aCSF resulted in an immediate and significant decrease in 5-HT overflow, with a maximal decrease of 93.0 ± 3.67 % ($p < 0.001$). Upon reperfusion with aCSF containing calcium ions, 5-HT overflow began to increase, but remained significantly lower than pre-intervention controls 45 min after reperfusion (figure 3.2A). Modified aCSF containing 100 mM KCl was perfused for 60 min, causing an immediate and significant increase in 5-HT overflow. Maximal increase was 349 ± 80.8 % ($p < 0.01$). After reperfusion with normal aCSF, 5-HT levels returned to basal (figure 3.2B).

3.3.1.2 Effect of local infusion of RU24969 into the SCN

The effect of stimulation of the 5-HT_{1B} autoreceptor with RU24969 (5-$HT_{1A/1B}$ agonist; 1μM; 15 min infusion) was dependant upon the zeitgeber time at which the drug was infused.

During the light phase, infusion of RU24969 at ZT 3 and 6 produced a significant and prolonged decrease in 5-HT overflow, reaching a maximal decrease of 30.6 ± 11.9 and 41.0 ± 11.7 % mean ± s.e.m. of baseline, respectively ($p < 0.01$; figure 3.3A and 3.3B). At ZT 9 infusion of RU24969 failed to produce any significant change in dialysate 5-HT concentration (figure 3.3C).

During the dark phase, infusion of RU24969 at ZT 15 produced a significant and prolonged decrease in SCN 5-HT, reaching a nadir of 56.1 ± 17.2 % of baseline ($p < 0.05$; figure 3.3D). At ZT 18, RU24969 infusion failed to significantly change dialysate 5-HT concentration (figure 3.3E). At ZT 21, RU24969 infusion produced a significant, but short lived, decrease in SCN 5-HT overflow, reaching a low of 54.3 ± 17.0 % of baseline ($p < 0.05$; figure 3.3F).

These findings are summarised in figure 3.4 which plots the maximal percentage decrease in dialysate 5-HT post-RU24969 infusion, against the zeitgeber time, and demonstrates the functional ability of the 5-HT_{1B} autoreceptor across the light dark cycle.

3.3.1.3 Effect of WAY100635 on the RU24969 infusion at ZT 6

In addition to stimulation at the 5-HT_{1B} receptor site, RU24969 also demonstrates affinity for the 5-HT_{1A} receptor. Therefore, to exclude the involvement of the 5-HT_{1A} receptor in the observed response, the tissue was pretreated with WAY100635, an antagonist specific for the 5-HT_{1A} receptor site at ZT 6. WAY100635 (1 μM) was infused for 15 min prior to and 15 min during RU24969 infusion. The ability of RU24969 to decrease dialysate 5-HT levels was not affected by the presence of WAY100635 (figure 3.5A). Therefore, it can be assumed that RU24969 is acting solely by stimulation of the 5-HT_{1B} receptor under these given circumstances. WAY100635 infusion alone did not significantly affect SCN 5-HT levels at ZT 6 (figure 3.5B).

3.3.1.4 Effect of a local infusion of RU24969 into the hippocampus at ZT 6 and 18

There was such a contrast between the ability of RU24969 to decrease dialysate 5-HT at ZT 6 (mid-light) versus ZT 18 (mid-dark) in the SCN, that it was decided to test another serotonin-rich brain area with RU24969 to establish whether this effect was SCN-specific. Hippocampal 5-HT levels pre-drug infusion were 54.4 ± 20.1 and 40.9 ± 15.3 fmol for ZT 6 and 18, respectively (mean ± s.e.m.). A 15 min infusion of RU24969 (1 μM) in the hippocampus at ZT 6 produced a significant decline in dialysate 5-HT, evident 60 min after the start of the infusion (maximal decrease 32.3 ± 15.0 % of baseline; $p < 0.01$; figure 3.6). At ZT 18 the reduction in dialysate 5-HT post-RU24969

infusion was less pronounced but reached statistical significance 60 min after the start of the infusion (maximal decrease 58.4 ± 9.63 % of baseline; $p < 0.01$).

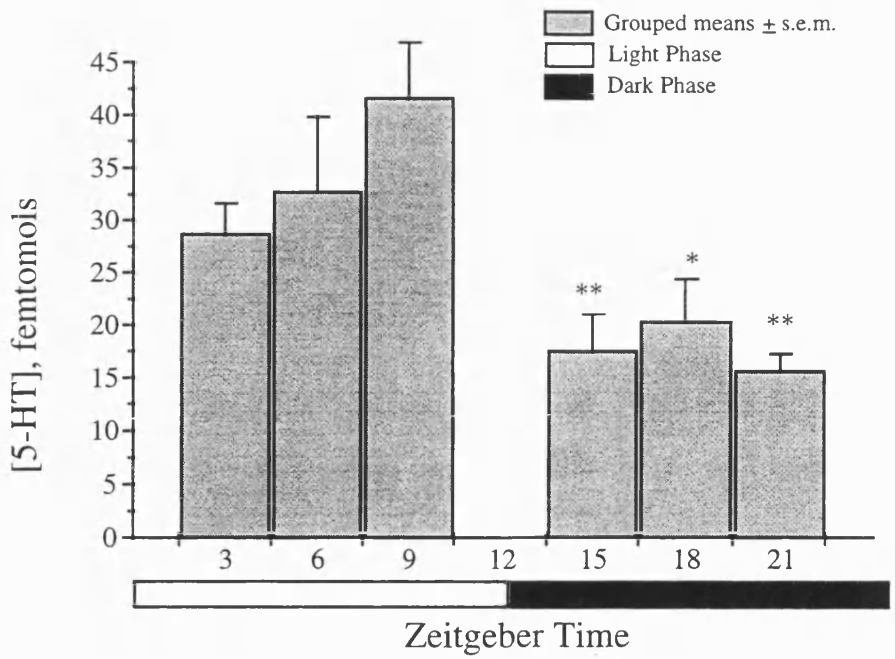

Figure 3.1. Basal 5-HT concentration as measured in SCN dialysate at six zeitgeber times across the 12:12 light:dark cycle. Data are expressed as mean ± s.e.m. (n = 4 - 8). Basal 5-HT levels at ZT 15, 18 and 21 are significantly different from basal levels measured at ZT 9. * $p < 0.05$; ** $p < 0.01$.

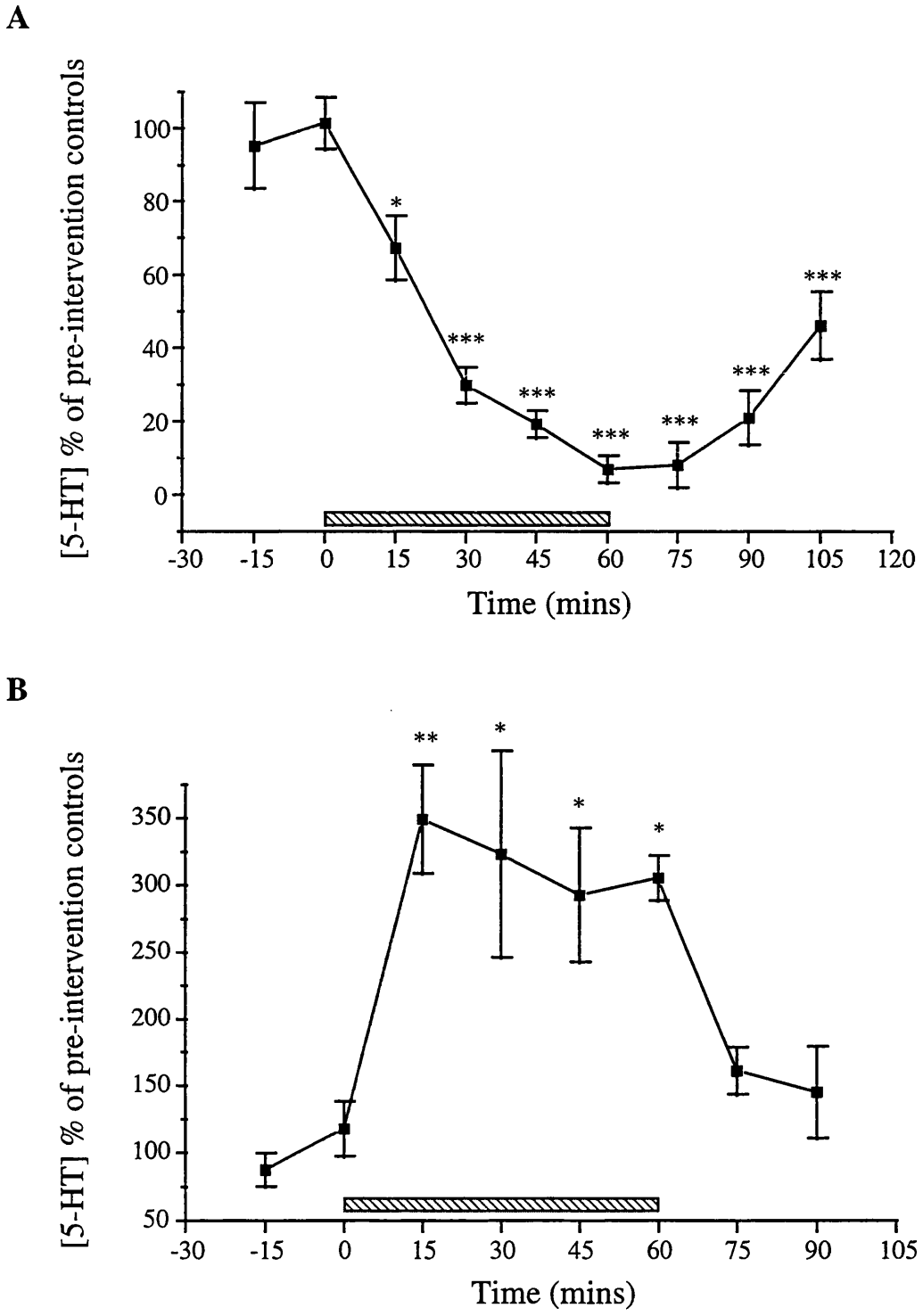

Figure 3.2. Effect of removal of calcium ions from (**A**) and increasing potassium ion concentration (100 mM) in (**B**) the perfusing aCSF on the 5-HT overflow from SCN dialysate. Calcium ions were removed from, or potassium ions were added to, the aCSF for a period of 60 min, denoted by the hatched bar. * $p<0.05$; ** $p<0.01$; *** $p<0.001$; n=3.

A

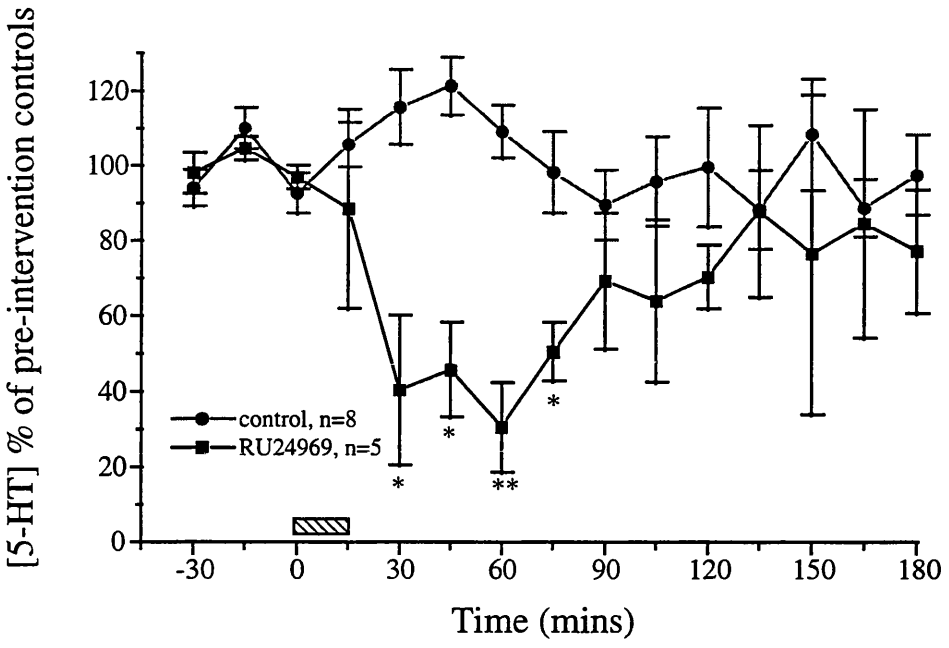

B

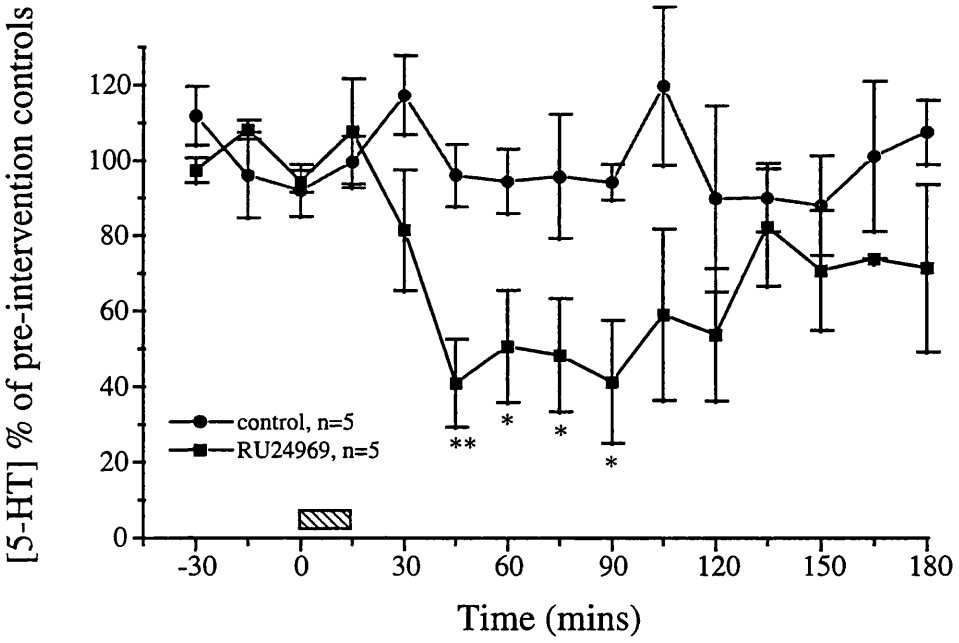

Figure 3.3 (A-F). Effect of RU24969 infusion (1 μM) on 5-HT overflow in the SCN at ZT 3 (**A**), 6 (**B**), 9 (**C**), 15 (**D**), 18 (**E**) and 21 (**F**). Values are mean ± s.e.m. expressed as a percentage of three pre-intervention control samples. RU24969 was infused for 15 min denoted by the hatched bar. * $p < 0.05$; ** $p < 0.01$.

C

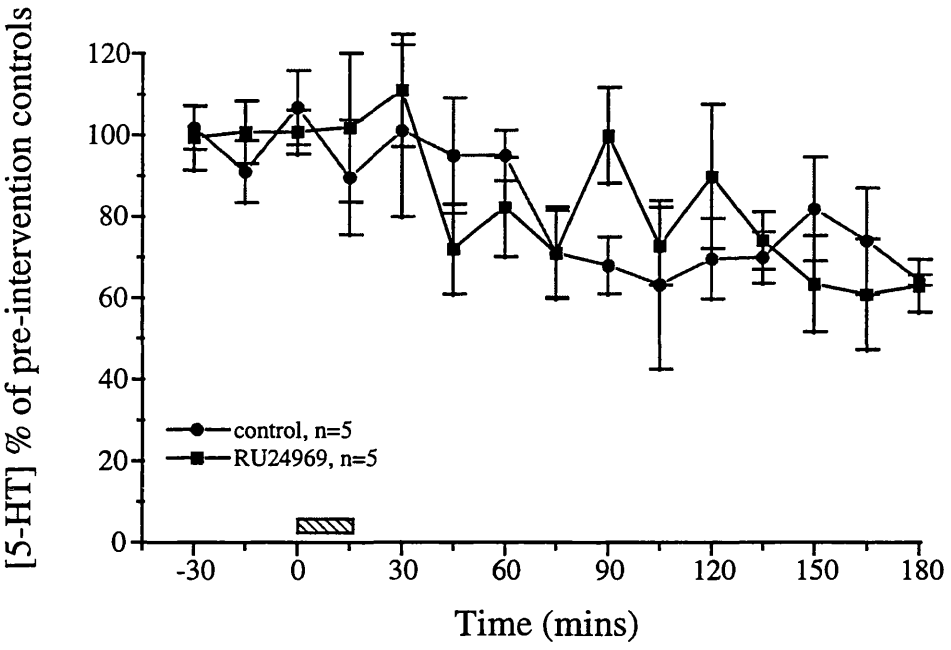

D

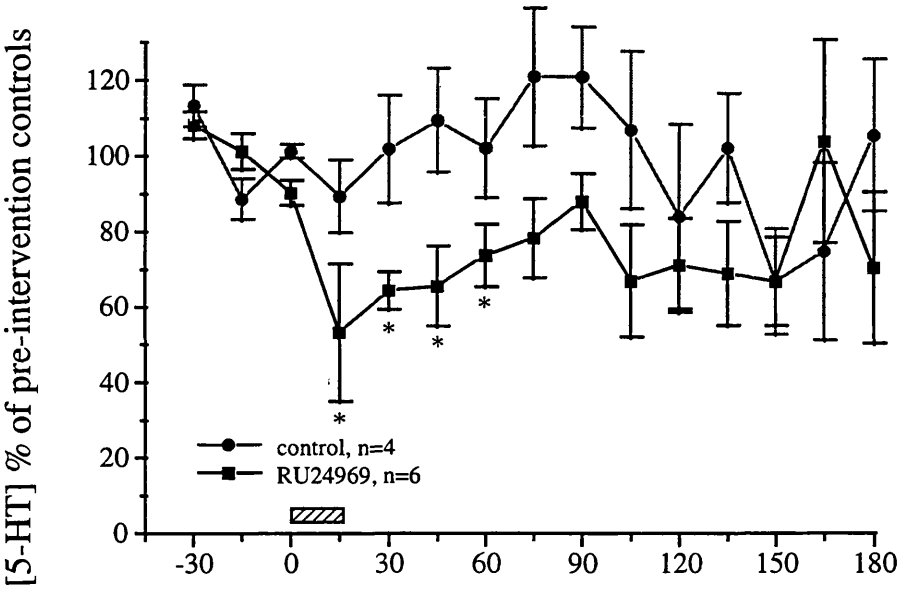

For figure legend see page 41

E

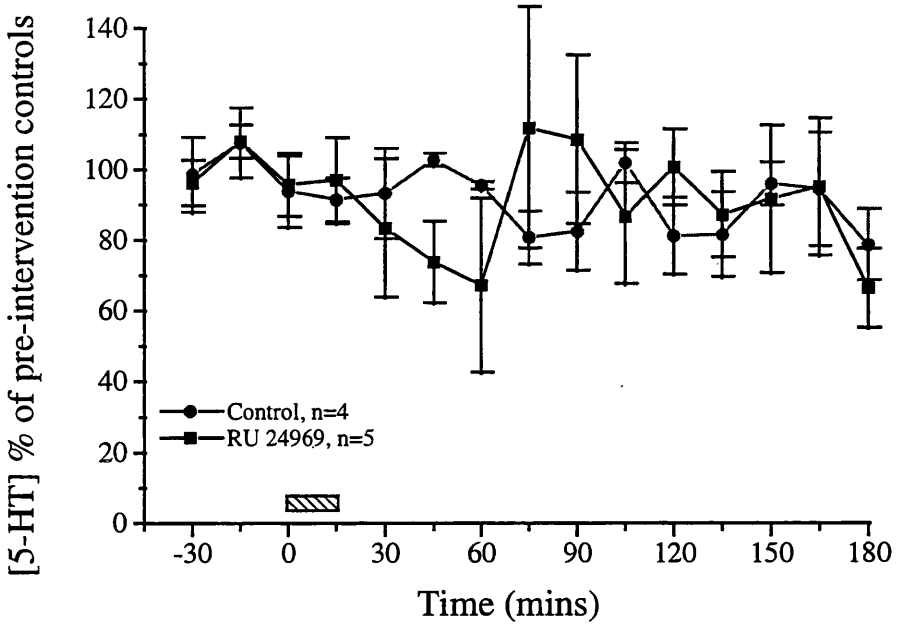

F

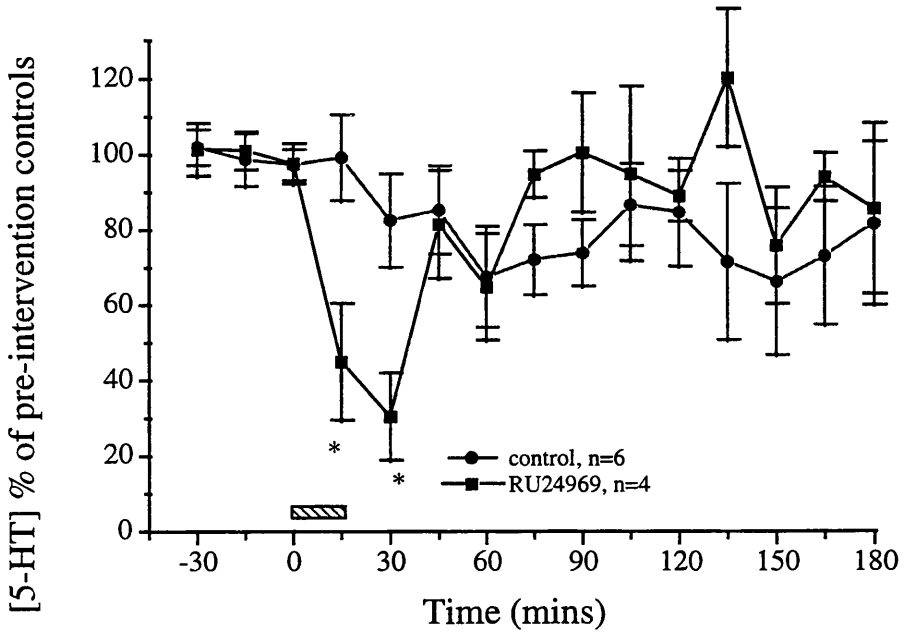

For figure legend see page 41

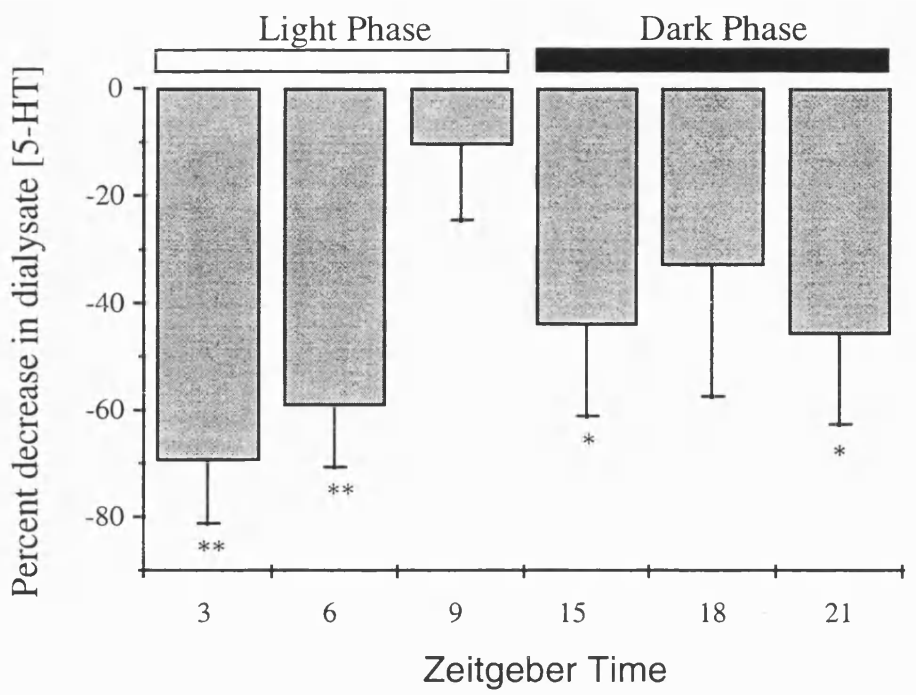

Figure 3.4. Percentage maximal decrease in 5-HT overflow following infusion of RU24969 (1 μM; 15 min) at zeitgeber times 3, 6, 9, 15, 18 and 21. * $p < 0.05$; ** $p < 0.01$. Maximal decrease in dialysate 5-HT concentration post-RU24969 infusion is plotted versus the zeitgeber time and represented as a negative percentage.

A

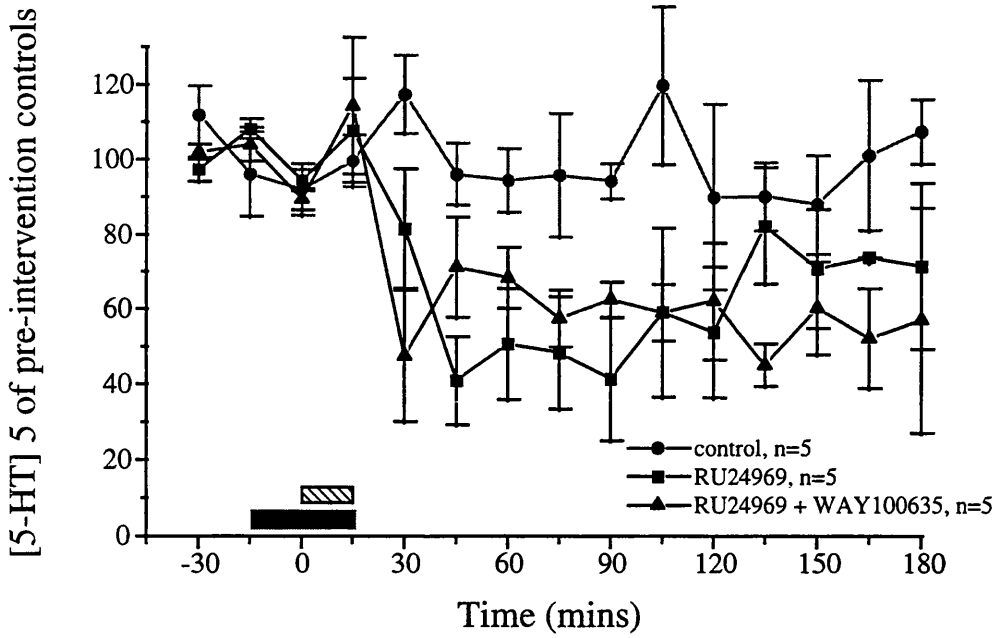

B

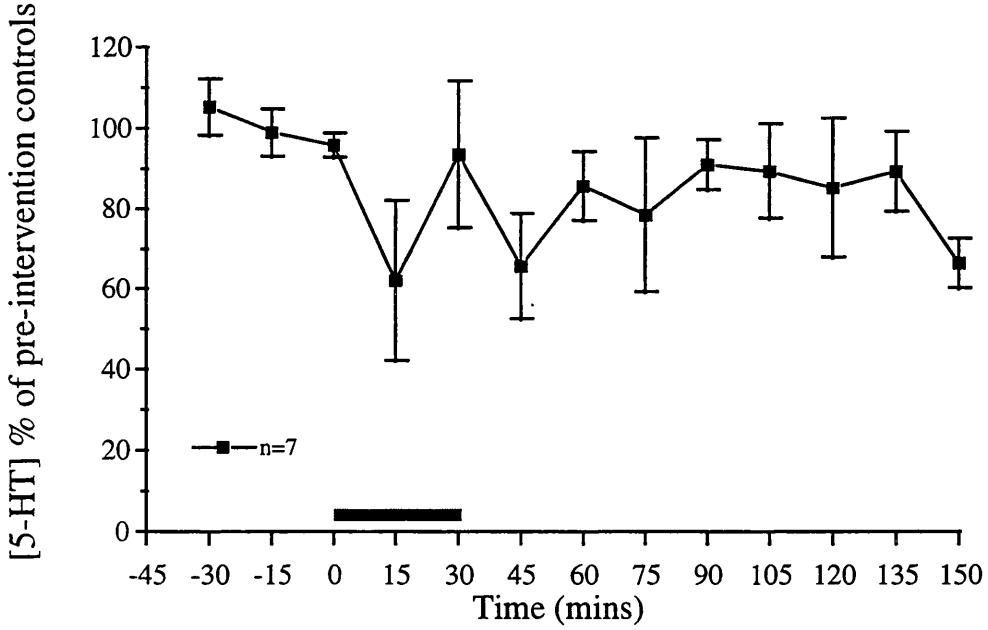

Figure 3.5. **A:** Effect of WAY100635 (1 μM) on the response to RU24969 (1 μM) on 5-HT overflow in the SCN at ZT 6. WAY100635 was infused 15 min prior to, and 15 min concurrently with RU24969. The solid bar denotes WAY100635 infusion, and the hatched bar the RU24969 infusion. Values are mean ± s.e.m. expressed as a percentage of three pre-intervention controls. **B:** Effect of WAY100635 (1 μM) alone on 5-HT overflow in the SCN at ZT 6.

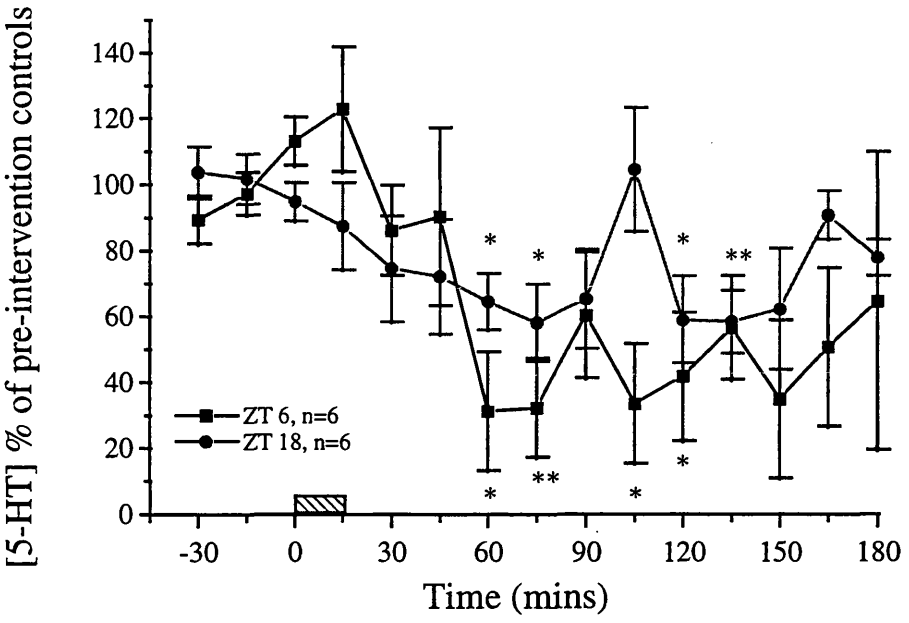

Figure 3.6. Effect of RU24969 infusion (1 μM) on hippocampal 5-HT overflow at ZT 6 and 18. Values are mean ± s.e.m. expressed as a percentage of three pre-intervention control samples. RU24969 was infused for 15 min denoted by the hatched bar. * $p < 0.05$; ** $p < 0.01$.

3.3.2 The 5-HT_{1B} heteroceptor

Basal glutamate overflow from the SCN differed at the two zeitgeber times tested. Higher levels were measured at ZT 18 versus ZT 6, being 1.82 ± 0.51 and 0.463 ± 0.21 picomols respectively ($p<0.05$).

3.3.2.1 Pharmacological controls

Modified aCSF containing 100 mM KCl was perfused via the probe for 30 min, producing a significant increase in glutamate overflow. Maximal increase was 338 ± 116 % of baseline ($p < 0.05$) occurring 30 min after the start of the infusion (figure 3.7A). Perfusion for 30 min with the voltage-dependant calcium channel blocker nickel chloride (NiCl; 2 mM), significantly decreased glutamate overflow from the SCN. Thirty min after the start of the infusion dialysate glutamate concentration dropped to 15.2 ± 5.39 % of baseline ($p < 0.05$; figure 3.7B).

3.3.2.2 Effect of local infusion of RU24969 into the SCN

A 15 min infusion of RU24969 (1 μM) into the SCN significantly decreased glutamate overflow in the dialysate samples at ZT 6 and ZT 18. The effect was more pronounced at ZT 6, reaching a nadir of 40.8 ± 12.5 % of baseline within 20 min of the start of the infusion ($p < 0.05$; figure 3.8A). At ZT 18, RU24969 infusion did result in a significant decrease in SCN glutamate to a level 37.9 ± 18.3 % of baseline, but not until 50 min after the start of the infusion (figure 3.8B)

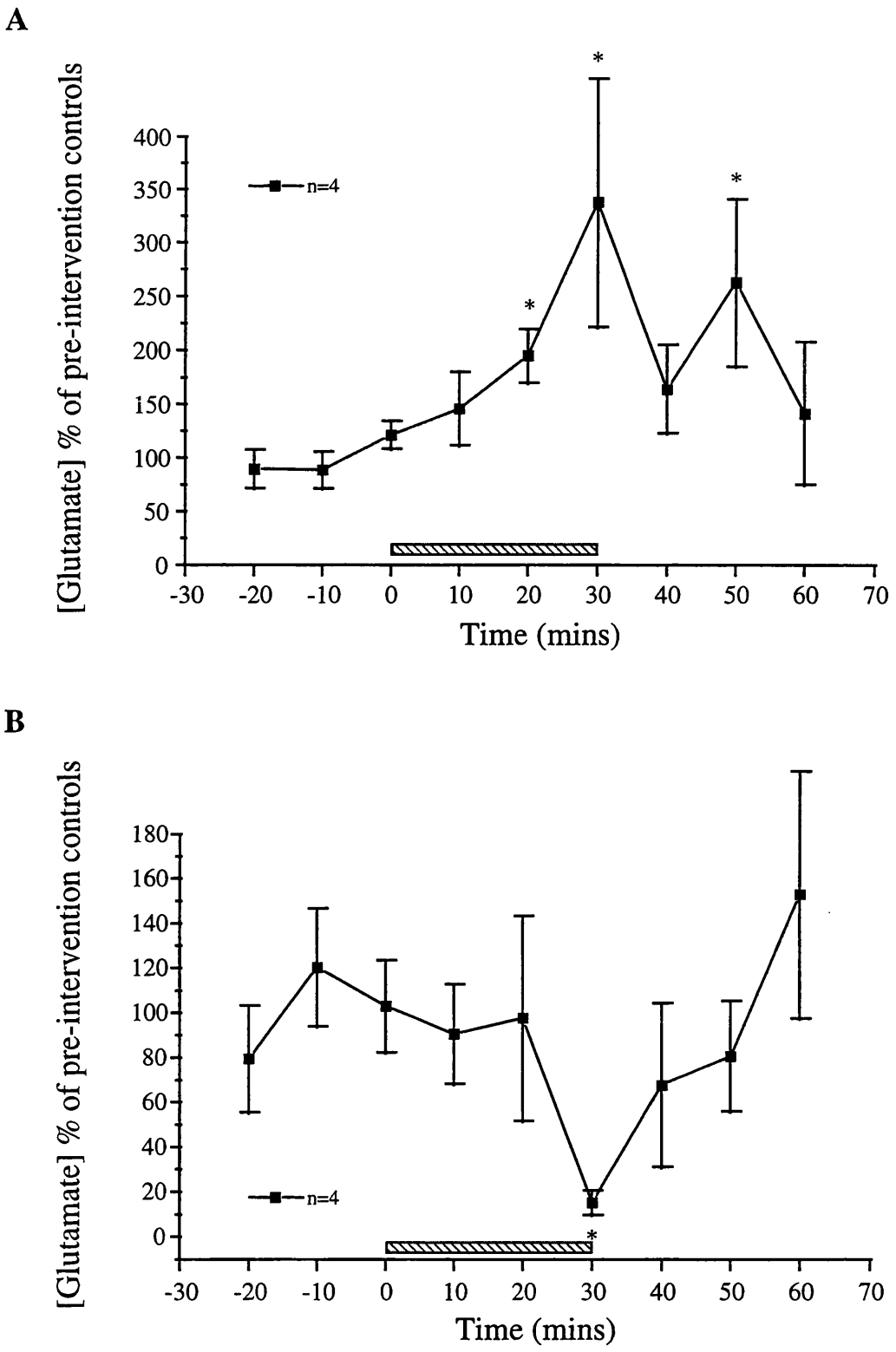

Figure 3.7. Effect of increasing potassium ion concentration (100 mM KCl; **A**) and including the voltage dependant calcium channel blocker, nickel chloride (NiCl; 2 mM; **B**) in the perfusing aCSF on the glutamate overflow from SCN dialysate. Potassium ions or NiCl was added to the aCSF for a period of 30 min, denoted by the hatched bar. * $p < 0.05$.

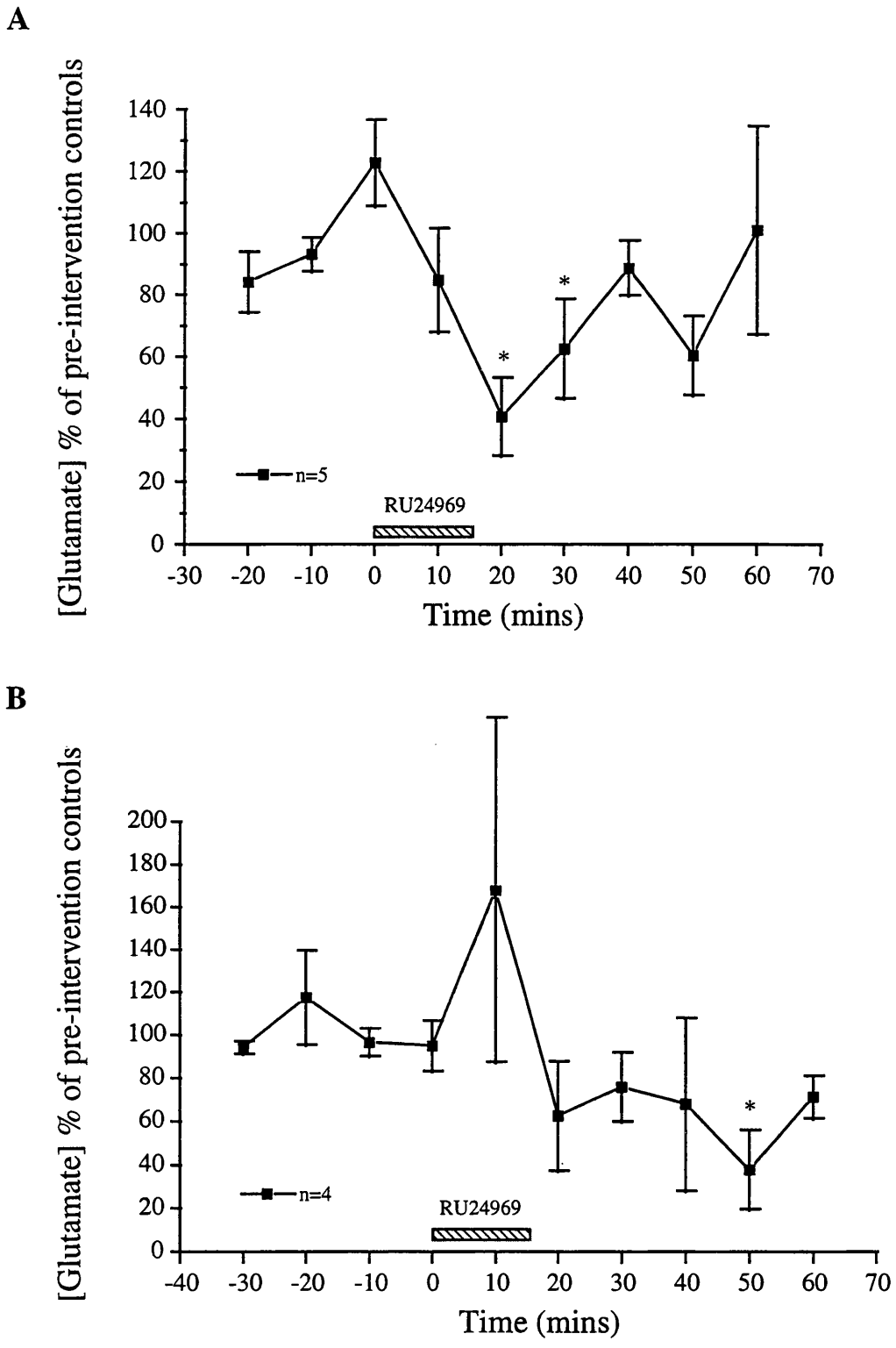

Figure 3.8. Effect of RU24969 (1 μM) on glutamate overflow in the SCN at ZT 6 (**A**) and ZT 18 (**B**). Results are mean ± s.e.m. values expressed as a percentage of pre-intervention controls. RU24969 was infused into the SCN via the dialysis probe for 15 min as indicated by the hatched bar.

3.4 DISCUSSION

3.4.1 The 5-HT_{1B} autoreceptor

Basal 5-HT levels from the SCN region showed a very distinct diurnal variation, with maximal levels being recorded at ZT 9, towards the end of the light period, and the lowest levels recorded through the dark period. This diurnal variation is very similar to results presented in a review by Martin and Marsden (1984) as unpublished data from their laboratories. They also obtained peak 5-HT levels from the microdialysate samples of the SCN after mid-light, with the levels declining toward the dark phase, and during the dark phase. A few laboratories have measured the output of the 5-HT metabolite 5-hydroxyindole acetic acid (5-HIAA) by *in vivo* voltametry or microdialysis across the light dark cycle. 5-HIAA is elevated during the hours of darkness and reaches a nadir during the light phase (Faradji *et al.*, 1983; ; Ramirez *et al.*, 1987; Glass *et al.*, 1992), and is closely correlated with an increase in locomotor activity. This rhythm in 5-HIAA exactly mirrors the rhythm for 5-HT I observed here. Glass and his coworkers (1992) account for the nocturnal rise in 5-HIAA by an increased metabolism and release of 5-HT, because local application to the SCN of the sodium channel blocker tetrodotoxin significantly reduced microdialysate concentrations of 5-HIAA during the dark phase whilst having no effect during the light phase. Also, addition of 5-HT to the perfusate significantly enhanced 5-HIAA levels, indicating that increased extracellular serotonin may be reflected by increased 5-HIAA concentrations, presumably due to additional metabolic breakdown of the 5-HT. From these experiments one might asssume that the higher rate of conversion of 5-HT to 5-HIAA during the dark phase indicates that the clearance of 5-HT is enhanced at night. If clearance is enhanced at night one might expect extracellular 5-HT measured in dialysate samples to be low, which is what I observed.

The firing of raphe serotonergic neurones correlates with the state of arousal of the animal. Raphe firing is low during sleep and periods of inactivity, and high during periods of activity. Therefore, terminal 5-HT release would be expected to be low during the light phase and high during the dark phase of a nocturnal animal. This however does not match the extracellular concentrations measured by microdialysis. As already suggested, however, clearance rates of 5-HT are higher during the dark, and it may be that during this phase greater release of 5-HT from serotonergic neurones is

more than compensated by greater neuronal reuptake and/or more rapid breakdown. Indeed the uptake of tritiated 5-HT into SCN slices shows a diurnal variation with the highest levels recorded at the start of the dark phase (Meyer and Quay, 1976) and imipramine labelling of the 5-HT presynaptic reuptake site is highest at end dark (Wirz-Justice *et al.*, 1983). It must be borne in mind, however, that the perfusion media contained the reuptake blocker citalopram, and so variation in dialysate 5-HT observed here cannot easily be attributable to alterations in the capacity of the neurones to take up 5-HT. The diurnal variation in measured 5-HT from the dialysate samples of the SCN is therefore most likely to be due to increased breakdown of 5-HT during the dark phase (supported by findings of high nocturnal 5-HIAA levels).

It was important to establish the origin of the 5-HT in the dialysate. Exocytotic release of neurotransmitter is considered to be a calcium dependent process and removal of calcium ions from the perfusion fluid resulted in an immediate and significant decrease in dialysate 5-HT. Conversely, increasing the concentration of potassium ions in the perfusing aCSF will lead to depolarisation of the nerve membrane and concomitant release of neurotransmitter similar to that seen when an action potential travels down the nerve. Indeed, infusion of 100 mM KCl led to an immediate and significant increase in 5-HT overflow. Two essential criteria for establishing a neuronal origin of the 5-HT present in the dialysate have thus been fulfilled. This is in agreement with other authors who have dialysed the hypothalamus and measured 5-HT levels (Auerbach *et al.*, 1989).

RU24969 has been shown previously to be an agonist at 5-HT_{1B} autoreceptors regulating 5-HT release in the hippocampus (Sharp et al., 1989; Martin *et al.*, 1992), the frontal cortex (Middlemiss, 1985) and the amygdala (Bosker et al., 1997). Unfortunately RU24969 has been shown to act as a 5-HT reuptake blocker in the absence of a reuptake blocker in the perfusing aCSF (Auerbach *et al.*, 1991; Hjorth and Tao, 1991). However, in the presence of citalopram, RU24969 was shown to act as an agonist at the 5-HT_{1B} autoreceptor. Thus, in the given experimental conditions, RU24969 is expected to act soley as an agonist. Although RU24969 is an agonist at 5-HT_{1B} receptors (Sills et al, 1984) it does have an affinity for the 5-HT_{1A} receptor. It was thus important to establish whether the RU24969 was acting via its actions on the 5-HT_{1A} or 5-HT_{1B} receptor. Simultaneous infusion of RU24969 and the 5-HT_{1A} receptor antagonist WAY100635 at ZT 6 did not alter the profile of inhibition by RU24969 alone

(figure 3.4), and we may assume that under the given experimental conditions, RU24969 was acting by activation of 5-HT_{1B} receptors. There was no apparent tonic influence of 5-HT_{1A} receptors in the SCN, demonstrated by the absence of response to infusion of WAY100635 alone. A previous report by Sayer (1994) failed to demonstrate any significant effects on 5-HT overflow in the SCN following infusion of the 5-HT_{1A} receptor agonist 8-OH-DPAT into the SCN at mid-light, thereby confirming that local stimulation of the 5-HT_{1A} receptor does not alter local 5-HToverflow.

The effect of 5-HT_{1B} receptor stimulation by RU24969 on 5-HT overflow from the SCN was strikingly dependent upon the zeitgeber time at which the drug was applied. During the early- and mid-light phase (ZTs 3 and 6) and the early-dark phase (ZT 15) RU24969 produced a significant and prolonged decrease in dialysate 5-HT levels. Towards the end of the dark period (ZT 21) the response to RU24969 was to produce a significant, but short acting reduction in dialysate 5-HT levels. Surprising RU24969 produced no effect on dialyate 5-HT levels towards the end of the light period (ZT 9) or at the mid-dark phase (ZT 18). During the dark phase, when RU24969 elicited a decrease in 5-HT overflow, it did so to a lesser degree than when RU24969 decreased 5-HT overflow during the light phase (figure 3.3). Previous *in vivo* studies that have investigated the function of the terminal 5-HT_{1B} autoreceptor have done so only at a single time point during either the light or dark phase. Rollema and coworkers (1996) investigated guinea pig hypothalamic 5-HT release with the 5-HT_{1D} agonist CP-135807 (the guinea pig terminal autoreceptor is of the 5-HT_{1D} subtype; Limberger *et al.*, 1991). CP-135807 dose-dependently reduced 5-HT overflow, and at a concentration of 1 μM decreased 5-HT levels to 30 % of basal, which is comparable to the results presented here for ZT 3 and ZT 6.

Acute stress has been shown to affect 5-HT_{1B} autoreceptor function (Bolanos-Jimenez *et al.*, 1995). During the light phase a 40 min restraint stress significantly reduced the efficacy of the 5-HT_{1B} receptor agonist CP93129 in decreasing potassium evoked tritiated 5-HT release in a synaptosome preparation. However, in my experiments all animals were prepared in the same manner and all experiments were performed under the same conditions. Additionally, the use of the round experimental cages equipped with a liquid swivvel ensured no contact with the animal (see Chapter 2 section 2.3.4). The variation in receptor function is not likely to be explained by stress of the animals.

This diurnal variation in 5-HT_{1B} autoreceptor function in the rat in response to RU24969 stimulation has not been reported before. However, a study by Martin and coworkers (1987) did suggest that the behavioural response to RU24969 in the mouse exhibited a circadian variation. The effects of RU24969 on locomotor activity was examined at different time points during the light dark cycle. The ability of the drug to induce locomotor activity did not vary across the light dark cycle, but the ability of the antagonist metergoline to antagonise the response varied at ZT 8 versus ZT 17. The antagonist was 3-5 fold more effective at blocking the response to RU24969 at ZT 8 than at ZT 18 (i.e. just after mid-light versus mid -dark). Although the authors were incorrect in stating that the behavioural response to 5-HT_{1B} receptor stimulation exhibited a *circadian* variation, it did appear to exhibit a *diurnal* variation; the degree of pre- and postsynaptic receptor contribution is unknown. Another behavioural study performed by Moser and Redfern (1984) set out to examine the activity of 5-HT receptors over 24 hours by administration of a mixed 5-HT receptor agonist, 5-methoxy-N,N-dimethyltryptamine, with a slightly higher affinity for the 5-HT_2 class of receptor. There was a clear diurnal variation in head twitch responses with peak activity occurring at mid-light. Although they postulated the effect to be attributable to *post*synaptic receptor stimulation it does reflect a diurnal rhythm in central 5-HT receptor function. Because the agonist used in their studies had affinity for receptor subtypes other than the 5-HT_2 receptor, it is possible that the observed affect on rat behaviour was due to the stimulation of the 5-HT_1 receptor class. This effect is unlikely to be attributable to 5-HT_{1A} receptors as extensive behavioural studies carried out by Lu and Nagayama (1996; Nagayama and Lu, 1997) administering the 5-HT_{1A} agonist 8-OH-DPAT, measured peak responses at mid-dark with a nadir at mid-light. These experiments by Moser and Redfern (1984) may thus be attributable to 5-HT_{1B} receptor stimulation considering the peak locomotor response was during the mid-light phase.

Subsequent *in vitro* studies have failed to identify variation in the function of the terminal 5-HT_{1B} receptor. Singh and Redfern (1994a) failed to demonstrate a circadian variation in the function of rat terminal 5-HT_{1B} autoreceptors even though they sampled at four equally spaced time points across the light dark cycle. However, these authors (1) sampled from hippocampus and cortex and not the hypothalamus where the SCN is situated (2) used an *in vitro* superfusion preparation, which whilst giving an indication

as to the mechanisms of neuronal release, cannot get as full a picture as those experiments performed *in vivo* and (3) they based their assumptions on the ability of methiothepin (a putative autoreceptor antagonist) to antagonise the inhibition by 5-HT, rather than seeing the effect of 5-HT_{1B} agonist stimulation. The results reported from these *in vivo* microdialysis experiments in the freely moving animal can be assumed to provide a more accurate reflection of autoreceptor function. In another *in vitro* study the ability of RU24969 to decrease stimulation-induced release of tritiated 5-HT from preloaded rat hypothalamic slices was similar in slices obtained from the light phase and the dark phase (Blier *et al*., 1989). These experiments were carried out only at two time points over the light dark cycle, and not at a fixed zeitgeber time, as in our experiments. It is thus possible that Blier and collaborators (1989) have sampled tissues in the dark phase either side of the mid-dark period, in which case they would indeed observe decreases in 5-HT overflow. The results from the data presented in this chapter therefore highlight the importance of stating the zeitgeber time in reports and sampling (*in vivo*) or collecting samples (*in vitro*) at equally spaced time points.

Many possibilities exist as to why there is a variation in 5-HT_{1B} receptor function including differential expression of receptor message over the light:dark cycle, 5-HT_{1B} receptor occupation by endogenous agonists, changes in the density of the 5-HT_{1B} autoreceptors in the nuclei, differential second messenger systems and receptor phosphorylation or internalisation. Messenger RNA (mRNA) for the 5-HT_{1B} receptors has been shown not to vary at two equally spaced time points across the light:dark cycle (Roca *et al.*, 1993). However these experiments examined SCN tissue from rats held in constant darkness, and so although there was no circadian variation, there may be a diurnal variation. Even so, one must bear in mind that mRNA expression within the SCN will measure receptor expression in the cell body relating to postsynaptic receptors, and will not measure the presynaptic autoreceptor as examined in these microdialysis experiments.

If the function of the 5-HT_{1B} autoreceptor varied in accordance with basal 5-HT levels then the reduced efficacy of the 5-HT_{1B} agonist to inhibit the release of 5-HT might result from the competition at 5-HT_{1B} receptors with the endogenous 5-HT released. During the dark phase when the basal 5-HT levels are low the autoreceptor function appears to be reduced because at ZT 18 there is no effect of 5-HT_{1B} autoreceptor

stimulation and at ZTs 15 and 18 the maximal decrease in 5-HT overflow following RU24969 infusion is only approximately 50 %, whereas at ZTs 3 and 6 maximal reduction is between 60 and 70 % of basal. This unfortunately does not account for why there is an apparent absence of 5-HT_{1B} autoreceptor function at ZT 9 when the basal 5-HT levels are at their peak. It may be that high extracellular 5-HT levels down regulate the receptor in response to being continually activated, although it is an anomaly why this would happen specifically at this time point.

5-HT_{1B} receptor binding has been shown in one study to be significantly higher during the dark phase than during the light phase (Prosser *et al.*, 1993). Unfortunately this does not correlate with our findings in which the response is absent at mid-dark. It may be that at mid-dark the receptor occupation by endogenous ligand is at its highest and therefore exogenously applied agonist cannot displace the natural ligand to exert its effect. If occupation of the 5-HT_{1B} receptor by endogenous 5-HT is higher during the dark phase, this may explain why extracellular 5-HT levels are lower during the dark. It is importanat to remember that the 5-HT concentration detected in the microdialysate is only a reflection of extracellular 5-HT and not synaptic 5-HT concentration.

5-HT_{1B} receptors are negatively coupled to adenylate cyclase (Bouhelal *et al.*, 1988), stimulatation of which will lead to changes in intracellular levels of cAMP. The functional activity of the 5-HT_{1B} autoreceptors is related to availability of the second messengers and the substrate cAMP. Circadian variation in the levels of endogenous cAMP have been detected in rat SCN micropunches (Prosser and Gillette, 1991; Yamazaki *et al.*, 1994) with peak levels during the late day and late night, but low during early night. This pattern does not really follow the function of the 5-HT_{1B} receptor but the experiments examining the levels of cAMP were carried out *in vitro* and under constant darkness. In animals maintained under a 12:12 light:dark cycle, the levels of endogenous cAMP may follow 5-HT_{1B} receptor activity. If cAMP levels were low towards the end of the light period and throughout the dark period, one might speculate that the low availability of substarate for the enzyme adenylate cyclase accounts for the variation in receptor function. However, the 5-HT_{1B} receptor is negatively coupled to adenylate cyclase; stimulation of the receptor will prevent rather than promote cAMP conversion. It would therefore be a more accurate parameter to measure the activity of the enzyme adenylate cyclase itself. Prosser and Gillette (1991)

did measure adenylate cyclase activity in addition to cAMP levels in the same setup, but found no significant variation in activity over the four different sampling times. Once again this is a measurement of circadian variation, and not diurnal variation as we have identified the 5-HT_{1B} autoreceptor to exhibit. It is still possible that underlying variations in adenylate cyclase activity account for the variation in 5-HT_{1B} autoreceptor function in the SCN.

Another exciting candidate for why this variation in autoreceptor function exists in rodent and bovine brains. It was proposed in 1996 that an endogenous ligand may be present in cerebral tissue capable of interacting with the 5-HT_1 receptor function and more specifically the 5-HT_{1B} receptor. This simple 4 amino acid peptide (Leu-Ser-Ala-Leu) was purified and named 5-HT moduline (Massot *et al.*, 1996). This molecule specifically inhibited the binding of tritiated 5-HT to 5-HT_{1B} receptors, thus acting as an allosteric modulator at the 5-HT_{1B} site, and was shown in behavioural experiments to have an antagonistic effect on 5-HT_{1B} receptor activity. Since that time, 5-HT moduline has been localised immunocytochemically in rodent brain after an antibody was raised against the peptide (Grimaldi *et al.*, 1997) Localisation of 5-HT moduline appeared to overlap binding at 5-HT_{1B} receptors, giving strength to the suggestion that it specifically interacts with 5-HT_{1B} receptors. Indeed in mutant mice lacking the gene encoding the 5-HT_{1B} receptor there was no binding of 5-HT moduline (Cloez-Tayarani *et al.*, 1997). If 5-HT moduline were present in the hypothalamus, as indeed has been shown (Grimaldi *et al.*, 1997), at levels that fluctuated throughout the course of a 24 hour day, then this would be a leading candidate for variation of 5-HT_{1B} receptor function *in vivo*. At this time no detection system other than that set up in the laboratory of Grimaldi and collaborators is available to us. If the four amino acid compound were readily detectable by HPLC-ED in microdialysate samples, then it paves the way for a 24 hour analysis of SCN samples to determine if the levels correlate with the function of the 5-HT_{1B} autoreceptor as identified in this study.

Many studies have centred on the effect of 5-HT_{1B} autoreceptor stimulation in the hippocampus (Sharp *et al.*, 1989; Hjorth and Tao, 1991; Martin *et al.*, 1992; Bolanos-Jimenez *et al.*, 1995; Bosker *et al.*, 1995). The hippocampus was dialysed as a comparison between this serotonergic rich terminal area and that of the SCN, to determine whether the diurnal variation in 5-HT_{1B} receptor function was site-specific for

the SCN. In the SCN mid-light and mid-dark 5-HT_{1B} receptor stimulation had very different effects; these two time points were therefore chosen for investigation of the hippocampus. In all the studies quoted above experiments were performed during the light phase, and application of an agonist for the 5-HT_{1B} autoreceptor produced comparable reductions in 5-HT overflow (between 33 and 67 % reduction of basal). In my experiments at both mid-light and mid-dark, infusion with RU24969 produced significant and prolonged decreases in dialysate 5-HT concentration (figure 3.6). Although the maximal decrease in 5-HT overflow was greater at mid-light (32.3 ± 15.0 % of basal) compared to mid-dark (58.4 ± 9.63 % of basal), the statistical significance level reached was the same ($p < 0.01$) and the time course of the decrease was similar. The hippocampal terminal 5-HT_{1B} autoreceptors therefore do not exhibit such pronounced diurnal variation in function as seen in the SCN. The diurnal rhythm in 5-HT_{1B} autoreceptor function, which manifests itself with a complete absence of a response at mid-light upon agonist stimulation appears region-specific for the SCN.

3.4.2 The 5-HT_{1B} heteroreceptor

Basal glutamate (Glu) levels recorded in this study were very similar to those obtained in the SCN previously (Srkalovic *et al.*, 1994; 800 ± 90 nanomol) and in the the basal hippocampus by Rowley *et al.* (1995; 0.60 ± 0.02 picomol). As in our study, many authors have observed higher basal Glu during the dark phase than during the light phase of animals synchronised to an environmental light:dark cycle (Glass *et al.*, 1993; Selim *et al.*, 1993; Srkalovic *et al.*, 1994). Glutamate is released at RHT terminals (Liou *et al.*, 1986) after stimulation by light. Therefore, one might assume that the Glu concentration measured during the light phase will be greater than that during the dark phase. However, measured Glu concentration does not necessarily reflect Glu released. The microdialysis samples record fluctuations in extracellular tissue concentrations, and it may be that during the light period the Glu is taken up and utilised more quickly by neurones. This possibility cannot be ruled out since the perfusing medium did not contain a selective Glu reuptake blocker.

A recent paper (Timmerman and Westerink, 1997) highlighted the problems associated with brain microdialyis of Glu. The authors reviewed a number of papers and highlighted that a number of studies failed to fulfill the classical criteria for exocytotic

release for Glu, whilst assuming that the origin of measured Glu in their dialysates was neuronal. However, I have shown that the Glu measured in the SCN dialysates is both calcium- and potassium-dependent. One problem that was quite obvious during the sampling of Glu was the fluctuation in Glu concentration from one collection sample to the next, an effect that was in contrast to the majority of studies collecting for 5-HT. This is apparent in the size of the error bars, i.e. inter-sample variation, of the pre-intervention control samples. However, the effect of the voltage-dependent calcium channel blocker, NiCl, and an increase in perfusing potassium ion concentration, was such that the effects were quite striking. The maximal increase in Glu efflux following stimulation with potassium ions was similar to that in hippocampus (Lu *et al.*, 1996; 280-320 % of baseline and Rowley *et al.*, 1995; 298 ± 11 % of baseline). Removal of calcium ions from the perfusing aCSF by Rowley and coworkers (1995) reduced Glu levels to 38 ± 3 % of baseline, which is not disimilar to our results.

Infusion with the mixed 5-$HT_{1A/1B}$ receptor agonist RU24969 for 15 min, produced a decrease in dialysate Glu concentration, which is consistent with the view that 5-HT_{1B} heteroceptors are present on retinal afferent terminals (Pickard *et al.*, 1996). The agonist produced comparable maximal decreases in Glu overflow during the light and dark phases. However, the 5-$HT_{1A/1B}$ receptor mediated reduction in dialysate Glu during the light phase occurred sooner (20 min after the start of the infusion) than that during the dark phase (50 min after the start of the infusion), which may reflect changes in the ability of the RU24969 to activate the 5-HT_{1B} inhibitory heteroceptors during the dark phase. Whether this effect is attributable to 5-HT_{1A} or 5-HT_{1B} receptor stimulation we cannot be certain. Although RU24969 is known to be a specific agonist at the 5-HT_{1B} receptor site (Sills *et al.*, 1984) it does show moderate agonist properties at the 5-HT_{1A} receptor site. Srkalovic and co-workers (1994) infused both a 5-HT_{1A} receptor agonist (8-OH-DPAT) and a 5-HT_{1B} receptor agonist (TFMPP) into the SCN region and compared effects on Glu overflow at ZT 18. Both drugs significantly decreased extracellular Glu concentration when infused separately, although the inhibitory effect of 8-OH-DPAT was greater than that of TFMPP; a reduction by 60 % of basal compared with a reduction by only 20% of basal, respectively. The RU24969 induced reduction in dialysate Glu by approximately 60 % may thus be attributable only to 5-HT_{1A} receptor stimulation. The likelyhood is that both 5-HT_{1A} and 5-HT_{1B} receptors lead to this reduction, because both 5-HT_{1A} and 5-HT_{1B} receptor stimulation can decrease Glu

overflow from the SCN (Srkalovic *et al.*, 1994). The degree of 5-HT_{1B} receptor involvement in the inhibition of Glu overflow in the SCN must therefore be clarified by further experimentation.

In the rat SCN approximately 40 % of all cells respond to 5-HT with a dose-dependent suppression of the spontaneous or glutamate-evoked discharge (Meijer and Groos, 1988). This is further evidence for 5-HT modulation of RHT transmission, although the receptor subtype(s) involved were not identified. In another terminal projection site originating from the retina, the superior colliculus, 5-HT_{1B} hereroceptors have been shown to modulate retinotectal neurones (Mooney *et al.*, 1994). Stimulation of the optic tract *in vitro* in hamsters evoked excitatory postsynaptic potentials (EPSPs) in the superior colliculus, which was consistently inhibited by application of 5-HT, and more specifically, the 5-HT_{1B} receptor agonists TFMPP and CGS12066B. With this in mind, if one extrapolates the effects of 5-HT_{1B} receptor agonists from one retinal projection area to another, 5-HT_{1B} inhibitory heteroceptors are likely to modulate the retinohypothalamic neurones

Other studies have provided data indicating that 5-HT and more specifically 5-HT_{1B} receptor stimulation has presynapic inhibitory effects in other structures. Singer *et al.* (1996) measured glutamate EPSPs in rat hyperglossal motorneurones, which were inhibited by 5-HT and the 5-HT_{1B} receptor agonist CP93129. In the guinea pig substantia gelatinosa frequency-mediated and spontaneous EPSPs were reduced by 5-HT and agonists acting at the 5-HT_{1D} receptor site, which is equivelent to the rat 5-HT_{1B} receptor (Travagli and Williams, 1996). More specific to our studies, in the SCN of anaestheised hamsters, light-activated neurones have been shown to be inhibited by microiontophoretic application of 5-HT (Ying and Rusak, 1994). These authors tested the ability of the 5-HT_{1A} receptor agonists 8-OH-DPAT and 5-CT to mimic the effects of 5-HT but failed to test other classes of 5-HT receptor, specifically the 5-HT_{1B} receptor. Using the experimental setup of Ying and Rusak (1994) it is likely that 5-HT_{1B} receptor agonist application in the SCN would also result in a decrease in the activity of light activated neurones.

3.5 CONCLUSIONS

The activity of the 5-HT_{1B} autoreceptor in the suprachiasmatic nucleus is not constant across the light:dark cycle and this seems to be a phenomenon unique to the SCN. This may be significant in terms of control and release of 5-HT with subsequent influence on clock functioning in the SCN. The mechanism(s) by which variation in receptor function is mediated remains to be elucidated.

Although at this stage one is speculating that the actions of RU24969 are via the 5-HT_{1B} heteroceptor, it can be concluded that the inhibitory action of the drug on Glu release does not exhibit variation at mid-light versus mid-dark, unlike the 5-HT_{1B} autoreceptor. The maximal reduction on Glu overflow is similar when the agonist is applied at ZT 6 or ZT 18. It is possible that the receptor regulating presynaptic inhibition of Glu does undergo a diurnal variation which we have failed to detect because we have only sampled at two time points across the light:dark cycle. As is evident from the experiments on the function of the 5-HT_{1B} autoreceptor, it is necessary to sample at frequent intervals across the light:dark cycle to detect diurnal rhythm in receptor function.

CHAPTER 4

5-HT_{1B} AUTO-, HETERO- AND POSTSYNAPTIC RECEPTOR mRNA AND 5-HT_{1B} RECEPTOR EXPRESSION IN THE SCN

4.1 INTRODUCTION

In the preceding chapter I described how the function of the 5-HT_{1B} autoreceptor in the SCN varied over the course of a 24 hour day. Many suggestions were put forward as to why the function might fluctuate, but at this stage the mechanisms behind this variation are purely speculative. Before examination in minute detail of the intricate intracellular mechanisms of receptor regulation, one might begin to examine the initial cascade of receptor production i.e. the amount of message produced that might be subsequently transcribed into receptor, and then the amount of 5-HT_{1B} receptor protein present in the brain tissue.

One study has examined the amount of mRNA present in the rat SCN by *in situ* hybridization (Roca *et al.*, 1993). These authors detected a weak signal for the 5-HT_{1B} receptor and found no variation in signal intensity at two time points; mid-subjective day and mid-subjective night. The animals used in their study had been allowed to free-run in constant darkness, and so although no circadian variation in receptor expression was identified, it still remains possible that the 5-HT_{1B} receptor undergoes a diurnal rhythm in animals entrained to a light:dark cycle. Therefore, although 5-HT_{1B} receptor expression in the SCN itself represents a *post*synaptic receptor it would be of considerable interest to the chronobiologist to evaluate whether the receptor mRNA levels were influenced by the light dark cycle.

In Chapter 3, in addition to investigating the function of the 5-HT_{1B} autoreceptor, the function of the 5-HT_{1B} heteroceptor was examined. Although no variation was observed in the heteroceptor function at the two time points studied it was nevertheless of interest to examine whether the mRNA for the heteroceptor varied across the 24 hour light:dark cycle, extending the study to incorporate eight equally spaced time points. Assuming that the heteroceptor is located on retinal afferents, the mRNA for this receptor will be produced in the cell body region located in the retina. Indeed, enucleation of hamsters significantly decreases the density of 5-HT_{1B} receptors in the SCN suggesting a retinal terminal location (Pickard *et al.*, 1996).

The mRNA for the terminal 5-HT_{1B} autoreceptor will be located in the cell body of the serotonergic neuron in the midbrain raphe nuclei (Moore *et al.*, 1978). Rats lesioned

with the selective serotonergic neurotoxin 5,7-dihydroxytryptamine show a significant decline in the amount of 5-HT_{1B} receptor mRNA level in the median and dorsal raphe nuclei as measured by in situ hybridization (Doucet *et al*, 1995). This indicates that the synthesis of the 5-HT_{1B} receptor is within the serotonergic neurones, as predicted by their presynaptic autoreceptor function at the level of the serotonergic neuron. A diurnal variation at the level of 5-HT_{1B} receptor mRNA in the raphe nuclei projecting to the SCN might contribute to the diurnal variation in function observed in the *in vivo* microdialysis studies. However, the exact location of the cell body projecting to the SCN i.e. whether the median raphe nuclei (MRN) or the dorsal raphe nuclei (DRN) project to the SCN is in dispute (see Chapter 6 Discussion).

5-HT receptor binding experiments have utilized radioligand binding combined with autoradiagraphy detection to localize 5-HT_{1B} receptors in the mammalian brain (Hoyer *et al.*, 1985; Engel *et al.*, 1986). Only one such study to date has investigated 5-HT_{1B} receptor binding in the circadian pacemaker at two time points across the light:dark cycle (Prosser *et al.*, 1993) and demonstrated increased receptor binding during the dark phase. The number of available receptors present in the brain tissue at a given time point will determine the ability of an exogenously applied agonist to produce a response. The aim was to do a more thorough investigation of the 5-HT_{1B} receptor protein present in the SCN across the light:dark cycle, sampling brain tissue every three hours and to show whether levels in 5-HT_{1B} receptor protein in the SCN correlated with the receptor function.

It was therefore the aim of the experiments described in this chapter to first investigate the amount of mRNA present in the SCN (postsynaptic receptor), the retina (heteroceptor) and the raphe nuclei (autoreceptor) at eight equally spaced time points over the 24 hour light:dark cycle using the sensitive semi-quantitative technique of reverse-transcriptase polymerase chain reaction (RT-PCR). Secondly, I intended to investigate the amount of 5-HT_{1B} receptor protein in the SCN. The initial aims were to use immunocytochemistry using a specific antibody raised against the 5-HT_{1B} receptor to quantitatively detect and localize the 5-HT_{1B} receptor in the SCN. Subsequent to detection of the 5-HT_{1B} receptor in the SCN, it was intended to use double labelling studies using a combination of 5-HT_{1B} /glutamate immunoreactivity and 5-HT_{1B} /serotonin immunoreactivity to quantify the number of receptors present on retinal

terminals (glutamate immunoreactivity) and/or ascending raphe projections (serotonin). The amount of 5-HT_{1B} receptor protein present in the SCN brain tissue was then to be verified across the light dark cycle using the protein detection method of Western blotting.

4.2 METHODS

Male Wistar rats (University of Bath strain; 260-320 g) were maintained under a 12:12 light:dark cycle regime (lights on 07.00; temperature 22 ± 2°C) with food and water available *ad libitum.*

4.2.1 REVERSE-TRANSCRIPTASE POLYMERASE CHAIN REACTION (RT-PCR)

4.2.1.1 Preparation of tissue samples

The animals were killed by CO_2 asphyxiation, brains removed and snap-frozen onto dry ice. Not allowing the brains to become brittle with prolonged freezing, the dissections were carried out quickly within a couple of minutes whilst the brains were still malleable. The dissection of blocks of tissue containing the SCN and the midbrain raphe was achieved by using 'landmarks' on the surface of the brain as indicators of location. The eyes were removed and placed in cold physiological saline for the dissection of the retina. Tissue from four animals were pooled for the RT-PCR reaction.

(1) SCN. The optic chiasm was used as the main indicator of the location of the SCN. Against the pinkish tinge of the whole brain, the optic nerves are easily visible as white thread-like structures, extending from the orbit encapsulating the eyes, along the base of the brain. The optic nerves join in the midline and are seen to form a cross as they bifurcate continuing in their path into the brain where they disappear out of sight of the whole brain. Two cuts are made with a clean razor blade perpendicular to the midline of the brain, the first at the point on the surface of the brain where the optic chiasm bifurcates, and the second approximately 1.5 mm rostral to this point, cutting the optic chiasm. A coronal brain slice of approximately 1.5 mm thickness remained (see figure 4.1a). Roughly 1 mm either side of the midline, two cuts were made leaving a section of brain requiring one further cut. Approximately 2 mm above the base of the optic chiasm a final cut was made, and a small block of tissue remained (2 x 2 x 1.5 mm) encapsulating the whole rostral caudal extent of the SCN. The tissue was stored at -70°C.

(2) Raphe. The initial cut in the brain was made using the cerebellum as a point of reference. With the brain dorsal surface up, a cut was made between the cerebellar and

cerebral cortices perpendicular to the midline of the brain. Using the stereotaxic atlas of Paxinos and Watson (1982) as a guide, tissue was cut away in very fine strips until all cerebellar tissue was removed except for a small part lobule 2 encapsulated in the centre of the brain surrounded by what is to become the cerebral aqueduct. At this point in the dissection, the shape of the brain and the amount of entorhinal cortex present were the principal guiding factors. A second major cut was made approximately 1.5 mm rostral to the exposed segment of brain to leave a 1.5 mm thick coronal slice of brain (see figure 1b). Two cuts were made approximately 1 mm parallel to either side of the midline, using the central grey area as a marker; so called due to the grey appearance of the tissue surrounding the cerebral aqueduct. The block of tissue containing the midbrain raphe nuclei was then isolated with two further cuts; one through the centre of the aqueduct, and one 4 mm ventral to that site. The small block of tissue remaining was approximately 2 x 4 x 1.5 mm in size and was stored at -70°C.

(3) Retina. The dissection of the retina was carried out under a standard bifocal dissecting microscope. The stump of the optic nerve was held with broad forceps in an attempt to maintain the eye in a fixed position, whilst the cornea was punctured using a sharp 23 gauge needle. A pair of fine microdissecting scissors were then inserted into the puncture hole, and the cornea cut and removed to leave a 'cup'. The lens was also removed at this point, and the vitreous humor expelled using a pair of fine forceps. The retina was visible as the 'lining' of the cup and slightly orange in colour. A small incision was made on the edge of the cup and the retina gently teased away. The retina was then rinsed in physiological saline, placed on foil and frozen onto dry ice. The tissue was stored at -70°C.

4.2.1.2 Isolation of total RNA

The isolation of *total* RNA from SCN samples was achieved using the TRIzol™ Reagent (GIBCO BRL, Life Technologies).

50 mg of frozen SCN tissue was homogenized in 1 ml of TRIzol Reagent, before being incubated for 5 min at room temperature to permit the complete dissociation of nucleoprotein complexes. After adding 0.2 ml chloroform and mixed thoroughly by shaking vigorously by hand for 15 sec, the samples were incubated at room temperature for 3 min prior to centrifugation at 12,000 x g for 15 min at 4°C. Separation of the

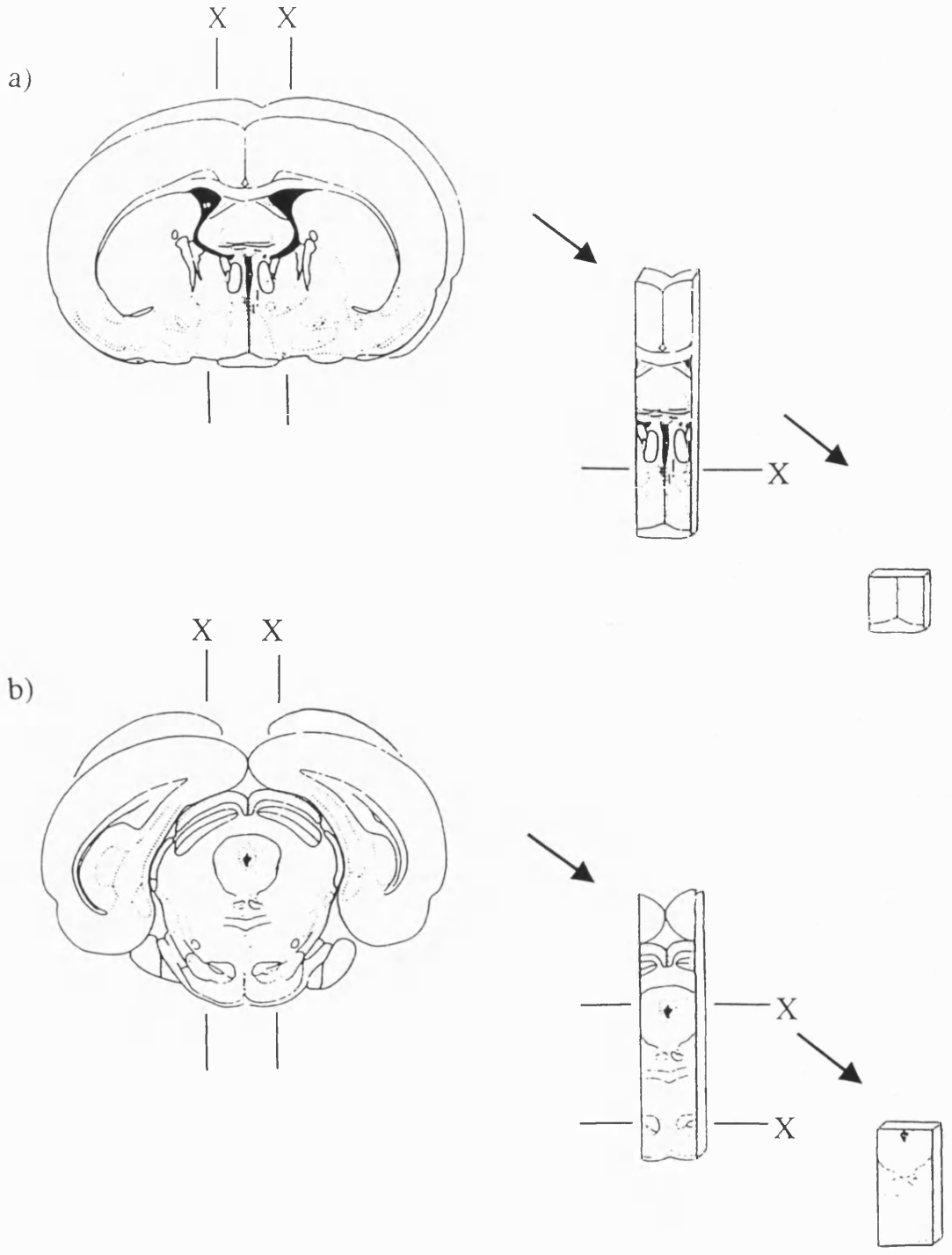

Figure 4.1. Dissection of (a) SCN and (b) raphe tissue. A 2 mm coronal section of the SCN or raphe was dissected from the rat brain, and two cuts were made approximately 1 mm either side of the midline, designated by X, to leave a columnar section of brain tissue. For the SCN dissection, a further cut was made approximately 2 mm from the base of the brain to leave a block of tissue 2 x 2 x 1.5 mm (a). For the midbrain raphe dissection, two further cuts were made; one in line with the cerebral aqueduct, and one 4 mm ventral to this site, to leave a block of tissue 2 x 4 x 1.5 mm (b).

mixture into a lower red, phenol-chloroform phase, an interphase, and a colourless upper aqueous phase was now visible with the RNA present exclusively in the aqueous phase. The aqueous phase was transferred into a fresh tube and the organic phase discarded. Using 0.5 ml isopropyl alcohol, the RNA was precipitated from the aqueous phase, incubated for 30 min at room temperature and then centrifuged at 12,000 x g for 15 min at 4°C. The supernatant was removed to expose the RNA pellet remaining, and the pellet washed with 1 ml 75% ethanol, mixed thoroughly and then centrifuged at 7,500 x g for 5 min at 4°C. The Pellet was then exposed and air-dried for 10 min, ensuring that it did not dry completely. The pellet was redisolved in 20 µl diethylpyrocarbonate-treate Milli Q water (DEPC/Q) to make a final 'stock' solution of total RNA and stored at -80°C.

4.2.1.3 Isolation of mRNA

The separation of *m*RNA from the retinal (RET), raphe (RAP) and SCN samples was achieved using a Dynabeads® mRNA DIRECT kit (DYNAL®, Norway). The solutions supplied with the kit are shown in the appendix.

50 mg of frozen RAP and SCN sample and 100 mg of frozen RET sample were homogenized in Lysis/binding buffer (1 ml per 50 mg of tissue) until complete lysis was obtained, and the samples then spun in a microcentrifuge for 1-2 mins to remove debris. 1 ml of the supernatant (lysate) was then mixed with the prewashed Dynabeads Oligo $(dT)_{25}$ on a roller for 5 min at room temperature. The vials containing the lysate and Dynabeads Oligo $(dT)_{25}$ (1.5 ml eppendorf tubes) were then placed in a Dynal magnetic particle concentrator (MPC) for 5 min before discarding the supernatant. The poly-$(A)^+$ RNA will now have annealed to the Oligo dT sequence that is bound to the Dynabeads surface. The Dynabeads were then washed twice with 1 ml washing buffer with LiDS and once with 1 ml washing buffer using the Dynal MPC. The beads were then washed a further two times with 0.5 ml washing buffer before elution of the mRNA from the Dynabeads Oligo $(dT)_{25}$ with 20 µl of elution solution. The tubes were maintained at 65°C for 2 min, and the supernatant containing the mRNA was transferred to RNase-free tubes. The Dynabeads Oligo $(dT)_{25}$ were then regenerated ready for subsequent use as directed in the Dynabeads® mRNA DIRECT kit handbook.

The quantity of *total* and *m*RNA in the individual samples was assessed by the absorbance at 260 nm and calculated by:

Amount of RNA (μg/ml) = A_{260} x dilution factor x 40*

*1 μg/ml of RNA gives an A_{260} reading of 40

(A280 assesses the amount of DNA in the sample)

4.2.1.4 Reverse-Transcriptase reaction (RT)

Total or Poly-(A) mRNA was reverse transcribed to generate cDNA. 200 ng of RNA in a volume of 9.75 μl was required for the RT. All RET, RAP and SCN samples ZTs 0-21 plus a blank solution containing no RNA underwent the RT reaction in duplicate. To 9.75 μl of the RNA/blank was added 4 μl 25 mM $MgCl_2$, 2 μl 10xPCR buffer 2, 2 μl 10 mM dNTPs, 1 μl RNAse inhibitor 35 units/μl, 0.25 μl Moloney-murine leukemia virus (M-MLV) R.T. 200 units/μl and 1 μl Oligo (dT) 0.5 mg/ml into PCR tubes to make final concentration of 5 mM, 1x, 1 mM, 1.75 units/μl, 2.5 units/μl and 25 μg/μl for each of $MgCl_2$, PCR buffer 2, dNTPs, RNAse inhibitor, M-MLV R.T. and Oligo (dT), respectively and a total volume of 20 μl. The tubes were then allowed to stand for 10 minutes at room temperature before being subjected to 42°C for 1 hour and 94°C for 3 minutes.

Following generation of the first strand cDNAs, the tubes were stored on ice for 5 minutes before being used in the cDNA amplification step.

4.2.1.5 cDNA Amplification

(1) PCR

To the 20 μl of cDNA produced from the RT reaction was added 4 μl 25 mM $MgCl_2$ (2 mM final concentration), 8 μl 10xPCR buffer (final concentration 1x), 47.5 μl DEPC/Q, 0.5 μl 5 U/μl Amplitaq DNA polymerase (final concentration 2.5 U/100 μl) and 10 μl of each of the forward and reverse primers 50 μg/ml (GIBCO BRL) for β-actin and 5-HT1B, to give a total volume of 100 μl. Each tube was topped with 4 drops of mineral oil before being subjected to cDNA amplification in a 35 cycle PCR reaction; one cycle of 94°C for 5 min followed by 35 cycles of 94°C for 45 sec, 60°C for 45 sec and 72°C for 90 sec and a final cycle of 72°C for 10 min.

(2) "Hot Start" PCR

To a sterile PCR tube was added 4 µl 25 mM $MgCl_2$ (2 mM final concentration) and 10 µl of each of the forward and reverse primers 50 µg/ml for β-actin and 5-HT_{1B}. A wax pellet (Ampliwax PCR Gem 100, Perkin Elmer) was then added, and heated at 77°C for 7 min. Once re-solidified a mixture of 20 µl cDNA (produced by the RT reaction), 8 µl 10xPCR buffer (final concentration 1x), 47.5 µl DEPC/Q water and 0.5 µl 5 U/µl (final concentration 2.5 U/100 µl) Amplitaq DNA Polymerase was added to each tube. The tubes containing a final total volume of 100 µl was then subjected to 35 cycles as described previously.

Primers (5' - 3'):

5-HT_{1B}:	Forward	CTA TGG AGG AGC AGG GTA TTC
	Reverse	CCG TGT ACA TGG TGC TGA TG
β-Actin:	Forward	CCT AGC ACC AAG AAG ATC AA
	Reverse	TTT CTG CGC AAG TTA GGT TTT GTC AA

4.2.1.6 Visualization of RT-PCR product

The RT-PCR products were run on a 2.5% agarose gel. 5 µl of the β-actin product and 20 µl of the 5-HT_{1B} product were loaded with dye (1x final concentration). The gel was then stained with ethidium bromide (0.5 µg/ml) for 30 minutes, before being visualized under U.V. light. The density of each 5-HT_{1B} band was calculated at each time point and normalized to the corresponding β-actin band using a Molecular Analyst computer package.

4.2.1.7 Statistics

Each 5-HT_{1B} mRNA band that was normalized to the corresponding β-actin band produced a value that represented 'adjusted volume counts per mm^2'. The mean number of counts was calculated for each gel run (ZTs 0, 3, 6, 9, 12, 15, 18 and 21), and at each zeitgeber time a percentage value of this mean count value was obtained. Since the gels were run three times with the SCN, RET and RAP samples, the mean ± s.e.m. of the three gel 'percentage average counts' were plotted against the zeitgeber time. Statistical

differences between the density of each band of the RT-PCR reaction product across the eight zeitgeber times in the SCN, RET or RAP tissue was calculated using a one way analysis of variance with a Tukey-Kramer multiple comparison *post hoc* test. $p < 0.05$ was considered significant.

4.2.2 IMMUNOCYTOCHEMISTRY

The antibody raised against the rat 5-HT_{1B} receptor corresponding to amino acids 365-383 mapping at the carboxy terminus was obtained from Santa Cruz Biotechnology (Autogen Bioclear UK Ltd, Wiltshire). The method of immunocytochemistry using frozen tissue sections was provided by the company, and it was this protocol that was followed and amended.

Brains were collected at zeitgeber times 0, 3, 6, 9, 12, 15, 18 and 21 (n=3 per time point) from animals that had been asphyxiated with CO_2. The brains were rapidly removed and snap frozen onto dry ice. During the dark phase brains were removed under low red light illumination. Brains were wrapped in silver foil and stored at -80°C prior to immunocytochemical processing. Consecutive coronal sections (15 μm) were cut on a cryostat (Bright Instruments) set at -20°C. Sections were taken of the full rostrocaudal extent of the SCN and every third section mounted onto gelatinized slides. Sections were air dried and stored at -80°C in sealed plastic slide boxes containing a small sachet of silica gel.

One hour prior to commencement of immunocytochemical staining, the slide boxes were removed from the freezer and allowed to stand at room temperature. Slides were then placed into glass slide racks and placed on a rocking platform, where all subsequent stages were carried out unless specified. Sections were fixed in a solution of either cold acetone (15 min) or 4% paraformaldehyde (30 min). After two washes (all washes were carried out over a 15 min period) in phosphate buffer saline (PBS) the slides were incubated for 30 min in 1 % hydrogen peroxide (H_2O_2) in a solution of 20 % methanol in PBS to block endogenous peroxidase activity. The sections were then washed twice in PBS before incubating the sections in 1.5 % normal rabbit serum (NRS) in PBS for 60 min. After two further washes in PBS the sections were incubated in primary antibody (0.1-2.0 μg/ml; 60 min-30 hours) in PBS containing 1 % NRS at 4°C in a

humidified chamber on a level surface. Sections were then washed three times in PBS, and incubated in peroxidase labeled rabbit antigoat secondary antibody (Sigma) diluted 1:200 in PBS containing 1 % NRS for 60 min in the humidified chamber at room temperature. The tertiary ABC complex (Dako) was prepared according to the manufacturers instructions and allowed to incubate at 4°C prior to use. Sections were washed twice in PBS and then incubated in ABC complex for 30 min in the humidified chamber at room temperature. Sections were then washed twice in PBS prior to a further wash in PBS containing 0.5 % triton-X 100 for 60 seconds. The chromagen diaminobenzidine (DAB) was available in tablet form in which each tablet weighed 1 mg, and came supplied with a tablet of H_2O_2 (Sigma). To 1 ml PBS was added the DAB tablet and H_2O_2 tablet, and vortexed before use. The slides were incubated for a period of time in the DAB mixture (10-20 min), during which time the antigenic site should be exposed with a brown precipitate. The reaction was stopped rinsing in 50:50 PBS: H_2O for 5 min before rinsing in distilled water. The slides were passed through graded alcohols (70, 80, 100 %) to dehydrate the sections, and then passed through a clearing agent, citroclear. The sections were mounted using a non-aqueous mounting medium, DPX.

4.2.2.1 Chymotrypsin treatment

Some sections were treated with the enzyme chymotrpsin. 2 μg/ml of chymotrypsin was prepared in Tris-buffered HCl (pH 7.8) containing 2 μg/ml $CaCl_2$ and warmed to 37°C. Sections were incubated for 15 min at 37°C prior to blocking endogenous peroxidase activity. Sections were washed twice in PBS before continuing the immunocytochemical protocol.

4.2.2.2 Heat treatment

After the fixation process some sections were placed in a container, covered with 10 mM citrate buffer, pH 3.5 containing 0.01 % (w/v) EDTA. The sections were microwaved for 5 min, then immersed in fresh citrate buffer prior to a further 5 min microwave treatment. The sections were then allowed to cool before commencement of the immunocytochemical staining.

4.2.3 WESTERN BLOTTING

4.2.3.1 Preparation of tissue samples

Brain tissue samples were dissected as previously described in section 4.2.1.1, and stored at -70°C until use. Samples from two animals were pooled, weighed and homogenized, in ice cold RIPA buffer (PBS containing 1% nonidet P40 (NP40), 0.5% sodium deoxycholate, 0.1% sodium dodecyl sulphate (SDS); 6 ml / gram tissue) containing 100 µg/ml PMSF, 30 µg/ml aprotonin and 1mM sodium orthovanadate, until there was no visible solid matter remaining. The samples were then transferred into a 1 ml Eppendorf tube and 10 µl of 10 mg/ml PMSF stock added. An incubation period of 30 min was allowed prior to centrifugation at 15,000xg for 20 min at 4°C. The supernatant was decanted and contained the total cell lysate.

4.2.3.2 Bradford protein assay

This is a relatively simple and accurate method for the determination of most proteins. Prior to the assay, the 'Bradford Reagent' was prepared by dissolving 200 mg Coomassie Blue (G form) into 200 ml of 85% phosphoric acid, made up to 1 L with distilled water, and stored in the dark. A series of protein samples were prepared (0-10 µg) with bovine serum albumin in 500 µl distilled water for a standard curve. 1 µl of tissue extract to be assayed for protein concentration was added to 500 µl distilled water (the same medium in which the protein standards were prepared). To each standard and sample solution was added 500 µl Bradford Reagent and vortexed thoroughly. 100 µl of each solution was added to a well of a 96 well tray and the absorbance read at 595 nm. The protein concentration in the tissue extracts were expressed as µg/µl.

4.2.3.3 Electrophoresis

Total proteins were separated on a 10% running polyacrylamide gel under denaturing conditions using a Bio-Rad Mini Protean system. 20 - 80 µg of total protein were loaded per well in a total volume of 20 µl electrophoreis sample buffer. Molecular weight markers were run in parallel on each gel. Gels were submerged in SDS-PAGE running buffer and run at 80 V for 20 min through the stacking gel (4%), and at 180 V for a further 60 min through the running gel. Following electrophoresis, the stacking gel was removed and the gel rinsed in semi-dry transfer buffer.

4.2.3.4 Immunoblotting

Transfer of proteins onto a nitrocellulose membrane (Bio-Rad) was achieved by sandwiching the gel with the nitrocellulose membrane and placing it between absorbent paper soaked in semi-dry transfer buffer. The gel-membrane sandwich was placed between carbon plate electrodes and run at 100 V and 40 mA for 60 min (0.8 mA per cm^2 of gel).

The membrane was blocked overnight in blocking buffer prior to incubation with primary antibody (anti-5-HT_{1B} polyclonal raised in goat, Santa Cruz Biotechnology, Inc.; 0.1 - 2.0 μg) diluted in blocking buffer. After 3 hours the membranes were washed once in TBS, three times in TBS containing 0.05% Tween-20 (TBS-T) and a further wash in TBS (all washes 10 min). The secondary antibody (peroxidase-conjugated anti-goat IgG raised in rabbit, DAKO; 1:5,000 - 1:40,000) diluted in TBS-T was applied for 1.5 hours. The secondary antibody was removed by repeating the washes following primary antibody incubation with an additional TBS wash. Bound antibody was detected by incubating the membranes in Amersham Enhanced Chemiluminescence (ECL) reagents for exactly 1 min, and being exposed in a darkroom to Kodak Scientific Imaging Film for 1 min, 5 min and 2 hours.

Optimal conditions for Western blotting were first identified and then SCN samples were obtained at ZTs 0, 3, 6, 9, 12, 15, 18 and 21. At each zeitgeber time 2xSCN were dissected and the tissue pooled. This was performed in duplicate providing two sets of SCN samples at each ZT. The density of the protein band was taken as an indication of the amount of 5-HT_{1B} receptor protein present in each SCN sample.

4.3 RESULTS

4.3.1 REVERSE-TRANSCRIPTASE POLYMERASE CHAIN REACTION

4.3.1.1 Total RNA extraction from SCN tissue

Using the TRIzol™ Reagent, total RNA was extracted from SCN tissue (ZTs 0, 3, 6, 9, 12, 15, 18 & 21). The purity of each sample was estimated using the A_{260}/A_{280} ratio; ratios less than 1.6 were deemed contaminated by proteins and DNA and consequently RNA was re-extracted. The quantity of RNA present in each sample was calculated using A_{260} (see Table 4.1). The mean RNA concentration for all the samples (± s.e.m) was 0.51 ± 0.10.

Sample ZT	0	3	6	9	12	15	18	21
[RNA]μg/μl	0.43	0.50	0.53	0.52	0.67	0.57	0.35	0.48

Table 4.1: Total RNA concentration expressed as μg/μl in each SCN sample calculated by the absorbance at 260 nm.

To ensure that the RNA was intact, and to verify that there was no DNA contamination, a 1% agarose gel was run loading 1 μg of RNA for each sample against a ribosomal RNA marker. Figure 4.2 shows the separation of the rRNA bands into 18S and 28S sized fragments. There was no DNA contamination and samples 0, 3, 6, 9, 12 & 15 all had intact rRNA bands. Samples 18 and 21 did not appear to have rRNA bands which would suggest that the RNA in these samples had broken down, but it was decided to proceed with the RT-PCR reaction with all the samples. Sample 0 had very feint rRNA bands due to loss of sample upon loading onto the gel.

4.3.1.2 RT-PCR reaction

Figure 4.3 shows the products of the first RT-PCR reaction run on a 2.5% agarose gel. β-actin primed-samples showed clear bands between the 200 and 300 base pair (bp) marker, being 276 bp in length. Unfortunately, the samples primed for 5-HT_{1B} mRNA displayed a double band between 300 and 400 bp (5-HT_{1B} mRNA - 356 bp using primers), implying that the primers used in the reaction had annealed non-specifically

during the cDNA amplification stage. To eliminate the contaminating band, a protocol for "hot-start" PCR was followed. This involved the prior separation of the specific primers from the cDNA and Amplitaq polymerase by a solid wax pellet. This prevents non-specific annealing by the primers at temperatures below that of the specified annealing temperature of the individual primers. When the samples reach the annealing temperature during the PCR reaction, the wax melts allowing the total volume in each PCR tube to mix thoroughly, so commencing the reaction.

A 'test-run' was performed on two samples (ZTs 0 and 12) and a further brain-RNA sample, in duplicate, using both the original PCR method and the 'hot-start' method for each β-actin and 5-HT_{1B} primers. The results are shown in figure 4.4, and demonstrates quite clearly that the 'hot-start' method eliminates the non-specific bands associated with the 5-HT_{1B} primers. The 'hot-start' PCR method was therefore employed hereafter.

The RT-PCR reaction was repeated a further three times on all samples. Unfortunately, the bands corresponding to the 5-HT_{1B} mRNA was so feint on all three runs that the computer program was unable to differentiate the density of the bands from background. If the bands were intensified using the computer program to make them visible, the bands corresponding to the β-actin mRNA became so intense that it was no longer possible to quantitate the PCR reaction (see figure 4.5). The RT-PCR reaction can be quantified by normalizing the density of each 5-HT_{1B} band to the corresponding β-actin band to give a value of 'adjusted volume counts x mm^2'. However, it is only possible to do so if the value for 'maximum counts' i.e. the density of an individual band, is less than 255 as calculated by the computer package. On all three RT-PCR reactions, the density of the β-actin bands gave values greater than 255, and were thus saturated.

The level of 5-HT_{1B} mRNA in the extracted RNA from these SCN samples must therefore be minimal. It was consequently decided to 'start from scratch' and repeat the RNA extraction using a different method. The Dynabead® mRNA separation kit has the advantage of extracting only *m*RNA, and not *total* RNA as extracted using the TRIzol reagent. The extraction product is therefore more specific and more concentrated.

4.3.1.3 mRNA extraction from SCN, retinal and raphe brain samples

Using the Dynabead® mRNA DIRECT kit mRNA was extracted from SCN, RET and RAP samples at ZTs 0, 3, 6, 9, 12, 15, 18 & 21. The quantity of RNA present in each sample was calculated using the absorbance value at 260 nm (see Table 4.2). The mean mRNA concentration for SCN, RET and RAP samples (± s.e.m) were 0.15 ± 0.04, 0.16 ± 0.02 and 0.24 ± 0.07 μg/μl, respectively.

Sample ZT	0	3	6	9	12	15	18	21
SCN	0.22	0.14	0.14	0.14	0.10	0.12	0.18	0.12
RET	0.16	0.15	0.14	0.18	0.16	0.17	0.12	0.19
RAP	0.37	0.24	0.32	0.20	0.24	0.22	0.16	0.20

Table 4.2: mRNA concentration of SCN, retinal (RET) and Raphe (RAP) brain tissue expressed as μg/μl, calculated by the absorbance at 260 nm.

4.3.1.4 RT-PCR reaction

To ensure that the mRNA separated by following the protocol from the Dynabead® mRNA DIRECT kit would produce bands of a sufficient intensity to quantify the reaction, an RT-PCR reaction was performed on each brain region at a single time point, and different volumes of RT product loaded onto the gel. Figure 4.6 shows the effect of differential loading of 5-HT_{1B} RT product of RET, RAP and SCN samples taken at ZT 0. For each sample, 5 and 10 μl of 5-HT_{1B} product was loaded along with 5 μl of the β-actin product. As anticipated, the β-actin product produced a very intense signal. Loading 5 μl of 5-HT_{1B} product was sufficient to produce detectable bands, although for SCN sample this was only very feint. Loading 10 μl of product was an improvement and produced bands of greater intensity, although these were still not as intense as the signal generated from the β-actin product. For subsequent RT-PCR reaction products, it was decided to load 20 μl for the 5-HT_{1B}-primed samples so that the samples would be of equal intensity to the 5 μl of loaded β-actin product.

All SCN, RET and RAP samples at ZTs 0, 3, 6, 9, 12, 15, 18 and 21 underwent an RT-PCR reaction which was repeated three times. Figures 4.7, 4.8 and 4.9 respectively,

show representative gels for SCN, RET and RAP tissues. The 5-HT_{1B} mRNA was quantified by normalizing each band to the corresponding β-acin mRNA band.

The intensity of the band produced by the RT-PCR reaction product across the eight zeitgeber times showed significant variations in both the SCN and the RET tissues, but not in the RAP tissue. In the SCN, the signal for the 5-HT_{1B} mRNA at both ZTs 0 and 3 were significantly higher than that at ZT 12 ($p < 0.05$; $p < 0.01$), and ZT 3 was significantly higher than ZT 21 ($p < 0.05$). In the RET tissue the intensity at ZT 0 was significantly higher than at all other zeitgeber times ($p < 0.05$).

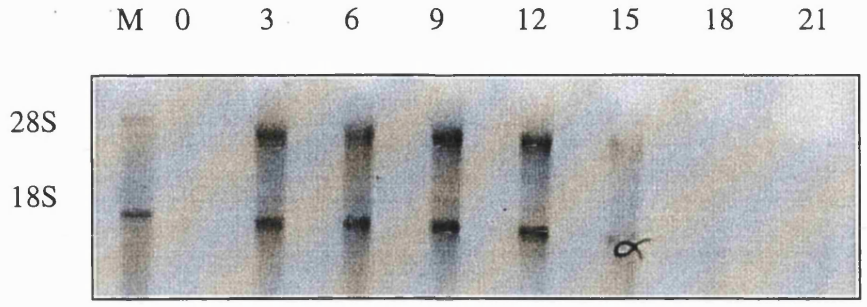

Figure 4.2. Separation of the isolated total RNA from rat brain SCN samples. 1 μg of each sample was loaded and run against a ribosomal RNA marker (M) which separates the 28S and 18S fragments (annotated on the left hand side of the gel). Zeitgeber times are indicated above the corresponding band. Samples 0, 3, 6, 9, 12 and 15 all have intact 28S and 18S fragments. Samples 18 and 21 do not appear to have rRNA bands, although there was no evidence of RNA breakdown products or DNA contaminating bands.

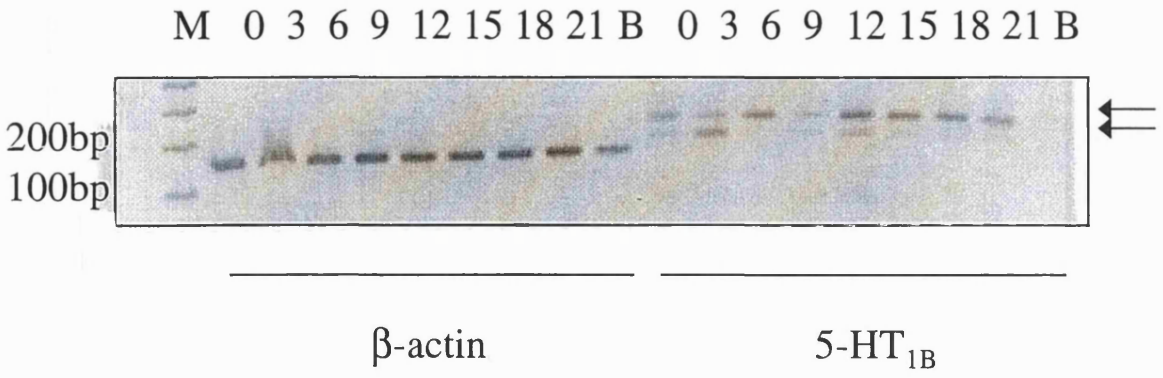

Figure 4.3. Initial RT-PCR analysis using total RNA from rat brain SCN tissue resulted in non-specific annealing of the 5-HT_{1B} mRNA primer producing a double band indicated by the black arrows to the right of the gel. β-actin mRNA is shown on the left and 5-HT_{1B} mRNA on the right of the gel. Zeitgeber times are indicated above the corresponding band. M=100bp molecular weight marker; B=blank.

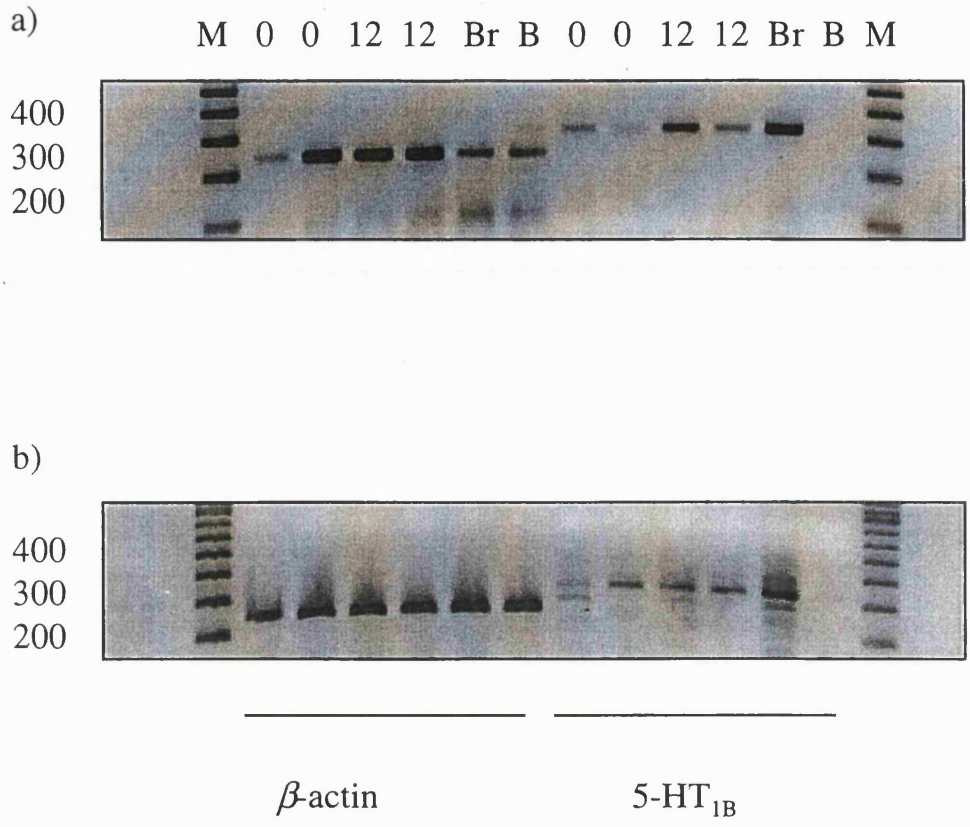

Figure 4.4. "Hot Start" PCR (**A**) versus "normal" PCR (**B**) on rat brain SCN tissue. Hot start PCR eliminates the double bands due to the non-specific annealing of the 5-HT_{1B} primer (refer to figure 4.3). β-actin mRNA is shown on the left and 5-HT_{1B} mRNA on the right of the gel. M=100bp molecular weight marker, indicated on the left hand side of the gel; 0=ZT 0; 12=ZT 12; Br=whole brain; B=blank.

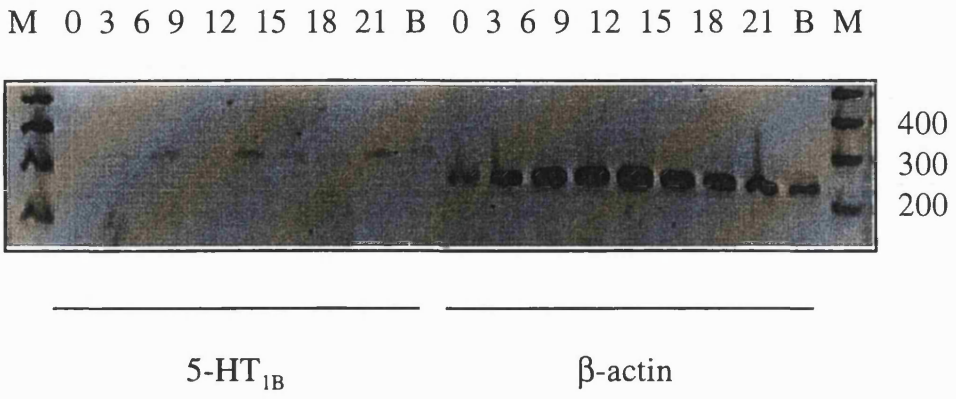

Figure 4.5. RT-PCR on total mRNA extracted from rat brain SCN tissue. The bands corresponding to 5-HT_{1B} mRNA (left) are too feint for analysis by density, and the β-actin bands (right) are too intense. Zeitgeber times are indicated above the corresponding band. M=100bp molecular weight marker, indicated on the right hand side of the gel; B=blank.

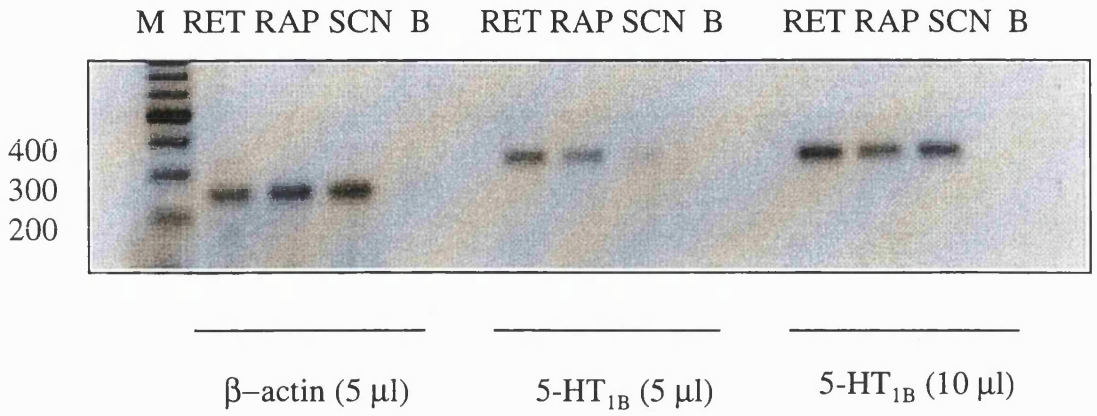

Figure 4.6. Effect of differential loading of the 5-HT_{1B} RT-PCR product. 200 ng of retinal (RET), raphe (RAP) and SCN mRNA were used in the RT-PCR reaction. 5 µl of β-actin product (left) was loaded against 5 µl (middle) and 10 µl (right) of 5-HT_{1B} product. M=100bp molecular weight marker, indicated on the left hand side of the gel; B=blank.

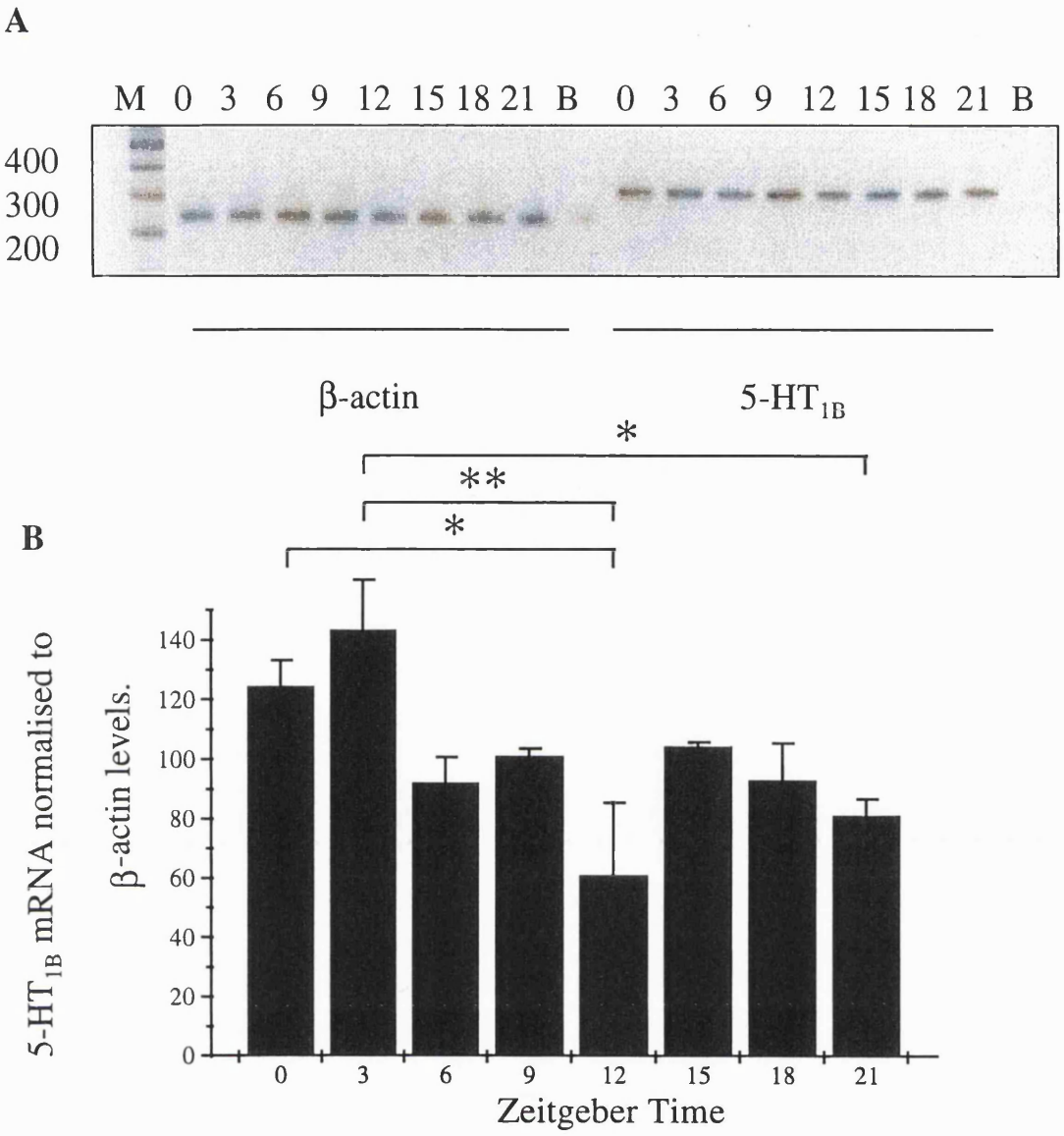

Figure 4.7. (**A**) A representative blot from isolated rat brain SCN tissue at eight zeitgeber times over twenty four hours. β-actin expression is shown on the left and 5-HT_{1B} expression on the right of the gel. Zeitgeber times are indicated above the corresponding band. M=100bp molecular weight marker, indicated on the left hand side of the gel. (**B**) SCN 5-HT_{1B} mRNA at ZTs 0, 3, 6, 9, 12, 15, 18 and 21 normalised to β-actin levels and plotted as a percentage of the mean value. Values are mean ± s.e.m. (n=3). *$p < 0.05$; **$p < 0.01$.

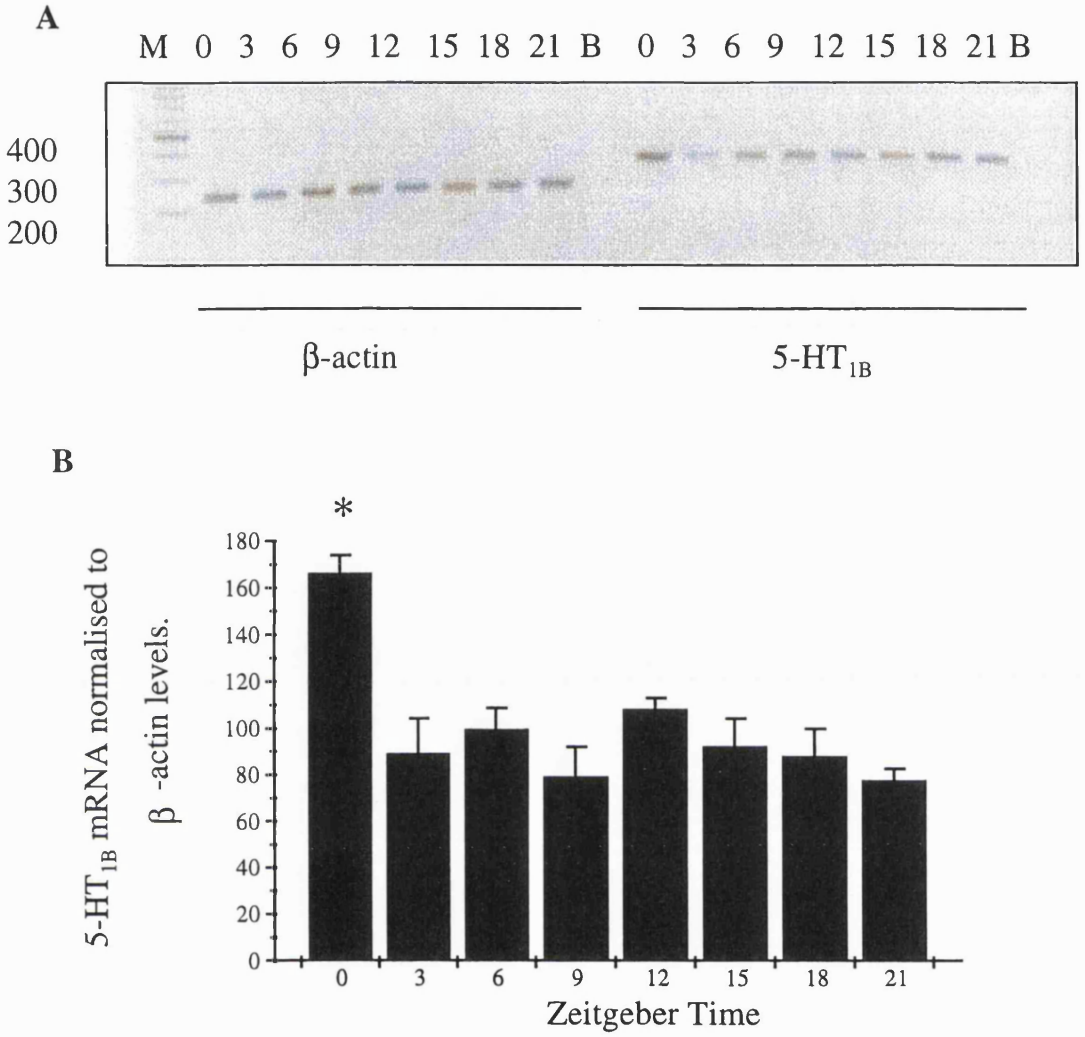

Figure 4.8. (**A**) A representative blot from isolated rat retinal mRNA at eight zeitgeber times over twenty four hours. β-actin expression is shown on the left and 5-HT_{1B} expression on the right of the gel. Zeitgeber times are indicated above the corresponding band. M=100bp molecular weight marker, indicated on the left hand side of the gel. (**B**) Retinal 5-HT_{1B} mRNA at ZTs 0, 3, 6, 9, 12, 15, 18 and 21 normalised to β-actin levels and plotted as a percentage of the mean value. Data are mean ± s.e.m. (n=3). *$p < 0.05$.

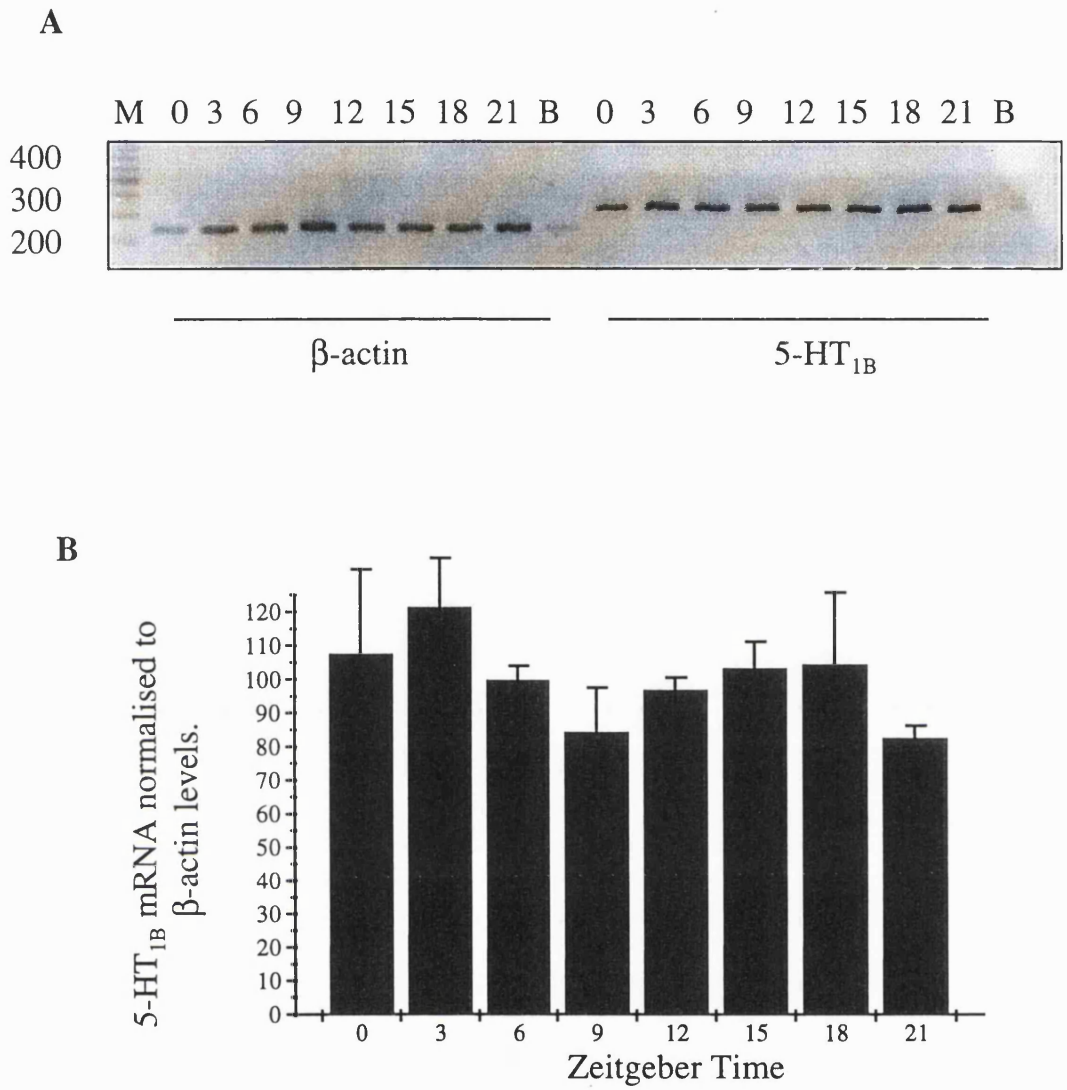

Figure 4.9. (**A**) A representative blot from isolated rat brain raphe nuclei mRNA at eight zeitgeber times over twenty four hours. β-actin expression is shown on the left and 5-HT_{1B} expression on the right of the gel. Zeitgeber times are indicated above the corresponding band. M=100bp molecular weight marker, indicated on the left hand side of the gel. (**B**) Raphe 5-HT_{1B} mRNA at ZTs 0, 3, 6, 9, 12, 15, 18 and 21 normalised to β-actin levels and plotted as a percentage of the mean. Values are mean ± s.e.m. (n=3).

4.3.2 IMMUNOCYTOCHEMISTRY

The SCN is known to contain a high density of 5-HT_{1B} receptors as verified by receptor binding experiments of the hypothalamus (Prosser *et al*, 1993; Manrique *et al*, 1994), and it is on this basis that the microdialysis experiments were performed in the preceding chapter to investigate the 5-HT_{1B} hetero- and auto-receptors. Thus, the SCN serves as its own positive control for immunocytochemical staining for the 5-HT_{1B} receptor protein.

Each slide had four brain sections mounted on them. The first set of experiments involved two slides from two of the three triplicate brains chosen from ZTs 0 and 12 i.e. a total of eight slides. Four groups of two slides were fixed in a solution of 4 % paraformaldehyde and incubated separately in 0.1, 0.5, 1.0 and 2.0 μg of primary antibody for an initial period of 60 min. Figure 4.10A represent a photomicrograph of a brain section at the level of the mid SCN which was incubated in 2.0 μg of primary antibody. There is a complete absence of staining in the region of the SCN and indeed on any of the brain tissue in any of the sections incubated in the range of the primary antibody. There was however, an intense staining above that of the background in the cerebral arteries/choroid plexus present in the lateral ventricles (figure 4.10B). This observation that no staining was evident anywhere in the brain tissue but was seemingly picked up in non-neuronal tissue was very puzzling.

The experiment was repeated on a further eight slides changing the fixative to cold acetone, using 2.0 μg of the primary antibody and increasing the primary antibody incubation period to 30 hours on half of the slides. Once again there was a complete absence of 5-HT_{1B} receptor staining in any of the brain tissue above that of background staining (data not shown). It was thus decided to enzyme treat and heat treat some of the sections in case the antigenic determinant was being masked by the fixation process. It was hoped that the antigenic site might be exposed by the chymotrypsin or heat treatment. Half of the sections prepared for the enzyme or heat treatment were fixed in 4 % paraformaldehyde, whist the other half were fixed in cold acetone. The chymotrpsin treated sections looked no different to those sections that had not been treated with enzyme, whereas the microwave treatment, as recommended by Santa Cruz

Biotechnology, seemingly destroyed the tissue, and nothing was detected post-DAB incubation (data not shown).

In addition to following the protocol supplied, other brain sections were treated slightly differently. Triton-X 100 is a detergent often used to permeabilise the section to allow entry of the antibody without opening up the tissue so far that you lose the target. It is most often used in all PBS washes and incubation solutions up until the DAB incubation stage. Due to the nature of the 5-HT_{1B} receptor being present on the surface of the cell, it is not necessary to add Triton-X 100 to the PBS wash stages. However, in an attempt to aid detection of the 5-HT_{1B} receptor protein in the neuronal tissue Triton-X 100 was added to all PBS washes (0.3 %). Again, the antibody failed to detect any antigenic sites within the neuronal tissue (data not shown).

Communicating directly with Santa Cruz Biotechnology who developed the antibody failed to shed light onto the inability of the antibody to detect 5-HT_{1B} receptor protein in neural tissue. Upon further communication with the company it was revealed that the antibody had never been tested for its ability to immunocytochemically detect the protein in animal tissue, let alone brain tissue, and no institution had ever used the antibody successfully so that they had published papers quoting Santa Cruz as the suppliers.

This failure to detect the 5-HT_{1B} receptor protein in the brain tissue was very disappointing, and also prevented the planned double labeling studies (5-HT_{1B}/glutamate and 5-HT_{1B}/serotonin) to proceed. The antibody was thus tested in a homogenate of brain tissue and detected by Western blotting, which in itself is a far from ideal method of detecting what may be very delicate changes in levels of receptor protein.

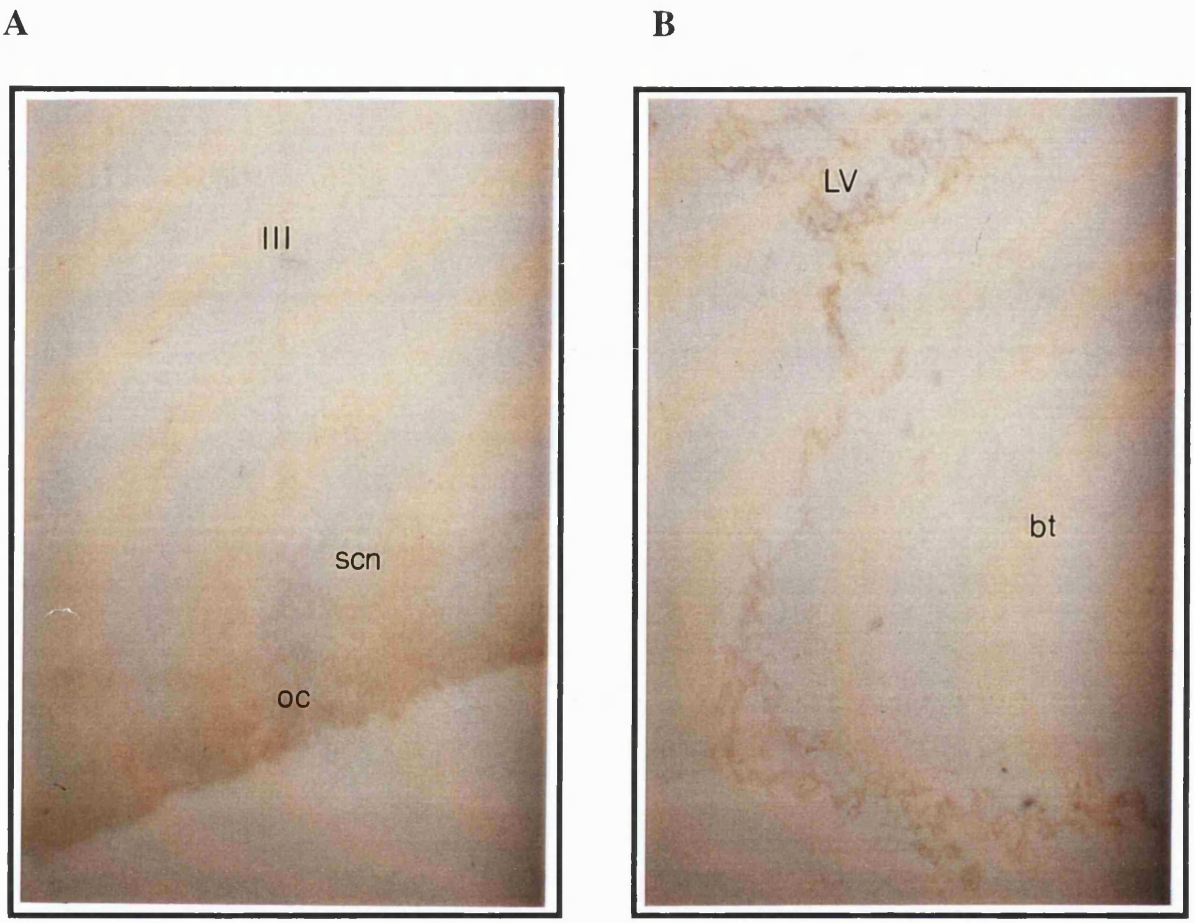

Figure 4.10. Representative brain sections at the level of the hypothalamus after immunocytochemical detection with an antibody raised against the 5-HT_{1B} receptor. For methods see text. Brain sections were fixed using a solution of 4 % paraformaldehyde and incubated in 2 µg primary antibody for a period of 60 min. (**A**) At the level of the suprachiasmatic nucleus (scn). Note the complete absence of immunocytochemical staining in the brain tissue. oc = optic chiasm; III = third ventricle. (**B**) Immunolabelled cells were observed in the lateral ventricles (LV) in non-neuronal tissue. Again, note the absence of staining in the brain tissue (bt). Magnification x 40.

4.3.3 WESTERN BLOTTING

4.3.3.1 Determination of tissue protein concentration

The Bradford Protein Assay was used to assess total protein concentration of the prepared SCN, raphe (RAP) and whole brain (WB) tissue. Table 4.3 shows the protein concentration of SCN samples at ZTs 0, 3, 6, 9, 12, 15, 18 and 21 (2xSCN at each ZT, duplicated). The average protein concentrations were 12.2 ± 0.78 and 13.0 ± 0.62 μg/μl for duplicate A and duplicate B, respectively. The total protein concentration of whole brain, raphe (2xRAP) and SCN 'test' (4xSCN) samples were 27.02 μg/μl, 10.81 μg/μl and 15.56 μg/μl, respectively.

Sample ZT	0	3	6	9	12	15	18	21
A:[protein]μg/μl	10.65	14.39	12.81	15.18	12.23	8.27	13.02	10.86
B;[protein]μg/μl	11.29	15.47	14.03	13.81	13.02	12.81	13.74	9.78

Table 4.3: Total protein concentration expressed as μg/μl in each SCN sample as determined by the Bradford Protein Assay. A and B represent the two sets of samples for each zeitgeber time (ZT). Each ZT represents 2xSCN samples.

4.3.3.2 Optimization of conditions for Immunoblotting

In order to optimize the conditions for immunoblotting 4x SCN samples were dissected at ZT 6, pooled and used as SCN 'test' samples, along with one whole brain and 2x raphe samples (ZT 6) for use as positive controls. It was necessary to optimize each of the following parameters; blocking buffer, primary antibody concentration, secondary antibody concentration and total protein concentration loaded per well on the gel.

A preliminary experiment was performed varying the primary antibody concentration (0.1 and 0.5 μg), varying the amount of total protein loaded (20 - 80 μg; SCN and WB) and utilizing a blocking buffer consisting of 5% BSA, 1% ovalbumin and 0.05% azide in TBS. Secondary antibody concentration was 1:40,000. Figure 4.11 shows the resultant blots with very high background and no distinct band at approximately 43 KD (molecular weight of 5-HT_{1B} receptor 43,162 KD), which would suggest either non-specific binding of the secondary antibody or insufficient 'blocking' by the blocking

buffer, providing that the primary antibody was specific and sensitive enough to detect the low amount of 5-HT_{1B} protein anticipated in the samples. The specificity of the secondary antibody was confirmed when another membrane was prepared for immunoblotting as above, but with the primary antibody step excluded. The developed blot had no staining (data not shown) which was to be expected if the secondary antibody was not responsible for the non-specific bands. Therefore the non-specific binding was due either to the primary antibody or the blocking buffer. Repeating the experiment using 2 μg primary antibody in an attempt to increase binding to the 5-HT_{1B} protein, 1:40,000 secondary antibody, loading 60 μg total protein (SCN, RAP and WB) and replacing the blocking buffer with a solution of 5% dried milk (Marvel), 0.05% azide in TBS-T resulted in much 'cleaner' blots with a single intense band just below the 45 KD molecular weight marker (see Figure 4.12). From this result it was decided to run RAP as a positive control as it gave a more intense signal than the WB.

Using 5% dried milk in TBS-T as the blocking buffer of choice, the experiment was repeated once again in a bid to optimize the primary and secondary antibody concentration as well as the amount of total protein loaded. Six gels were run in parallel varying the primary antibody concentration (0.1, 0.5 and 1.0 μg), secondary antibody concentration (1:10,000 and 1:20,000) and running RAP and SCN tissue at 20, 40 and 60 μg total protein (see Figure 4.13). The most intense signal was generated by a primary antibody concentration of 1 μg and a secondary concentration of 1:10,000 (Figure 4.13E). All three blots blotted with 1:10,000 secondary antibody had higher non-specific binding than those blotted with 1:20,000, although there remained some background staining at this dilution. The lower primary antibody concentrations resulted in very weak staining of the 5-HT_{1B} protein and at the lowest concentration failed to result in specific staining (Figure 4.13A and B). Taking these results into consideration, a primary antibody concentration of 1.0 μg in combination with a secondary antibody concentration of 1:40,000 was postulated to result in the 'cleanest' blots - it was thought that lowering the secondary antibody concentration further would eliminate background staining.

With regard to varying the total protein concentration loaded per well, the intensity of the protein band of interest varied; 20 μg resulted in weakest staining and 60 μg resulted

in the greatest staining, most evident in Figure 4.13F. Occasionally loading a high protein concentration results in characteristic 'smearing' of the bands but this was absent and it was therefore decided to load 60 μg of total protein per well.

Consequently, the optimal conditions for analysis of the 5-HT_{1B} receptor protein in SCN samples were identified as being: 1 μg primary antibody; 1:40,000 secondary antibody dilution whilst loading 60 μg total protein and using 5% dried milk in TBS-T as a blocking buffer.

The SCN samples (ZT 0, 3, 6, 9, 12, 15, 18 and 21) were run on a gel with RAP as a positive control. Each set of samples were run twice. Figure 4.14 shows the effect of zeitgeber time on SCN 5-HT_{1B} receptor protein expression in the two groups of samples, measured by Western blotting. There is no marked difference in the density of the bands at any zeitgeber time.

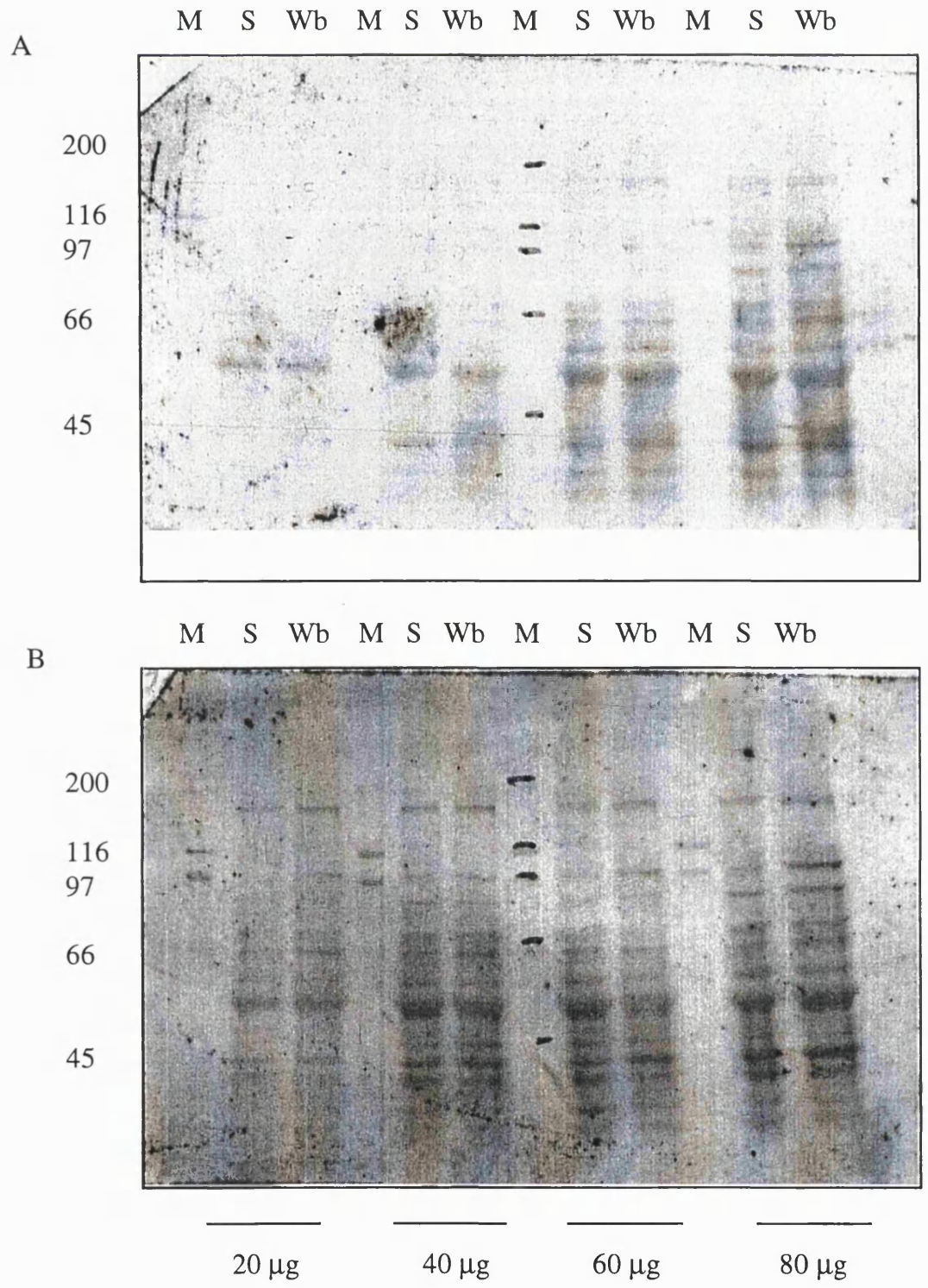

Figure 4.11. Preliminary Western blot analysis of SCN (S) and whole brain (Wb) tissue varying the primary antibody concentration and total protein loading. Secondary antibody dilution 1:40,000; blocking buffer 5 % BSA, 1 % ovalbumin, 0.05 % azide in TBS. Differential total protein loading is displayed along the bottom of blot B. Primary antibody concentration 0.1 µg (A) and 0.5 µg (B). M = Molecular weight markers (100 bp), indicated on the left hand side of the gel.

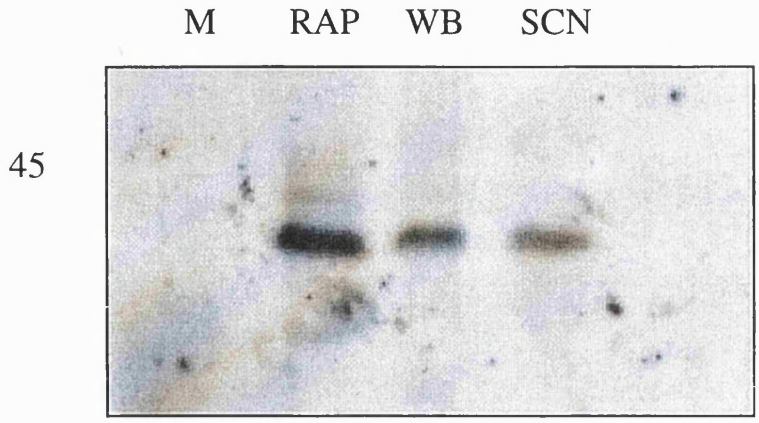

Figure 4.12. Western blot analysis of raphe (RAP), whole brain (WB) and SCN tissue. 60 µg of total protein was loaded in each lane and blotted with 2 µg of primary antibody with a secondary antibody antibody dilution of 1:40,000. The blocking buffer utilised consisted of 5 % dried milk in TBS-T. M = molecular weight marker (100 bp), indicated on the left hand side of the gel.

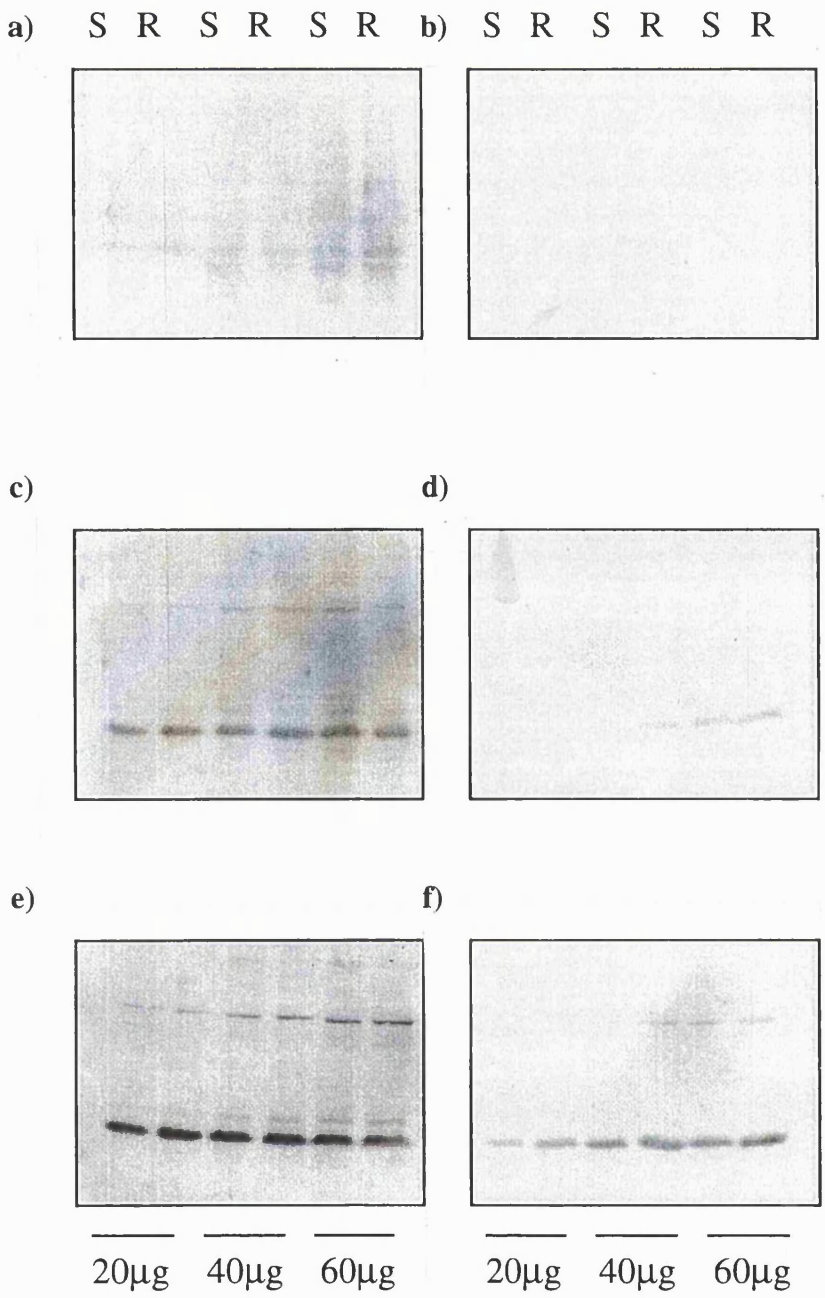

Figure 4.13. Western blot analysis of SCN (S) and raphe (RAP) tissue using 5% milk in TBS-T as the blocking buffer. Varying the primary antibody concentration; (a) and (b) 0.1 µg; (c) and (d) 0.5 µg; (e) and (f) 1.0 µg, the secondary antibody dilution; (a), (c) and (e) 1:10,000; (b), (d) and (f) 1:20,000, and the total protein loaded per well (displayed along the bottom of the blots).

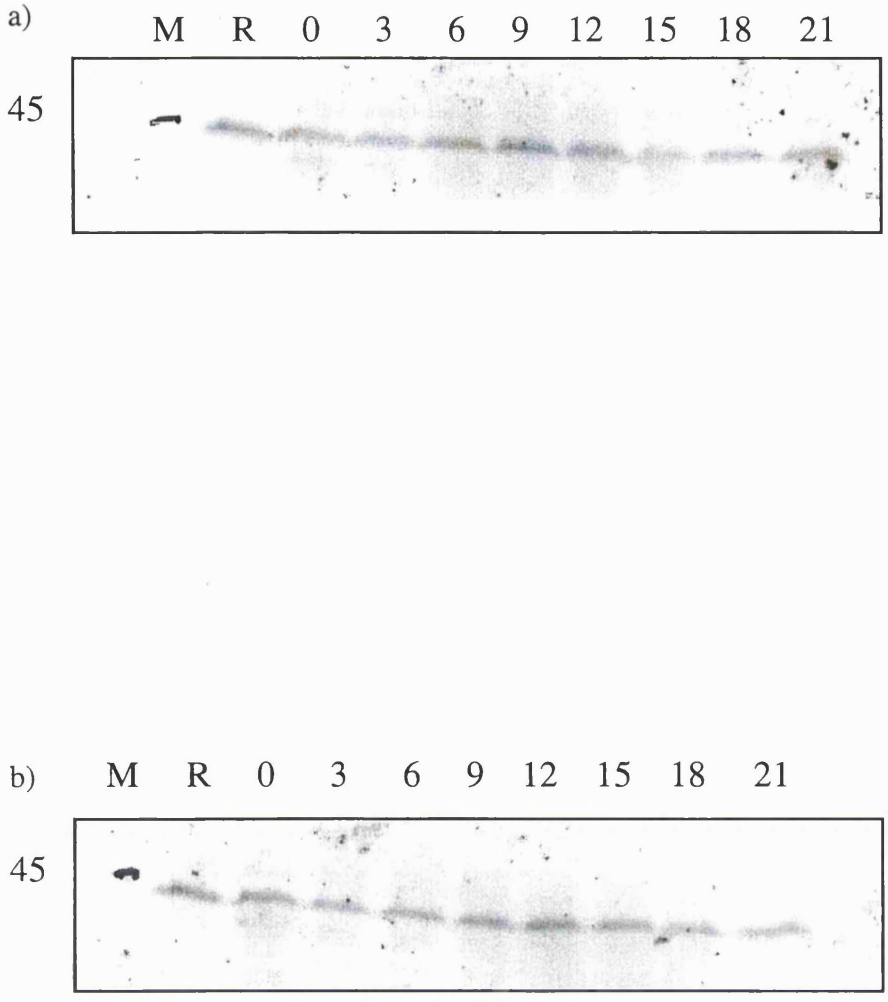

Figure 4.14. Western blot analysis of 5-HT_{1B} receptor protein in SCN tissue at zeitgeber times (ZTs) 0, 3, 6, 9, 12, 15, 18 and 21. At each ZT 2x SCN were dissected and the tissue pooled. This was performed in duplicate to provide two sets of SCN samples at each ZT. a) and b) represent the results from each duplicate. Proteins were extracted from the tissue and separated on a 10% SDS-PAGE gel (60 µg of total protein loaded per sample) and transferred to a nitrocellulose membrane. The 5-HT_{1B} receptor protein was probed using 1 µg of primary antibody and 1:40,000 dilution of secondary antibody. The blocking buffer used was 5% dried milk in TBS-T. M = molecular weight marker; RAP = raphe sample (positive control).

4.4 DISCUSSION

4.4.1 5-HT_{1B} receptor mRNA levels in SCN, raphe and retina

Reverse transcriptase-polymerase chain reaction was used to identify day-night differences in the expression of the 5-HT_{1B} receptor in the SCN, retina and midbrain raphe nuclei of the rat. RT-PCR is a method widely used to identify different mRNA products in various brain areas and has been used previously to identify day-night or circadian changes in gene expression in SCN (e.g. Ghosh *et al.*, 1997) and retina (e.g. Gauer *et al.*, 1995) and to analyse 5-HT receptor subtypes in a presumptive serotonin cell line derived from the rat raphe (Jackson *et al.*, 1997). The method of RT-PCR can produce results with small quantities of total RNA as it is based on significant signal amplification and is relatively sensitive. This is crucial when working with limited sample size such as the dissected SCN, retina or raphe, which will contain limited amounts of mRNA.

The primer used for the amplification of the 5-HT_{1B} receptor was specific for the rat 5-HT_{1B} receptor, as the PCR product of the "hot-start" PCR produced a single band with the ethidium bromide under UV light (figure 4.12). When the "normal" PCR reaction was performed, multiple bands were present, indicative of non-specific annealing of the primers, before the commencement of the reaction i.e. before the reaction mixture has reached the starting temperature of 94°C.

The amount of total mRNA isolated by the TRIzol reagent in this study was similar to total RNA isolated from mouse SCN (O'Hara *et al*, 1995). O'Hara and colleagues (1995) isolated 0.6 μg of total RNA from 1 mm^3 sections of SCN, which although a smaller block of tissue than obtained in this study, they were using mouse brain which is expected to yield a smaller amount of brain tissue. The method of isolation of total RNA with the TRIzol Reagent produced only very feint bands upon amplification with the 5-HT_{1B} primers (figure 4.13), possibly because of loss of mRNA fragments in the separation procedure, which is a somewhat lengthy process. However, the isolation of mRNA with the Dynabeads® mRNA DIRECT kit, produced a much cleaner and more intense signal (figure 4.15), and was therefore the separation method of choice for the SCN, raphe and retinal mRNA. It can be seen from the amount of total RNA versus the amount of mRNA isolated from similar sized blocks of tissue that a vast amount of total

RNA is lost during the isolation procedure. mRNA constitutes only about 5 % of total RNA and if one compares the amount of total RNA (0.51 ± 0.10 μg/μl) with that of mRNA (0.15 ± 0.04 μg/μl) in the SCN tissue, it would appear that the mRNA represents almost 30 % of the total RNA. The actual total RNA concentration is most probably higher than the value reported here and it can be assumed to have been lost during the separation procedure.

Because of the semi-quantitative and subjective nature of the densitometry of the PCR products, this method of detection of mRNA within the tissue cannot be expected to provide us with definitive answers, but rather to give a perspective on what is going on. However, changes in receptor expression in different tissue samples are visible. For example, the expression of 5-HT_{1B} mRNA in the retina, appears to be greater than in the raphe, which is greater than in the SCN (figure 4.14). It is known that the SCN contains very little 5-HT_{1B} mRNA (Roca *et al.*, 1993), which is often missed by *in situ* hybridization analysis (Neumaier *et al.*, 1996). Bruinvels *et al.* (1994) failed to detect high 5-HT_{1B} mRNA in the SCN, although they did so in the arcuate hypothalamic nuclei. Since the dissection of the SCN also included a small section of surrounding hypothalamic tissue, it is possible that the mRNA amplified by the RT-PCR reaction originated from hypothalamic nuclei other than the SCN. Indeed, Neumaier and colleagues (1996) detected high levels of 5-HT_{1B} mRNA in the dorsomedial hypothalamic area and in the anteroventral preoptic area, which might have contaminated the SCN tissue. However, since the PCR reaction is a very sensitive technique, it will be able to detect changes in expression in the SCN against a constant background in other nuclei. Bruinvels and his coworkers (1994) also measured a more intense signal in the midbrain raphe nuclei than in the hypothalamus, and this is visible in my data as a higher density band.

In the SCN the peak signal was generated at ZTs 0 and 3 and the nadir at ZT 12 and 21. None of the other 4 time points were significantly different from each other, although as a general trend, intensity was lower than at ZT 0 and 3. Gene expression, measured by *in situ* hybridization, of peptides (somatostatin; Nishiwaki *et al.*, 1995; vasointestinal peptide and gastrin releasing peptide; Zoeller *et al.*, 1991), immediate early genes (c-fos; Prosser *et al.*, 1994a) and receptors (vasointestinal peptide 2 receptor; Cagampang *et al.*, 1998) have all been shown to exhibit day-night differences in the SCN of rats.

Therefore, the finding of a day-night difference in 5-HT_{1B} mRNA is not surprising, and allows us to add another receptor to the list of a growing number of factors displaying fluctuating levels throughout the 24 hour cycle of darkness and light in the SCN. Only one study performed to date has investigated the relationship between the 5-HT_{1B} receptor and the SCN and involved detection by *in situ* hybridization of brain tissue from animals maintained in constant darkness (Roca *et al.*, 1993). As outlined in the Introduction to this chapter, maintainance of the animals in constant darkness will measure circadian rather than diurnal variation. The results presented in this thesis are the first to demonstrate that light can influence the regulation of the 5-HT_{1B} receptor gene. The fluctuation in 5-HT_{1B} mRNA in the SCN represents variations in the number of terminal region 5-HT_{1B} receptors, located in SCN projection sites (for efferent projection of SCN neurones see Watts and Swanson, 1987). mRNA is generated in the cell body region, and in the case of the 5-HT_{1B} receptor, is transported to neuronal terminals where it exerts its effects. Therefore, this fluctuation in expression would not account for a variation in SCN 5-HT_{1B} receptor sensitivity.

As mentioned in the discussion section of the preceding chapter behavioural investigation of the 5-HT_{1B} postsynaptic receptor suggests that the function of the receptor undergoes diurnal variation, with the ability of a receptor antagonist to block the behavioural response to administration of the 5-HT_{1B} agonist RU24969 more pronounced during the light phase (Martin *et al.*, 1987). Similarly a study by Moser and Redfern (1984) identified a diurnal variation in the ability of a serotonergic agonist to produce a behavioural response with peak activity occurring at mid-light. Although in their study they could not identify the receptor subtype involved, it is possible that the agonist is acting via 5-HT_{1B} receptors. The results of these behavioural experiments may be explicable by variation in the number of 5-HT_{1B} receptors produced in the SCN across the light:dark cycle as identified in this study. An increased expression of the receptor will probably manifest itself by an increase in available receptors and a greater cumilative response to agonist stimulation.

In the retina, there was a peak signal generated at ZT 0, which was significantly different from all other time points. None of the other seven time points were significantly different from each other. Circadian changes in gene expression in the retina have previously been examined by the use of Northern blot analysis (Sakamoto

and Ishida, 1998) and RT-PCR analysis (Gauer *et al.*, 1995), but to my knowledge no author has looked at 5-HT_{1B} receptor expression across the light dark cycle in the retina. Isolation of the mRNA from the retina, with subsequent amplification of the 5-HT_{1B} signal, unfortunately does not identify the cell types in which the signal was generated. Retinal ganglion cells project to the SCN (Moore *et al.*, 1995), but one cannot establish using this method, whether it is these cells are displaying the variation in expression. Therefore, we cannot be sure that the variation in expression shown here will ultimately lead to a variation in the number 5-HT_{1B} receptors on RHT nerve terminals in the SCN. Other retinal projection sites include the lateral geniculate nucleus, raphe nuclei, thalamic nuclei and the superior colliculus (e.g. Shen and Semba, 1994), all of which might synthesize the 5-HT_{1B} receptor. Indeed, the afferents to the superior colliculus are known to have 5-HT_{1B} heteroceptors at their terminals (Mooney *et al.*, 1994), and it is possible that the variation in 5-HT_{1B} receptor mRNA in the retina will lead to a variation in receptor expression in the superior colliculus, or one of the other projection sites. The presence of the 5-HT_{1B} mRNA in the retinal ganglion cells projecting to the SCN must therefore be verified by techniques such as *in situ* hybridization in which the cells producing the mRNA can be identified.

If the increased production of 5-HT_{1B} receptor mRNA at ZT 0 was indeed located in the retinal ganglion cells projecting to the SCN, it is important to remember that these receptors are heteroceptors. A variation in the density of 5-HT_{1B} heteroceptors would not explain the variation in 5-HT_{1B} autoreceptor function as identified by the *in vivo* microdialysis studies. The relevant tissue here is the raphe, in which the serotonergic neurones projecting to the SCN would house the 5-HT_{1B} receptor mRNA production.

In the raphe tissue there was no difference in signal intensity generated over the eight zeitgeber times i.e. the expression of the 5-HT_{1B} receptor was constant across the light dark cycle. The block of tissue containing the midbrain raphe, was the largest of the three dissected tissues, and contained the largest quantity of total mRNA (table 4.3). Because of the uncertainty about whether the MRN or the DRN sends projections to the SCN (see discussion Chapter 6), the block of tissue dissected had to encapsulate both the MRN and DRN. It is possible that variation in MRN and DRN could display different phases and thus cancel each other out. Therefore, a fluctuation in expression in the raphe neurones projecting to the SCN was masked by a reversed fluctuation in gene

expression in other neurones within the block of tissue. However, it is unlikely that gene expression for a single receptor will show such contrasting rhythms as to cancel each other out, in what is still a relatively small amount of tissue. High levels of 5-HT_{1B} receptor mRNA have previously been located to the raphe nuclei using *in situ* hybridization (Bruinvels *et al.*, 1994). The DRN has been shown to express higher levels than the MRN (Neumaier *et al.*, 1996). The observation that 5-HT_{1B} receptor mRNA levels are reduced by 75 % in the MRN and DRN after serotonergic lesioning by 5,7-dihydroxytryptamine (Doucet *et al.*, 1995) indicates that this receptor is synthesized in serotonergic neurones. However, the remaining 25 % of receptor mRNA not destroyed by the neurotoxin may represent 5-HT_{1B} receptors that are present on non-serotonergic neurones in the raphe. In my study I could not distinguish between receptors in serotonergic or non-serotonergic neurones. In addition, firing rate of raphe neurones has been shown to be controlled by 5-HT_{1B} receptors on the cell body (Davidson and Stamford, 1995) and the RT-PCR reaction will also include these receptors in its amplification.

Assuming that the lack of diurnal variation in the whole block of raphe tissue represents those receptors projecting to the SCN, the SCN will receive a constant signal for this receptor across the light:dark cycle. If so, one must assume that the number of receptors expressed and transported to the SCN terminals will be constant during the day and night.

4.4.2 5-HT_{1B} receptor protein in the SCN

Immunocytochemistry and Western blotting were the techniques employed to detect 5-HT_{1B} receptor protein in the SCN at eight equally spaced time points across the light:dark cycle.

Immunocytochemistry is a commonly used technique capable of giving a high degree of spatial information in locating specific proteins either within individual cells or to a small sub-population of cells within a tissue sample. It is therefore the method of choice to detect small changes in receptor numbers in a given area of tissue in the brain due to the quantitative nature of the technique. Unfortunately, I was unable to detect any staining in the neuronal tissue using the antibody supplied to us by Santa Cruz Biotechnology. In biological tissues proteins can be lost by metabolism if the biological

processes of the tissue are not arrested. However, because of the rapid freezing of the brain after removal, one cannot assume that the 5-HT_{1B} receptor protein was lost due to inadequate handling of the tissue. Indeed, confirmation by Western blotting showed that the 5-HT_{1B} receptor protein was present in the neuronal tissue. Changing the fixative, incubating the primary antibody for much longer periods and even trying to expose the antigenic site by enzymatic digestion and heat treatment failed to result in the antibody detecting the 5-HT_{1B} receptor in the neuronal tissue, and I was forced to conclude that the antibody is not suited to this method of detection.

The method of Western blotting to detect proteins in a supernatant fraction of brain tissue thus had to be relied upon. Once the system has been optimized for each particular antibody and tissue sample, this method is a reliable way of detecting proteins. However, it has the disadvantage of not giving a spatial relationship between brain nuclei and protein location. That is, immunocytochemistry can locate proteins in brain nuclei and individual neurones, whereas Western blotting can only give an indication that a protein is present in the tissue, and in that respect the technique is much like that of RT-PCR. Also, a relatively large block of tissue is dissected which encapsulates the SCN and, like the experiments using RT-PCR, the amount of protein detected may be contaminated by nuclei other than the one of interest. That does not mean however that changes in receptor protein levels cannot be detected by this method.

Western blotting has served to locate proteins in the SCN of rats in previous studies (Reuss *et al.*, 1995; Spessert *et al.*, 1995). The methodology followed in both of these studies was similar to that used here, in which the SCN of four animals were pooled for subsequent analysis. One of these studies (Spessert *et al.*, 1995) tried to identify variations in tissue protein levels of the enzyme neuronal nitric oxide synthase during manipulation of the light:dark cycle. Although they failed to detect changes in protein levels in the SCN using Western blotting at two time points across the light dark cycle, they were able to detect differences in another important structure, the pineal gland. This study thus demonstrates that Western blotting can be used to identify changes in protein levels in tissue samples.

As is evident from the sample blots shown in figure 4.14 there were no marked differences in the intensity of bands corresponding to any zeitgeber time tested. A

densitometer was not used to compare the density of each band, because although the amount of total protein loaded was equal, there was no 'internal standard', unlike the β-actin housekeeping gene in the RT-PCR studies. It therefore remains subjective whether a change is visible. From the blots shown in figure 4.14, it appears the band corresponding to ZT 9 is more intense than the other bands, and that the band at ZT 15 is less intense (figure 4.14A). However, from the second set of samples run one can see that the bands are of a more equal density (figure 4.14B). This stresses the importance of repeating the immunoblotting on more than one set of samples.

5-HT_{1B} receptor detected by radioligand binding in the SCN has been shown to be significantly higher during the dark than during the light phase (Posser *et al.*, 1993). The results from my Western blot analysis do not agree with these findings. However, from the limitations of the Western blot technique outlined already, one must be cautious to come to a definite conclusion. The difference between the results from the binding study (Prosser *et al.*, 1993) and the Western blot analysis (present study) may reflect the fact that the two methods are identifying different receptor populations. The functional 5-HT_{1B} receptor is located on the cell surface *in situ* and radioligand binding will detect the receptors that are at the cell surface. Western blotting on the other hand will detect all protein in the tissue homogenate that the antibody recognises. It may be that at different phases in the circadian cycle, the receptor is internalised and so not functional, although still detected by the Western blotting technique. By contrast, the radioligand binding study would only detect receptors expressed at the external surface of the cell. The advent of a commercially available antibody raised against the 5-HT_{1B} receptor that can be used immunologically to detect the receptor in brain slices is much awaited.

4.5 CONCLUSIONS

The expression of the 5-HT_{1B} receptor in the rat has been shown, using RT-PCR, to differ across the light dark cycle in the SCN and retina, but not in the midbrain raphe nuclei. In the SCN the highest levels of 5-HT_{1B} mRNA were seen at the start of the light period at ZTs 0 and 3, whilst the lowest levels were at ZT 12, the very start of the dark period, and at ZT 21, towards the end of the dark period. In the retina, there was a

very distinct peak in expression at ZT 0, with expression across the remainder of the light dark cycle showing no fluctuation.

Because the 5-HT_{1B} mRNA levels in the block of raphe tissue did not vary across the light:dark cycle. as measured by RT-PCR, it is unlikely that changes in 5-HT_{1B} mRNA, leading ultimately to changes in receptor levels on neuronal terminals, will account for the variation in the 5-HT_{1B} receptor sensitivity as measured by *in vivo* microdialysis experiments.

On the basis of these Western blotting experiments, the amount of 5-HT_{1B} receptor protein present in the dissected SCN tissue remains constant across the light:dark cycle. The variation in 5-HT_{1B} receptor function detected using *in vivo* microdialysis is therefore unlikely to be due to variation in the *total* number of receptors available, but rather to internalisation/phosphorylation of the receptor rendering it insensitive to agonist stimulation, or to changes in second messenger systems as discussed in the preceding chapter.

CHAPTER 5

GLUTAMATERGIC RECEPTOR AGONIST REGULATION OF 5-HT RELEASE IN THE SCN

5.1 INTRODUCTION

The significant number of serotonergic and glutamatergic fibres and pathways in the mammalian brain give rise to the possibility of an interaction between these two transmitter systems. 5-HT often serves as a neuromodulator for glutamatergic transmission in many different animal species and brain regions including cerebellum (Maura *et al.*, 1988; Maura and Raiteri, 1996), substantia gelatinosa of the spinal cord (Travagli and Williams, 1996), the locus coeruleus in the midbrain (Aston-Jones *et al.*, 1991) and even human neocortical slices (Maura *et al.*, 1998). Likewise, excitatory amino acid regulation of serotonergic transmission is evident in many midbrain and forebrain areas (Whitton *et al.*, 1994; Fink *et al.*, 1996; Tao and Auerbach, 1996; Tao *et al.*, 1997).

The SCN of the hypothalamus receive a dense innervation from the retina, terminating in the ventral-lateral aspect of the nuclei (Moore and Lenn, 1972). The putative transmitter of this pathway is glutamate (see Chapter 1: 1.2.1). Another principle pathway to the SCN is that originating in the midbrain raphe (Moore *et al.*, 1978), releasing 5-HT at its terminals (see Chapter 1: 1.2.2), which also terminates in the ventral-lateral region of the nuclei. The close proximity of the serotonergic and glutaminergic terminals in the SCN lead to the possibility that interaction between these two systems is necessary to maintain efficient functioning of the circadian pacemaker. Data from several laboratories suggest that the serotonergic projection to the SCN may serve to modulate the responses of the circadian system to light (e.g. Bradbury *et al.*, 1997).

The brief insight into the role of the serotonergic system as outlined in the General Introduction (Chapter 1) in regulating circadian rhythms gives some indications of the complexity of the interactions between just these two systems amongst the plethora of neurotransmitter substances within the pacemaker (van den Pol and Tsujimoto, 1985; Watts and Swanson, 1987). In the preceding chapter we confirmed (Selim *et al.*, 1993; Srkalovic *et al.*, 1994) that stimulation with a 5-$HT_{1A/1B}$ receptor agonist decreases extracellular glutamate in the SCN region, presumably at the terminals of the RHT. The aim of the experiments described in this chapter was to establish the role of exitatory amino acid (EAA) receptor stimulation in the SCN on the response to 5-HT. NMDA-

(Whitton *et al.*, 1994; Fink *et al.*, 1995; 1996; Tao *et al.*, 1996; Pallotta *et al.*, 1998), AMPA- (Ohta *et al.*, 1994; Maione *et al.*, 1997; Tao and Auerbach, 1997; Singewald *et al.*, 1998) and kainate- (Tao *et al.*, 1997) induced changes in extracellular 5-HT levels as measured *in vitro* using brain slices or more often *in vivo* using microdialysis have all been recorded in various brain nuclei. The ionotropic NMDA, AMPA, kainate and the metabotropic glutamate receptor mRNA levels have all been detected in the SCN of rodents (Gannon and Rea, 1994; van den Pol, 1994; Mick *et al.*, 1995; O'Hara *et al.*, 1995; van den Pol *et al.*, 1995; Ghosh *et al.*, 1997), and thus the possibility exists that stimulation of these EAA receptors might affect 5-HT release within the SCN.

It was the aim of this study to elucidate a role for the excitatory amino acid agonists in the release of 5-HT from the circadian pacemaker. *In vivo* microdialysis was utilised in this study to determine the effect of a local infusion of ionotropic and metabotropic glutamate receptors on 5-HT overflow in the SCN. Ampa, kainate and NMDA were used to elucidate a role for each class of ionotropic glutamate receptor in the regulation of 5-HT release from the SCN. To date, there are eight subtypes of metabotropic glutamate receptors grouped into three classes (group I,II and III) (Pin and Duvoisin, 1995), but only mRNA for group I and II receptors have been located to the SCN (van den Pol, 1994; Mick *et al.*, 1995; van den Pol *et al.*, 1995). Therefore, the group I / group II metabotropic agonist 1S,3R-ACPD was chosen to establish a role of this class of receptor in the control of 5-HT release in the SCN. Experiments were carried out at ZT 6 (mid-light) and ZT 18 (mid-dark) to establish diurnal variation in the action of these drugs.

5.2 PROTOCOL

5.2.1 Animals

Male Wistar rats (University of Bath strain; 260-320 g) were maintained under a 12:12 light:dark cycle regime (lights on 07:00 "normal" light:dark cycle; lights on 19:00 "reverse" light:dark cycle; temperature 22 ± 2°C). The animals were housed in cages of six prior to experimentation, with food and water available *ad libitum*.

5.2.2 Microdialysis

Each animal was implanted with a microdialysis probe as described in chapter 2 section 2.2.3 directed at the SCN, and introduced to the experimental cage. The probe was continuously perfused with aCSF (1.2 µl/min) containing 1 µM of the SSRI citalopram. Six 15 min control samples were collected, and the three samples immediately before drug infusion served as the pre-intervention controls. At zeitgeber times 6 or 18 drugs were infused for a period of 60 min via the probe. For antagonistic studies, the antagonist was infused for an additional 30 min prior to and during the 60 min infusion with the agonist. Dialysate samples were collected every 15 min over a period of 2 hours post-drug infusion, and analysed for 5-HT content using HPLC-ED, as described in chapter 2 section 2.3.5. Samples not being analysed immediately were snap frozen and maintained on dry ice until analysis. At the end of the experiments the animals were killed by CO_2 asphyxiation and the brains removed and frozen onto dry ice. Slicing freehand with a sharp razor blade, the probe tract was clearly visible as a fine line through the brain tissue. With the aid of a stereotaxic atlas (Paxinos and Watson, 1982) the position of the probe tract within the hypothalamus was established. The animals whose probe tracts were not in the target area were discarded for analysis.

5.2.3 Drugs

NMDA (*N*-methyl-D-aspartate), kainic acid (kainate), AMPA (α-amino-3-hydroxy-5-methyl-4-isoxazolapropionate) and idazoxan were obtained from Sigma Chemical Co.; ACPD [(1S,3R)-1-aminocyclopentane-1,3-dicarboxylic acid], AP5 [(±)-2-amino-5-phosphonopentanoic acid] and E4CPG [(RS)-α-ethyl-4-carboxyphenylglycine] from Tocris Cookson Ltd.; MK-801 [(5R,10S)-(+)-5-methyl-10,11-dihydro-5H-

dibenzo[a,d]cyclohepten-5,10-imine / dizocilpine) was provided by Dr. Chris Bolton and citalopram hydrobromide by Lundbeck (Copenhagen-Valby)

5.2.4 Statistics

5-HT concentration in the dialysate samples (not-corrected for probe recovery) were expressed as a percentage of the three pre-intervention controls samples. Values post-drug treatment were analysed by one-way analysis of variance (ANOVA) with repeated measures with Student Newman Keuls post hoc test to detect differences between pre-intervention controls samples. $p < 0.05$ was considered statistically significant.

5.3 RESULTS

Control infusion of the SCN with aCSF at ZT 6 and 18 resulted in a stable 5-HT output for the duration of the 120 min collection period (figure 5.1). The 5-HT concentration in the dialysate fractions did not vary significantly from the three pre-intervention control samples. Basal 5-HT concentrations at ZT 6 and 18 were 36.3 ± 8.89 and 28.1 ± 5.34 fmol respectively.

5.3.1 Effect of local infusion of AMPA into the SCN

A 60 min infusion of AMPA (10 mM and 1 mM) into the SCN at ZT 6 resulted in an increase in dialysate 5-HT (figure 5.2A). Unfortunately at these doses the animals died between 30 and 90 minutes after the start of the infusion. Infusion of 100 μM AMPA did not kill the animal but failed to affect 5-HT overflow at either ZT 6 or ZT 18 (figure 5.2B).

5.3.2 Effect of local infusion of kainate into the SCN

A 60 min infusion of kainate (100 μM) into the SCN at ZT 6 and 18 resulted in a significant increase in dialysate 5-HT concentration (figure 5.3). Maximal increase at ZT 6, expressed as a percentage change relative to three pre-intervention controls, was 233 ± 19.8 % ($p < 0.001$), and occurred 60 min after the start of the infusion. Thirty min after the end of the AMP infusion, 5-HT had returned to baseline levels. Maximal increase at ZT 18 was 198 ± 45.5 % ($p < 0.05$), 45 min after the start of the infusion. Before the end of the AMPA infusion the 5-HT levels were not significantly different from control levels.

5.3.3 Effect of local infusion of NMDA into the SCN

The effect of a 60 min infusion of NMDA into the SCN on 5-HT overflow was dependant upon the concentration, and the zeitgber time at which NMDA was applied. At ZT 6 (figure 5.4A), 100 μM NMDA failed to affect SCN 5-HT, whilst 1 mM NMDA resulted in a significantly elevated 5-HT overflow from the SCN (162 ± 26.9 %; $p < 0.05$) 30 min after the start of the infusion. Although the 5-HT levels remained elevated for the duration of the collection period, they were not significantly different from control levels. At ZT 18, 100 μM and 1 mM NMDA had contrasting effects (figure

5.4B). 100 μM NMDA resulted in a significant decrease in measured 5-HT 45 min after the start of the infusion (52.0 ± 21.5 % of baseline levels; $p < 0.05$). The 5-HT concentration then returned to basal before becoming significantly elevated 60 min after the end of the infusion (183 ± 38.3 %; $p < 0.05$). 1 mM NMDA significantly increased dialysate 5-HT levels 30 min after the start of the infusion; 5-HT levels remaining elevated until the end of the infusion (peak increase 206 ± 24.8 %; $p < 0.01$). After cessation of the infusion, the 5-HT concntration returned to levels not significantly different from baseline.

The effectiveness of the non-competitive NMDA antagonist (+)-MK801 was also dependant upon the zeitgeber time at which it was applied. Thirty min pretreatment with MK801 (10 μM) blocked the effect of 1 mM NMDA at ZT 6 (figure 5.5A), but failed to prevent the increase in 5-HT overflow following 1 mM NMDA, or the decrease following 100 μM NMDA (figure 5.6A and 5.6B, respectively). MK801 infusion (10 μM) alone for 90 min at ZT 6 resulted in a prolonged and significant decrease in dialysate 5-HT concentration (maximal decrease 48.6 ± 7.00 % of baseline; $p < 0.01$; figure 5B). MK801 infusion (10 μM; 90 min) at ZT 18 did not produce significant changes in dialysate 5-HT overflow (figure 5.7).

Thirty min pretreatment with the competitive NMDA antagonist AP5 (100 μM) prevented the increase in dialysis 5-HT overflow after 1 mM NMDA infusion, and the decrease after 100 μM NMDA at ZT 18 (figures 5.8A and 5.8B respectively).

Concurrent application of the α_2-adrenoreceptor antagonist idazoxan (1 μM) with 100 μM NMDA at ZT 6 significantly elevated the dialysate 5-HT concentration 30 min after NMDA infusion to 137 ± 9.20 % of pre-intervention control levels ($p < 0.01$; figure 5.9A), whereas when given alone the NMDA had failed significantly to affect the 5-HT levels. At ZT 18, application of idazoxan (1 μM) with NMDA (100 μM) resulted in a significantly increased dialysate 5-HT level (225 ± 58.2 % of pre-intervention controls; $p < 0.05$), 45 min after the start of the infusion, which exactly mirrored the effect of application of NMDA alone. A 60 min infusion of idazoxan alone (1 μM) failed significantly to change SCN 5-HT concentration at ZT 18 (figure 5.10).

5.3.4 Effect of local infusion of ACPD into the SCN

The effect of a 60 min infusion of ACPD into the SCN was both concentration- and zeitgeber time- dependant. At ZT 6 (figure 5.11A), 100 μM ACPD failed to significantly affect dialysate 5-HT concentration, although the trend was toward a drop in 5-HT levels; maximal decrease was 70.5 ± 14.2 % of the pre-intervention controls. 1 mM ACPD produced an immediate and significant increase in dialysate 5-HT to 183 ± 31.7 % of pre-intervention controls ($p < 0.05$). AT ZT 18, neither 100 μM or 1 mM ACPD produced significant changes in measured 5-HT (figure 5.11B).

30 min pretreatment with the metabotropic antagonist E4CPG (100 μM) completely blocked the effect of 1 mM ACPD at ZT 6 (figure 5.12A). Infusion of E4CPG alone (100 μM) for 90 min did not significantly effect SCN 5-HT levels (figure 5.12B).

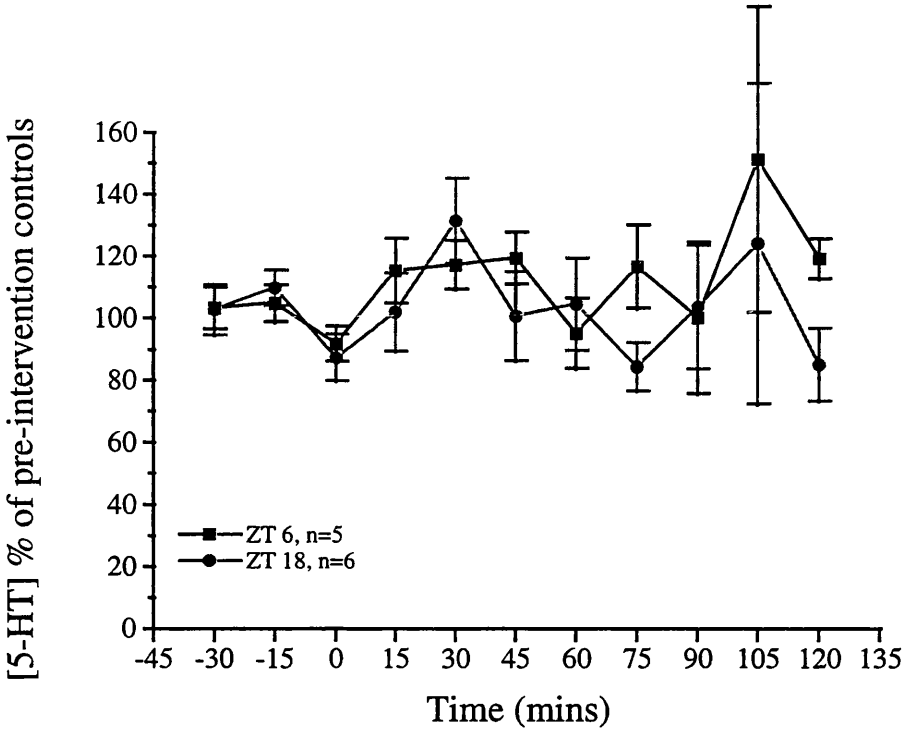

Figure 5.1: Control 5-HT concentration ([5-HT]) expressed as mean ± s.e.m percentage values of of three pre-intervention controls, at zeitgeber times (ZT) 6 and 18. Time 0 on the X-axis denotes the zeitgeber time.

A

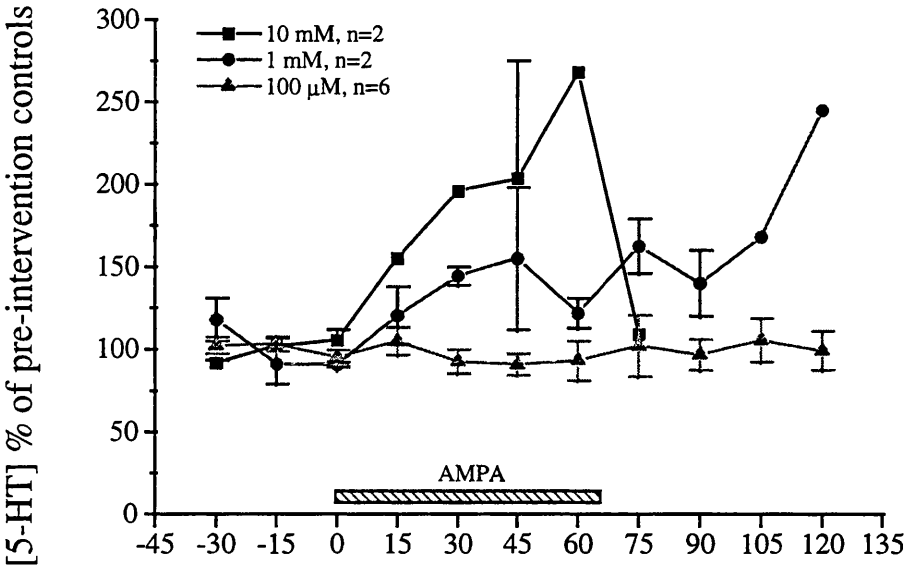

B

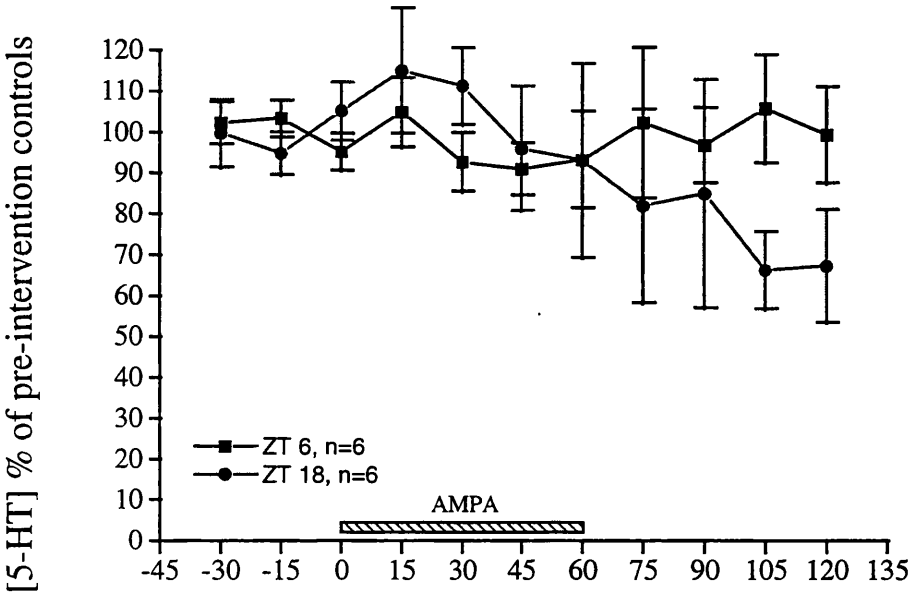

Figure 5.2. Effect of AMPA on 5-HT overflow in the SCN. Results are mean ± s.e.m. values expressed as a percentage of three pre-intervention controls. AMPA was infused into the SCN via the dialysis probe for 60 min as indicated by the hatched bar. Time 0 on the X-axis denotes the zeitgeber time. **A:** 10 mM, 1 mM and 100 µM AMPA, ZT 6. **B:** 100 µM AMPA at ZT 6 and ZT 18.

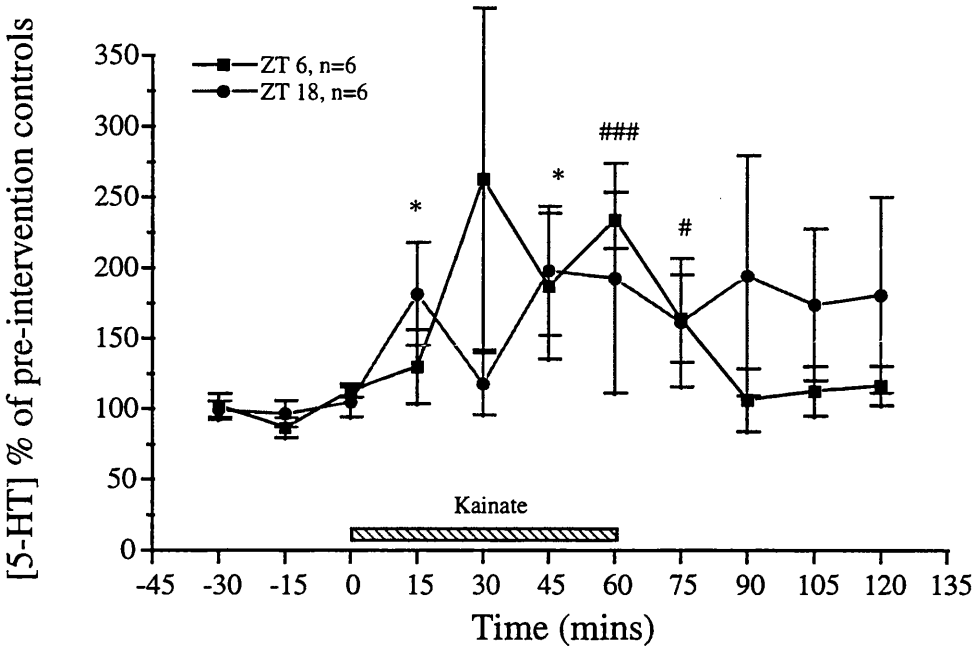

Figure 5.3. Effect of kainate (100 μM) on 5-HT overflow in the SCN. Results are mean ± s.e.m. values expressed as a percentage of three pre-intervention controls. Kainate was infused into the SCN via the dialysis probe for 60 min as indicated by the hatched bar. Time 0 on the X-axis denotes the zeitgeber time. For ZT 18 * $p < 0.05$; For ZT 6 # $p < 0.05$, ### $p < 0.001$.

A

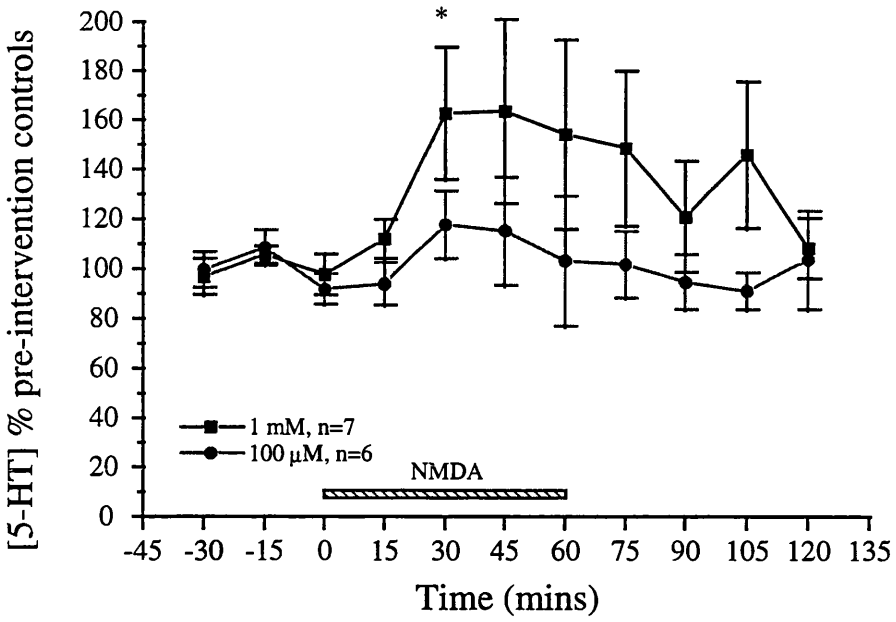

B

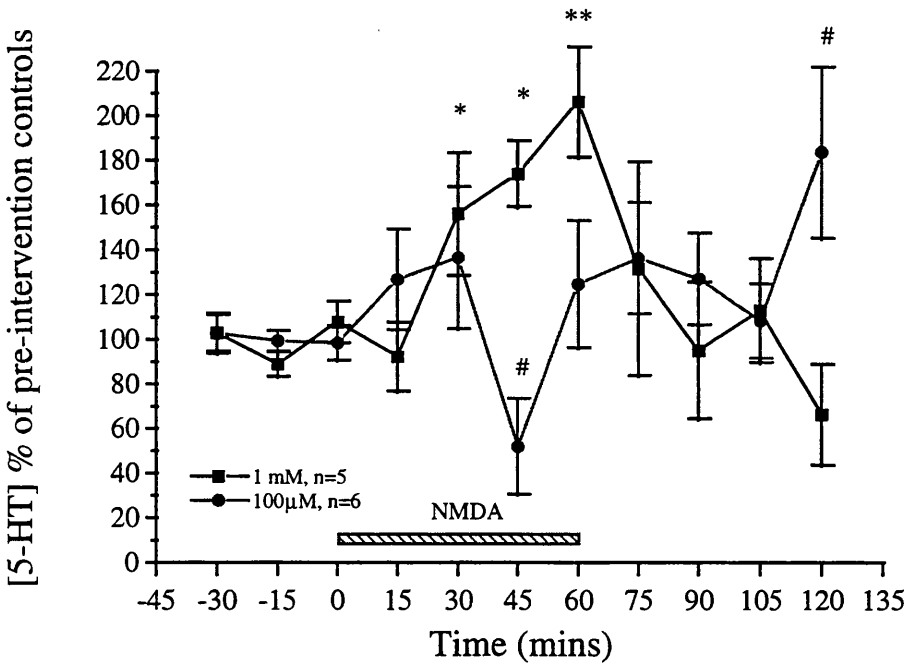

Figure 5.4. Effect of NMDA (1 mM and 100 µM) on 5-HT overflow in the SCN. Results are mean ± s.e.m. values expressed as a percentage of three pre-intervention controls. AMPA was infused into the SCN via the dialysis probe for 60 min as indicated by the hatched bar. Time 0 on the X-axis denotes the zeitgeber time. **A:** ZT 6; * $p < 0.05$. **B:** ZT 18; * $p < 0.05$ and ** $p < 0.01$ for 1 mM NMDA; # $p < 0.05$ for 100 µM NMDA.

A

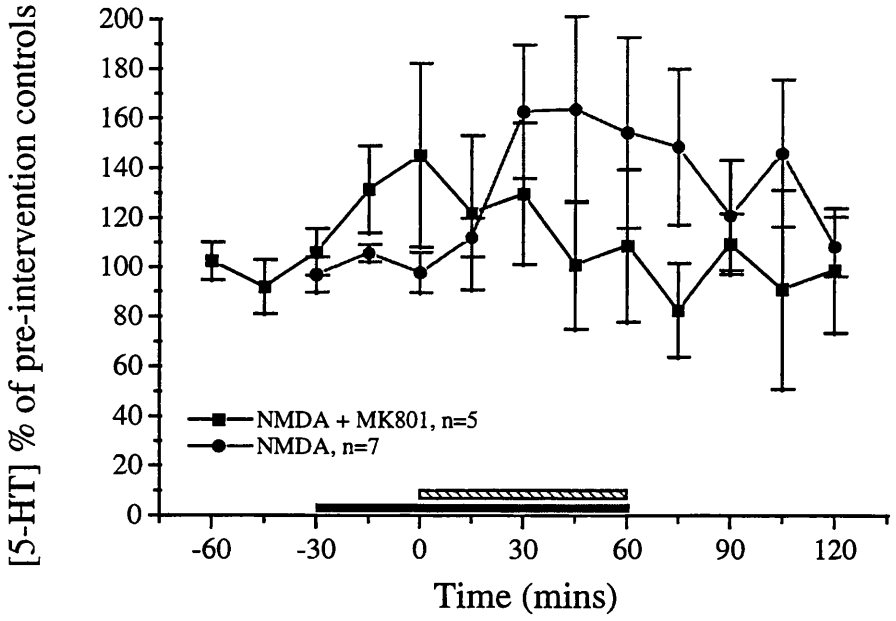

B

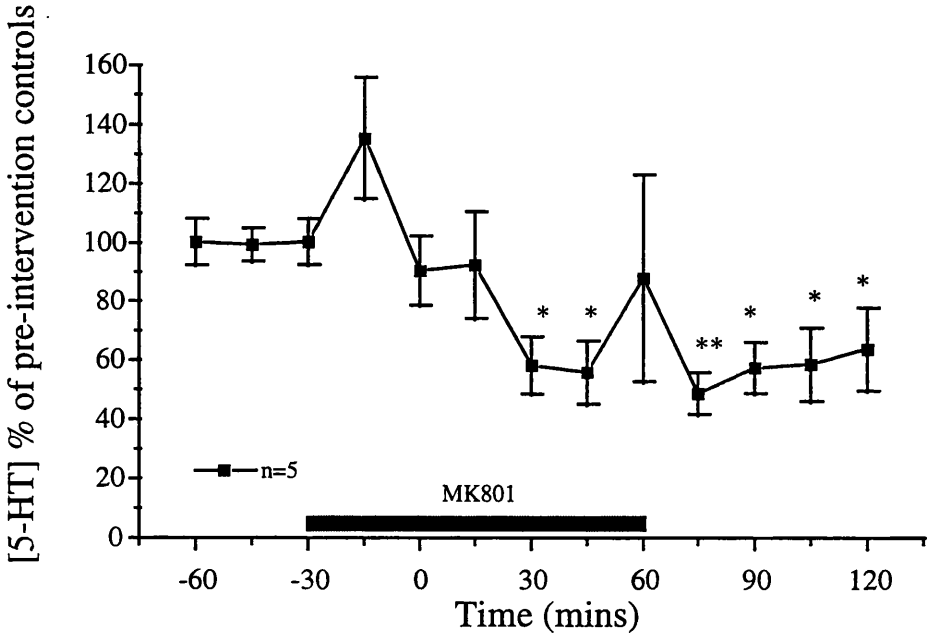

Figure 5.5. **A:** Effect of the non-competitive NMDA antagonist (+)-MK801 on the response to NMDA in the SCN at ZT 6. Results are mean ± s.e.m. values expressed as a percentage of three pre-intervention controls. MK801 (10 μM) was infused 30 min prior to, and 60 min concurrently with NMDA (100 μM), via the dialysis probe. The solid bar denotes MK801 infusion and the hatched bar NMDA infusion. **B:** Effect of MK801 (10 μM) infusion alone on SCN 5-HT concentration at ZT 6. MK801 was infused via the dialyis probe for 90 mins. * $p < 0.05$; ** $p < 0.01$.

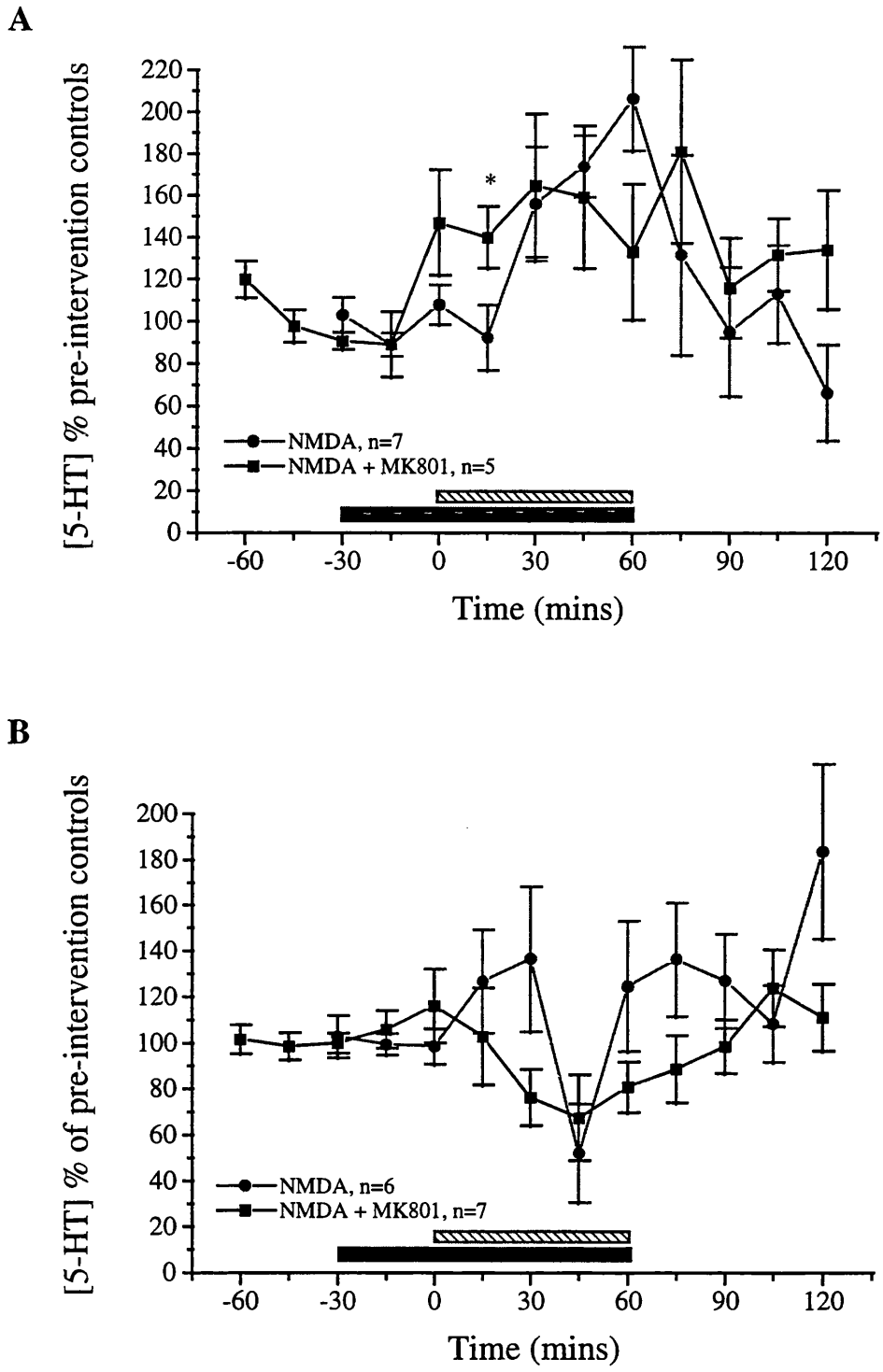

Figure 5.6. Effect of the non-competitive NMDA antagonist (+)-MK801 on the response to NMDA in the SCN at ZT 18. Results are mean ± s.e.m. values expressed as a percentage of three pre-intervention controls. MK801 (10 μM) was infused 30 min prior to, and 60 min concurrently with NMDA (1 mM, **A**; 100 μM, **B**), via the dialysis probe. The solid bar denotes MK801 infusion and the hatched bar NMDA infusion. * $p < 0.05$.

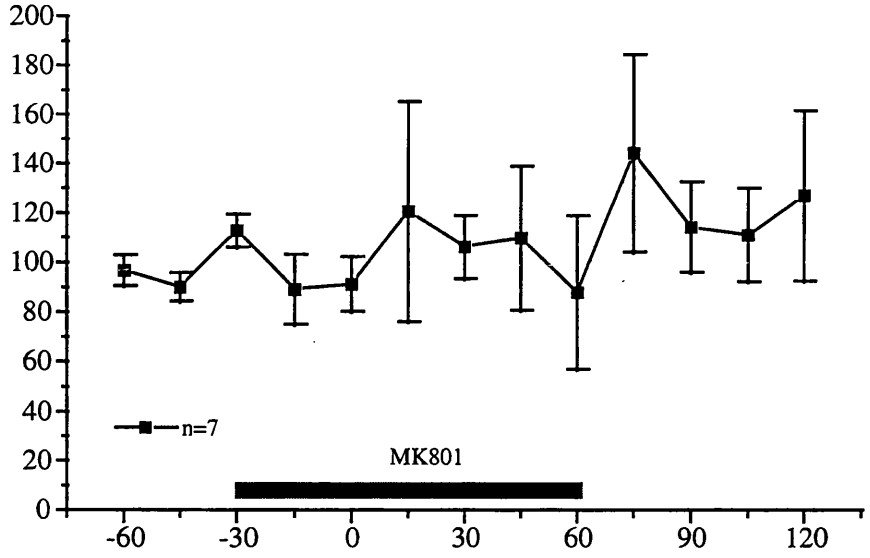

Figure 5.7. Effect of MK801 (10 μM) infusion alone on SCN 5-HT concentration at ZT 18. MK801 was infused via the dialyis probe for 90 mins, denoted by the solid bar. Results are mean ± s.e.m. values expressed as a percentage of three pre-intervention controls.

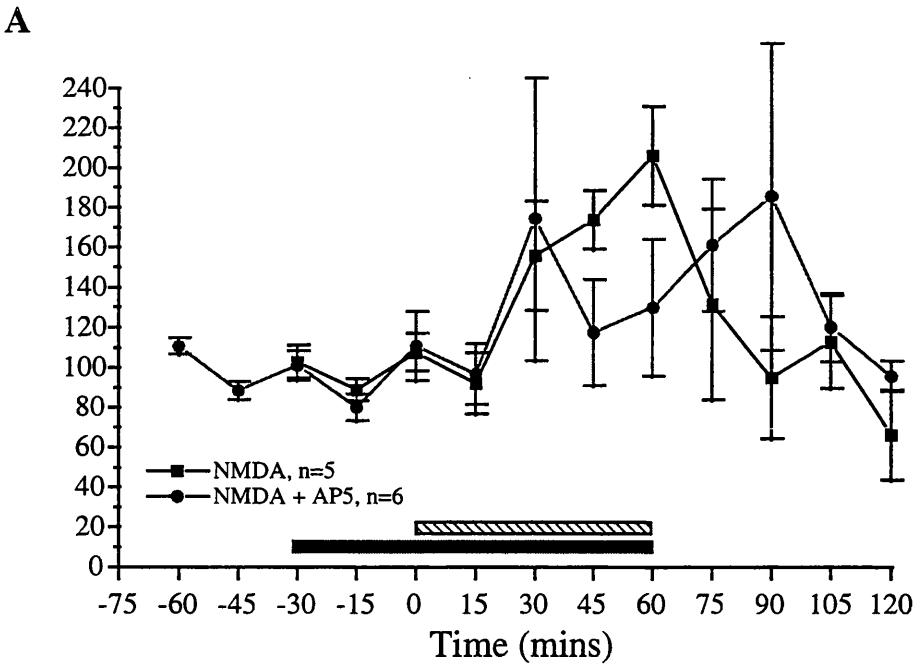

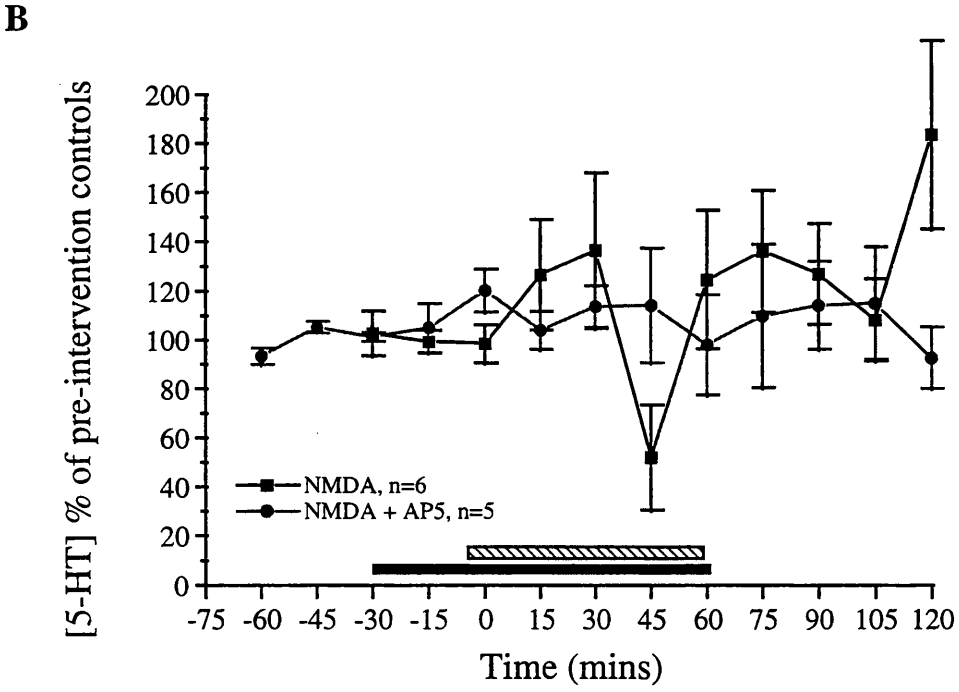

Figure 5.8. Effect of the competitive NMDA antagonist AP5 on the response to NMDA in the SCN at ZT 18. Results are mean ± s.e.m. values expressed as a percentage of three pre-intervention controls. AP5 (100 μM) was infused 30 min prior to, and 60 min concurrently with NMDA (1 mM, **A**; 100 μM, **B**), via the dialysis probe. The solid bar denotes AP5 infusion and the hatched bar the NMDA infusion.

A

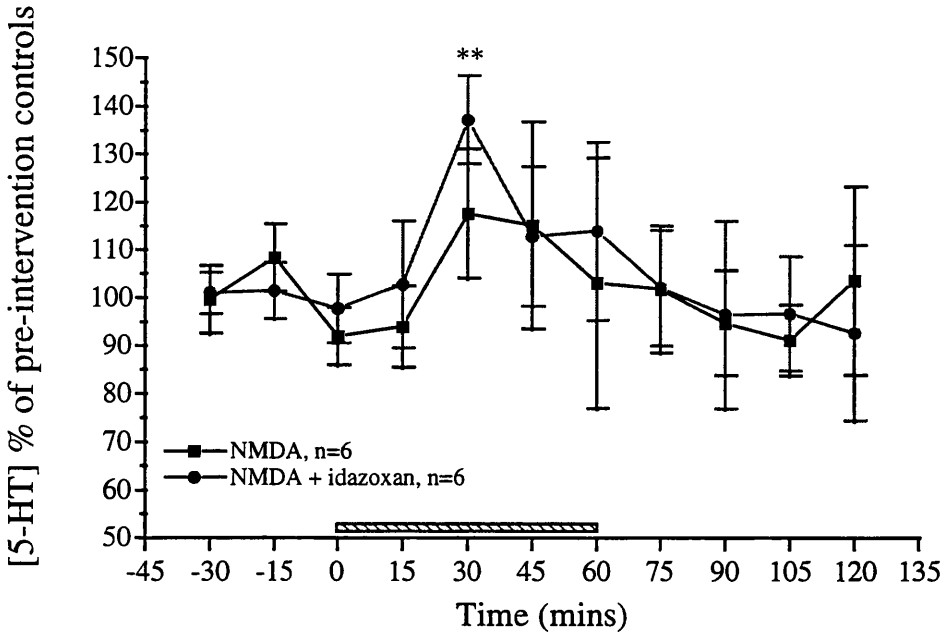

B

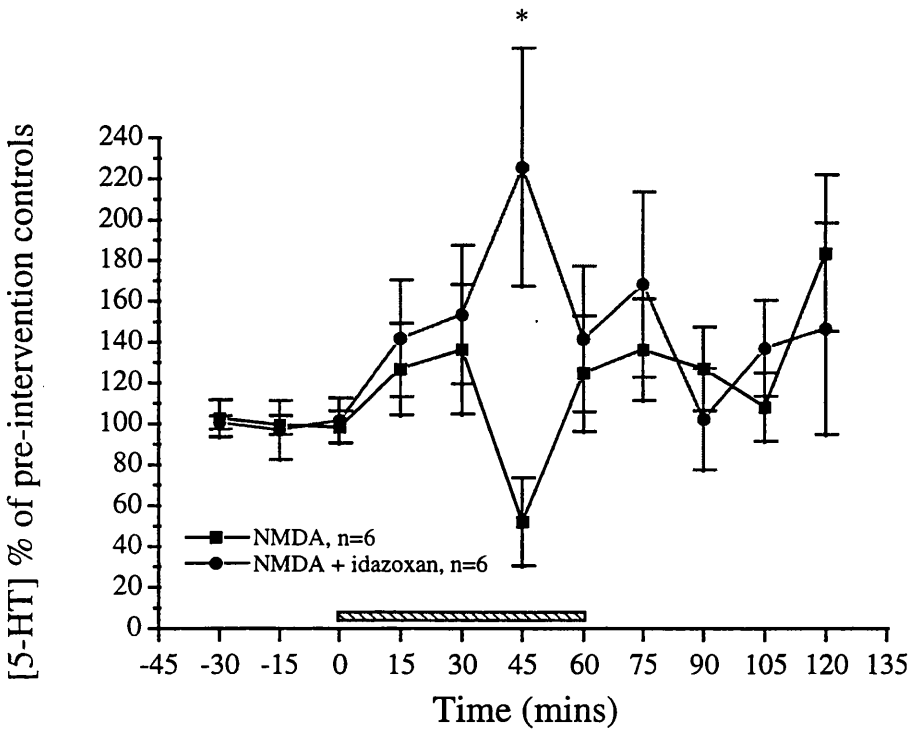

Figure 5.9. Effect of concurrent application of the α_2-antagonist idazoxan (1 μM) with NMDA (100 μM) at **A:** ZT 6 and **B:** ZT 18. Results are mean ± s.e.m. values expressed as a percentage of three pre-intervention controls. The hatched bar denotes infusion of NMDA, or NMDA + idazoxan, for 60 min via the dialysis probe. * $p < 0.05$; ** $p < 0.01$

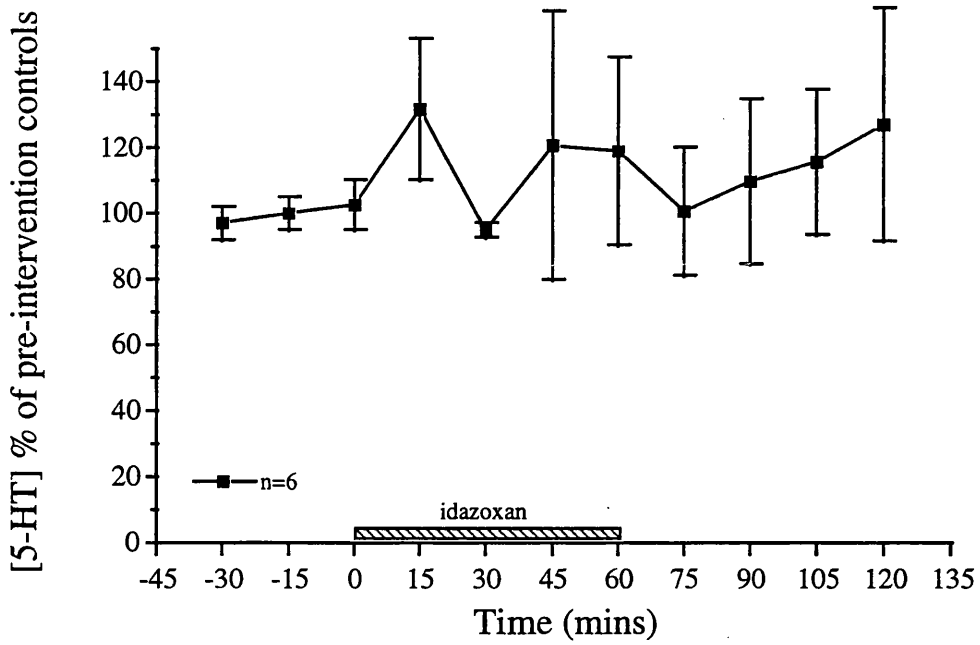

Figure 5.10. Effect of idazoxan (1 μM) infusion on SCN 5-HT concentration at ZT 18. Idazoxan was infused via the dialyis probe for 60 mins, denoted by the hatched bar. Results are mean ± s.e.m. values expressed as a percentage of three pre-intervention controls.

A

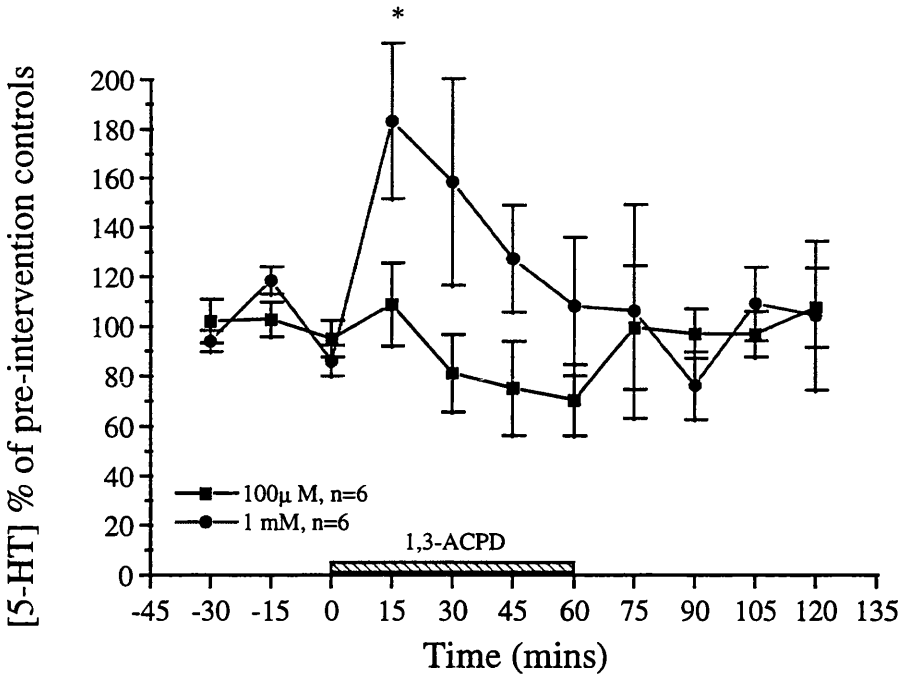

B

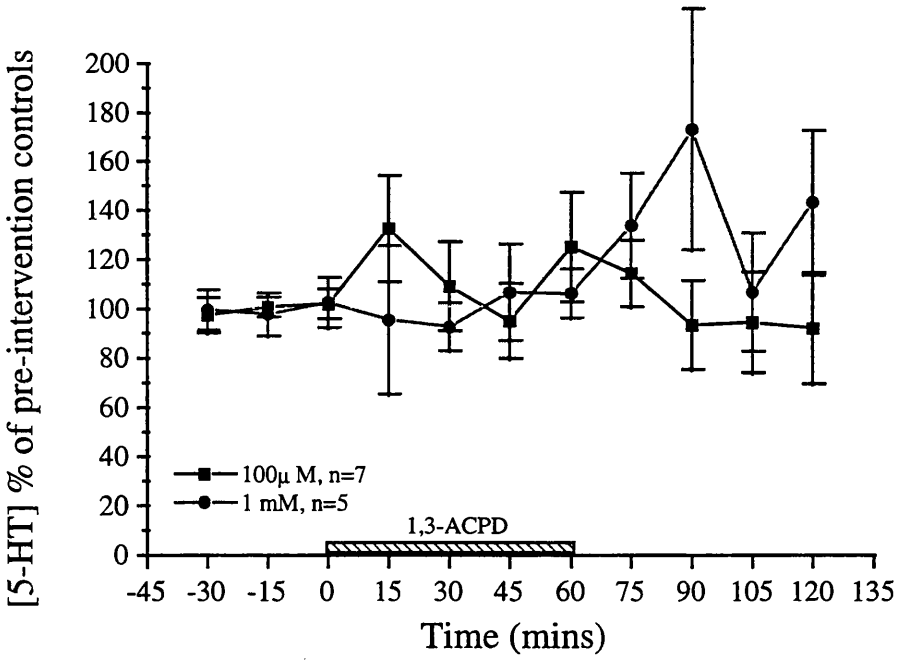

Figure 5.11. Effect of the metabotropic agonist 1S,3R-ACPD (1 mM and 100 μM) on 5-HT overflow in the SCN. Results are mean ± s.e.m. values expressed as a percentage of three pre-intervention controls. ACPD was infused into the SCN via the dialysis probe for 60 min as indicated by the hatched bar. **A:** ZT 6. **B:** ZT 18. * $p < 0.05$

A

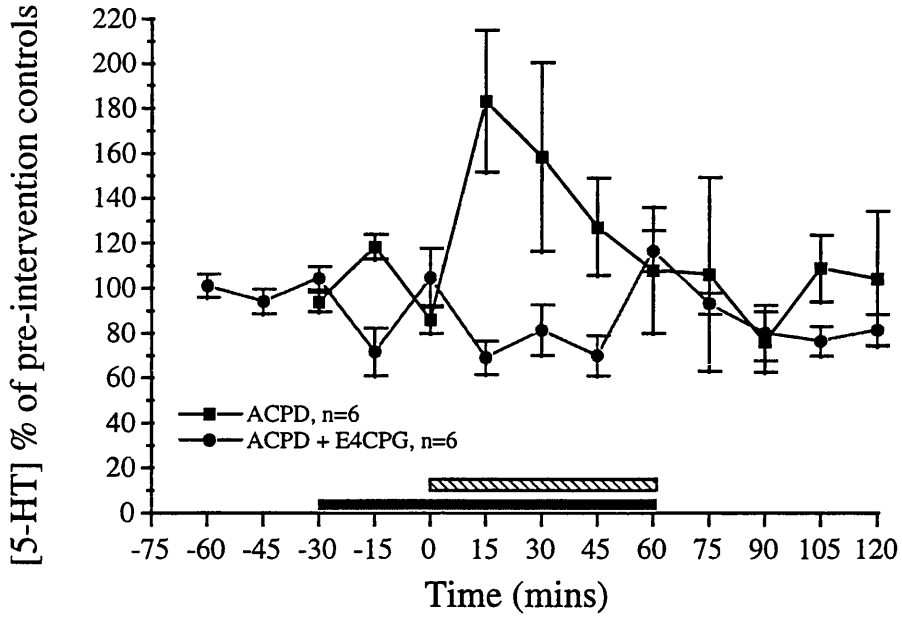

B

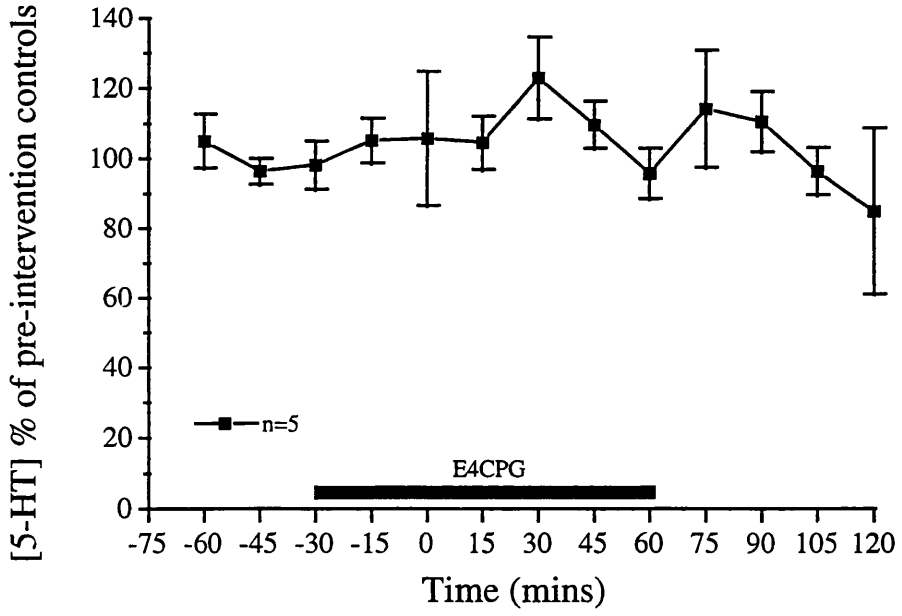

Figure 5.12. **A:** Effect of the metabotropic antagonist E4CPG on the response to 1S,3R-ACPD in the SCN at ZT 6. Results are mean ± s.e.m. values expressed as a percentage of three pre-intervention controls. E4CPG (100 μM) was infused 30 min prior to, and 60 min concurrently with ACPD via the dialysis probe. The solid bar denotes E4CPG infusion and the hatched bar the ACPD infusion. **B:** Effect of a 90 min infusion of E4CPG (100 μM) alone at ZT 6. The solid bar denotes E4CPG infusion.

5.4 DISCUSSION

In the preceding chapter I have shown that the 5-HT_{1B} heteroceptor can regulate glutamate release in the SCN during the light phase and during the dark phase of animals synchronised to an environmental light:dark cycle. The data presented here suggest that there is reciprocal regulation between the glutamatergic and serotonergic systems in the rat SCN, because both ionotropic and metabotropic glutamate receptor agonists can regulate 5-HT overflow in the SCN.

Previous studies have investigated the effects of serotonin and sertonin receptor agonists on photically responsive cells (Huang and Pan, 1993; Ying and Rusak, 1994), photically induced Fos immunoreactivity in the SCN (Selim *et al.*, 1993; Reico *et al.*, 1996), photic phase shifting of the circadian activity rhythm (Rea *et al.*, 1995) and more specifically using microdialysis, serotonergic inhibition of extracellular glutamate in the SCN region (Selim *et al.*, 1993; Srkalovic *et al.*, 1994). All these studies centred on the effects of serotonin on photic or glutamatergic transmission in the SCN, whereas I have investigated the effects of glutamatergic agonists on 5-HT overflow in the SCN region, to further our understanding of the regulation of circadian entrainment.

A few studies have utilised microdialysis to investigate the effects of L-glutamate and selective agonists on 5-HT overflow in the raphe nuclei and/or forebrain projection sites, namely hippocampus, striatum, nucleus accumbens, locus coeruleus or frontal cortex (Ohta *et al.*, 1994; Whitton *et al.*, 1994; Tao and Auerbach, 1996; Maione *et al.*, 1997; Pallotta *et al.*, 1998; Tao *et al.*, 1997; Singewald *et al.*, 1998). In my experiments local infusion of AMPA into the SCN region at 1-10 mM increased 5-HT overflow in this area, but associated with a significant increase in locomotor activity, eventually leading to death before the end of the experiment. The reason for the animals' death was not ascertained, although upon a rough post-mortem, the animals appeared to have severe oedema of the lungs, and to have effectively asphyxiated. Infusing AMPA at the lower concentration of 100 μM did not result in death, nor did it appear to place the animals in any discomfort, although it still increased locomotor activity. At this concentration the AMPA infused into the SCN region at both ZT 6 and ZT 18 failed significantly to affect 5-HT overflow. In other forebrain areas such as the striatum (Ohta *et al.*, 1996; Maione *et al.*, 1997) and the locus coeruleus (Singewald *et al.*, 1998)

AMPA has the ability to increase dialysate 5-HT in a concentration dependent (10-500 μM) manner, but Tao and co-workers (1997) infused AMPA into either the DRN (300/1000 μM) or the nucleus accumbens (300 μM) without significant effect. However, AMPA receptors are known to desensitise rapidly (see Bettler and Mulle, 1995). This desensitisation can be prevented by pre-treatment with cyclothiazide or diazoxide. Indeed, the effect of pre-treating the DRN with either cyclothiazide or diazoxide was to produce a transient increase in 5-HT release (Tao *et al.*, 1997). The effect of AMPA in the SCN may thus be masked by desensitisation of the AMPA receptor. However, Tao *et al.* (1997) also pre-treated the nucleus accumbens (a forebrain projection site of the DRN) with diazoxide with no enhancement of 5-HT release. In the absence of data on the effect preventing AMPA receptor desensitisation in the SCN, one must assume that AMPA receptor stimulation in this brain area does not produce any effect on 5-HT overflow. 5-HT release following AMPA receptor stimulation is obviously dependent on the brain area studied.

Kainate infusion into the SCN produced comparable effects on 5-HT overflow in the SCN at ZT 6 and ZT 18. Stimulation of SCN neurones by kainate significantly enhanced 5-HT release. Infusion of kainate (30-300 μM) into the ventral hypothalamus, ventral hippocampus, nucleus accumbens (Tao *et al.*, 1997), locus coeruleus (Singewald *et al.*, 1998) or the striatum (Ohta *et al.*, 1994) increases 5-HT overflow. In the ventral hypothalamus the effect of kainate on 5-HT overflow was only apparent after the highest concentration of 300 μM was infused. The authors have suggested that this effect of kainate was due to excitotoxic effects of the drug as the increase in 5-HT overflow was delayed and prolonged. The results presented here do not appear to be due to neurotoxic lesions because at ZT 18 (Tao and co-workers performed their experiments during the dark phase) I observed an immediate and significant enhancement of 5-HT release in the SCN region, and at ZT 6 there was significant enhancement 45 min after the start of the infusion; in both cases, the increase did not last beyond the termination of the infusion with levels returning to values not significantly different from controls. Kainate is a drug often used to produce excitotoxic lesions. At the concentration of drug used here (100 μM) it is unlikely that 5-HT release results from cell death. Kainate (300 μM) infused into the nucleus accumbens for a period of 60 min produced no evidence of neuronal degeneration as determined by silver staining (Tao *et al.*, 1997).

Although retinohypothalamic transmission is a combination of non-NMDA and NMDA receptor effects, NMDA receptor stimulation is regarded as playing a key role in brain photic entrainment of circadian rhythms (e.g. Cahill and Menaker, 1989; Ohi et al., 1991). It is for this reason that a large part of this investigation concentrated on NMDA receptor stimulation. The effect of an infusion of NMDA on 5-HT overflow in the SCN was dependent largely on the concentration of drug infused, and the zeitgeber time at which the drug was applied. During the light phase (ZT 6) 100 μM NMDA produced no significant change in 5-HT overflow, whereas increasing the concentration ten-fold resulted in a significant enhancement of SCN 5-HT release. There was a striking effect of NMDA infusion during the dark phase (ZT 18). At the lowest concentration (100 μM) NMDA induced a decrease in measured 5-HT to 52 ± 21.5 % of baseline, evident 45 min after the start of the infusion. In contrast, 1 mM NMDA produced a large and prolonged increase in 5-HT release, starting 30 min after the start of the infusion and lasting for the duration of the infusion. The ability of NMDA to enhance 5-HT release in the SCN was greater when NMDA was administered during the dark phase (206 ± 24.8 % at ZT 18 compared with 162 ± 26.9 % of pre-intervention controls at ZT 6). There was an obvious diurnal variation in the function of the NMDA receptor.

Rat brain (Fink *et al.*, 1995) or guinea pig brain (Fink *et al.*, 1996) cortical slices pre-incubated with tritiated 5-HT in the presence of a specific noradrenaline reupake inhibitor, show concentration dependent release of 5-HT by NMDA. Although the circadian phase was not reported, it seems reasonable to assume that these experiments were undertaken during the light phase. Another experiment performed during the light phase involving microdialysis of the hippocampus and striatum also showed a dose-dependent increase in dialysate 5-HT concentration after a 30 min infusion of NMDA (1-100 μM; Whitton *et al.*, 1994). Tao and Auerbach (1996), who perform their experiments during the dark phase, observed a decrease in dialysate 5-HT concentration during a 60 min infusion of NMDA (100 and 300 μM) of the nucleus accumbens, frontal cortex and hippocampus. This is consistent with the observation in my experiments that 100 μM NMDA infused at ZT 18 into the SCN region produced a significant decline in dialysate 5-HT concentration. These authors did not, however, use NMDA at 1 mM, which in my experiments produced a contrasting increase in SCN 5-

HT overflow when administered at ZT 18. Pallotta and co-workers (1998) measuring 5-HT overflow from raphe dialysate samples during the light phase, also demonstrated opposing effects of the same drugs on 5-HT release. At a low concentration of NMDA (25 μM), raphe dialysate 5-HT concentration decreased, whereas a four-fold increase in the concentration of infused NMDA (100 μM) significantly enhanced 5-HT levels. In the SCN, this differential activation of NMDA receptors leading to a significantly different outcome on measured 5-HT release appears to be important only during the dark phase. It is still possible however, that this effect would have become evident during the light phase if a broader range of concentration of NMDA had been used.

The ability of the non-competitive NMDA receptor antagonist MK-801 to antagonise the effects on dialysate 5-HT concentration elicited by NMDA infusion into the SCN, was dependent upon the zeitgeber time at which it was applied. MK-801 was able to block the increase in 5-HT overflow from the SCN induced by NMDA (1 mM) at ZT 6, whilst having no effect on the decrease induced by NMDA (100 μM) or the increase following NMDA (1 mM) at ZT 18.

For MK-801 to exert its effects the voltage dependent ion channel must be open and active. During the light phase, light falling on the retinal ganglion cells activate the retinal hypothalamic tract (RHT) sending signals to the SCN. During the dark phase, the RHT is not stimulated. Therefore, one might assume that in the light the NMDA receptors in the SCN have been activated, whilst the same receptors are quiescent during the dark phase. Thus, at ZT 6, the MK-801 is able to gain access to the ion channel. At ZT 18 the channel remains closed until the receptor is activated by NMDA; presumably under these circumstances the MK-801 cannot surmount the effects of the agonist. This phenomenon that MK-801 administration during the dark phase does not block NMDA responses is possibly unique to the SCN, because MK-801 infused into the DRN by microdialysis has been used successfully to antagonise NMDA-induced increases during the dark phase (Tao and Auerbach, 1996).

MK-801 when administered alone had a significant effect on SCN 5-HT overflow at ZT 6 and no effect at ZT 18. During the light phase MK-801 significantly reduced 5-HT overflow indicative of tonic NMDA receptor mediated glutamatergic control over 5-HT

release in the SCN. This tone is absent during the dark phase, and may possibly reflect the absence of RHT stimulation.

In direct comparison to pre-infusing MK801, the competitive NMDA receptor antagonist AP5, prevented the NMDA from significantly increasing (1 mM) or decreasing (100 μM) dialysate 5-HT concentration at ZT 18. This reflects the ability of AP5 to access the NMDA site directly and prevent stimulation of the receptor by exogenously applied agonist.

The release of 5-HT can be regulated by pre-synaptic receptors such as α_2-adrenoceptors. Electrically stimulated tritium release from rat brain cortex slices pre-incubated with tritiated 5-HT is reduced by application of the α-adrenoceptor agonist noradrenaline and increased with the α-adrenoceptor antagonist phentolamine (Gothert and Huth, 1980). Additional characterisation of this inhibitory receptor present at pre-synaptic serotonergic terminals in rat hippocampal or cortical slices classified it as an α_2-autoreceptor (Frankhuyzen and Mulder, 1982; Trendelenburg *et al.*, 1994)). It has been suggested that within the SCN, 5-HT release and metabolism is influenced by tonic adrenergic inputs, because idazoxan administered intravenously was shown by voltametric recordings to increase the height of the indole oxidation peak *in vivo* (Marsden and Martin, 1986). Moreover, NMDA-induced tritiated 5-HT overflow from rat brain cortex was facilitated by the addition of the α_2-adrenoceptor antagonist idazoxan (Fink *et al.*, 1995). It was on this basis that idazoxan was co-infused with NMDA (100 μM) at ZT 6 and 18, to establish whether the response to NMDA in the SCN could be augmented by the α_2-adrenoceptor antagonist.

The response to NMDA at ZT 6 was indeed augmented by the addition of the α_2-adrenoceptor antagonist, suggesting that during the light period NMDA-induced 5-HT release was inhibited by endogenous α_2-adrenoceptor agonists, namely noradrenaline, released at the same time. During the dark phase, the NMDA-induced decrease in 5-HT release is evidently a result of inhibition by endogenous noradrenaline, as this decrease is prevented by idazoxan and the effect is to significantly elevate the 5-HT overflow. The possibility exists during the dark phase that more noradrenaline is released by NMDA receptor stimulation to act upon α_2-adrenoceptors thereby inhibiting 5-HT

terminal release, or that these α_2-adrenoceptors are more receptive to stimulation at this time as opposed to during the light phase. Pronounced fluctuations in hippocampal noradrenaline output over the normal light:dark cycle do suggest that levels are higher during the period of darkness, and when the animal is most active (Kalen *et al*, 1989). During the dark phase there does not appear to be any tonic control of 5-HT release by endogenous α_2-adrenoceptor agonists, as infusion of idazoxan at ZT 18 failed significantly to affect the 5-HT concentration collected in the dialysate. Indeed, in rat hypothalamic slices selective α_2-adrenoceptor antagonists failed to enhance the release of tritiated 5-HT (Blier *et al*, 1990), corroborating the data that indicate that there is no tonic control of 5-HT by α_2-adrenoceptors in the hypothalamus, which is contrary to the data of Marsden and Martin (1986). The α_2-adrenoceptor influence over 5-HT release in the SCN appears to rely upon neuronal release of transmitter.

The metabotropic glutamate receptors (mGluR) constitute a family of G-protein coupled receptors that can exert their effects by influencing cytoplasmic second messenger systems. The ability of the mixed Group I / group II agonist 1S,3R-ACPD (ACPD) to influence 5-HT release in the SCN was concentration- and zeitgeber time-dependent. During the dark phase, ACPD had no influence over SCN 5-HT release. At ZT 6 on the other hand, although 100 μM ACPD failed significantly to affect 5-HT release, 1 mM caused an immediate and significant increase in 5-HT overflow, which was blocked by the group I / group II antagonist E4CPG. There is no evidence to date that expression of mGluR in the SCN or immunoreactivity for the mGluR shows circadian variation. *In vitro* preparations of hamster SCN cells show increased neuronal activity following ionophoretic application of ACPD, but this was only tested during the light phase (Scott and Rusak, 1996). It may be that SCN cells do not respond to ACPD during the dark phase.

The effect observed here after stimulation with the metabotropic glutamate receptor agonist ACPD on 5-HT overflow might be an indirect effect of glutamate. ACPD has been used to look at the effects of mGluR stimulation on glutamate and aspatate levels by *in vivo* microdialysis of the nucleus tractus solitarius (Jones et al, 1998). ACPD significantly elevated glutamate and aspatate overflow, which is blocked by the antagonist E4CPG. However, the effect observed in my experimenst is immediate, and

one might expect the response to take longer to establish if it was caused by indirect stimulation of glutamate release. An interesting aspect of mGluR stimulation is the facilitation of NMDA depolarisation of cortical wedges (Rahman and Neuman, 1996). It may be that in the SCN mGluR and NMDA receptors work together to modulate 5-HT neurotransmission to the SCN.

5.5 CONCLUSIONS

With the exception of the AMPA receptor, ionotropic and metabotropic glutamate receptor activation has the ability to affect serotonergic transmission in the SCN. During the light phase NMDA receptor stimulation exerts tonic control over the terminal release of 5-HT, which is absent during the dark phase. This is presumably influenced by the activation of the retinohypothalamic tract during the day, releasing excitatory amino acids at it terminals. NMDA receptor activation has the ability to increase 5-HT release in the SCN during both the light and the dark phase, but the degree of receptor activation during the dark period is important in mediating the effects on 5-HT overflow. The difference between an NMDA-induced decrease in 5-HT release during the dark phase, and an NMDA-induced increase may be important for phase resetting of the circadian pacemaker during the dark phase. This NMDA-induced decrease in 5-HT release is mediated by parallel activation of monoamine transmitter systems activating inhibitory α_2-adrenoceptor heteroceptors present on the serotonergic nerve terminals. Endogenous monoamines in the SCN serve to regulate neuronally released 5-HT, and therefore must be taken into consideration when examining the effects of drugs on 5-HT release in this brain region. The regulation of 5-HT by metabotropic glutamate receptors exhibits a definite diurnal variation. The activation of these receptors can only regulate 5-HT release during the light phase and may thus be influenced by activation of the retinohypothalamic tract.

CHAPTER 6

THE RAPHE 5-HT$_{1A}$ SOMATODENDRITIC AUTORECEPTOR AND NMDA RECEPTOR REGULATION OF 5-HT RELEASE IN THE SCN

6.1 INTRODUCTION

Although not a recognised pathway for the integration and regulation of circadian rhythms, there is growing evidence of a retinal-raphe-SCN projection. The raphe-SCN projection is a well established pathway sending serotonergic nerve fibres to the circadian pacemaker (Moore *et al.*, 1978). Anterograde tracers injected into the posterior chamber of the eye reveal a bilateral projection to the DRN in the cat (Foote *et al.*, 1978) and rat (Villar *et al.*, 1987; Shen and Semba, 1994; Kawano *et al.*, 1996), although these fibres are scarce in comparison to well established retinal projections such as the SCN (Moore and Lenn, 1972) and IGL (Card and Moore, 1989). Retrograde tracers injected into the DRN of the rat have confirmed the presence of this pathway, by detecting equivalent numbers of labeled ganglion cells in the retina (Shen and Semba, 1994). Whether there is a reciprocal projection from the raphe to the retina is under dispute with retrograde retinal labeled fibres reportedly present (Villar *et al.*, 1987) or absent (Kawano *et al.*, 1996) from the DRN.

The growing controversy about whether the raphe-SCN projection originates in the median or dorsal raphe nuclei (see Discussion, this chapter) might tempt the interested reader to dispute the existence of a retino-raphe-SCN projection, as from the evidence presented, the retinal fibres terminating in the raphe nuclei do so solely in the DRN and in small numbers. Indeed, one paper dedicated to answering the question of "Is there a direct retina-raphe-suprachiasmatic nucleus pathway in the rat?" (Kawano *et al.*, 1996) suggests that this presumed third visual input to the circadian pacemaker may include further neuronal connections or brain sites. These authors anterogradely labeled fibres from the retina, labeled SCN neurones with retrograde tracers, and identified DRN neurones by means of serotonin immunohistochemistry of brain sections. Approximately half of the retrograde-labeled SCN neurones detected in the DRN were serotonin-immunoreactive, but no close spatial relationship between anterogradely and retrogradely labeled structures in the DRN were observed, and at best, only a very few neurones retrogradely labeled from the SCN were distributed in the rostral DRN where retinal afferents terminated.

Structural evidence therefore suggests that the retinal-raphe pathway exists, but whether this pathway is functional in the regulation of SCN neurotransmitters, namely serotonin,

and the control of circadian rhythms remains unanswered. The leading contender for the transmitter of the retinal afferents to the SCN and IGL is glutamate (e.g. Liou *et al.*, 1986; de Vries *et al.*, 1993; 1994) and the involvement of ionotropic and metabotropic glutamate receptors in neurotransmission of photic information through the RHT is well established (Cahill and Menaker, 1989; Ohi *et al.*, 1991). It seems reasonable to extrapolate this to the retinal-raphe pathway until the transmitter of the retinal-raphe pathway has been identified.

The aim of this chapter was first to investigate the feasibility of a dual probe paradigm which would involve implanting two dialysis probes into a single animal to measure the 5-HT overflow simultaneously in the midbrain raphe and SCN. For this, the 5-HT_{1A} receptor agonist 8-OH-DPAT was infused via the probe implanted into the raphe nuclei and terminal 5-HT release monitored in the SCN. Stimulation of the somatodendritic 5-HT_{1A} receptor has been shown to decrease raphe neuronal firing and thus decrease terminal release (Sprouse and Aghajanian, 1987). Therefore, for the dual probe paradigm to function efficiently, after stimulation with 8-OH-DPAT, terminal 5-HT release is expected to decline. Once this was established, the aim was to investigate the application of the ionotropic glutamate agonist NMDA to the raphe nucleus of the rat, whilst measuring the effects on 5-HT release in the SCN and thus examining the functional capacity of a retinal-raphe-hypothalamic pathway.

6.2 PROTOCOL

6.2.1 Animals

Male Wistar rats (University of Bath strain; 260-320 g) were maintained under a 12:12 light:dark cycle regime (lights on 07:00 "normal" light:dark cycle; lights on 19:00 "reverse" light:dark cycle; temperature 22 ± 2°C). The animals were caged in groups of six prior to experimentation, with food and water available *ad libitum.*

6.2.2 Microdialysis

Each animal was implanted with two microdialysis probes as described in chapter 2 section 2.3.3 directed at the SCN and the midbrain raphe, and introduced to the experimental cage. The probes were continuously perfused with aCSF (1.2 µl/min); only the probe to the SCN region receiving the SSRI citalopram. Six 15 min control samples were collected, and the three samples immediately before drug infusion served as the pre-intervention controls. At zeitgeber times 6 or 18 drugs were infused for a period of 60 min into the raphe nuclear region via the probe. For antagonistic studies, the antagonist was infused for an additional 30 min prior to and during the 60 min infusion with the agonist. Dialysate samples were collected every 15 min simultaneously from the SCN and raphe regions over a period of 2 hours post-drug infusion, and analysed for 5-HT content using HPLC-ED, as described in chapter 2 section 2.3.5. Samples not being analysed immediately were snap frozen and maintained on dry ice until analysis. At the end of the experiments the animals were killed by CO_2 asphyxiation and the brains removed and frozen onto dry ice. Slicing freehand with a sharp razor blade, the probe tract was clearly visible as a fine line through the brain tissue. With the aid of a stereotaxic atlas (Paxinos and Watson, 1982) the position of the probe tract within the hypothalamus or midbrain raphe was established. The animals whose probe tracts were not in the target area were discarded for analysis.

6.2.3 Drugs

8-OH-DPAT [(±)-8-Hydroxy-2-(di-*n*-propylamino)tetralin] and NMDA (*N*-methyl-D-aspartate) were obtained from Sigma Chemical Co., AP5 [(±)-2-amino-5-phosphonopentanoic acid] from Tocris Cookson Ltd. and WAY100635 (N-[2-[4-(2-

methoxyphenyl)-1-piperazinyl]ethyl]-N-(2-pyridinyl)cyclohexanecarboxamide trihydrochloride) from Wyeth-Ayerst Research. Citalopram hydrobromide was provided by Lundbeck (Copenhagen-Valby)

6.2.4 Statistics

5-HT concentration in the dialysate samples (not-corrected for probe recovery) were expressed as a percentage of the three pre-intervention controls samples. Values post-drug treatment were analysed by one-way analysis of variance (ANOVA) with repeated measures with Student Newman Keuls post hoc test to detect differences between pre-intervention controls samples. $p < 0.05$ was considered statistically significant.

6.3 RESULTS

At ZT 6, the basal 5-HT concentration prior to any drug treatment for raphe and SCN dialysates were 23.39 ± 5.14 and 15.48 ± 2.80 fmol respectively. At ZT 18 basal 5-HT overflow was 62.77 ± 17.20 and 19.98 ± 2.52 femtomols for raphe and SCN dialysates respectively.

6.3.1 Effect of local infusion of 8-OH-DPAT in the midbrain raphe nuclei on 5-HT overflow in the raphe and SCN

At ZT 18 two concentrations of 8-OH-DPAT were infused into the raphe for a period of 60 min. The initial concentration of 1 μM failed to affect significantly either raphe or SCN 5-HT overflow (figure 6.1A and 6.1B, respectively). It was therefore decided to increase the concentration 1000-fold to 1 mM. In raphe dialysate 1 mM 8-OH-DPAT appeared to produce a transient rise in 5-HT overflow, although this was not statistically significant. Thereafter, 5-HT levels became significantly lower than pre-intervention controls 30 min after the end of the infusion, and remained low for the duration of the experiment (figure 6.1A). Maximal drop in raphe 5-HT levels was 33.3 ± 15.7 % of baseline ($p < 0.01$). The effect of 1 mM 8-OH-DPAT applied to the raphe was to decrease SCN 5-HT overflow to levels significantly lower than pre-intervention controls 45 min after the start of the infusion; 5-HT levels staying low for the remainder of the 2 hour collection period, reaching a nadir of 21.7 ± 8.19 % of baseline ($p < 0.01$; figure 6.1B).

At ZT 6, 1 mM 8-OH-DPAT into the raphe caused a dramatic and significant increase in raphe 5-HT 45 min after the start of the infusion, reaching a peak of 516 ± 104 % of baseline ($p < 0.001$). Thirty min after the end of the infusion, raphe 5-HT concentration fell to levels not significantly different from pre-intervention controls (figure 6.2A). In the SCN dialysate, 5-HT levels decreased significantly 45 min after the start of the raphe infusion and remained low for the duration of the collection period, reaching a nadir of 32.3 ± 9.61 % of baseline ($p < 0.01$; figure 6.2B).

Pretreatment and co-infusion of the specific 5-HT_{1A} receptor antagonist WAY100635 (10 μM) with 8-OH-DPAT (1 mM) failed to prevent the decrease in SCN 5-HT levels at

ZT 6 (figure 6.3B). In the SCN, 5-HT overflow fell significantly within 30 min of the start of the infusion, and remained so for the whole of the collection period, reaching a nadir of 13.4 ± 9.87 % of baseline ($p < 0.001$). This concentration of WAY100635 did, however, prevent the increase in raphe 5-HT (figure 6.3A). Forty five min after the end of the infusion, raphe 5-HT fell to 55.6 ± 14.5 % of baseline ($p < 0.05$). At ZT 18, the concentration of WAY100635 was increased 100-fold to match that of the infused 8-OH-DPAT (1 mM). In the presence of the antagonist, 8-OH-DPAT failed to decrease SCN 5-HT throughout the duration of the infusion, although the last collection sample, 60 min after the end of the infusion, SCN 5-HT did fall to 35.7 ± 13.5 % of baseline ($p < 0.05$; figure 6.4B). The effect of pretreatment with WAY100635 on raphe 5-HT, on the other hand, was to augment the increase in 5-HT to levels significantly higher than baseline 30 min after the start of the infusion, reaching a peak of 460 ± 110 % ($p < 0.01$; figure 6.4A). WAY100635 did prevent the decrease in raphe 5-HT observed after 8-OH-DPAT alone, during the period after the infusion, (figure 6.1A).

6.3.2 Effect of local infusion of NMDA in the midbrain raphe nuclei on 5-HT overflow in the raphe and SCN

Similar effects of NMDA (100 μM) were observed at ZT 6 and 18 (figure 6.5A and 6.5B, respectively). At ZT 6, a 60 min infusion of NMDA into the raphe increased raphe 5-HT, reaching significance 15 min after the end of the infusion (214 ± 29.3 % of baseline; $p < 0.05$). This increase was mirrored by a decrease in SCN 5-HT, reaching significance 30 min after the end of the infusion (54.6 ± 16.0 % of baseline; $p < 0.05$). At ZT 18, a 60 min infusion of NMDA into the raphe also increased raphe 5-HT levels. Peak levels were achieved 60 min after the start of the infusion (158 ± 31.7 % of baseline). A decrease in SCN 5-HT levels were observed after the infusion in the raphe, reaching significance 15 min after the end of the infusion, but reaching a nadir of 17.7 ± 17.7 % ($p < 0.01$) 45 min after the end of the infusion.

The decrease in SCN 5-HT overflow following NMDA (100 μM) infusion of the raphe nuclei at ZT 18 was prevented by pretreatment and co-infusion with the NMDA antagonist AP5 (100 μM; figure 6.6B). However, the increase in raphe 5-HT observed after NMDA infusion was not blocked by the antagonist, and still reached statistical significance 60 min after the start of the experiment (173 ± 26.3 % of baseline; $p <$

0.01). However, 45 min after the end of the infusion, raphe 5-HT levels fell significantly to 59.3 ± 8.61 % of baseline ($p < 0.05$).

To establish whether the decrease in 5-HT overflow from the SCN following NMDA infusion into the raphe at ZT 18 was due to stimulation of the 5-HT_{1A} autoreceptor on the serotonergic neurones, WAY100635 (1 mM) was infused before and during the NMDA infusion (100 μM). WAY100635 failed to prevent the decline in SCN 5-HT overflow 30 min after the end of the infusion, although the drop in SCN 5-HT levels was less pronounced than with NMDA alone, reaching a nadir of only 57.4 ± 13.5 % of baseline ($p < 0.05$; figure 6.7B), in comparison to 17.7 ± 17.7 % (figure 6.5B). A very striking effect of WAY100635 pretreatment was observed in the raphe nuclei. The increase in raphe 5-HT concentration following NMDA alone (100 μM; figure 6.5B) was augmented considerably after treatment with WAY100635 (figure 6.7A), evident after 15 min of the NMDA infusion and remaining elevated for the whole collection period. Maximal increase was 914 ± 204 % of baseline ($p < 0.01$).

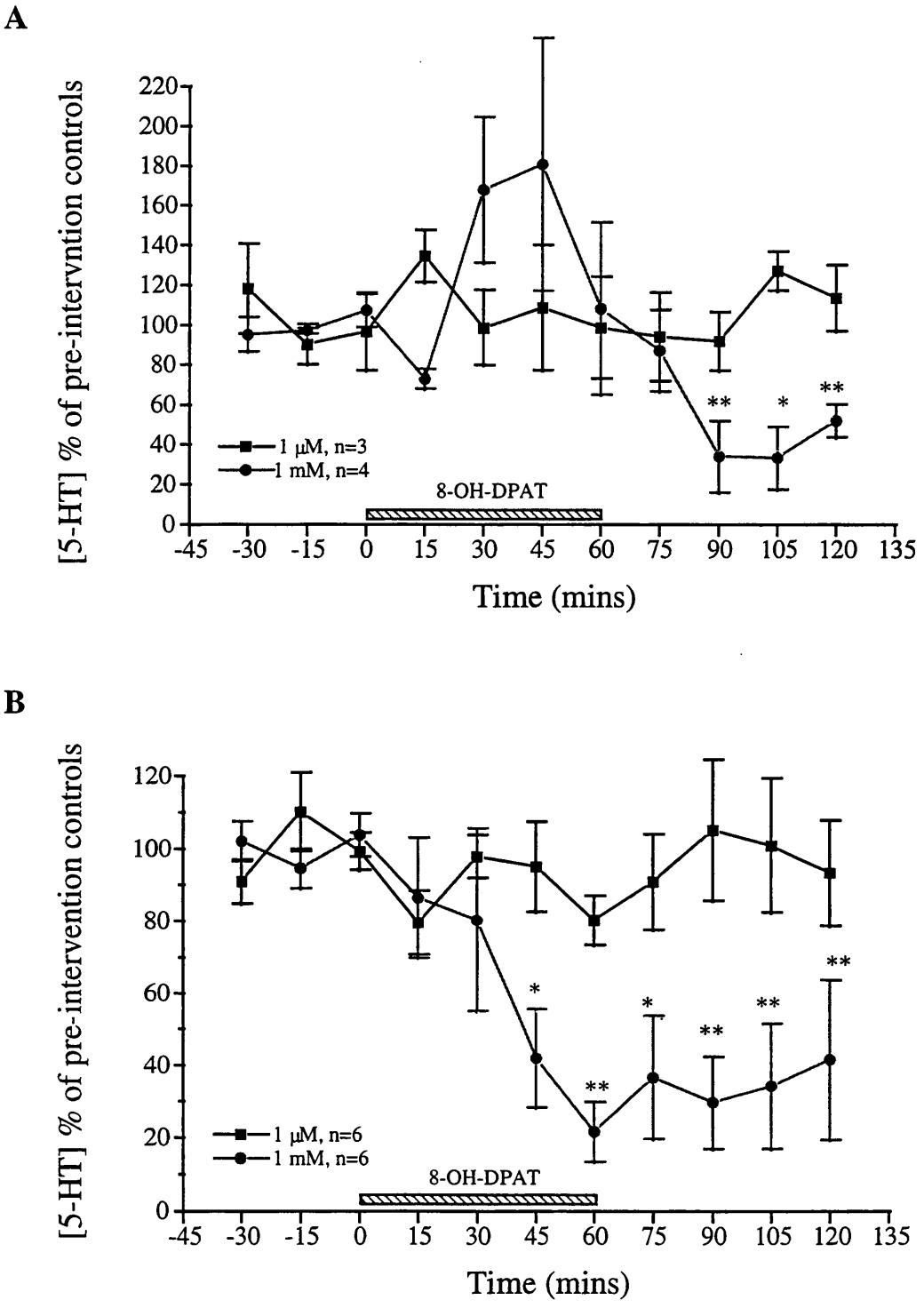

Figure 6.1. Effect of 8-OH-DPAT infusion (1 μM and 1 mM) in the midbrain raphe nuclei on 5-HT overflow in raphe nuclei (**A**) and in the SCN (**B**) at ZT 18. Simultaneous collection of samples was carried out in a single animal implanted with two microdialysis probes. Values are mean ± s.e.m. expressed as a percentage of three pre-intervention control samples. 8-OH-DPAT was infused for 60 min denoted by the hatched bar. * $p < 0.05$; ** $p < 0.01$.

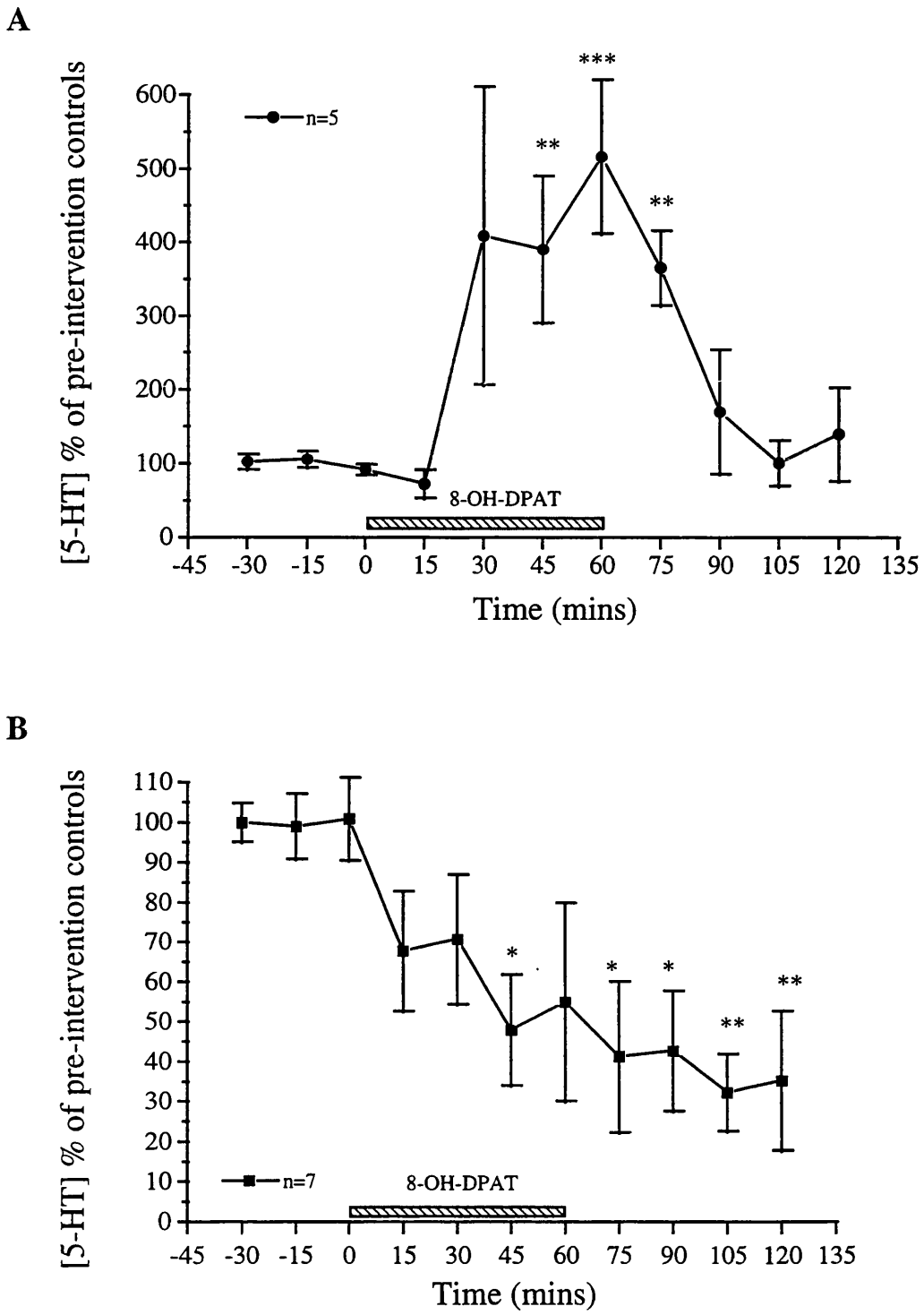

Figure 6.2. Effect of 8-OH-DPAT infusion (1 mM) in the midbrain raphe nuclei on 5-HT overflow in raphe nuclei (**A**) and in the SCN (**B**) at ZT 6. Simultaneous collection of samples was carried out in a single animal implanted with two microdialysis probes. Values are mean ± s.e.m. expressed as a percentage of three pre-intervention control samples. 8-OH-DPAT was infused for 60 min denoted by the hatched bar. * $p < 0.05$; ** $p < 0.01$

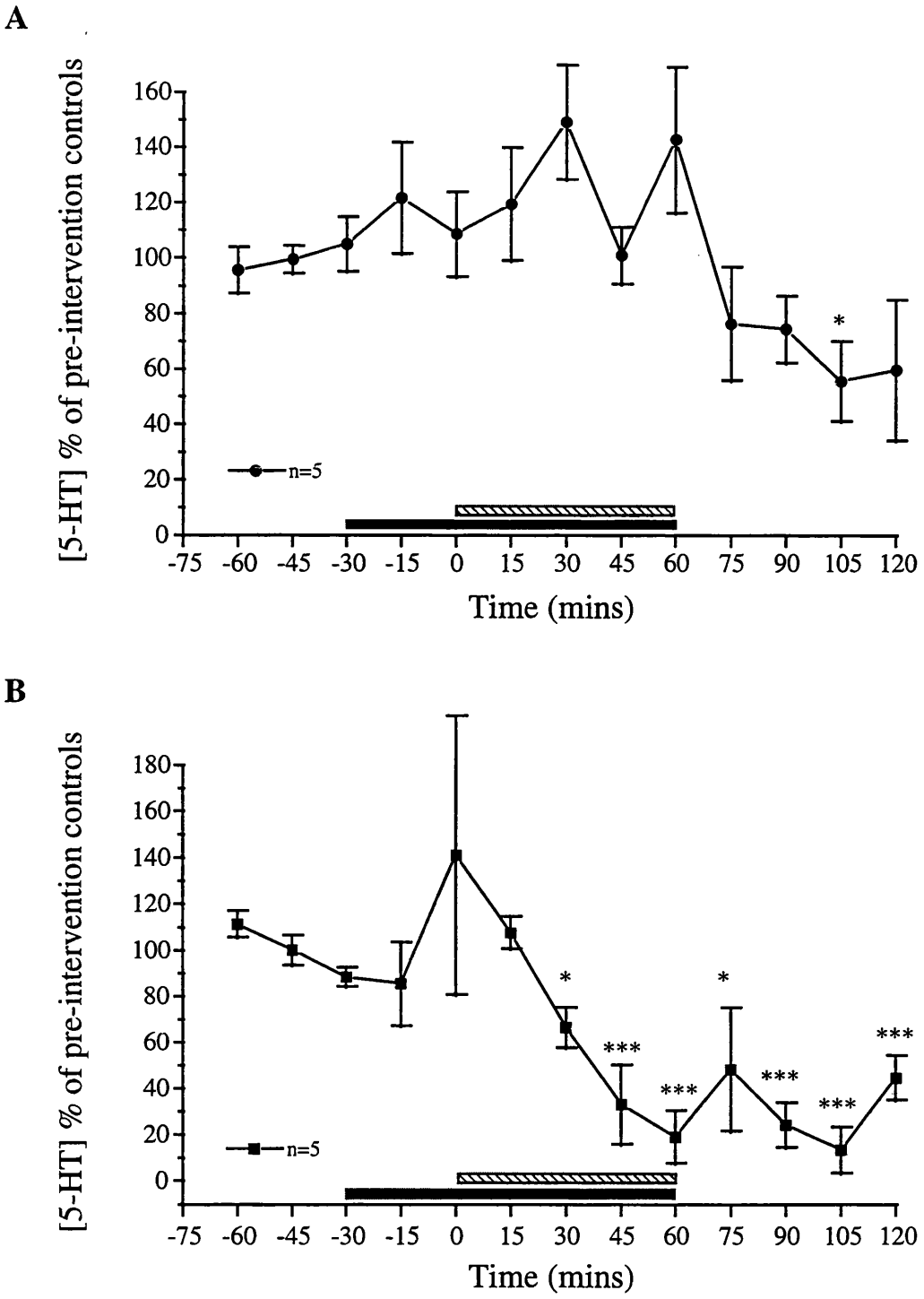

Figure 6.3. Effect of the specific 5-HT_{1A} antagonist WAY100635 (10 μM) on the effect of 8-OH-DPAT (1 mM) infusion in the midbrain raphe on 5-HT overflow in the raphe (**A**) and the SCN (**B**) at ZT 6. WAY100635 was infused 30 min prior to, and 60 min concurrently with 8-OH-DPAT. The solid bar denotes WAY100635 infusion and the hatched bar the 8-OH-DPAT. Values are mean ± s.e.m. expressed as a percentage of three pre-intervention controls. * $p < 0.05$; *** $p < 0.001$. Compare the effect of WAY100635 with the infusion of 8-OH-DPAT alone at ZT 6 (figure 6.2)

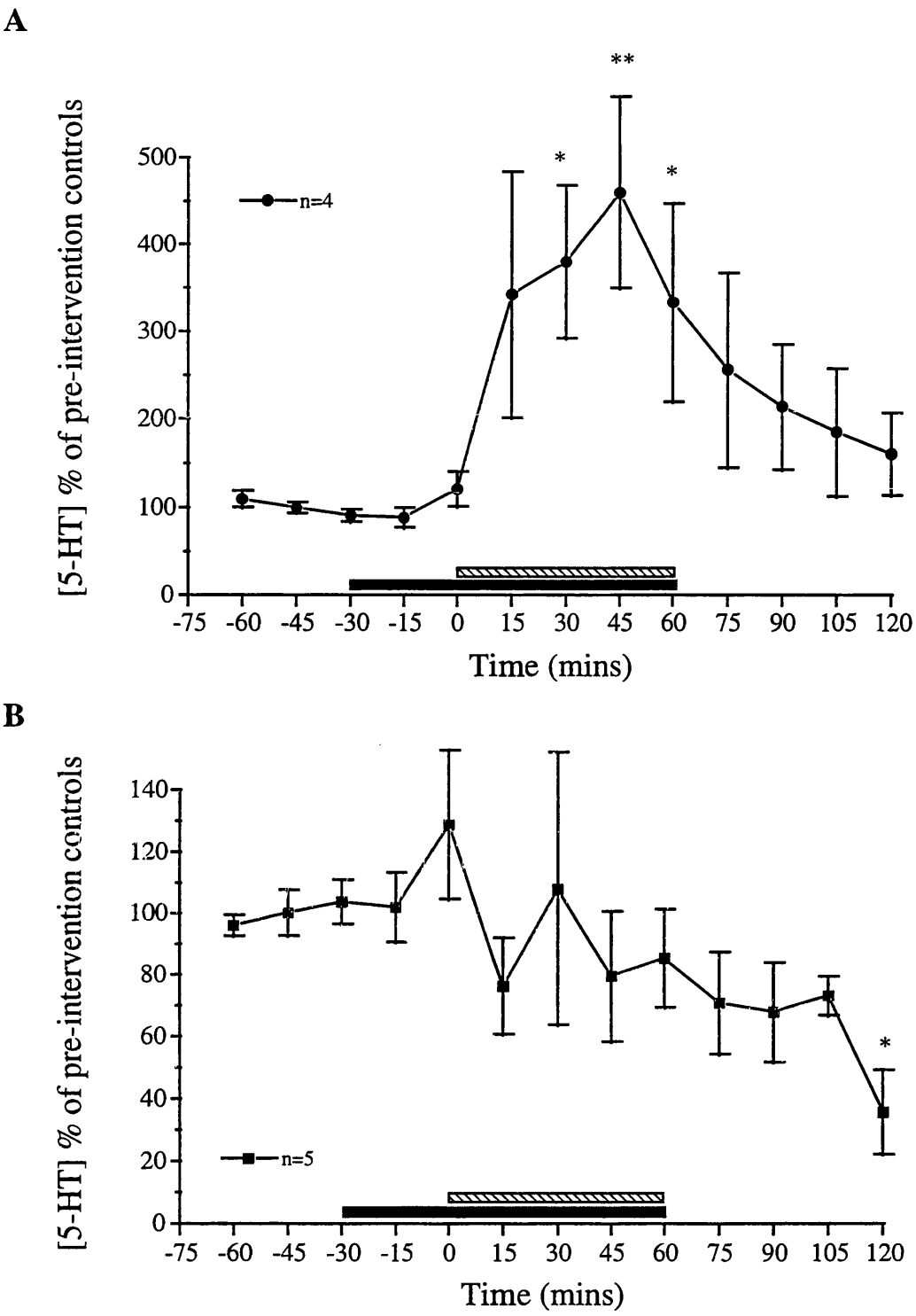

Figure 6.4. Effect of the specific 5-HT_{1A} antagonist WAY100635 (1 mM) on the effect of 8-OH-DPAT (1 mM) infusion in the midbrain raphe on 5-HT overflow in the raphe (**A**) and the SCN (**B**) at ZT 18. WAY100635 was infused 30 min prior to, and 60 min concurrently with 8-OH-DPAT. The solid bar denotes WAY100635 infusion and the hatched bar the 8-OH-DPAT. Values are mean ± s.e.m. expressed as a percentage of three pre-intervention controls. * $p < 0.05$; ** $p < 0.01$. Compare the effect of WAY100635 with the infusion of 8-OH-DPAT alone at ZT 18 (figure 6.1)

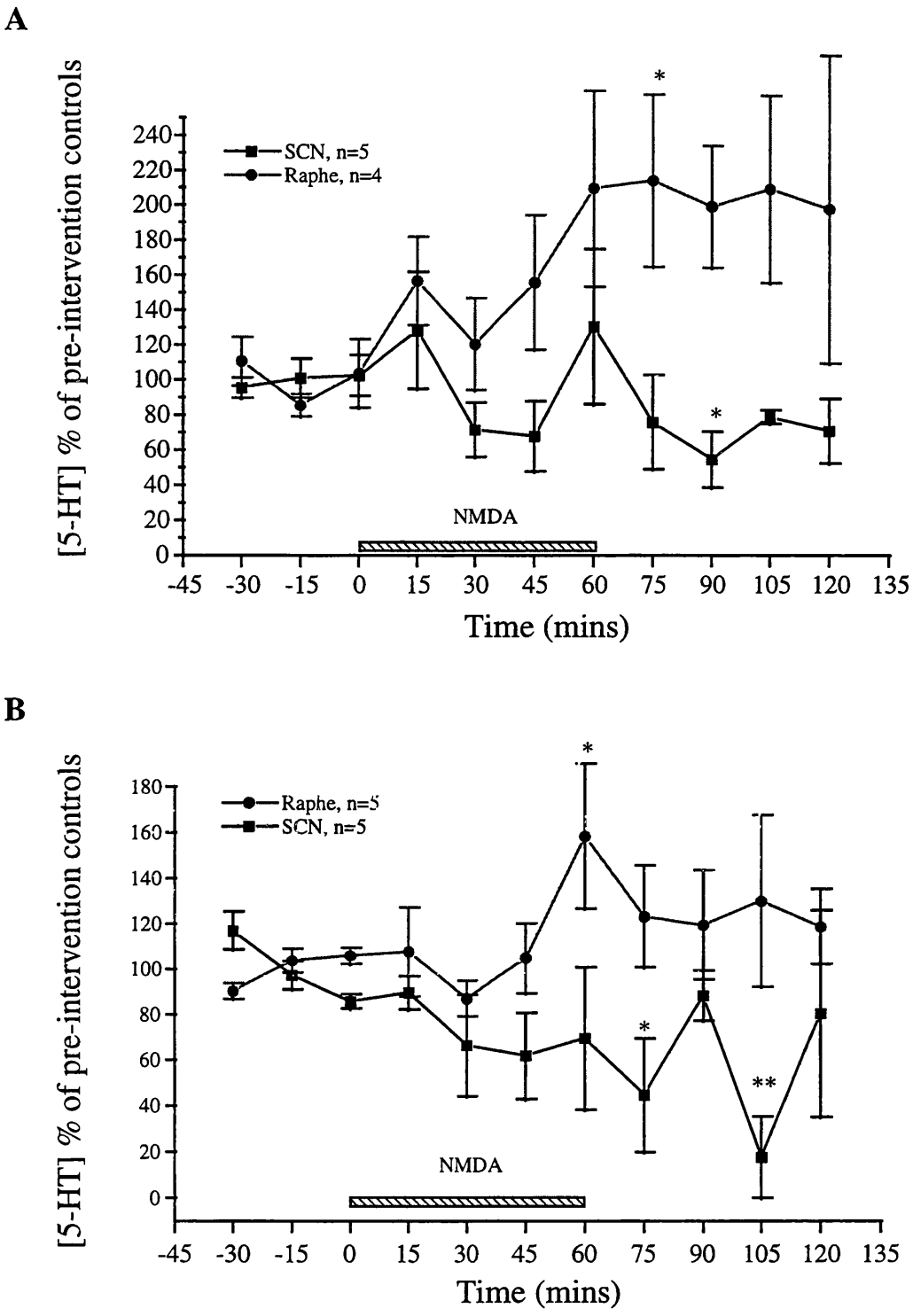

Figure 6.5. Effect of NMDA infusion (100 μM) in the midbrain raphe nuclei on 5-HT overflow in raphe nuclei and in the SCN at ZT 6 (**A**) and ZT 18 (**B**). Simultaneous collection of samples was carried out in a single animal implanted with two microdialysis probes. Values are mean ± s.e.m. expressed as a percentage of three pre-intervention control samples. NMDA was infused for 60 min denoted by the hatched bar. * $p < 0.05$; ** $p < 0.01$.

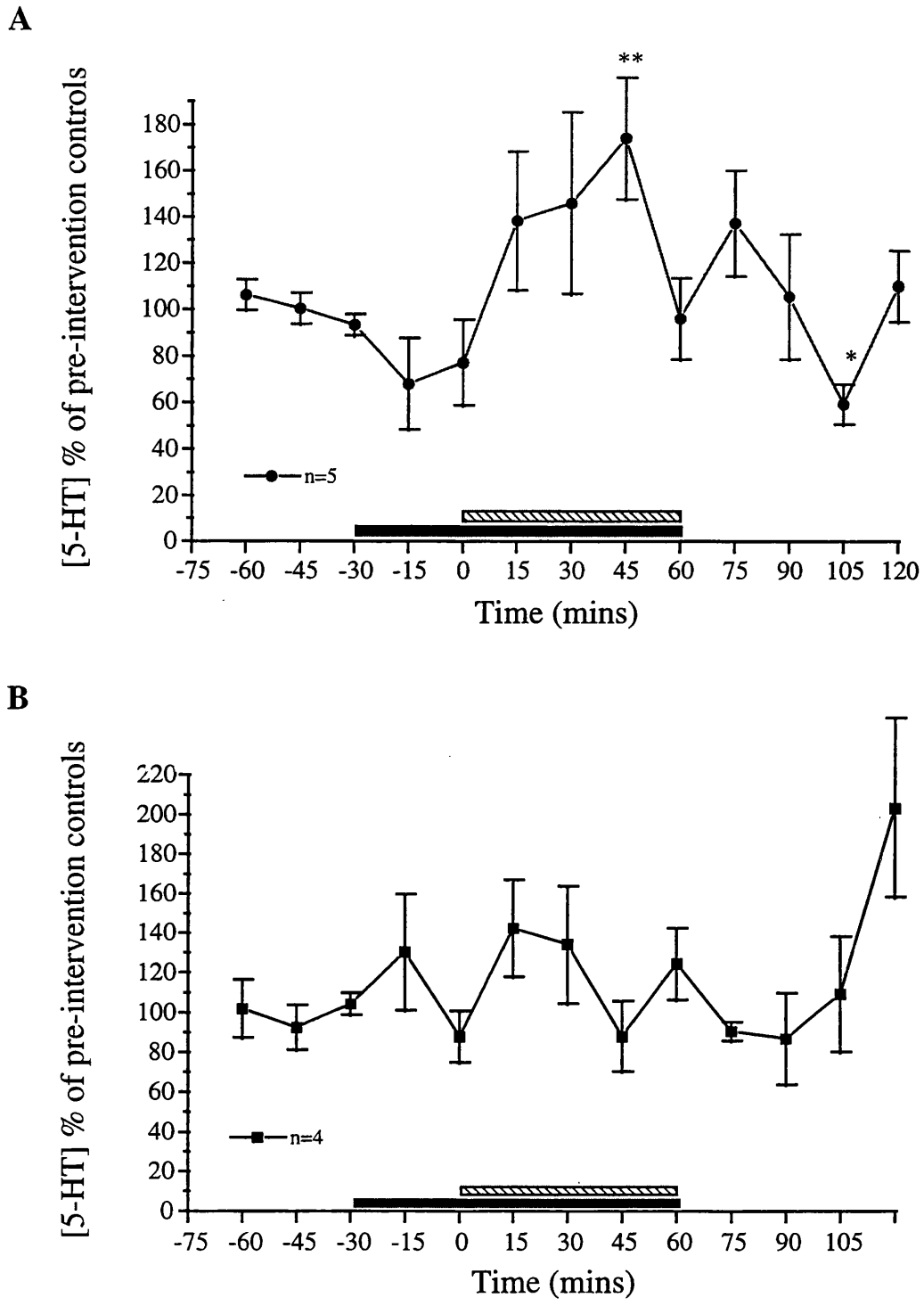

Figure 6.6. Effect of the specific antagonist AP5 (100 μM) on the effect of NMDA (100 μM) infusion in the midbrain raphe on 5-HT overflow in the raphe (**A**) and the SCN (**B**) at ZT 18. AP5 was infused 30 min prior to, and 60 min concurrently with NMDA. The solid bar denotes AP5 infusion and the hatched bar the NMDA. Values are mean ± s.e.m. expressed as a percentage of three pre-intervention controls. * $p < 0.05$; ** $p < 0.01$.

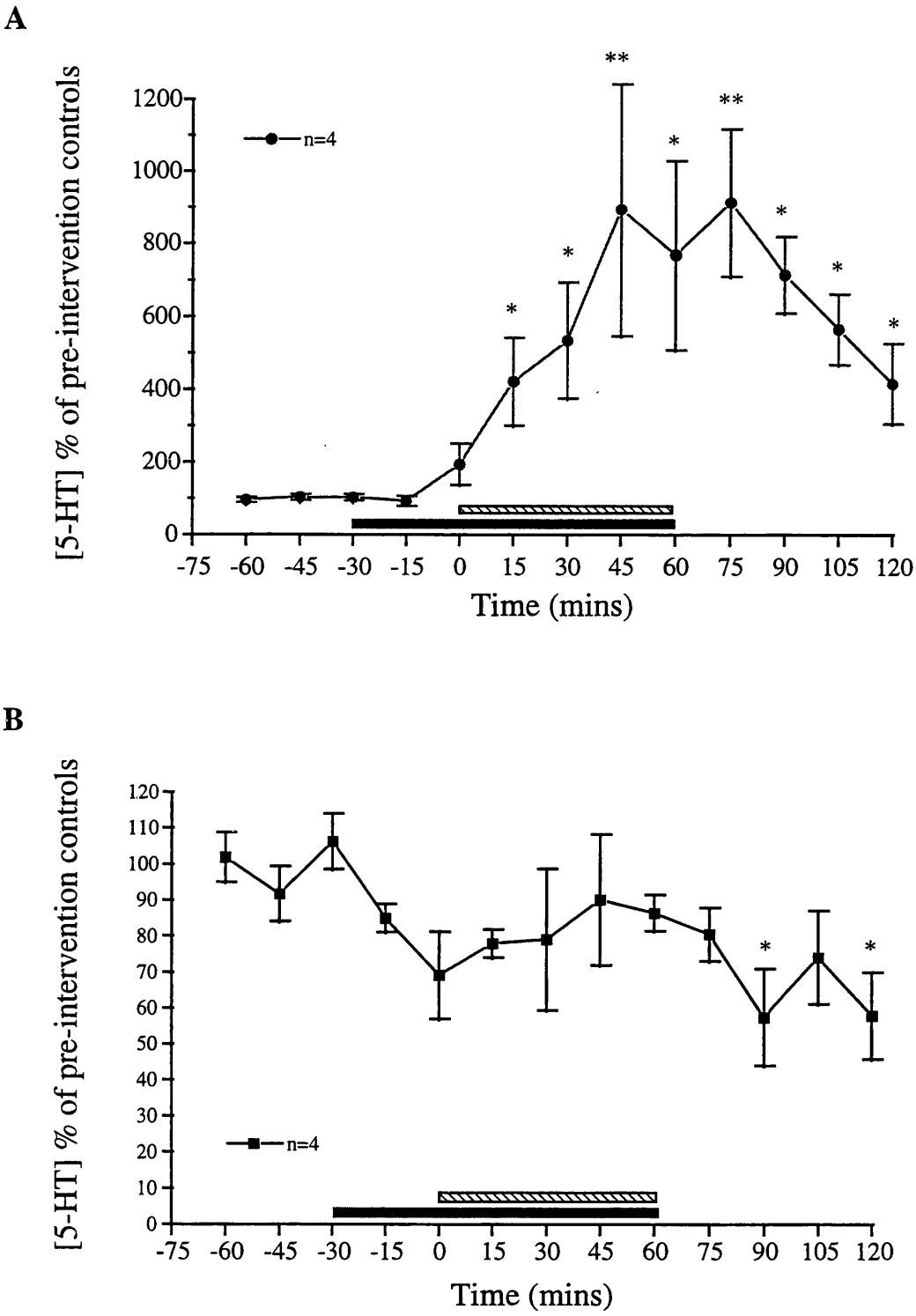

Figure 6.7. Effect of the specific 5-HT_{1A} antagonist WAY100635 (1 mM) on the effect of NMDA (100 μM) infusion in the midbrain raphe on 5-HT overflow in the raphe (**A**) and the SCN (**B**) at ZT 18. WAY100635 was infused 30 min prior to, and 60 min concurrently with NMDA. The solid bar denotes WAY100635 infusion and the hatched bar the NMDA. Values are mean ± s.e.m. expressed as a percentage of three pre-intervention controls. * $p < 0.05$; ** $p < 0.01$.

6.4 DISCUSSION

The double probe paradigm used in these experiments has been employed to detect changes in 5-HT concentration in the midbrain raphe and SCN dialysate samples simultaneously. Previous studies have successfully implanted two microdialysis probes into different areas of the brain to measure local changes in neurotransmitter release (Adell *et al.*, 1993; Matos *et al.*, 1996a; Tao and Auerbach, 1996; Bosker *et al.*, 1997; Morari *et al.*, 1998 and Pallotta *et al.*, 1998). With the exception of Matos *et al.* (1996a) and Morari *et al.* (1998) all these cited authors infused drugs by 'reverse-dialysis' into either the median or dorsal raphe nuclei, and detected changes in 5-HT concentration in forebrain projection sites, namely the nucleus accumbens, hippocampus, amygdala or the frontal cortex.

The application of drugs via one microdialysis probe implanted in the midbrain raphe enables us to detect changes in neurotransmitter release in a forebrain projection area. Because of the local area of the infusion via the microdialysis probe one has a reasonable idea of where the drug is acting. This provides an advantage compared to systemic administration of drugs, with subsequent detection of changes in a given transmitter in a particular area of the brain by microdialysis. For example, Hjorth and Sharp (1991) administered 8-OH-DPAT subcutaneously to anaesthetised animals, and measured 5-HT release in six separate forebrain sites by microdialysis. The 8-OH-DPAT decreased the 5-HT overflow in all forebrain sites, but the authors were left to speculate about the location of drug action, although they did postulate the midbrain raphe nuclei. They were however, unable to verify at which midbrain raphe nucleus the drug was exerting its effect. In experiments using a dual probe system, the experimenter is able to specifically apply drugs to particular brain nuclei, for example, separately to the median (MRN) or dorsal raphe nuclei (DRN) (Tao and Auerbach, 1996).

In the experiments reported in this thesis, I used a microdialysis probe with a functional membrane length of 4 mm which, when implanted, spanned the whole of the raphe nuclei -7.8 mm relative to Bregma (coordinates relative to Paxinos and Watson, 1982). This implantation site incorporated both MRN and DRN. Early autoradiaographic studies utilizing anterograde tracers combined with selective lesions of the serotonergic neurones with 5,6-dihydroxytryptamine in the rat, identified the midbrain raphe as the

principle source of the serotonergic terminals in the SCN (Moore *et al.*, 1978). However, since then there has been dispute over which raphe nucleus sends its projection to the SCN. Azmitia and Segal (1978) used anterograde tracing of the raphe nuclei in the rat, and concluded that the SCN receive input from both MRN and DRN. However, van de Kar and Lorens (1979) lesioned the MRN and DRN in separate groups of rats and measured isolated hypothalamic nuclei for serotonin content. A significant decrease in 5-HT content of the SCN was only achieved in animals that had received lesions to the MRN (by 70 %); electrolytic lesion of the DRN failed to significantly affect SCN 5-HT content. Retrograde tracer injected into the hamster SCN supports input from both MRN and DRN (Pickard, 1982), whereas functional studies looking at the effects of specific lesions on wheel running activity in hamsters (Meyer-Bernstein and Morin, 1996) have implicated only the MRN. More recent studies are still in disagreement as to the site of the projection from the midbrain raphe in the rat. Kawano *et al.* (1996) labeled SCN neurones with retrograde tracer and detected deposits in the DRN, whereas Moga and Moore (1997), using complimentary retrograde and anterograde tracers, suggested that the majority of fibres originate in the MRN. On the basis of this disagreement amongst individual groups, it was decided to incorporate both MRN and DRN in our experiments.

Basal 5-HT concentration collected in the dialysate collected from the raphe nuclei in this study was very similar to those of many authors who detected levels between 5 and 50 femtomols in the MRN or DRN with or without an SSRI in the perfusing aCSF (Agneter and Singer, 1993; Casanovas and Artigas, 1996; Matos *et al.*, 1996a; Bosker *et al.*, 1997; Casanovas *et al.*, 1997). However, Tao *et al.* (1997) were able to detect much higher basal levels, between 4 and 7 picograms, with the inclusion of an SSRI in the aCSF. Interestingly, Tao *et al.*, (1997) Casanovas and Artigas (1996), and Casanovas *et al.* (1997) were all able to detect higher basal 5-HT overflow from the MRN compared to the DRN. In my experiments, the basal raphe 5-HT concentration was higher during the dark phase compared to the light phase. Agren *et al.* (1986) measured the 5-HT concentration in micropunches of rat raphe nuclei assayed by HPLC, and detected highest levels at the end of the light phase with a nadir at end dark, which directly opposes our results. This may simply reflect differences in total tissue concentration (Agren *et al.* 1986) versus extracellular 5-HT concentration (this study).

To determine the effectiveness of this dual probe experimental model, initial experiments were performed infusing the 5-HT_{1A} agonist 8-OH-DPAT. 5-HT_{1A} receptor agonists are known to decrease firing of raphe neurones when administered systemically (Mundey *et al.*, 1996) or microiontophoretically (Dong *et al.*, 1997), and thus I postulated that administration of 8-OH-DPAT locally via the microdialysis probe would also decrease raphe neuronal firing. A decrease in neuronal firing should produce a concomitant decrease in 5-HT released at the terminal region, in this case the SCN. Initial experiments were performed at ZT 18. Lu and Nagayama (1996) demonstrated that the effectiveness of systemically applied 8-OH-DPAT to produce 5-HT_{1A} behavioural syndrome was dependent on circadian phase. Peak responses were observed in the mid-dark phase, and it was on this basis that preliminary experiments were performed at ZT 18, in an attempt to demonstrate what was expected to be a peak effect.

Bosker *et al.* (1997) successfully applied 1μM of the 5-HT_{1A} agonist flesinoxan via a microdialysis probe to produce an effect in the nucleus accumbens, and therefore I chose a concentration of 1 μM. At this concentration 8-OH-DPAT failed to demonstrate any significant effects on either raphe or SCN 5-HT overflow (figure 6.1). This may be due to different specificity of flesinoxan versus 8-OH-DPAT, or the diffusable properties of the agonist through the membrane. Casanovas and Artigas (1996) and Matos *et al.* (1996a) failed to detect changes in raphe 5-HT levels following administration of the lowest concentration of agonist in their experiments (0.3 mg/Kg and 5 mg/Kg respectively), and more specifically, 8-OH-DPAT (1 μM) infused via the probe into the raphe nuclei in rats implanted with two dialysis probes (raphe and hippocampus) failed to significantly affect 5-HT overflow in either midbrain or forebrain (Adell *et al.*, 1993). Additionally, a study by Bosker *et al.* (1994) also failed to demonstrate any effect of 8-OH-DPAT (1 μM) in MRN. Some forms of stress, such as placing rats in novel uncontrolled environmental conditions for 16 hours has been shown to decrease significantly DRN cell responses to the 5-HT_{1A} agonist iasaspirone, indicating a decreased sensitivity of somatodendritic 5-HT_{1A} autoreceptors (Laaris *et al.*, 1997). The rats in my study may therefore be undergoing a form of mild stress, as they have been placed in an unfamiliar experimental cage, and the inability of 1 μM 8-OH-DPAT to affect either SCN or raphe 5-HT overflow might thus be explained.

The concentration of 8-OH-DPAT was therefore increased to 1 mM. The ability of 8-OH-DPAT (1 mM) to reduce raphe 5-HT levels at ZT 18 was consistent with data from *in vivo* microdialysis experiments following systemic or local administration during the dark phase (Tao and Auerbach, 1996) and other *in vitro* (Davidson and Stamford, 1995) and *in vivo* (Casanovas *et al.*, 1997) data following application of 8-OH-DPAT in which the authors do not state the circadian phase. Other 5-HT_{1A} agonists administered systemically also significantly decreased raphe 5-HT overflow (isaspirone, Casanovas and Artigas, 1996; BMY14802, Matos *et al.*, 1996a; alnespirone, Casanovas *et al.*, 1997) and the 5-HT_{1A} agonist flesinoxan delivered via the dialysis probe significantly decreased caudal linear raphe and MRN 5-HT concentration (Bosker *et al.*, 1996).

In my experiments, raphe 5-HT levels fell significantly 90 min after the start of the infusion, which is similar to Matos *et al.* (1996a) who observed an effect 125 min post-systemic administration of the 5-HT_{1A} agonist BMY-14802 but longer than Casanovas and Artigas (1996) (40 min post-systemic injection of the 5-HT_{1A} agonist isaspirone), Casanovas *et al.* (1996) (40 min post-systemic injection of the 5-HT_{1A} agonist alnespirone and 8-OH-DPAT) and Bosker *et al.* (1996) (25 min post reverse dialysis infusion of the 5-HT_{1A} agonist flesinoxan). It is likely that the decrease in raphe 5-HT concentration induced by 8-OH-DPAT at ZT 18 is due to activation of 5-HT_{1A} receptors located on the soma and dendrites of the neurones in the serotonergic neuronal pool in the DRN and MRN. Additionally, 8-OH-DPAT which shows moderate affinity for the 5-HT_{1B} receptor may stimulate 5-HT_{1B} autoreceptors present on serotonergic nerve terminals in the raphe nuclei. Stimulation of the 5-HT_{1B} autoreceptor would be expected to decrease terminal 5-HT release (see Chapter 3).

The reduction in 5-HT overflow from the SCN following 1 mM 8-OH-DPAT to the raphe nuclei at ZT 18 is in keeping with the assumption that the applied 8-OH-DPAT is stimulating somatodendritic 5-HT_{1A} autoreceptors in the raphe. However, Romero *et al.* (1994) raised the possibility that other 8-OH-DPAT-sensitive serotonergic receptors different from 5-HT_{1A} autoreceptors, may be involved in the control of terminal 5-HT release. They monitored the effects of striatal 5-HT release (a forebrain projection site of the DRN) after subcutaneous administration of 8-OH-DPAT, before and after application of pertussis toxin to selectively destroy G_i/G_o proteins. Surprisingly, the

destruction of the G-proteins failed to modulate the effect of 8-OH-DPAT, and on this their conclusions were based. Further experiments need to be carried out before one can speculate if the 8-OH-DPAT in my experiments was stimulating receptors in the raphe other than the 5-HT_{1A} autoreceptor. Until some evidence is produced to the contrary I will assume that the 8-OH-DPAT was stimulating 5-HT_{1A} cell body autoreceptors.

The effect of 1 mM 8-OH-DPAT applied during the light phase at ZT 6 on SCN 5-HT levels is comparable to the effect demonstrated at ZT 18 during the dark phase, resulting in a decreased 5-HT overflow. The effect on raphe 5-HT overflow, on the other hand was quite dramatic. The 5-HT_{1A} agonist produced a huge increase in raphe 5-HT to a peak of 516 ± 104 % of pre-intervention controls.

The ability of 8-OH-DPAT to increase raphe 5-HT concentration at ZT 6 represents differences in the route of administration of the drug. Most studies (with the exception of Tao and Auerbach, 1996, who performed their experiments during the dark phase) have involved systemic administration of the 5-HT_{1A} agonist with subsequent measurement of raphe 5-HT levels from microdialysis probes implanted into the raphe nuclei. Three studies that have involved infusion of a 5-HT_{1A} agonist locally via reverse dialysis to the raphe nuclei have all reported an increase in 5-HT concentration (Adell *et al.*, 1993; Bosker *et al.*, 1994; Matos *et al.*, 1996b). All three studies also demonstrated that systemic administration of the same agonists consistently decreased significantly raphe 5-HT overflow. Local application of the 5-HT_{1A} agonist buspirone, at low concentration (10-100 nM) had no effect, whilst at the highest concentration (1 mM), equivalent to that used in my experiments, significantly enhanced DRN 5-HT release (Matos *et al.*, 1996b). The two other studies infused 8-OH-DPAT. At concentrations between 0.1-10 µM (Bosker *et al.*, 1994) and 1-100 µM (Adell *et al.*, 1993), 8-OH-DPAT infusion had no effect on raphe 5-HT overflow, whilst higher concentrations (100 µM, Bosker *et al.*, 1994; 1-10 mM, Adell *et al.*, 1993) enhanced significantly raphe 5-HT concentration. In addition, this response to locally infused 8-OH-DPAT appears to be a biphasic response as very low concentrations (30-100 nM) significantly decreased raphe 5-HT overflow (Bosker *et al.*, 1994).

The application of the 5-HT_{1A} agonist via the probe represents a local effect on neurones in close proximity of the probe tip, whereas with systemic administration one cannot ascertain where the drug is acting. The systemically administered drug may act at brain areas other than the raphe nucleus to produce an overall effect of lowering raphe nuclei 5-HT concentration. At high concentrations, 8-OH-DPAT has the ability to bind to the 5-HT reuptake system. Tritiated 8-OH-DPAT has been shown to label two sites in preparations of human platelets (Ieni and Meyerson, 1987) and homogenates of raphe nuclei from rat brain (Wootton and Hazelwood, 1990). The higher affinity site corresponds to the 5-HT_{1A} binding site, and the lower to the 5-HT uptake sites. Indeed, 8-OH-DPAT competitively inhibited tritiated 5-HT uptake into rat cortical synaptosomes (Hamon *et al.*, 1984). Therefore, the increase in raphe 5-HT concentration may be a consequence of reuptake blockade, since the aCSF perfusing the raphe did not contain a 5-HT reuptake blocker. However, if the 8-OH-DPAT did bind to the reuptake system, I would have expected the effect to be apparent during both the light and dark phase. The possibility remains that the affinity of 8-OH-DPAT to bind to the 5-HT uptake site exhibits a diurnal variation. Bearing in mind that the results of my experiments performed at ZT 18 and those performed by Tao and Auerbach (1996) during the dark phase, did not exhibit a significant increase in raphe 5-HT concentration after 8-OH-DPAT infusion, the effect of locally infused 8-OH-DPAT appears to undergo a diurnal variation.

The experiments of Lu and Nagayama (1996; Nagayama and Lu, 1997) demonstrated a circadian rhythm in the behavioural response to subcutaneous (s.c.) or intracerebroventricular (i.c.v.) administration of 8-OH-DPAT. Stimulation of the central 5-HT_{1A} receptors with 8-OH-DPAT at mid-dark produced maximal responses in forepaw treading, head weaving (s.c. and i.c.v. administration) and flatbody posture (s.c. administration). The results presented in this thesis do not support the hypothesis that the somatodendritic 5-HT_{1A} autoreceptor exhibits diurnal variation in function. The ability of 8-OH-DPAT applied to the raphe nuclei to decrease 5-HT concentration in the SCN did not vary at ZT 6 versus ZT 18. However, the experiments by Lu and Nagayama (1996) suggest that it is a *post*-synaptic 5-HT_{1A} receptor that exhibits a circadian rhythm in its function. Therefore, my results, stimulating a *pre*-synaptic receptor in the raphe nuclei, cannot explain the variation demonstrated by these authors. Indeed, behavioural experiments performed by Moser and Redfern (1985) in which they

measured the hypothermic response to 8-OH-DPAT did not demonstrate variation in the ability of the drug to induce a hypothermia. The 8-OH-DPAT induces hypothermia in rodents through an action on 5-HT cell body autoreceptors (Goodwin *et al.*, 1985), thus suggesting that the somatodendritic 5-HT_{1A} autoreceptor does not exhibit diurnal variation, as confirmed in my study. As mentioned above, the variation lies in the ability of 8-OH-DPAT to influence raphe 5-HT levels. At ZT 18, 8-OH-DPAT significantly decreased 5-HT overflow, whereas at ZT 6, 8-OH-DPAT significantly increased 5-HT overflow. Whether this is a direct effect 5-HT_{1A} receptor stimulation, or an indirect effect, remains to be elucidated.

WAY100635 is a potent and selective 5-HT_{1A} receptor antagonist (Fletcher *et al.*, 1994). Subcutaneous administration of 8-OH-DPAT (1 mg/Kg) can inhibit the firing rate of dorsal raphe neurones and induce specific behaviours in the guinea pig (Mundey *et al.*, 1996). The effect of 8-OH-DPAT can be antagonised by prior administration of WAY100635 (1 mg/Kg s.c.). Similarly in rat DRN slices, reduction in electrically stimulated 5-HT release by application of 8-OH-DPAT (1 μM) was prevented by WAY100635 (0.1 μM) (Davidson and Stamford, 1995). Administration of WAY100635 (s.c.) also antagonised the reduction in forebrain 5-HT levels following systemic administration of a 5-HT_{1A} agonist (Bosker *et al.*, 1996; Matos *et al.*, 1996a; Bosker *et al.*, 1997) in addition to blocking the reduction in raphe 5-HT levels.

In my study, 30 min pre-treatment with 10 μM WAY100635 followed by 60 min concomitant infusion with 1 mM 8-OH-DPAT at ZT 6, successfully attenuated the increase in raphe 5-HT concentration following 8-OH-DPAT infusion. The increase in 5-HT can, therefore, be assumed to be due to stimulation of 5-HT_{1A} receptors. Interestingly, 45 min after the end of the combined infusion of WAY100635 and 8-OH-DPAT, raphe 5-HT levels fell significantly. Unfortunately, the concentration of WAY100635 was insufficient to block the decrease in 5-HT levels in the SCN. It appears that the concentration of antagonist required to block the 5-HT_{1A} autoreceptor is greater than that required to block the 5-HT_{1A} receptors responsible for the local increase in raphe 5-HT concentration. Interestingly, Matos *et al.* (1996b) also observed that different concentrations of antagonist was required to block 5-HT_{1A}-induced 5-HT decrease in the forebrain (hippocampus) and in the raphe nuclei. They applied the 5-

HT_{1A} agonist systemically whilst the antagonist was applied locally to the raphe. A greater concentration of antagonist was required to block the decrease in raphe 5-HT versus the hippocampal 5-HT. Although this runs counter to my data (a greater antagonist concentration was required to prevent the decrease in SCN 5-HT concentration versus the increase in raphe 5-HT), this might reflect a difference in systemic versus local administration of the 5-HT_{1A} agonist.

Increasing the concentration of WAY100635 onehundred-fold (1 mM) successfully antagonised the effect of 8-OH-DPAT on terminal 5-HT concentration at ZT 18. However, the concentration in the final dialysate fraction collected 60 min after the end of the drug infusion remained significantly below pre-intervention control samples (figure 6.4B). The decrease in raphe 5-HT overflow following infusion of 8-OH-DPAT at ZT 18 was also prevented by pretreatment with the antagonist. However, the combined effect of 5-HT_{1A} agonist and antagonist was to increase dramatically raphe 5-HT release. It was assumed that WAY100635 was not acting as a partial agonist (Fornal *et al.*, 1994) and that the effect was due to the antagonism of the 5-HT_{1A} receptor.

There is evidence of serotonergic tone in the DRN, possibly modulated by an inhibitory 5-HT_{1A} autoreceptor. WAY100635 administration in the cat increases raphe neuronal firing in the dark phase, and not in the light phase (Fornal *et al.*, 1994), whereas in the guinea pig, WAY100635 (s.c.) causes a dose dependent increase in DRN firing in the light phase (Mundey *et al.*, 1996). The circadian phase of this appears to be species dependent. Additionally, local infusion of the 5-HT_{1A} antagonist (-)pindolol in the rat DRN increased 5-HT levels (circadian phase not stated) (Matos *et al.*, 1996b). It is possible that *in situ*, somatodendritic 5-HT_{1A} autoreceptors on raphe interneurones are activated by extracellular 5-HT to produce inhibition of 5-HT release in the soma region. Administration of the 5-HT_{1A} antagonist would thus remove the tonic inhibition thereby increasing extracellular 5-HT at the cell body region.

The dual probe paradigm has thus successfully applied drugs to the raphe with subsequent monitoring of release from the terminal SCN region. The effect of direct application of the ionotropic glutamate receptor agonist NMDA via the probe to the midbrain raphe was next investigated. Similar effects of NMDA (100 μM) on raphe and

SCN 5-HT overflow were obtained at mid-light and mid-dark. Maximal increase in raphe 5-HT levels was slightly higher at ZT 6 versus ZT 18; 214 ± 19.3 versus 158 ± 31.7 % of baseline respectively. Conversely, at ZT 18, the decrease in SCN 5-HT following NMDA infusion of the raphe nuclei was greater than that produced at ZT 6; 17.7 ± 17.7 versus 54.6 ± 16.9 % of baseline respectively. Tao and Auerbach (1996) infused NMDA via 'reverse' dialysis into the DRN and MRN during the dark phase, and at a concentration of 100 μM produced an increase in 5-HT overflow comparable to that produced in my experiments. They also monitored the effect of NMDA into either the DRN or MRN on 5-HT release in the projection sites (nucleus accumbens and hippocampus respectively). Unlike the decrease in SCN terminal 5-HT release I observed with 100 μM NMDA, they could not produce an effect with 100 μM. They did, however, elicit an increase in terminal 5-HT release upon increasing the NMDA concentration to 300 μM. Pallotta *et al.* (1998) used the dual probe model to monitor 5-HT release in the raphe nucleus and concomitant release in the frontal cortex after infusion of NMDA. Not unlike the results presented here, the authors reported an increase in raphe 5-HT overflow, with a parallel decrease in frontal cortex 5-HT concentration. The effect of increased 5-HT in the nucleus accumbens and hippocampus, reported by Tao and Auerbach (1996), may be pathway-specific.

Pre-treatment and co-administration with the competitive NMDA antagonist AP5 at ZT 18 failed to antagonise the increase in raphe 5-HT concentration evident after NMDA alone, but did block the decrease in 5-HT levels in the SCN. This would lead to the suggestion that the increase in raphe 5-HT overflow post-NMDA infusion was not mediated by NMDA receptors but was a non-specific effect of the amino acid agonist. However, the decrease in terminal 5-HT levels measured in the SCN was a direct consequence of the stimulation of NMDA receptors. The ability of AP5 to prevent the decrease in SCN 5-HT levels is a positive result, but it is unusual that the AP5 was unable to block the increase in raphe 5-HT overflow. Results from *in vitro* raphe culture preparations suggest that the rise in raphe 5-HT overflow following application of NMDA is mediated by NMDA receptors as it is prevented by pre-treatment with AP5 (Becquet *et al.*, 1993). Tao and Auerbach (1996) were able to block the rise in DRN 5-HT levels with the application of both non-competitive and competitive antagonists. Indeed, the same concentration of agonist and antagonist used in these experiments were

used by Tao and Auerbach (1996) (i.e. 100 μM NMDA and AP5 by 'reverse' dialysis). Pallotta *et al.* (1998) also demonstrated that AP5 (100 μM by 'reverse' dialysis) was able to prevent the rise in raphe 5-HT levels following 100 μM NMDA. The reason for the inability of AP5 to antagonise the NMDA-induced increase in raphe 5-HT overflow in my experiments is not clear and requires further experiments perhaps using higher concentrations of AP5.

NMDA receptors are excitatory. Stimulation would be expected to increase neuronal firing due to an influx of calcium ions into the cell. It is, therefore, unlikely that NMDA receptors are present on the ascending raphe neurones projecting to the SCN, considering that stimulation of these receptors produced a decrease in 5-HT overflow in the SCN. The ability of NMDA to decrease SCN 5-HT levels is more likely to be an indirect effect. The NMDA receptors may be located on inhibitory GABA-ergic interneurones in the raphe nuclei. Stimulation of these receptors would be expected to increase the local concentration of GABA in the raphe, thus decreasing neuronal firing. Alternatively, the NMDA receptors might be present on serotonergic interneurones in the raphe nuclei. NMDA receptor stimulation would, therefore, increase the concentration of 5-HT within the raphe nuclei (as was observed after NMDA infusion via the probe in my experiments at both ZT 6 and ZT 18), increasing the amount of 5-HT available to stimulate the somatodendritic 5-HT_{1A} autoreceptor. Stimulation of the 5-HT_{1A} autoreceptor would then be expected to decrease the 5-HT concentration in the SCN. Consistent with the suggestion that NMDA receptor stimulation can indirectly affect ascending serotonergic neuronal firing, intravenous administration of the non-competitive (MK801) or competitive (CPP) NMDA receptor antagonist to rats, facilitated DRN firing of ascending serotonergic neurones (Lejeune *et al.*, 1994). However, these authors reported that NMDA administered alone did not significantly modify DRN firing.

To examine the theory that the NMDA infused into the raphe nuclei was indirectly stimulating the 5-HT_{1A} cell body autoreceptor, the 5-HT_{1A} antagonist WAY100635 was pre- and co-infused with NMDA. At a concentration previously shown to attenuate the decrease in SCN 5-HT levels by 1 mM 8-OH-DPAT at ZT 18, 1 mM WAY100635 did not prevent the inhibition of terminal 5-HT release in the SCN by NMDA (100 μM).

However, the maximal decrease in SCN 5-HT concentration was attenuated (57.4 ± 13.5 versus 17.7 ± 17.7 % of baseline, respectively). From this it would appear that the decrease in SCN 5-HT concentration following NMDA infusion in the raphe is only partially, if at all, mediated by the 5-HT_{1A} autoreceptor. The rise in raphe 5-HT release post-NMDA infusion was not blocked by WAY100635, but was augmented ten-fold by co-application with the 5-HT_{1A} receptor antagonist. Pallotta *et al.* (1998) were able to block the fall in frontal cortex 5-HT overflow following 100 μM NMDA with WAY100635 (1 μM) administered to the raphe nuclei via 'reverse' dialysis, but unable to prevent the increase in raphe 5-HT. The difference in the results obtained by these authors and the data presented here is the large difference in concentration of WAY100635 administered although the concentration of NMDA was comparable. The concentration of WAY100635 I used was 1000 times greater than that used by Pallotta and co-workers (1998), and this may go a little way to explaining the observed differences.

In the absence of a 5-HT_{1A} agonist but in the presence of NMDA, WAY100635 may result in a disihibition of serotonergic interneurones. Postulating that there is serotonergic tone in the raphe modulated by inhibitory 5-HT_{1A} autoreceptors (as discussed previously), stimulation by the antagonist would increase local 5-HT concentration. 5-HT_{1A} receptors and NMDA receptors may co-exist on serotonergic interneurone cell bodies or be present on separate groups of serotonergic interneurones. The regulation of local raphe 5-HT concentration may be a balance between stimulation of 5-HT_{1A} receptors decreasing interneurone output of 5-HT, and NMDA receptor stimulation increasing the output. Simultaneous blockade of the 5-HT_{1A} receptor and stimulation of the NMDA receptor might therefore evoke a greater response than would be predicted from the responses of the two drugs administered alone. This however, might lead to depletion of neuronal stores of 5-HT because the increase in raphe 5-HT following both WAY100635 and NMDA is sustained for the whole experimental collection period. However, the area that the probe is spanning is quite large, and activation of all neurones might have led to a sustained increase in 5-HT overflow.

The combined effect of the 5-HT_{1A} antagonist and NMDA receptor stimulation might be an indirect effect of glutamate. A study by Dijk an co-workers (1995) applied drugs

topically to the striatum, collected samples from the frontal cortex by means of microdialysis, and measured glutamate release. Although these workers did not measure 5-HT and they did not monitor levels in the raphe nuclei, they did demonstrate a significant potentiation of glutamate release in the frontal cortex after co-application of WAY100635 with NMDA as compared to release with NMDA stimulation alone. This potentiating effect of WAY100635 on NMDA-induced glutamate release is obviously occurring at the cell body region, as they were applying drugs to the cell body, whilst monitoring terminal transmitter release. The possibility remains that the disinhibition of a glutaminergic neurone by WAY100635 increases glutamate release, thereby activating NMDA receptors in addition to other ionotropic glutamate receptors present on serotonergic interneurones, to increase 5-HT release in the raphe nuclei. Of course all of the possibilities proposed in this discussion to explain the combined effect of NMDA and the 5-HT_{1A} antagonist, and others, might occur in the raphe nuclei. It is only with further studies that the mechanisms behind the potentiation of NMDA-induced 5-HT release in the raphe by a 5-HT_{1A} receptor antagonists will be elucidated.

6.5 CONCLUSIONS

The dual probe paradigm has been a very useful tool in examining the effects of drugs administrated locally to the midbrain raphe nuclei, whilst measuring 5-HT overflow in the raphe itself and in a terminal projection area, the SCN.

The somatodendritic 5-HT_{1A} inhibitory autoreceptor, stimulated by 8-OH-DPAT does not exhibit a diurnal variation in function as tested at mid light versus mid dark phases. On the other hand, the local raphe response to a high concentration (1 mM) of 8-OH-DPAT does exhibit a diurnal variation. A significant decrease in raphe 5-HT overflow is observed following infusion at ZT 18 (dark phase) compared with a significant increase at ZT 6 (light phase).

These results give support to a functional role of a retino-raphe-SCN projection in the rat, which may be important in the control of circadian rhythms. NMDA released from retinal afferents might, indirectly by the incorporation of raphe interneurones, result in a decrease in SCN terminal 5-HT release. The increase in 5-HT release in the raphe by

stimulation of NMDA receptors, in part stimulates inhibitory 5-HT_{1A} autoreceptors to inhibit neuronal firing and decrease 5-HT release in the SCN.

CHAPTER 7

GENERAL DISCUSSION

In the following chapter I shall summarize the data collected in this thesis, discuss the relevance of the results and discuss possibilities for future work.

7.1 SUMMARY OF THESIS

The microdialysis technique has proved to be an excellent method of sampling *in vivo* neurotransmitter levels from the SCN, hippocampus and raphe nuclei regions. Using this technique the terminal 5-HT_{1B} auto- and hetero-receptor and somatodendritic 5-HT_{1A} autoreceptor function have been examined in the conscious rat. In addition, the interaction between the serotonergic and glutamatergic systems were examined in the somatodendritic (raphe nuclei) and terminal (SCN) regions. The aims were to further the understanding of the regulation of 5-HT release within the circadian pacemaker and to examine the relationship between the serotonergic and glutamatergic systems.

The striking feature of the 5-HT_{1B} autoreceptor in the SCN was the difference in responsiveness to agonist stimulation at the different zeitgeber times examined. This variation in function did not follow either the pattern of extracellular 5-HT concentration or the light:dark cycle, although in general the greatest response to agonist stimulation occured during the light period. This variation in function seemed to be specific to the SCN; when the 5-HT_{1B} autoreceptor was tested in another serotonergic rich brain region, namely the hippocampus, at mid-light and mid-dark, the inhibition of neuronal 5-HT following agonist stimulation did not follow that of the SCN. That is, in the hippocampus agonist stimulation at mid-light and mid-dark produced a significant reduction in dialysate 5-HT overflow, whilst in the SCN the response is absent during mid-dark. The variation in 5-HT_{1B} receptor function also seemed specific to the autoreceptor because the 5-HT_{1B} heteroceptor showed no variation to agonist stimulation at the two time points tested (mid-light and mid-dark).

The reason behind the variation in function of the 5-HT_{1B} autoreceptor was unknown. Thus, I next examined whether the messenger RNA for the 5-HT_{1B} receptor varied in parallel to the variation in SCN receptor function. The reverse transcriptase-polymerase chain reaction method was utilised to examine the 5-HT_{1B} postsynaptic, auto- and hetero- receptor mRNA in dissected SCN, raphe, and retinal tissues, respectively. The variation in function of the 5-HT_{1B} autoreceptor could not be explained by alterations in

mRNA for the receptor since no variation in 5-HT_{1B} autoreceptor mRNA was detected using this method. Interestingly, the mRNA for both the 5-HT_{1B} heteroreceptor and the postsynaptic receptor did show variation over 24 hours. The variation in SCN 5-HT_{1B} receptor mRNA may contribute to a variation in the number of postsynaptic receptors in the SCN, and a diurnal variation in receptor function. The variation in retinal 5-HT_{1B} receptor mRNA may also reflect variation in the number of 5-HT_{1B} heteroreceptors present on retinal afferents in the SCN, and perhaps receptor function. The absence of a diurnal variation in the function of the 5-HT_{1B} heteroreceptor in the SCN demonstrated in this thesis may reflect the two sampling times. It remains a possibility that the 5-HT_{1B} heteroceptor exhibits a diurnal variation evident at time points other than those sampled in my experiments.

The absence of variation in mRNA for the 5-HT_{1B} autoreceptor led me to speculate that it was the number of receptors available for agonist stimulation that was important in determining the receptor function. The method of choice to examine the receptor protein was immunocytochemistry. Unfortunately the antibody raised against the 5-HT_{1B} receptor was unable to detect the receptor protein in brain slices. Therefore, Western blotting was employed to detect 5-HT_{1B} receptor protein levels in dissected SCN tissue. There were a number of limitations of this technique as outlined in Chapter 4 but from the results obtained there did not appear to be significant differences in receptor protein level over the eight zeitgeber times tested. Thus, the mechanism(s) behind this variation of receptor function has yet to be elucidated.

The extensive sampling across the light:dark cycle whilst examining the 5-HT_{1B} autoreceptor function demonstrates the need for more than one time point when examining the function of a particular receptor. Some authors (e.g. Tao and Auerbach) who detect 5-HT in microdialysate samples collect only during the dark phase. If I had applied RU24969 to the SCN during the mid-dark phase only, I might have eroneously concluded that in the SCN there was no function of a 5-HT_{1B} autoreceptor. Although this effect appeared to be specific to the SCN when compared to the hippoampus, other brain regions such as SCN effector areas might be likewise affected.

In contrast to the terminal 5-HT_{1B} autoreceptor, the somatodendritic 5-HT_{1A} autoreceptor failed to exhibit variation in function as examined by the dual probe microdialysis experiments at two time points (mid-light and mid-dark).

The regulation of 5-HT release by excitatory amino acids was examined in the SCN at both the terminal and soma regions. The close proximity of the serotonergic and glutamatergic terminals in the SCN provides spatial evidence for interaction between the two systems. Indeed, 5-HT release in the SCN was regulated by the ionotropic glutamate receptor agonists kainate and NMDA and by the metabotropic glutamate receptor agonist 1S,3R-ACPD. AMPA receptor stimulation failed to affect 5-HT release in the SCN. The response to NMDA and ACPD showed diurnal variation. Metabotropic receptor stimulation with ACPD at the highest dose enhanced significantly the measured 5-HT concentration at mid-light whilst having no effect at mid-dark. On the other hand, at the lowest dose tested, NMDA receptor stimulation at mid-dark reduced significantly 5-HT overflow in the SCN whilst having no effect at mid-light. This reduction in 5-HT overflow by NMDA appeared to involve the endogenous release of noradrenaline acting on presynaptic α_2-adrenoreceptors, because addition of the α_2-adrenoreceptor antagonist idazoxan potentiated the release of 5-HT. At mid-dark, there was no reduction in 5-HT following NMDA receptor stimulation; this may be because of a diurnal variation in either the ability of NMDA to release noradrenaline, or the function of the α_2-adrenoreceptor. At the highest dose tested, NMDA increased significantly the 5-HT overflow from the SCN at both time points tested.

The regulation of 5-HT release in the SCN by NMDA application to the soma region did not appear to exhibit a diurnal variation under the given conditions and the dose tested. NMDA administration to the raphe nuclei significantly decreased SCN 5-HT overflow at both mid-light and mid-dark. The effect was likely to be the result of indirect stimulation of raphe interneurones, and to be partly mediated by an increased 5-HT concentration in the soma region acting on the 5-HT_{1A} inhibitory autoreceptors. This modulation of the ascending raphe nuclei projection to the SCN by the excitatory amino acid agonist provides functional evidence for a retinal-raphe-SCN projection in the rat.

7.2 DISCUSSION

Research into circadian rhythms has increased within the last few years and the results presented in this thesis have gone a little way to extending the information known about the function of the circadian pacemaker in mammals. A knowledge of the normally functioning circadian pacemaker aside from any intrinsic scientific interest can also inform studies of abnormalities in clock function such as jet-lag and depressive illness. In addition, the importance of timing during drug delivery in certain medical manipulations such as cancer chemotherapy, is now being recognised (for a review on clinical chronopharmacology see Lemmer, 1995). However, the differences in the intricate workings of the clock in two mammalian species, namely the rat and hamster, casts doubt upon the extrapolation of the results obtained in rodents to man.

One clinical condition that may have direct relevance to the results obtained in this thesis is that of depression. Over the past few years an increasing amount of evidence has indicated that depression, one of the most common mental illnesses in man, is associated with abnormalities in circadian rhythms (for a recent review see Rosenwasser and Wirz-Justice, 1997). Depressed patients may present with similar symptoms, but the causal mechanisms of each individual may be completely different. Difficulty in getting to sleep and early morning wakening are of the most common complaints in depressive illness. This latter abnormal timing is suggestive of a phase advance in the sleep wake cycle, and is one of the most robust findings that suggest that depression involves a disorder of time keeping. However, disruption of circadian parameters cannot simply be diagnosed as a phase advance in the sleep wake cycle, as these changes are not consistent in all humans or animal models of depression. It still remains obscure whether depressive illness leads to altered circadian rhythms, or whether a disruption in the normal time keeping function is responsible for an unstable state of mind.

The treatment of depressive illness has commonly been to enhance monoamine neurotransmitter levels in the brain (Blier and de Montigny, 1994; Leonard, 1995). The involvement of serotonin in depression and antidepressant therapies has been extensively studied (Meltzer, 1990; Briley and Moret, 1993; Willner, 1985) and has led to the development of selective serotonin reuptake inhibitors (SSRI) for the treatment of depression. Antidepressant therapies have a delay of approximately two weeks before

the clinical benefits are observed. This is thought to be because of adaptive changes at serotonin receptors, but could also be the result of resynchronising the malfunctioning circadian pacemaker. Experiments on human subjects have shown that after a trans-Atlantic flight, the body clock (measured as blood pressure and heart rate rhythms) does not resynchronise to the new time zone even after eleven days after the time change (Nold *et al.*, 1996). This provides evidence that a long period of time is needed to restore synchronisation of the body clock to its environment.

The terminal 5-HT_{1B} receptor function has been shown to be affected in animal models of depression (Edwards *et al.*, 1991), by acute stress (Bolanos-Jimenez *et al.*, 1995) and following antidepressant therapies (Moret and Briley, 1988; 1990). In addition, the 5-HT_{1A} somatodendritic autoreceptor is also modified following chronic antidepressant treatment (O'Connor and Kruk, 1994). In general, long term serotonin reuptake blockade desensitizes the terminal 5-HT_{1B} autoreceptor, and sensitizes the 5-HT_{1A} autoreceptor thus enhancing synaptic availability of serotonin.

The 5-HT_{1B} autoreceptor function has been shown in this thesis to vary over 24 hours. Surely, therefore, the timing of drug delivery for antidepressant therapy is crucially important. If the drug is administered when the 5-HT_{1B} receptor is least active i.e. naturally down regulated, then how can the antidepressant therapy down regulate the receptor further? The antidepressant drug must therefore be administered when the autoreceptor is responsive to agonist stimulation, so that the benefits of receptor down regulation can be reaped. It can be argued that with respect to the 5-HT_{1A} autoreceptor, time of day is not an important consideration during antidepressant treatments as this receptor did not exhibit a diurnal variation.

Recently, functional antagonists at the NMDA receptor complex have also been shown to exhibit antidepressant actions in an animal model of depression (Trullas and Skolnick, 1990). The effect of the NMDA antagonists on the function of the NMDA receptor mimics that of chronic but not acute treatment with a range of antidepressant therapies including tricyclics and SSRIs (Nowak *et al.*, 1993, 1996, 1998; Paul *et al.*, 1993). The NMDA receptors can be regulated by glycine and polyamines and substances such as Mg^{2+} and MK801 can sit in the ion channel and block receptor activation. Chronic antidepressant treatment decreased the ability of glycine to displace

radioligand binding in mice cortical membranes (Paul *et al.*, 1993; Nowak *et al.*, 1993, 1996, 1998) in addition to other effects on NMDA receptor function (see Nowak *et al.*, 1993). This effect was a slowly developed adaptive phenomenon, which would correlate with clinical improvement following antidepressant therapies, and was persistent after the cessation of treatment (Paul *et al.*, 1993). Additionally this effect appeared to be specific to the neocortex, since the response was absent in the hippocampus (Nowak *et al.*, 1993, 1996). Interestingly, in the frontal cortex of suicide victims the high affinity glycine displaceable ligand binding to glutamate receptors is decreased significantly compared to age matched controls (Nowak *et al.*, 1995). The consensus of opinion is that the NMDA ion channel might serve as a final common pathway of antidepressant action and indicates glutamatergic pathway involvement in the pathophysiology of depression. However, the relationship between NMDA receptor activity to depression is likely to be a very complex phenomenon (see Discussion Nowak *et al.*, 1995).

In animal models of depression, abnormalities in the function of the NMDA receptor have not been looked at in the hypothalamus, or more specifically, in the SCN. Likewise, the effect of antidepressant therapies on the NDMA receptor has not been studied in the SCN. Although the effect on the NMDA receptor after antidepressant drugs appeared specific to the neocortex, until a full examination of the brain is done, one cannot exclude the possibility that changes occur in the SCN after such treatments. On the otherhand, the effect of antidepressant therapies on the 5-HT_{1B} autoreceptor have been studied in the rat hypothalamus (Moret and Briley, 1990) and SCN (O'Connor and Kruk, 1994). A down regulation of the 5-HT_{1B} autoreceptor results and would indicate a decreased sensitivity to endogenous 5-HT or to agonist stimulation.

As regards to the NMDA receptor involvement in the SCN during antidepressant therapies, one can only speculate. It does seem a viable possibility that either during a depressive episode, or after antidepressant treatment that there are alterations in the NMDA receptor complex. As Nowak *et al.* (1995) have already suggested, the likelihood of the involvement of the NDMA receptor in antidepressant therapies is complex. However, because of the reciprocal control of the serotonergic and glutamatergic systems in the SCN, it is possible that a dysfunction in either the serotonergic or glutamatergic system may lead to a dysfunction in both transmitter

systems leading to the depressive episode. If NMDA receptor antagonists are the way ahead for antidepressant therapies and one considers the circadian parameters, then once again time of day must be taken into account during administration of the drugs. Administration during the light phase would be expected to decrease 5-HT concentration in the SCN, whereas during the dark period there would be no effect on SCN 5-HT concentration, as demonstrated in this thesis. Brain 5-HT levels are already reduced in depression, and if the antidepressant therapy, in the form of an NMDA receptor antagonist, was to decrease the 5-HT concentration further, then surely the depressive symptoms would be made worse. It must be borne in mind, however, that the results of this thesis demonstrate the function of the clock under normal conditions, and in the case of depression, disruptions in the transmitter balance may contradict the theories put forward here for the time of day administration. Therefore, many more experiments must be performed in animal models of depression as regards to the diurnal variation in 5-HT_{1B} receptor function and the effect NMDA receptor agonists and antagonists would have on 5-HT concentration in the SCN. Suggestions for future work are discussed in the next section.

7.3 FUTURE WORK

The work presented in this thesis has opened up many avenues. Firstly, regarding the data from Chapter 3 on the function of both the 5-HT_{1B} hetero- and auto-receptors, it would be of great interest to examine the function of the heteroceptor across the light:dark cycle at more time points in order to establish whether there is a variation in its function. In addition, it must be clarified whether the response to the agonist RU24969 is via stimulation of the 5-HT_{1B} or the 5-HT_{1A} receptor.

The remarkable variability in the function of the terminal 5-HT_{1B} autoreceptor must have an underlying cause. Possibilities for this variation in function have already been outlined in the discussion section of Chapter 3, and it would be worthwhile investigating these suggestions, particularly the involvement of the novel four amino acid peptide 5-HT moduline which is postulated to act as an endogenous antagonist at 5-HT_{1B} receptors, and the involvement of the second messenger cascade that leads to the response.

The variation in 5-HT_{1B} autoreceptor function is a diurnal variation. Of considerable interest to the chronobiologist is whether the receptor exhibits a circadian variation, that is whether it is influenced by the internal pacemaker. This can be tested in animals maintained under constant environmental conditions such as continuous darkness. Under these conditions, the function of the receptor can be tested again by microdialysis. The disadvantage of performing microdialysis experiments in animals allowed to free run in constant darkness is the need to monitor locomotor activity. Animals present with individual activity rhythms that are slightly out of synchronization with their litter mates. Therefore, each individual used in microdialysis experiments for drug infusion at a set zeitgeber time must have locomotor rhythms monitored constantly. The onset of locomotor activity in animals allowed to free run is designated ZT 12.

The advent of a commercially available antibody that can detect the 5-HT_{1B} receptor protein immunocytochemically in slices of rat brain would create a number of experiments localizing the receptor within the nucleus. As stated in Chapter 4, the initial aims of the immunocytochemical procedure were to utilise the 5-HT_{1B} antibody to a) examine the density of the receptor across the light:dark cycle, and to b) carry out double-labeling studies with antibodies to glutamate and serotonin to calculate the relative degree of hetero- and auto-receptors in the nucleus. The results of these experiments would still be of great interest.

As discussed in the preceding section (7.2), the results obtained in this thesis are interesting regarding antidepressant therapies. Animal models of depression are often used to test antidepressant therapies on aspects of behaviour and neurochemical levels in the brain. An animal model of depression could be set up and the experiments of this thesis repeated to identify differences in receptor function under normal conditions and during a depressive episode.

The question of whether there is a retinal-raphe-hypothalamic tract has been addressed briefly in this thesis with an attempt to give credence to a functional pathway. The problem here is that there is a dispute over whether the serotonergic projection to the SCN originates in the MRN or the DRN (outlined in the discussion section of Chapter 6). Lesion studies and comprehensive tract tracing techniques might be employed to verify this problem in the Wistar rat, which would subsequently make the initial

question easier to answer. A four millimeter probe membrane had to be utilised in these studies to span the whole dorsal-medial extent of the raphe nuclei. More specifically one could implant probes with smaller membrane surfaces (e.g. 1-2 mm) into specific raphe nuclei and determine if the ability of drugs (8-OH-DPAT or NMDA) to affect SCN 5-HT release specific to the MRN or DRN. Indeed there may be a number of drugs that might affect SCN 5-HT release when infused into the raphe, and a broad range of drugs can be tested in this system. Continuing along the theme of excitatory amino acid involvement in the regulation of 5-HT release, one could test the same excitatory amino acid agonists as used in Chapter 5. The regulation of 5-HT release in the SCN by somatodendritic 5-HT_{1A} autoreceptors was shown in this study not to exhibit a diurnal variation. Only two time points were investigated in this study and it might be worthwhile examining the 5-HT_{1A} autoreceptor at additional time points across the light:dark cycle.

One way of confirming a projection to the raphe nucleus from the retina would be to implant dialysis probes into the individual raphe nuclei and determine whether retinal stimulation increases retinal transmitter release. The prime candidate transmitter of this pathway is probably glutamate, and with an HPLC set up for the detection of glutamate in the laboratory, this might be a logical step forward. The animals could either be maintained on a 12:12 light dark cycle or one of continuous darkness. During the (subjective) dark phase retinal illumination will excite the retinal neurones and release transmitter at their terminals. If there were a retinal projection to the SCN and it released glutamate at the terminals then it would be detectable by microdialysis and HPLC-ED, provided the circulating aCSF contained a selective glutamate reuptake inhibitor.

If retinal stimulation of the raphe nuclei occurs, and if this pathway is functional in, for example modulation of light-induced phase shifting of the circadian clock, as is postulated, then light might induce the expression of immediate early genes in these nuclei. Light will induce the expression of immediate early genes, particularly the most studied c-fos gene and its protein product Fos, in the SCN (e.g. Rea, 1989) and in the intergeniculate leaflet (Park *et al.*, 1993). A longer period of illumination is required to stimulate Fos-like immunoreactivity in the IGL than in the SCN (Park *et al.*, 1993), and it might be that the raphe nuclei respond in a similar manner to the IGL. Different

lengths of illumination during the dark phase, and different zeitgeber times must be tested for the ability to induce Fos protein in the raphe. This would establish a role of the retinal-raphe pathway in the regulation of circadian rhythms.

Some preliminary experiments have been carried out that were not reported in the bulk of this thesis, but might pave the way for some exciting experiments. Firstly, immuocytochemical staining for the enzyme neuronal nitric oxide synthase (nNOS) was carried out in rat brain sections collected at six time points across the light dark cycle. The methodology for the collection of brains and subsequent processing of brains was similar to that reported in Chapter 4 for the detection of the 5-HT_{1B} receptor protein, but with the inclusion of the detergent agent Triton-X 100 present in all PBS wash stages. The primary antibody used (1:10,000; 48 hours) was donated by G. Leng from the university of Edinburgh and was raised in sheep.. The secondary antibody was thus donkey anti-sheep HRP (1:500; 24 hours, Sigma) normal donkey serum was used as a blocking agent. As outlined in the Introduction (Chapter 1), nitric oxide has a putative role in the regulation of circadian entrainment and is thought to be released upon stimulation of the RHT. One study has demonstrated NOS activity to exhibit increases in activity from mid-light to mid-dark (Ayers *et al.*, 1996) and it was therefore my aim to detect nNOS in the SCN of animals collected at six time points across the 12:12 light:dark cycle. Three animals at each time point were sacrificed and processed for nNOS staining.

Figure 7.1 shows representative sections of the mid-SCN region at each time point. A startling finding was that the SCN did not appear to contain any nNOS. A positive control section of the supraoptic nucleus verified the functional capacity of the antibody under the given conditions (figure 7.2). Neuronal NOS staining was seen on the medial and dorsal borders of the nuclei, and in the subparaventricular area closely associated with the third ventricle and no day-night difference in the number of NOS-containing neurones were detected in the six time points across the light:dark cycle. Previous reports have also used immunocytochemical detection methods to detect nNOS within the nucleus and have failed to detect significant amounts within the nuclei (Decker and Reuss, 1994; Amir *et al.*, 1995; Reuss *et al.*, 1995; Lupi *et al.*, 1996). Whilst the areas in which nNOS containing neurones were found are not the major retinorecipient area of the hypothalamus, they do receive afferents from the retinae (Johnson *et al.*, 1988a). It is

possible therefore, that stimulation of the NOS-containing cells in this region release NO which diffuses into the SCN to exert its effect. Alternatively, the release of NO could be secondary to stimulation of the SCN neurones by retinal afferents. Watts and Swanson (1987) performed an extensive tract tracing study detailing the efferents of the SCN, and identified that the densest projection ends just dorsal to the SCN in a comma-shaped region named the subparaventricular zone; this area contains NO-producing cells. Indeed, the authors have suggested that circadian patterns of neuronal activity generated in the SCN are relayed to effector circuitry in two stages with cells being innervated by the subparaventricular plexus, subsequently supplying greater input to the target nuclei. It is possible, therefore, that NOS plays a significant role in the effector circuitry of the nuclei.

Unfortunately, a report by Amir (1992) casts doubt upon this hypothesis. Increases in heart rate, stimulated by a brief light pulse in urethane anaesthetised rats, were blocked by antagonists of NMDA receptors and competitive blockers of NO production only when infused directly into the SCN and not when infusions were made in a region 2 mm dorsal to the SCN. This suggests a retinal pathway utilising NO only within the SCN itself, and not dorsal to the nuclei where, in the present study, NOS staining cells were most prominent.

Wang and Morris (1996) who successfully detected NOS-containing neurones in the SCN by immunocytochemical methods, used an antibody directed against whole recombinant rat neuronal nitric oxide synthase, and in parallel stained for NADPH-diaphorase, an enzyme whose colocalisation with NOS-containing neurones was considered a suitable marker for neuronal NOS (Dawson et al, 1991). Although they detected NOS-immunoreactive fibres in the SCN they failed to detect NADPH-diaphorase activity, suggesting that their antibody for NOS recognised a yet unidentified from of neuronal nitric oxide synthase. This might explain why the present study and others have been unable to detect NOS-containing neurones within the SCN, in the presence of accumulating evidence for a role of nitric oxide in the signal transduction pathway in the suprachiasmatic nucleus.

Studies branching from these preliminary data are extensive. First, there must be more than one type of neuronal NOS in the central nervous system as is evident from the

apparent lack of nNOS within the SCN despite the plethora of evidence for a role for nitric oxide in circadian rhythms. The study by Wang and Morris (1996) support this view. Molecular biology techniques must therefore be undertaken to identify the NOS molecule that is present in the SCN of rodents, and indeed why this protein is perhaps unique to the circadian pacemaker. A NOS molecule present in the SCN, but not present elsewhere in the central nervous system might be a feature of pacemaker cells, and thus upon identification of the molecule specific inhibitors or stimulatory agents might be able to modulate specifically the circadian pacemaker, and alleviate symptoms unique to disruptions of the circadian pacemaker, such as jet lag.

Specific HPLC methodology able to detect nitrates, one of the breakdown products of nitric oxide, commonly used to identify nitric oxide usage, is available commercially (Presearch Ltd.) and may enable the detection of nitrate in microdialysis samples. The detection of nitrite in dialysate samples would therefore be possible across the light:dark cycle and possible diurnal variations in this nitric oxide breakdown product identified.

A second set of preliminary experiments involved microdialysis of animals during the dark period. Animals were implanted with probes into the SCN region as described previously and maintained on a reverse lighting schedule. Initially a short 15 min light pulse was administered at ZT 15 and ZT 21 in separate individuals. At these zeitgeber times a short light pulse delivered to the animals has the ability to induce phase shifts in behavioural rhythms and to induce c-fos expression in the SCN (Rea, 1989). In three animals, a light pulse delivered at ZT 15 induced a 3-4 fold increase in 5-HT as measured in the microdialysate sample (figure 7.3). The increase in magnitude of the response was similar in all animals although the timing of the increase after light exposure did vary. This experiment was repeated on a further six animals with only one third of the animals responding in a similar manner. In addition, a further three animals received a light pulse delivered an hour earlier at ZT 14 without effect. At ZT 21 the first two animals exposed to a light pulse exhibited a four fold increase in 5-HT concentration in the dialysate samples (figure 7.4). This was repeated on a further five animals with only two out of the five responding in a similar manner. Two more animals received a light pulse at ZT 20 and two others a light pulse at ZT 22. None of these animals responded to the light pulse with an altered dialysate 5-HT level.

To my knowledge this effect of light on 5-HT release is novel. Unfortunately the inconsistency of the response in separate animals casts a shadow on the validity of the data. Forty four percent of the animals exposed to a light pulse at ZT 15 and 43 % of the animals at ZT 21 failed to respond with an effect on dialysate 5-HT concentration.

The effect of a light pulse on 5-HT release may be a very specific time-dependent occurrence with a very narrow window during which light can affect 5-HT release. As is seen in the few animals presented with a light pulse at ZT 14, 20 and 22, there was no effect on 5-HT release in any of these animals tested. Each individual used in these experiments although entrained to the same 12:12 light dark cycle, may have subtle variations in circadian parameters to his litter mates and the time window in each individual may vary slightly. The maximal phase delay or phase advance shown by any one individual to a light pulse delivered at the early or late (subjective) night, respectively, is also a very time specific event and the time specificity may reflect the ability of light to affect 5-HT release. Although as a general rule 5-HT applied to animals (hamster or mouse) inhibits light-induced Fos induction (Chapter 1 section1.2.2) the effect of 5-HT on light-induced Fos production in the rat is different. In the rat application of an antagonist at the 5-HT_{1A} receptor blocks Fos induction (Recio et al, 1996) and qupazine applied systemically to rats can induce c-fos in the VL-SCN similar to that produced by light during the dark phase (Moyer *et al.*, 1997). In this latter study, the author suggests that, in the rat, serotonin might mediate the effects of light on SCN Fos induction. The results from this brief experiment supports this theory.

From this point where can one take these experiments? Firstly one must repeat the experiments, perhaps using a longer duration light pulse and determine the true window in which light can affect 5-HT release. Verification that the light pulse is indeed capable of phase shifting circadian parameters can be done in the same animals by processing the brains for Fos-immunoreactivity after the presentation of a light pulse. A very interesting and logical progression from here will be whether administration of 5-HT and then more specifically 5-HT receptor agonists via the microdialysis probe can indeed induce Fos protein expression in the SCN similar to that seen after a light pulse, which would give functional purpose to an increase in 5-HT release after the presentation of a light pulse.

This effect of light on 5-HT release is a very short acting response. From the experiments performed to elucidate a role of excitatory amino acid receptor regulation of 5-HT release in the SCN (Chapter 5), agonist stimulation usually produced a long lasting and sustained response on 5-HT concentration. However, agonists were applied for a much longer period than the duration of the light pulse and it is therefore possible that excitatory amino acid receptor stimulation results in the effect on SCN 5-HT concentration. A good candidate for this effect must be the diffusable molecule nitric oxide. If the response of 5-HT to light were a consistent response, nitric oxide synthase inhibitors such as L-NAME could be administered either systemically or via the probe before the presentation of the light pulse to see whether the increase in 5-HT concentration could be inhibited. Conversely, nitric oxide donors could be administered via the probe to determine their effects of 5-HT release. A suitable model for determination of the substance responsible for the rise in 5-HT concentration would be if the light pulse could be administered on two consecutive days to have a reproducible effect of 5-HT release. The animal could therefore act as its own control, and on day 2 various inhibitors or agonists could be applied to identify the mediator of the response.

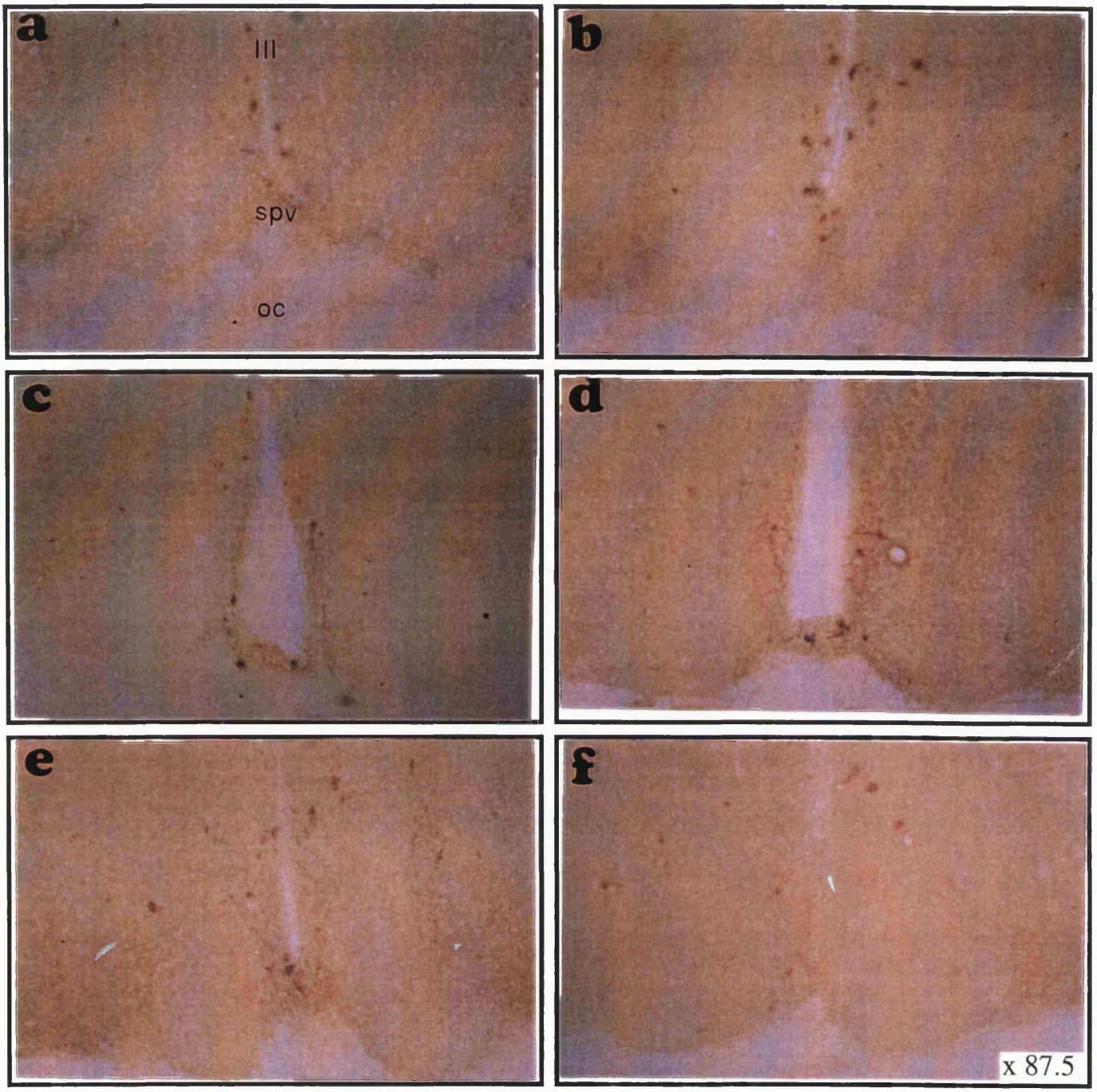

Figure 7.1. Reprasentative brain sections at the level of the hypothalamic suprachiasmatic nuclei at (**a**) ZT 3, (**b**) ZT 6, (**c**) ZT 9, (**d**) ZT 15, (**e**) ZT 18 and (**f**) ZT 21. Neuronal nitric oxide synthase (nNOS) neurones are visible as those containing a dark brown precipitate. Note the absence of nNOS within the suprachiasmatic nuclei, which are almond-shaped nuclei either side if the third ventricle (III) and above the optic chiasm (oc), but its presence in the subparaventricular zone (spv), on the borders of the nuclei and on the borders of the third ventricle. Magnification x 87.5.

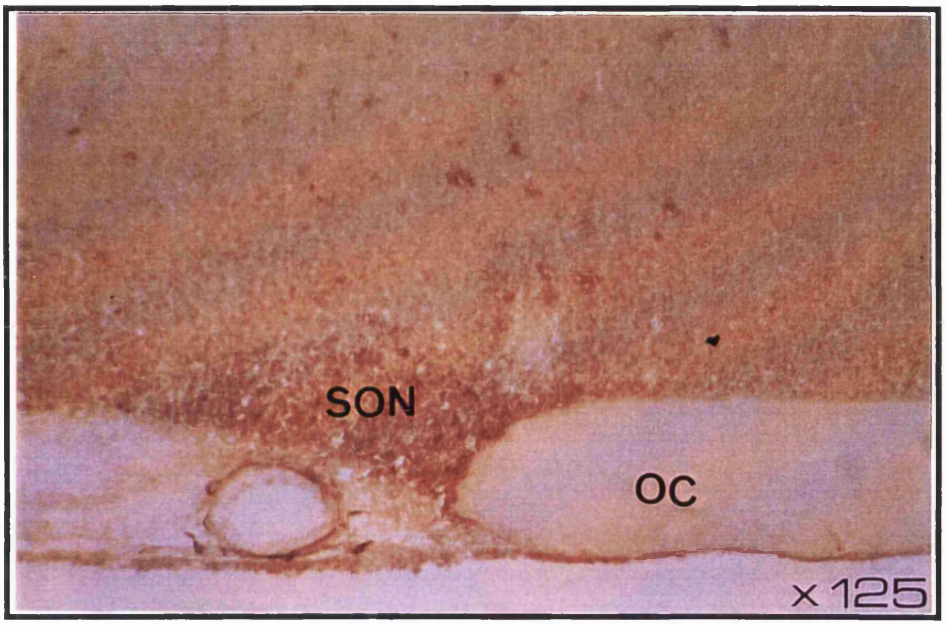

Figure 7.2. Representative brain section at the level of the supraoptic nucleus (SON) at ZT 6. Note the high density of brown precipitate indicative of neuronal nitric oxide synthase within the nucleus. oc = optic chiasm. Magnification x 125.

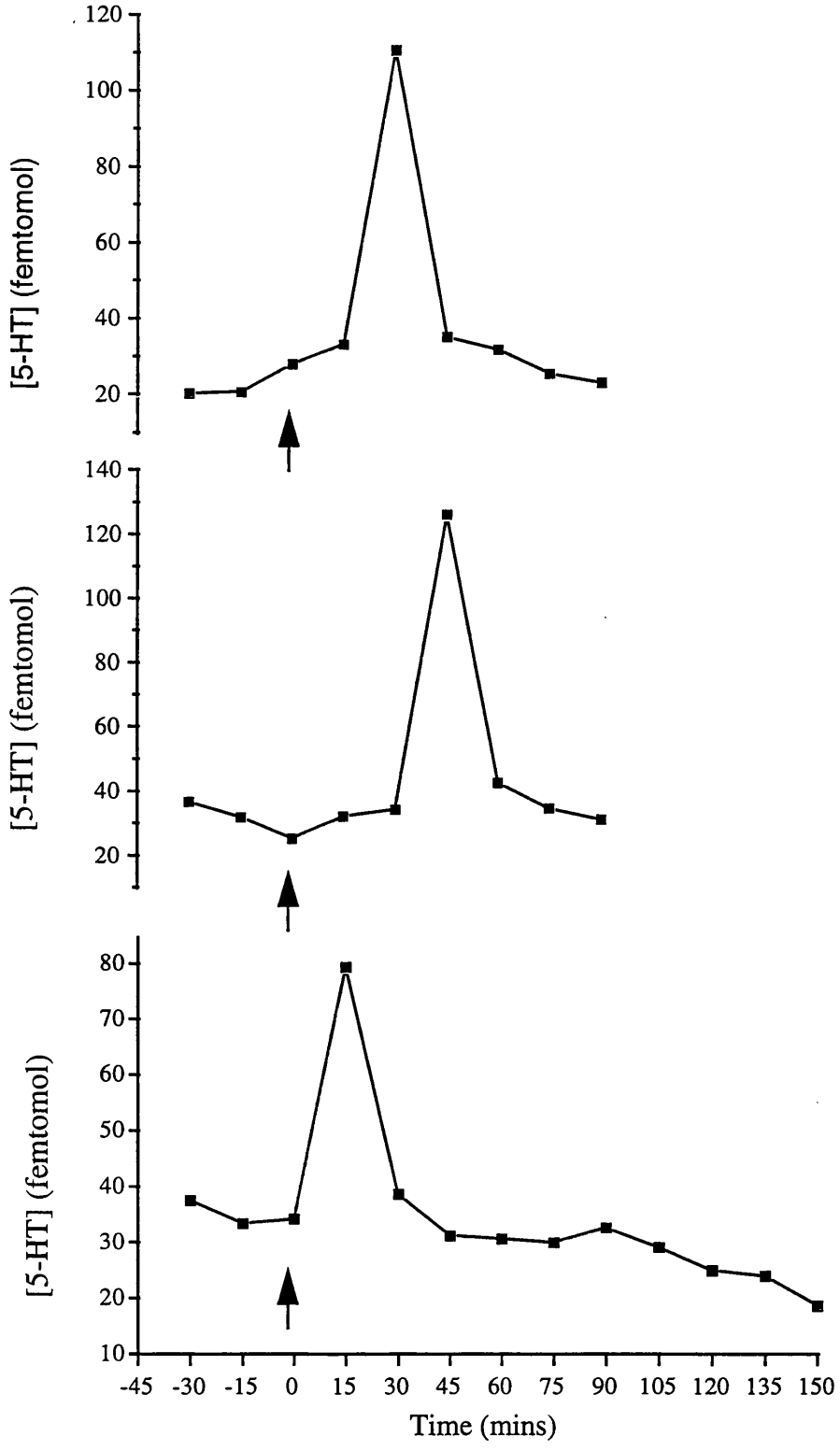

Figure 7.3. The effect of a short (15 min) light pulse, indicated by the black arrow, on extracellular 5-HT concentration from the SCN region. The light pulse was presented at ZT 15 and the figure represents data from three separate animals. Values are actual 5-HT concentration collected from a 22 µl dialysis sample, not corrected for probe recovery.

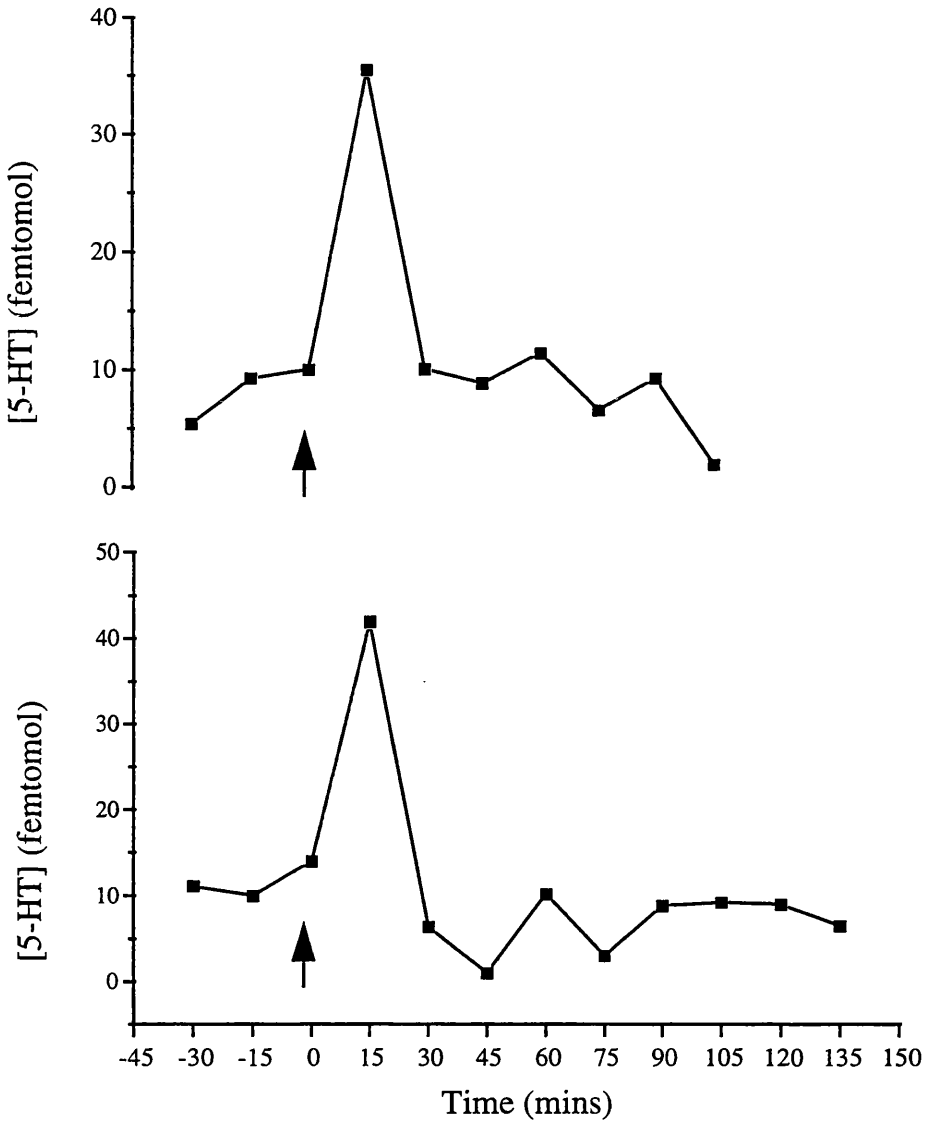

Figure 7.4. The effect of a short (15 min) light pulse, indicated by the black arrow, on extracellular 5-HT concentration from the SCN region. The light pulse was presented at ZT 21 and the figure represents data from two separate animals. Values are actual 5-HT concentration collected from a 22 µl dialysis sample, not corrected for probe recovery.

PUBLICATIONS

PUBLICATION LIST

GARABETTE, M.L., MARTIN, K.F., REDFERN, P.H. (1996). Nitric oxide synthase (NOS) activity in the suprachiasmatic nucleus (SCN) of the rat. *Chronobiol. Int. (Suppl.)* **13**:35.

GARABETTE, M.L., MARTIN, K.F., REDFERN, P.H. (1997). Circadian variation in terminal 5-HT_{1B} autoreceptor function in rat SCN. *Chronobiol. Int. (Suppl.)* **14**:52.

GARABETTE, M.L., MARTIN, K.F., REDFERN, P.H. (1997). Circadian variation in terminal 5-HT_{1B} autoreceptor in the SCN of the rat. *J. Psychopharmacol. (Suppl.)* **11**:A40.

GARABETTE, M.L., MARTIN, K.F., REDFERN, P.H. (1998). Twenty four hour variation in the function of the terminal 5-HT_{1B} autoreceptor in the rat SCN. In: *Biological clocks Mechanisms and applications*. Ed. Yvan Touitou. pp 103-106.

REFERENCES

ABE, H. and RUSAK, B. (1992). Stimulation of the hamster ventral lateral geniculate nucleus induces Fos-like immunoreactivity in suprachiasmatic nucleus cells. *Neurosci.Letts.* **148**:185-189.

ADELL, A., CARCELLER, A., ARTIGAS, F. (1993). In vivo brain dialysis study of the somatodendritic release of serotonin in the raphe nuclei of the rat: Effects of 8-hydroxy-2-(di-*n*-propylamino)tetralin. *J. Neurochem.* **60**:1673-1681.

AGNETER, E. and SINGER, E.A. (1993). Autoreceptor-mediated control of 5-hydroxytryptamine release from medullary raphe nuclei in the freely moving rat. *N.S. Arch. Pharmacol.* **R124**:493.

AGREN, H., KOULU, M., SAAVEDRA, J.M., POTTER, W.Z., LINNOILA, M. (1986). Circadian covariation of norepinephrine and serotonin in the locus coeruleus and dorsal raphe nucleus in the rat. *Brain Res.* **397**:353-358.

ALBRECHT, P., VISSCHER, M.B., BITTNER, J.J., HALBERG, F. (1956). Daily changes in 5-hydroxytryptamine concentration in mouse brain. *P.S.E.B.M.* **92**:703-706.

AMIR, S. (1992). Blocking NMDA receptors or nitric oxide production disrupts light transmission to the suprachiasmatic nucleus. *Brain Res.* **586**: 336-339.

AMIR, S., ROBINSON, B., EDELSTEIN, K. (1995). Distribution of NADPH-diaphorase staining and light-induced Fos expression in the rat suprachiasmatic nucleus region supports a role for nitric oxide in the circadian system. *Neurosci.* **69**:545-555.

ASTON-JONES, G., AKAOKA, H., CHARLETY, P., CHOUVET, G. (1991). Serotonin selectively attenuates glutamate-evoked activation of noradrenergic locus coeruleus neurons. *J. Neurosci.* **11**: 760-769.

AUERBACH, S.B., MINZENBERG, M.J., WILKINSON, L.O. (1989). Extracellular serotonin and 5-hydroxyindoleacetic acid in hypothalamus of the unanesthetized rat measured by in vivo dialysis coupled to high-performance liquid chromatography with electrochemical detection: dialysate seotonin reflects neuronal release. *Brain Res.* **499**: 281-290.

AUERBACH, S.B., RUTTER, J.J., JULIANO, P.J. (1991). Substituted piperazine and indole compounds increase extracellular serotonin in rat diencephalon as determined by *in vivo* microdialysis. *Neuropharmacol.* **30**:307-311.

AYERS, N.A., KAPAS, L., KRUEGER, J.M. (1996). Circadian variation of nitric oxide synthase activity and cytosolic protein levels in rat brain. *Brain Res.* **707**:127-130.

AZMITIA, E.C. and SEGAL, M. (1978). An autoradiographic analysis of the differential ascending projections of the dorsal and median raphe nuclei in the rat. *J. Comp. Neurol.* **179**:641-668.

BECQUET, D., HERY, M., DEPREZ, P., FAUDON, M., FACHE, M.P., GIRAUD, P., HERY, F. (1993). N-methyl-D-aspartate acid/glycine interactions on the control of 5-hydroxytryptamine release in raphe primary cultures. *J.Neurochem.* **61**:1692-1697.

BENVENISTE, H. (1989). Brain microdialysis. *J. Neurochem.* **52**: 1667-1679.

BENVENISTE, H. and DIEMER, N.H. (1987). Cellular reactions to implantation of a dialysis tube in the rat hippocampus. *Acta Neuropathologica* **74**:234-238.

BENVENISTE, H. and HUTTEMEIER, P.C. (1990). Microdialysis - theory and application. *Prog. Neurobiol.* **35**:195-215.

BETTLER, B. and MULLE, C. (1995). Review: neurotransmitter receptors. II. AMPA and kainate receptors. *Neuropharmacol.* **34**:123-129.

BLIER, P. and DE MONTIGNY, C. (1994). Current advances and trends in the treatment of depression. *Trends in Pharmacol. Sci.* **15**:220-226.

BLIER, P., GALZIN, A-M., LANGER, S.Z. (1989). Diurnal varuation in the function of serotonin terminals in the rat hypothalamus. *J. Neurochem.* **52**: 453-459.

BLIER, P., GALZIN, A-M., LANGER, S.Z. (1990). Interaction between serotonin uptake inhibitors and alpha-2-adrenergic heteroceptors in the rat hypothalamus. *J.Pharmacol.Exp.Ther.* **254**:236-254.

BOBRZYNSKA, K.J., VRANG, N., MROSOVSKY,N. (1996a). Persistence of non-photic phase shifts in hamsters after serotonin depletion in the suprachiasmatic nucleus. *Brain Res.* **741**:205-214.

BOBRZYNSKA, K.J., GODFREY, M.H., MROSOVSKY, N. (1996b). Serotonergic stimulation and non-photic phase shifting in hamsters. *Physiol. Behav.* **59**:221-230.

BOLANOS-JIMENEZ, F., DECASTRO, R.M., SEGUIN, L., CLOEZ-TAYARANI, I., MONNERET, V., DRIEU, K., FILLION. G. (1995). Effects of stress on the functional properties of presynaptic and postsynaptic 5-HT_{1B} receptors in the rat brain. *Eur. J. Pharmacol.* **294**:531-540.

BOSKER, F.J., DEWINTER, T.Y.C.E., KLOMPMAKERS, A.A., WESTENBERG, H.G.M. (1996). Flesinoxan dose-dependently reduces extracellular 5-hydroxytryptamine (5-HT) in rat median raphe and dorsal hippocampus through activation of 5-HT_{1A} receptors. *J.Neurochem.* **66**:2546-2555.

BOSKER, , F.J., KLOMPMAKERS, A.A., WESTENBERG, H.G.M. (1994). Extracellular 5-hydroxytryptamine in median raphe nucleus of the conscious rat is decreased by nanomolar concentrations of 8-hydroxy-2-(di-*n*-propylamino)tetralin and is sensitive to tetrodotoxin. *J. Neurochem.* **63**:2165-2171.

BOSKER, , F.J., VANESSEVELDT, K.E., KLOMPMAKERS, A.A., WESTENBERG, H.G.M. (1995). Chronic treatment with fluvoxamine by osmotic minipumps fails to induce persistent functional changes in central 5-HT_{1A} and 5-HT_{1B} receptors, as measured by in vivo microdialysis in dorsal hippocampus of conscious rats. *Psychopharmacol.* **117**:358-363.

BOSKER, F., VRITEN, D., KLOMPMAKERS, A., WESTENBERG, H. (1997). The effects of a 5-HT_{1A} receptor agonist and antagonist on the 5-hydroxytryptamine release in the central nucleus of the amygdala: a microdialysis study with flesinoxan and WAY 100635. *N.S.Arch.Pharmacol.* **355**:347-353.

BOUHELAL, R., SMOUNYA, L., BOCKAERT, J. (1988). 5-HT_{1B} receptors are negatively coupled with adenylate cyclase in rat substancia nigra. *Eur.J.Pharmacol.* **151**:189-196.

BRADBURY, M.J., DEMENT, W.C., EDGAR, D.M. (1997). Serotonin-containing fibres in the suprachiasmatic hypothalaums attenuate light-induced phase delays in mice. *Brain Res.* **768**:125-134.

BRILEY, M. and MORET, C. (1993). Neurobiological mechanisms involved in antidepressant therapies. *Clin.Neuropharmacol.* **16**:387-400.

BRUINVELS, A.T., LANDWEHRMEYER, B., GUSTAFSON, E.L., DURKIN, M.M., MENGOD, G., BRANCHEK, T.A., HOYER, D., PALACIOS. J.M. (1994). Localization of 5-HT_{1B}, 5-HT_{1D_α}, 5-HT_{1E}, and 5-HT_{1F} receptor messenger RNA in rodent and primate brain. *Neuropharmacol.* **33**:367-386.

CAGAMPANG, F.R.A. and INOUYE, S.I.T. (1994). Diurnal and circadian changes of serotonin in the suprachiasmatic nuclei: regulation by light and an endogenous pacemaker. *Brain Res.* **639**: 175-179.

CAGAMPANG, F.R.A., SHEWARD, W.J., HARMAR, A.J., PIGGINS, H.D., COEN, C.W. (1998). Circadian changes in the expression of vasoactive intestinal peptide 2 receptor mRNA in the rat suprachiasmatic nuclei. *Mol. Brain Res.* **54**:108-112.

CAHILL, G.M. and MENAKER, M. (1989). Effects of excitatory amino acid receptor antagonists and agonists on suprachiasmatic nucleus responses to retinohypothalamic tract volleys. *Brain Res.* **479**:76-82.

CARD, J.P. and MOORE, R.Y. (1984). The suprachiasmatic nucleus of the golden hamster: immunohistochemical analysis of cell and fiber distribution. *Neurosci.* **13**:415-431.

CARD, J.P. and MOORE, R.Y. (1989). Organization of lateral geniculate-hypothalamic connections in the rat. *J.Comp.Neurol.* **284**:135-147.

CASANOVAS, J.M. and ARTIGAS, F. (1996). Differential effects of isaspirone on 5-hydroxytryptamine release in the dorsal and median raphe neuronal pathways. *J.Neurochem.* **67**:1945-1952.

CASANOVAS, J.M., LESOURD, ARTIGAS, F. (1997). The effect of the selective 5-HT_{1A} agonists alnespirone (S-20499) and 8-OH-DPAT on extracellular 5-hydroxytryptamine in different regions of rat brain. *Brit.J.Pharmacol.* **122**:733-741.

CLOEZ-TAYARANI, I., CARDONA, A., ROUSSELLE, J-C., MASSOT, O., EDELMAN, L., FILLION, G. (1997). Autoradiographic characterization of [^{3}H]-5-HT-moduline binding sites in rodent brain and their relationship to 5-HT_{1B} receptors. *Proc.Natl.Acad.Sci. USA* **94**:9899-9904.

CUTERA, R.A., OUAROUR,A., PEVET, P. (1994). Effects of the 5-HT_{1A} receptor agonist 8-OH-DPAT and other non-photic stimuli on the circadian rhythm of wheel-running activity uin hamsters under different constanat conditions. *Neurosci.Letts.* **172**:27-30.

CUTERA, R.A., SABOUREAU, M., PEVET, P. (1997). Phase-shifting effect of 8-OH-DPAT, a 5-HT_{1A} /5-HT_7 receptor agonist, on locomotor activity in golden hamster in constant darkness. *Neurosci.Letts.* **210**:1-4.

DAVIDSON, C. and STAMFORD, J.A. (1995). Evidence that 5-hydroxytryptamine release in rat dorsal raphe nucleus is controlled by 5-HT_{1A}, 5-HT_{1B} and 5-HT_{1D} autoreceptors. *Brit. J. Pharmacol.* **114**:1107-1109.

DAWSON, V.L., BREDT, D.S., FOTUHI, M., HWANG, P.M., SNYDER, S.H. (1991). Nitric oxide synthase and neuronal NADPH diaphorase are identical in brain and peripheral tissues. *Proc. Natl. Acad. Sci. USA* **88**: 7797-7801.

DECKER, K. and REUSS, S. (1994). Nitric oxide-synthesizing neurons in the hamster suprachiasmatic nucleus: a combined NOS- and NADPH- staining and retinohypothalamic tract tracing study. *Brain Res.* **666**: 284-288.

DECOURSEY, P.J. and BUGGY, J. (1989). Circadian rhythmicity after neural transplant to hamster third ventricle: specificity of suprachiasmatic nuclei. *Brain Res.* **500**:263-275.

DE VRIES, M.J., CARDOZO, B.N., VAN DER WANT, J., DE WOLF, A., MEIJER, J.H. (1993). Glutamate immunoreactivity in terminals of the retinohypothalamic tract of the brown Norwgian rat. *Brain Res.* **612**: 231-237.

DE VRIES, M.J., TREEP, J.A., DE PAUW, E.S.D., MEIJER , J.H. (1994). The effects of electrical stimulation of the optic nerves and anterior optic chiasm on the circadian activity rhythm of the Syrian hamster: involvement of excitatory amino acids. *Brain Res.* **642**:206-212.

DIJK, S.N., FRANCIS, P.T., STRATMANN, G.C., BOWEN, D.M. (1995). NMDA-induced glutamate and aspartate release from rat cortical pyramidal neurones: Evidence for modulation by a 5-HT_{1A} antagonist. *Brit.J.Pharmacol.* **115**:1169-1174.

DING, J.M., CHEN, D., WEBER, E.T., FAIMAN, L.E., REA, M.A., GILLETTE, M.U. (1994). Resetting the biological clock: mediation of nocturnal circadian shifts by glutamate and NO. *Sci.* **266**: 1713-1717.

DING, J.M., FAIMAN, L.E., HURST, W.J., KURIASHKINA, L.R., GILLETTE, M.U. (1997). Resetting the biological clock: mediation of nocturnal CREB phosphorylation via light, glutamate, and nitric oxide. *J.Neurosci.* **17**:667-675.

DONG, J., DE MONTIGNY, C., BLIER, P. (1997). Effect of acute and repeated versus sustained administration of the 5-HT_{1A} receptor agonist spipirone: electrophysiological studies in the rat hippocampus and dorsal raphe. *N.S.Arch.Pharmacol.* **356**:303-311.

DOUCET, E., POHL, M., FATTACCINI, C.M., ADRIEN, J., ELMESTIKAWY, S., HAMON, M. (1995). In situ htbridization evidence for the synthesis of 5-HT_{1B} receptor in serotonergic eurones of anterior raphe nucleus in the rat brain. *Synapse* **19**:18-28.

DYKSTRA, K.H., HSIAO, J.K., MORRISON, P.F., BUNGAY, P.M., MEFFORD, I.N., SCULLY, M.M. (1992). Quantitative examination of tissue concentration profiles associated with microdialysis. *J. Neurochem.* **58**:931-940.

EBLING, J.P., MAYWOOD, E.S., STALEY, K., HUMBY, T., HANCOCK, D.C., WATERS, C.M., EVAN, G.I., HASTINGS, M.H. (1991). The role of N-methyl-D-aspartate-type glutamatergic neurotransmission in the photic induction of immediate early gene expression in the suprachiasmatic nuclei of the Syrian hamster. *J.Neuroendocrinol.* **3**:641-652.

EDWARDS, E., HARKINS, K., WRIGHT, G., HENN, F.A. (1991). 5-HT_{1B} receptors in an animal model of depression. *Neuropharmacol.* **30**:101-105.

ENGEL, G., GOTHERT, M., HOYER, D., SCHUCKER, E., HILLENBRAND, K. (1986). Identity of inhibitory presynaptic 5-hydoxytryptamine (5-HT) autoreceptors in the rat brain cortex with 5-HT_{1B} binding sites. *N.S. Arch. Pharmacol.* **332**: 1-7.

FARADJI, H., CESPUGLIO, R., JOUVET, M. (1983). Voltametric measurements of 5-hydroxyindole compounds in the suprachiasmatic nuclei - circadian fluctuations. *Brain Res.* **279**:111-119.

FERRARO, J.S. and STEGER, R.W. (1990). Diurnal variations in brain serotonin are driven by the photic cycle and are not circadian in nature. *Brain Res.* **512**:121-124.

FINK, K., BOING, C, GOTHERT, M. (1996). Presynaptic 5-HT autoreceptors modulate *N*-methyl-D-aspartate-evoked 5-hydroxytryptamine release in the guinea-pig brain cortex. *Eur.J.Pharmacol.* **300**:79-82.

FINK, K., SCHMITZ, V., GOTHERT, M. (1995). Stimulation of serotonin release in the rat brain cortex by activation of ionotropic glutamate receptors and its modulation via α_2-heteroceptors. *N.S.Arch.Pharmacol.* **352**:394-401.

FLETCHER, A., BILL, D.J., CLIFFE, I.A., FORSTER, E.A., JONES, D., REILLY, Y. (1994). A pharmacological profile of WAY-100635, a potent and selective 5-HT_{1A} receptor antagonist. *Brit.J.Pharmacol.* **112**:91P.

FOOTE, W.E., TABER-PIERCE, E., EDWARDS, L. (1978). Evidence for a retinal projection to the midbrain raphe of the cat. *Brain Res.* **156**:135-140.

FORNAL, C.A., METZLER, C.W., VEASEY, S.C., McCREARY, A.C., DOURISH, C.T. (1994). Single unit receordings from freely-moving animals provide evidence that WAY-100635, but not (S)-WAY-100135, blocks the action of endogenous serotonin at the 5-HT autoreceptor. *Brit.J.Pharmacol.* **112**:92P.

FRANKHUYZEN, A.L. and MULDER, A.H. (1982). Pharmacological characterization of presynaptic α-adrenoceptors modulating [^{3}H]noradrenaline and [^{3}H]5-hydroxytryptamine release from slices of the hippocampus of the rat. *Eur.J.Pharmacol.* **81**:97-106.

GADDUM, J.H. (1961). Push-pull cannulae. *J. Physiol.* **155**: 1-2.

GANNON, R.L. and REA, M.A. (1993). Glutamate receptor immunoreactivity in the rat suprachiasmatic nucleus. *Brain Res.* **622**: 337-342.

GANNON, R.L. and REA, M.A. (1994). In situ hybridization of antisense mRNA oligonucleotides for AMPA, NMDA and metabotropic glutamate receptor subtypes in

the rat suprachiasmatic nucleus at different phases of the circadian cycle. *Mol. Brain Res.* **23**: 338-344.

GAUER, F., KEDZIERSKI, W., CRAFT, C.M. (1995). Identification of circadian gene expression in the rat pineal gland and retina by mRNA differential display. *Neurosci.Letts.* **187**:69-73.

GHOSH, P.K., BASKARAN, N., VAN DEN POL, A.N. (1997). Developmentally regulated gene expression of all eight metabotropic glutamate receptors in hypothalamic suprachiasmatic and arcuate nuclei - a PCR study. *Dev. Brain Res.* **102**:1-12.

GLASS, J.D., RANDOLF, W.W., FERREIRA, S.A., REA, M.A., HAUSER, U.E., BLANK, J.L., DE VRIES, M.J. (1992). Diurnal variation in 5-hydroxyindole acetic acid output in the suprachiasmatic region of the Siberian hamster assessed by in vivo microdialysis: evidence for nocturnal activation of serotonin release. *Neuroendocrinol.* **56**: 582-590.

GLASS, J.D., HAUSER, U.E., BLANK, J.L., SELIM, M., REA, M.A. (1993). Differential timing of amino acid acid and 5-HIAA rhythms in suprachiasmatic hypothalamus. *Am.J.Physiol.* **265**:R504-R511.

GOODWIN, G.M., DESOUZA, R.J., GREEN, A.R. (1985). The pharmacology of the hypothermic response in mice to 8-hydroxy-2-(di-*n*-propylamino)tetralin (8-OH-DPAT). A model of presynaptic 5-HT_1 function. *Neuropharmacol.* **24**:1187-1194.

GOTHERT, M. and HUTH, H. (1980). Alpha-adrenoceptor-mediated modulation of 5-hydroxytryptamine release from rat brain cortex slices. *N.S.Arch.Pharmacol.* **313**:21-26.

GRIFFIOEN, H.A., DUINDAM, H., VAN DER WOUDE, T.P., REITVELD, W.J., BOER, G.J. (1993). Functional development of fetal suprachiasmatic nucleus grafts in suprachiasmatic nucleus-lesioned rats. *Brain Res. Bull.* **31**:145-160.

GRIMALDI, B., FILLION, M.-P., BONNIN, A., ROUSSELLE, J.C., MASSOT, O., FILLION, G. (1997). Immunological localization of neurons expressing 5-HT-moduline in the mouse brain. *Neuropharmacol.* **36**:1079-1087.

HALLBUS, M., MAGNUSSON, T., MAGNUSSON, O. (1997). Influence of 5-$HT_{1B/1D}$ receptors on dopamine release in the guinea pig nucleus accumbens: A microdialysis study. *Neurosci. Letts.* **225**:57-60.

HAMON, M., BOURGOIN, S., GOZLAN, H., HALL, M.D., GOETZ, C., ARTAUD, F., HORN, A.S. (1984). Biochemical evidence for the 5-HT agonist properties of PAT

(8-hydroxy-2-(di-*n*-propylamino)tetralin) in the rat brain. *Eur. J. Pharmacol.* **100**:263-276.

HARRINGTON, M.E., NANCE, D.M., RUSAK, B. (1987). Double-labeling of neuropeptideY-immunoreactive neurons which project from the geniculate to the suprachiasmatic nuclei. *Brain Res.* **410**:275-282.

HJORTH, S. and SHARP, T. (1991). Effect of the 5-HT_{1A} receptor agonist 8-OH-DPAT on the release of 5-HT in dorsal and median raphe-innervated rat brain regions as measured by *in vivo* microdialysis. *Life Sci.* **48**:1779-1786.

HJORTH, S. and TAO, R. (1991). The putative 5-HT_{1B} agonist CP-93,129 suppresses rat hippocampal 5-HT release in vivo: comparison with RU 24969. *Eur. J. Pharmacol.* **209**: 249-252.

HOYER, D., ENGEL, G., KALKMAN, H.O. (1985). Characterization of the 5-HT_{1B} recognition site in rat brain: binding studies with (-)[^{125}I]iodocyanopindolol. *Eur.J.Pharmacol.* **118**:1-12.

HUANG, S.-K. and PAN, J.-T. (1993). Potentiating effects of serotonin and vasoactive intestinal peptide on the action of glutamate on suprachiasmatic neurons in brain slices. *Neurosci.Letts.* **159**:1-4.

IENI, J.R. and MEYERSON, L.R. (1987). The 5-HT_{1A} receptor probe [^{3}H]8-OH-DPAT labels the 5-HT transporter in human platelets. *Life Sci.* **42**:311-320.

JACKSON, Z.E., STRINGER, B.M.J., FOSTER, G.A. (1997). Identification of 5-HT receptor subtypes in a homogeneous population of presumptive serotonin neurones. *Neuropharmacol.* **36**:543-548.

JANIK, D. and MROSOVSKY, N. (1994). Intergeniculate leaflet lesions and behaviorally-induced shifts of circadian rhythms. *Brain Res.* **651**:174-182.

JOHNSON, R.D. and JUSTICE, J.B. (1983). Model studies for brain dialysis. *Brain Res. Bull.* **10**: 567-571.

JOHNSON, R., MORIN, L., MOORE, R. (1988a). Retinohypothalamic projections in the hamster and rat demonstrated using cholera toxin. *Brain Res.* **462**: 301-312.

JOHNSON, R., MOORE, R., MORIN, L. (1988b). Loss of entrainment and anatomical plasticity after lesions of the hamster retinohypothalamic tract. *Brain Res.* **460**:297-313.

JOHNSON, R.F., SMALE, L., MOORE, R.Y., MORIN, L.P. (1988c). Lateral geniculate lesions block circadian phase-shift responses to a benzodiazepine. *Proc. Natl. Acad. Sci. USA* **85**:5301-5304.

JOHNSON, R., MOORE, R., MORIN, L. (1989). Lateral geniculate lesions alter circadian rhythmicity in the hamster. *Brain Res. Bull.* **22**: 411-422.

JONES, N.M., LAWRENCE, A.J., BEART, P.M. (1998). In vivo microdialysis reveals facilitatory metabotropic glutamate receptors regulating excitatory amino acid release in rat nucleus tractus solitarius. *Neurochem. Int.* **32**:31-38.

KALEN, P., KARLSON, M., WIKLUND, L. (1985). Possible excitatory amino acid afferents to nucleus raphe dorsalis of the rat investigated with retrograde wheat germ agglutinin and D-[^{3}H]aspartate tracing. *Brain Res.* **360**:285-297.

KALEN, P., ROSEGREN, E., LINDVALL, O., BJORKLUND, A. (1989). Hippocampal noradrenaline and serotonin release over 24 hours as measured by the dialysis technique in freely moving rats: correlation to behavioural activity state, effect of handling and tail pinch. *Eur. J. Neurosci.* **1**:181-188.

KAWANO, H., DECKER, K., REUSS, S. (1996). Is there a direct retina-raphe-suprachiasmatic nucleus pathway in the rat? *Neurosci.Lett.* **212**:143-146.

KIM, Y.I. and DUDEK, F.E. (1991). Intracellular electrophysiological study of suprachiasmatic nucleus neurons in rodents: excitatory synaptic mechanisms. *J.Physiol.* **444**:269-287.

KNOWLES, R.G., PALACIOS, M., PALMER, R.M.J., MONCADA, S. (1989). Formation of nitric oxide from L-arginine in the central nervous system: a transduction mechanism for stimulation of the soluble guanylate cyclase. *Proc. Natl. Acad. sci. USA* **86**: 5159-5162.

LAARIS, N., LEPOUL, E., HAMON, M., LANFUMY, L. (1997). Stress-induced alteratins of somatodendritic 5-HT_{1A} autoreceptor sensitivity in the rat dorsal raphe nucleus - In vivo electropysiological evidence. *Fundamental & Clinic. Pharmacol.* **11**:206-214.

LEHMAN, M.N., SILVER, R., GLADSTONE, W.R., KAHN, R.M., GIBSON, M., BITTMAN, E.L. (1987). Circadian rhymicity restored by neural transplant. Immunocytochemical charactorization of the graft and its integration with the host brain. *J. Neurosci.* **7**: 1626-1638.

LEJEUNE, F., GOBERT, A., RIVET, J.M., MILLAN, M.J. (1994). Blockade of transmission at NMDA receptors facilitates the electrical and synthetic activity of ascending serotonergic neurons. *Brain Res.* **656**:427-431.

LEMMER, B. (1995). Clinical chronopharmacology: the importance of time in drug treatment. In: Circadian clocks and their adjustments. *Ciba Foundation Symposium 183* pp254-290.

LEONARD, B.E. (1995). Mechanisms of action of antidepressants. *CNS Drugs (Suppl.)* **4**:1-12.

LIMBERGER, N., DEICHER, R., STARKE, K. (1991). Species differences in presynaptic serotonin autoreceptors: mainly 5-HT_{1B} but possibly in addition 5-HT_{1D} in the rat, 5-HT_{1D} in the rabbit and guinea-pig brain cortex. *N.S. Arch.Pharmacol.* **343**:353-364.

LIOU, S.Y., SHIBATA, S., IWASAKI, K., UEKI, S. (1986). Optic nerve stimulation-induced increase of release of ^{3}H-glutamate and ^{3}H-aspartate but not ^{3}H-GABA from the suprachiasmatic nucleus in slices of rat hypothalamus. *Brain Res. Bull.* **16**:527-531.

LU, J-Q. and NAGAYAMA, H. (1996). Circadian rhythm in the response of central 5-HT_{1A} receptors to 8-OH-DPAT in rats. *Psychopharmacol.* **123**:42-45.

LU, Y.M., ZHANG, J.T., ZHAO, F.Q., QIN, Y.F. (1996). The effects of Ca^{2+} antagonists on glutamate release and Ca^{2+} influx in the hippocampus with in vivo intracerebral microdialysis. *Brit.J.Pharmacol.* **104**:222-226.

LUPI, D., DEBERNARDIS, D., VALLERGA, S., MORGAN, P.J., DJAMGOZ, M.B.A. (1996). NADPH diaphorase activity around the suprachiasmatic nucleus in rat brain. *Cell Tiss. Res.* **283**: 335-338.

MAIONE, S., ROSSI, F., BIGGS, C.S., FOWLER, L.J., WHITTON, P.S. (1997). AMPA receptors modulate extracellular 5-hydroxytryptamine concentration and metabolism in rat striatum in vivo. *Neurochem. Int.* **30**:299-304.

MANRIQUE, C., FRANCOIS-BELLAN, A.M., SEGU, L., BECQUET, D., HERY, M., FAUDON, M., HERY, F. (1994). Impairment of serotonergic transmission is followed by adaptive changes in 5-HT_{1B} binding sites in the rat suprachiasmatic nucleus. *Brain Res.* **663**:93-100.

MARSDEN, C.A. and MARTIN, K.F. (1986). Involvement of 5-HT_{1A} - and α_2-receptors in the decreased 5-hydroxytryptamine release and metabolism in rat suprachiasmatic nucleus after intravenous 8-hydroxy-2-(*n*-dipropylamino) tetralin. *Brit.J.Pharmacol.* **89**:277-286.

MARTIN, K.F., HANNON, S., PHILLIPS, I., HEAL, D.J. (1992). Opposing roles for $5HT_{1B}$ and $5HT_3$ receptors in the control of 5HT release in rat hippocampus in vivo. *Brit. J. Pharmacol.* **106**: 139-142.

MARTIN, K.F. and MARSDEN, C.A. (1984). In vivo diurnal variations of 5HT release in hypothalamic nuclei. In: Circadian rhythms in the central nervous system. Eds P.H. Redfern, I.C. Campbell, J.A. Davies, K.F. Martin. pp81-92. IUPHAR 9th International Congress of Pharmacology.

MARTIN, K.F. and REDFERN, P.H. (1997). 5-hydroxytryptamine and noradrenaline synthesis, release and metabolism in the central nervous system: circadian rhythms and control mechanisms. In *Physiology and pharmacology of biological rhythms*. Eds. Peter H.Redfern and Bjorn Lemmer. pp157-176.

MARTIN, K.F., WEBB, A.R., MARSDEN, C.A. (1987). The behavioural response to the 5-hydroxytryptamine$_{1B}$ (5-HT$_{1B}$) receptor agonist - RU24969 may exhibit a circadian variation in the mouse. *Chronobiol.Int.* **4**:493-498.

MASSOT, O., ROUSSELLE, J.-C., FILLION, M.-P., GRIMALDI, B., CLOEZ-TAYARANI, I., FUGELLI, A., PRUDHOMME, N., SEGUIN, L., ROUSSEAU, b., PLANTEFOL, M., HEN, R., FILLION, G. (1996). 5-hydroxytryptamine-moduline, a new endogenous cerebral peptide, controls the serotonergic activity via its specific interaction with 5-hydroxytryptamine$_{1B/1D}$ receptors. *Mol.Pharmacol.* **50**:752-762.

MATOS, F.F., KORPINEN, C., YOCCA, F.D. (1996a). 5-HT$_{1A}$ receptor agonist effects of BMY-14802 on serotonin release in dorsal raphe and hippocampus. *Eur.J.Pharmacol.* **317**:49-54.

MATOS, F.F., URBAN, C., YOCCA, F.D. (1996b). Serotonin (5-HT) release in the dorsal raphe and ventral hippocampus: raphe control of somatodendritic and terminal 5-HT release. *J. Neural. Transm.* **103**:173-190.

MATSUYAMA, S., NEI, K., TANAKA, C. (1996). Regulation of glutamate release via NMDA and 5-HT$_{1A}$ receptors in guinea pig dentate gyrus. *Brain Res.* **728**:175-180.

MAURA, G. and RAITERI, M. (1986). Cholinergic terminals in rat hippocampus possess 5-HT$_{1B}$ receptors mediating inhibition of acetylcholine release. *Eur.J.Pharmacol.* **129**:333-337.

MAURA, G., ROCCATAGLIATA, E., ULIVI, M., RAITERI, M. (1988). Serotonin-glutamate interaction in rat cerebellum: involvement of 5-HT$_1$ and 5-HT$_2$ receptors. *Eur.J.Pharmacol.* **145**:31-38.

MAURA, G. and RAITERI, M. (1996). Serotonin 5-HT$_{1D}$ and 5-HT$_{1A}$ receptors respectively mediate inhibition of glutamate release and inhibition of cyclic GMP production in rat cerebellum in vitro. *J.Neurochem.* **66**:203-209.

MAURA, G., MARCOLI, M, TORTAROLO, M., ANDRIOLI, G.C., RAITERI, M. (1998). Glutamate release in human cerebral cortex and its modulation by 5-hydroxytryptamine acting at h5-HT_{1D} receptors. *Brit.J.Pharmacol.* **123**:45-50.

MEDANIC, M. and GILLETTE, M.U. (1992). Serotonin regulates the phase of the rat suprachiasmatic circadian pacemaker *in vitro* only during the subjective day. *J. Physiol.* **450**: 629-642.

MEIJER, J.H. and GROOS, G.A. (1988). Responsiveness of suprachiasmatic and ventral lateral geniculate neurones to serotonin and imipramine - A microiontophoretic study in normal and imipramine treated rats. *Brain Res. Bull.* **20**:89-96.

MELTZER, H.Y. (1990). Role of serotonin in depression. *Ann.N.Y.Acad.Sci.* **600**:486-500.

MEYER, D.C. and QUAY, W.B. (1976). Hypothalamic and suprachiasmatic uptake of serotonin in vitro; twenty four hour changes in male and proestrous female rats. *Endocrinol.* **98**: 1160-1165.

MEYER-BERNSTEIN, E.L. and MORIN, L.P. (1996). Differential serotonergic innervation of the suprachiasmatic nucleus and the intergeniculate leaflet and its role in circadian rhythm modulation. *J.Neurosci.* **16**:2097-2111.

MICK, G., YOSHIMURA, R., OHNO, K., KIYAMA, H., TOHYAMA, M. (1995). The messenger RNAs encoding metabotropic glutamate receptor subtypes are expressed in different neuronal subpopulations of the rat suprachiasmatic nucleus. *Neurosci.* **66**:161-173.

MIDDLEMISS, D.N. (1985). The putative 5-HT_1 receptor agonist, RU24969, inhibits the efflux of 5-hydroxytryptamine from rat frontal cortex slices by stimulation of the 5-HT autoreceptor. *J.Pharm.Pharmacol.* **37**:434-437.

MOFFETT, J.R., WILLIAMSON, L., PALKOVITS, M., NAMBOODIRI, A.A. (1990). N-acetylaspartylglutamate: a transmitter candidate for the retinohypothalamic tract. *Proc.Natl.Acad.Sci. USA* **87**:8065-8069.

MOGA, M.M. and MOORE, R.Y. (1997). Organization of neural inputs to the suprachiasmatic nucleus in the rat. *J.Comp.Neurol.* **389**:508-534.

MOONEY, R.D., SHI, M.Y., RHOADES, R.W. (1994). Modulation of retinotectal transmission by presynaptic 5-HT_{1B} receptors in the superior colliculus of the adult hamster. *J.Neurophysiol.* **72**:3-13.

MOORE, R.Y. (1996). Entrainment pathways and the functional organization of the circadian system. *Prog. Brain Res.* **111**:103-119.

MOORE, R.Y. and CARD, J.P. (1990). Neuropeptide-Y in the circadian timing system. *Ann. N. Y. Acad. Sci.* **611**:247-257.

MOORE, R.Y. and CARD, J.P. (1994). The intergeniculate leaflet: an anatomically and functionally distinct subdivision of the lateral geniculate complex. *J. Comp. Neurol.* **344**:403-430.

MOORE, R.Y. and HALARIS, A.E. (1975). Hippocampal innervation by serotonin neurones of the midbrain raphe in the rat. *J. Comp. Neurol.* **164**:171-184.

MOORE, R.Y. and LENN, N.J. (1972). A retinohypothalamic projection in the rat. *J. Comp. Neurol.* **146**: 1-14.

MOORE, R.Y., HALARIS, A.E., JONES, B.E. (1978). Serotonin neurons of the midbrain raphe: Ascending projections. *J. Comp. Neurol.* **180**:417-438.

MOORE, R.Y., SPEH, J.C., CARD, J.P. (1995). The retinohypothalamic tract originates from a distinct subset of retinal ganglion cells. *J. Comp. Neurol.* **352**:351-366.

MORARI, M., SBRENNA, S., MARTI, M., O'CONNOR, W.T., BIANCHI, C., FUXE, K., BEANI, L. (1998). Evidence for a striatal NMDA receptor modulation of nigral glutamate release. A dual probe microdialysis study in the awake freely moving rat. *Eur. J. Neurosci.* **10**:1716-1722.

MORET, C. and BRILEY, M. (1988). Sensitivity of the response of 5-HT autoreceptors to drug modifying synaptic availability of 5-HT. *Neuropharmacol.* **27**:43.

MORET, C. and BRILEY, M. (1990). Serotonin autoreceptor subsensitivity and antidepressant activity. *Eur. J. Pharmacol.* **180**:351-356.

MORIN, L.P. and BLANCHARD, J. (1991). Depletion of brain serotonin by 5,7-DHT modifies hamster circadian rhythm response to light. *Brain Res.* **566**:173-185.

MORIN, L.P., BLANCHARD, J., MOORE, R.Y. (1992). Intergeniculate leaflet and suprachiasmatic nucleus organization and connections in the golden hamster. *Visual Neurosci.* **8**:219-230.

MORIYA, T., YAMANOUCHI, S., FUKUSHIMA, T., SHIMAZOE, T., SHIBATA, S., WATANABE, S. (1996). Involvement of 5-HT_{1A} receptor mechanisms in the inhibitory effects of metamphetamine on photic responses in the rodent suprachiasmatic nucleus. *Brain Res.* **740**:261-267.

MOSER, P.C. and REDFERN, P.H. (1984). Diurnal variation in behavioural responses to 5-HT receptor stimulation. *Brit.J.Pharmacol.* **82**:269P.

MOYER, R.W., KENNAWAY, D.J., FERGUSON, S.A., DIJSTELBLOEM, Y.P. (1997). Quipazine and light have similar effects on c-*fos* induction in the rat suprachiasmatic nucleus. *Brain Res.* **765**:337-342.

MUNDEY, M.K., FLETCHER, A., MARSDEN, C.A. (1996). Effects of 8-OH-DPAT and 5-HT_{1A} antagonists WAY100135 and WAY100635, on guinea-pig behaviour and dorsal raphe 5-HT neuron firing. *Brit.J.Pharmacol.* **117**:750-756.

NAGAYAMA, H. and LU, J-Q. (1997). Circadian rhythm in the response to intracerebroventricular administration of 8-OH-DPAT. *Brain Res.* **756**:92-95.

NEUMAIER, J.F., SZOT, P., PESKIND, E., DORSA, D.M., HAMBLIN, M.W. (1996). Serotonergic lesioning differentially affects presynaptic and postsynaptic 5-HT_{1B} receptor mRNA levels in rat brain. *Brain Res.* **722**:50-58.

NOLD, G., KERN, R., LOHRER, H., LEMMER, B. (1996). Effects of jet-lag on circadian blood pressure and herat rate rhythms in top athletes. *Chronobiol. Int. (Suppl.)* **13**:97.

NOWAK, G., LEGUTKO, B., SKOLNICK, P., POPIK, P. (1998). Adaptation of cortical NMDA receptors by chronic treatment with specific serotonin reuptake inhibitors. *Eur.J.Pharmacol.* **342**:367-370.

NOWAK, G., LI, Y., PAUL, I.A. (1996). Adaptation of cortical but not hippocampal NMDA receptors after chronic citalopram treatment. *Eur.J.Pharmacol.* **295**:75-85.

NOWAK, G., ORDWAY, G.A., PAUL, I.A. (1995). Alterations in the *N*-methyl-D-aspartate (NMDA) receptor complex in the frontal cortex of suicide victims. *Brain Res.* **675**:157-164.

NOWAK, G., TRULLAS, R., LAYER, R.T., SKOLNICK, P., PAUL, I.A. (1993). Adaptive changes in the N-methyl-D-aspartate receptor complex after chronic treatment with imipramine and 1-aminocyclopropanecarboxyl acid. *J.Pharm.Exp.Ther.* **265**:1380-1386.

O'CONNOR, J.J. and KRUK, Z.L. (1994). Effect of 21 days treatment with fluoxetine on stimulated endogenous 5-hydroxytryptamine overflow in the rat dorsal raphe and suprachiasmatic nucleus studied using fast cyclic voltametry in vitro. *Brain Res.* **640**:328-335.

O'HARA, B.F., ANDRETIC, R., HELLER, H.C., CARTER, D.B., KILDUFF, T.S. (1995). $GABA_A$, $GABA_C$, and NMDA receptor subunit expression in the suprachiasmatic nucleus and other brain regions. *Mol.Brain Res.* **28**:239-250.

OHI, K., TAKASHIMA, M., NISHIKAWA, T., TAKAHASHI, K. (1991). N-methyl-D-aspartate receptor participates in neuronal transmission of photic information through the retinohypothalamic tract. *Neuroendocrinol.* **53**: 344-348.

OHTA, K., ARAKI, N., SHIBATA, M., KOMATSUMOTO, S., SHIMAZU, K. (1994). Presynaptic ionotropic glutamate receptors modulate in-vivo release and mtabolism of striatal dopamine, noradrenaline and 5-hydroxytryptamine - involvement of both NMDA and AMPA kainate subtypes. *Neurosci. Res.* **21**:83-89.

OZAKI, N., NAKAHARA, D., KASAHARA, Y., NAGATSU, T. (1991). The effect of metamphetamine on serotonin and its metabolite in the suprachiasmatic nucleus - a microdialysis study. *J. Neural Transmission - General section* **86**:175-179.

PALLOTTA, M., SEGIETH, J., WHITTON, P.S. (1998). N-methyl-D-aspartate receptors regulate 5-HT release in the raphe nuclei and frontal cortex of freely moving rats: differential role of 5-HT_{1A} autoreceptors. *Brain Res.* **783**:173-178.

PARK, H.T., BAEK, S.Y., KIM, B.S., KIM, J.B., KIM, J.J. (1993). Profile of Fos-like immunoreactivity induction by light stimuli in the intergeniculate leaflet is different from that of the suprachiasmatic nucleus. *Brain Res.* **610**: 334-339.

PAUL, I.A., NOWAK, G., LAYER, R.T., POPIK, P., SKOLNICK, P. (1993). Adaptation of the N-methyl-D-aspartate receptor complex following chronic antidepressant treatments. *J.Pharm.Exp.Ther.* **269**:95-102.

PAXINOS, G. and WATSON, C. (1982). The rat brain in stereotaxic coordinates (2nd Edn). Academic Press, San Diego, CA.

PENEV, P.D., TUREK, F.W., ZEE, P.C. (1993). Monoamine depletion alters the entrainment and the responses to light of the circadian activity rhythm in hamsters. *Brain Res.* **156**-164.

PICKARD, G.E. (1982). The afferent connections of the suprachiasmatic nucleus of the golden hamster with emphasis on the retinohypothalamic projection. *J.Comp.Neurol.* **211**:65-83.

PICKARD, G. (1989). Entrainment of the circadian rhythm of whell-running activity is phase shifted by ablation of the IGL. *Brain Res.* **268**: 151-154.

PICKARD, G.E. and REA, M.A. (1997). TFMPP, a 5-HT_{1B} receptor agonist, inhibits light-induced phase shifts of the circadian activity rhythm and c-fos expression in the mouse suprachiasmatic nucleus. *Neurosci.Letts.* **231**:95-98.

PICKARD, G.E., WEBER, E.T., SCOTT, P.A., RIBERD, A.F., REA, M.A. (1996). 5-HT_{1B} receptor agonists inhibit light-induced phase shifts of behavioural circadian

rhythms and expression of the immediate early gene c-fos in the suprachiasmatic nucleus. *J.Neurosci.* **16**:8208-8220.

PIN, J.-P. and DUVOISIN, R. (1995). Review: Neurotransmitter receptors I. The metabotropic glutamate receptors: structure and functions. *Neuropharmacol.* **34**:1-26.

PORTAS, C.M., THAKKAR, M., RAINIE, D., McCARLEY, R.W. (1996). Microdialysis perfusion of 8-hydroxy-2-(di-*n*-propylamino)Tetralin (8-OH-DPAT) in the dorsal raphe nucleus decreases serotonin release and increases rapid eye movement sleep in the freely moving cat. *J.Neurosci.* **16**:2820-2828.

PROSSER, R.A., DEAN, R.R., EDGAR, D.M., HELLER, H.C., MILLER, J.D. (1993). Serotonin and the mammalian circadian system: I. *in vitro* phase shifts by serotonergic agonists and antagonists. *J. Biol. Rhythms* **8**: 1-16.

PROSSER, R.A. and GILLETTE, M.U. (1991). Cyclic changes in cAMP concentration and phosphodiesterase activity in mammalian circadian clock studies in vitro. *Brain Res.* **568**: 185-192.

PROSSER, R.A., MACDONALD, E.S., HELLER, H.C. (1994a). c-*fos* mRNA in the suprachiasmatic nuclei in vitro shows a circadian rhythm and responds to a serotonergic agonist. *Mol. Brain Res.* **25**:151-156.

PROSSER, R.A., HELLER, H.C., MILLER, J.D. (1994b). Serotonergic phase advances of the mammalian circadian clock involve protein kinase A and K^+ channel opening. *Brain Res.* **644**:67-73.

PROSSER, R.A., MILLER, J.D., HELLER, H.C. (1990). A serotonin agonist phase-shifts the circadian clock in the suprachiasmatic nuclei in vitro. *Brain Res.* **534**:336-339.

QUAY, W.B. (1968). Differences in circadian rhythms in 5-hydroxytryptamine according to brain region. *Am. J. Physiol.* **215**: 1448-1453.

RAHMAN, S. and NEUMAN, R.S. (1996). Characterization of metabotropic glutamate receptor-mediated facilitation of N-methyl-D-aspartate depolarization of neocortical neurones. *Brit. J. Pharmacol.* **117**:675-683.

RALPH, M.R. and LEHMAN, M.N. (1991). Transplantation: a new tool in the analysis of the mammalian hypothalamic circadian pacemaker. *Trends in Pharmacol. Sci.* **14**:362-366.

RALPH, M.R., FOSTER, R.G., DAVIS, F.C., MENAKER, M. (1990). Transplanted suprachiasmatic nucleus determines circadian period. *Science* **247**:975-978.

RAMIREZ, A.D., RAMIREZ, V.D., MEYER, D.C. (1987). The nature and magnitude of in vivo 5-hydroxyindoleacetic acid output from 5-hydroxytryptamine terminals is related to specific regions of the suprachiasmatic nucleus. *Neuroendocrinol.* **46**:430-43.

REA, M.A. (1989). Light increases Fos-related protein immunoreactivity in the rat suprachiasmatic nuclei. *Brain Res. Bull.* **23**:577-581.

REA, M.A., BARRERA, J., GLASS, J.D., GANNON, R.L. (1995). Serotonergic potentiation of photic phase shifts of the circadian activity rhythm. *Neuroreport* **6**:1289-1292.

REICO, J., PEVET, P. MASSON-PEVET, M. (1996). Serotonergic modulation of photically induced increase in melatonin receptor density and Fos immunoreactivity in the suprachiasmatic nuclei of the rat. *J.Neurochem.* **8**:839-845.

REUSS, S., DECKER, K., ROSSELER, L., LAYES, E., SCHOLLMAYER, A., SPESSERT, R. (1995). Nitric oxide synthase in the hypothalamic suprachiasmatic nucleus of rat: evidence from histochemistry, immunohistochemistry and Western blot; and colocalization with VIP. *Brain Res.* **695**:257-262.

ROCA, A.L., WEAVER, D.R., REPPERT, S.M. (1993). Serotonin receptor gene expression in the rat suprachiasmatic nuclei. *Brain Res.* **608**: 159-165.

ROLLEMA, H., CLARKE, T., LU, Y., SCHMIDT, A., SPROUSE, J. (1996). Comparison of the effects of CP-93,393 and buspirone on 5-HT and NE release - microdialysis studies in hippocampus of the freely moving rat and guinea pig. *J. Neurochem.* **66**:537.

ROMIJN, H.J., SLUITER, A.A., POOL, C.W., WORTEL, J., BUIJS, R.M. (1996). Differences in colocalization between Fos and PHI, GRP, VIP and VP in neurons of the rat suprachiasmatic nucleus after a light stimulus during the phase delay versus the phase advance period of the night. *J.Comp.Neurol.* **372**:1-8.

ROMERO, L., CELADA, P., ARTIGAS, F. (1994). Reduction of in vivo striatal 5-hydroxytryptamine release by 8-OH-DPAT after inactivation of G_i/G_o proteins in dorsal raphe nucleus. *Eur.J.Pharmacol.* **265**:103-106.

ROSENWASSER, A.M. and WIRZ-JUSTICE, A. (1997). Circadian rhythms and depression: clinical and experimental models. In: *Physiology and pharmacology of biological rhythms.* Eds. Peter H.Redfern and Bjorn Lemmer. pp458-486.

ROWLEY, H.L., MARTIN, K.F., MARSDEN, C.A. (1995). Determination of in vivo amino acid neurotransmitters by high-performance liquid chromatography with *o*-phthalaldehyde-sulphite derivatisation. *J.Neurosci.Meth.* **57**:93-99.

SANDBERG, M. and LINDSTROM, S. (1983). Amino acids in the dorsal lateral geniculate nucleus of the cat - collection in vivo. *J. Neurosci. Meth.* **9**: 65-74.

SAKAMOTO, K. and ISHIDA, N. (1998). Circadian expression of serotonin *N*-acetyltransferase mRNA in the rat retina. *Neurosci.Letts.* **245**:113-116.

SAYER, T.J.O (1994) Ph.D. Thesis. University of Bath.

SCOTT, G. and RUSAK, B. (1996). Activation of hamster suprachiasmatic neurons *in vitro* via metabotropic glutamate receptors. *Neurosci.* **71**:533-541.

SELIM, M., GLASS, J.D., HAUSER, U.E., REA, M.A. (1993). Serotonegic inhibition of light-induced Fos protein expression and extracellular glutamate in the suprachiasmatic nuclei. *Brain Res.* **621**: 181-188.

SHARP, T., BRAMWELL, S.R., GRAHAME-SMITH, D.G. (1989). 5-HT_1 agonists reduce 5-hydroxytryptamine release in rat hippocampus *in vivo* as determined by brain microdialysis. *Brit.J.Pharmacol.* **96**:283-290.

SHARP, T., BRAMWELL, S.R., GRAHAME-SMITH, D.G. (1990). Effect of endogenous 5-hydroxytryptamine in rat ventral hippocampus evoked by electrical stimulation of the dorsal raphe nucleus as detected by microdialysis: senstivity to tetrodotoxin, calcium and calcium antagonists. *Neurosci.* **39**: 629-637.

SHEN, H. and SEMBA, K. (1994). A direct retinal projection to the dorsal raphe nucleus in the rat. *Brain Res.* **635**:159-168.

SHENG, M. and GREENBERG, M.E. (1990). The regulation and function of c-fos and other immediate-early genes in the nervous system. *Neuron* **4**:477-485.

SHIBATA, S., TSUNEYOSHI, A., HAMADA, T., TOMINAGA, K., WATANABE, S. (1992a). Effect of substance P on circadian rhythms of firing activity and the 2-deoxyglucose uptake in the rat suprachismatic nucleus in vitro. *Brain Res.* **597**:257-263.

SHIBATA, S., TSUNEYOSHI, A., HAMADA, T., TOMINAGA, K., WATANABE, S. (1992b). Phase-resetting effect of 8-OH-DPAT, a serotonin$_{1A}$ receptor agonist, on the circadian rhythm of firing rate in the rat suprachiasmatic nuclei in vitro. *Brain Res.* **582**:353-356.

SHIBATA, S., WATANABE, A., HAMADA, T., ONO, M., WATANABE, S. (1994). *N*-methyl-D-aspartate induces phase shifts in circadian rhythm of neuronal activity of rat SCN in vitro. *Am.J.Physiol.* **267**:R360-R364.

SHINOHARA, K., TOMINAGA, K., ISOBE, Y., INOUYE, S.I.T. (1993). Photic regulation of peptides located in the ventral lateral subdivision of the suprachiasmatic

nucleus of the rat - daily variation of vasointestinal peptide, gastrin releasing peptide and neuropeptide-Y. *J. Neurosci.* **13**:793-800.

SHIRAKAWA, T., MOORE, R.Y. (1994a). Responses of rat suprachiasmatic nucleus neurons to substance P and glutamate in vitro. *Brain Res.* **642**:213-220.

SHIRAKAWA, T., MOORE, R.Y. (1994b). Glutamate shifts the phase of the circadian neuronal firing rhythm in the rat suprachiasmatic nucleus in vitro. *Neurosci. Lett.* **178**: 47-50.

SILLS, M.A., WOLFE, B.B., FRAZER, A. (1984). Determination of selective and non-selective compounds for the 5-HT_{1A} and 5-HT_{1B} receptor subtypes in rat frontal cortex. *J. Pharm. Exp. Ther.* **231**:480-487.

SILVER, R., LESAUTER, J., TRESCO, P.A., LEHMAN, M.N. (1996). A diffusable coupling signal from the transplanted suprachiasmatic nucleus controlling circadian locomotor rhythms. *Nature* **382**:810-813.

SINGH, A. and REDFERN, P. (1994a). Lack of circadian variation in the sensitivity of rat terminal 5-HT_{1B} autoreceptors. *J.Pharm.Pharmacol.* **46**:366-370.

SINGH, A. and REDFERN, P. (1994b). Guinea pig terminal 5-HT_{1D} autoreceptors do not display a circadain variation in their responsiveness to serotonin. *Chronobil.Int.* **11**:165-172.

SINGER, J.H., BELLINGHAM, M.C., BERGER, A.J. (1996). Presynaptic inhibiton of glutamatergic synaptic synaptic transmission to rat motor neurones by serotonin. *J.Neurophysiol.* **76**:799-807.

SINGEWALD, N., KAEHLER, S.T., HEMEIDA, R., PHILIPPU, A. (1998). Influence of excitatory amino acids on basal and sensory stimuli-induced release of 5-HT in the locus coeruleus. *Brit. J. Pharmacol.* **123**:746-752.

SKOLNICK, P., LAYER, R.T., POPIK, P., NOWAK, G., TRULLAS, P.R. (1996). *Pharmaopsychiat.* **29**:23-26.

SMALE, L., MICHELS, K.M., MOORE, R.Y., MORIN, L.P. (1990). Destruction of the hamster serotonergic system by 5,7-DHT: effects on circadian rhythm phase, entrainment and response to triazolam. *Brain Res.* **515**: 9-19.

SPESSERT, R., LAYES, E., SCHOLLMAYER, A., REUSS, S., VOLLRATH, L. (1995). In the rat pineal gland, but not in the suprachiasmatic nucleus, the amount of constitutive neuronal nitric oxide synthase is regulated by environmental lighting conditions. *Biochem.Biophys.Res.Comm.* **212**:70-76.

SPROUSE, J.S. and AGHAJANIAN, G.K. (1987). Electrophysiological responses of serotonergic dorsal raphe neurones to 5-HT_{1A} and 5-HT_{1B} agonists. *Synapse* **1**:3-9.

SRKALOVIC, G., SELIM, M., REA, M.A., GLASS, J.D. (1994). Serotonergic inhibition of extracellular glutamate in the suprchiasmatic nucear region assessed using in vivo brain microdialysis. *Brain Res.* **656**: 302-308.

STARKEY, S.J. (1996). Melatonin and 5-hydroxytryptamine phase-advance the rat circadian clock by activation of nitric oxide synthesis. *Neurosci.Letts.* **211**:199-202.

STEPHAN, F.K., ZUCKER, I. (1972). Circadian rhythms in drinking behaviour and locomator activity of rats are eliminated with hypothalamic lesions. *Proc. Nat. Acad. Sci. USA* **69**: 1583-1586.

SUTIN, E.L. and KILDUFF, T.S. (1992). Circadian and light-induced expression of immediate early gene mRNAs in the rat suprachiasmatic nucleus. *Mol. Brain Res.* **15**:281-290.

TAO, R. and AUERBACH, S.B. (1996). Differential effect of NMDA on extracellular serotonin in rat midbrain raphe and forebrain sites. *J. Neurochem.* **66**:1067-1075.

TAO, R, MA, Z., AUERBACH, S.B. (1997). Influence of AMPA/kainate receptors on extracellular 5-hydroxytryptamine in the rat midbrain raphe and forebrain. *Brit.J.Pharmacol.* **121**:1707-1715.

TAKATSUJI, K., MIGUELHIDALGO, J.J., TOHYAMA, M. (1991). Substance-P-immunoreactive innervation from the retina to the suprachiasmatic nucleus in the rat. *Brain Res.* **568**:223-229.

TIMMERMAN, W. and WESTERINK, B.H.C. (1997). Brain microdialysis of GABA and glutamate: what does it signify? *Synapse* **27**:242-261.

TOMINAGA, K., SHIBATA, S., UEKI, S., WATANABE, S. (1992). Effects of 5-HT_{1A} receptor agonists on the circadian rhythm of wheel-running activity in hamsters. *Eur.J.Pharmacol.* **214**:79-84.

TRAVAGLI, R.A. and WILLIAMS, J.T. (1996). Endogenous monoamines inhibit glutamate transmission in the spinal trigeminal nucleus of the guinea-pig. *J.Physiol.* **491**:177-185.

TRENDELENBURG, A-U., TRENDELENBURG, M., STARKE, K., LIMBERGER, N. (1994). Release-inhibiting α_2-adrenoceptors at serotonergic axons in rat and rabbit brain cortex: evidence for pharmacological identity with α_2-autoreceptors. *N.S.Arch.Pharmacol.* **349**:25-33.

TRILLAT, A.C., MALAGIE, I., SCEARSE, K., PONS, D., ANMELLA, M.C., JACQUOT, C., HEN, R., GARDIER, A.M. (1997). Regulation of serotonin release in the frontal cortex and ventral hippocmpus of homozygous mice lacking 5-HT_{1B} receptors: In vivo microdialysis studies. *J. Neurochem.* **69**:2019-2025.

TRULLAS, R. and SKOLNICK, P. (1990). Functional antagonists at the NMDA receptor complex exhibit antidepressant actions. *Eur.J.Pharmacol.* **185**:1-10.

TUREK, F.W. (1987). Pharmacological probes of the mammalian circadian clock: use of the phase response curve approach. *Trends in Pharmacol. Sci.* **8**:212-217.

VAN DE KAR, L.D. and LORENS, S.A. (1979). Differential serotonergic innervation of individual hypothalamic nuclei and other forebrain regions by the dorsal and median midbrain raphe nuclei. *Brain Res.* **162**:45-54.

VAN DEN POL, A.N. (1991). Glutamate and aspartate immunoreactivity in hypothalamic presynaptic axons. *J. Neurosci.* **11**: 2087-2101.

VAN DEN POL, A.N. (1994). Metabotropic glutamate receptor mGluR1 distribution and ultrastrucural localization in hypothalamus. *J.Comp.Neurol.* **349**:615-632.

VAN DEN POL, A.N., ROMANO, C., GHOSH, P. (1995). Metabotropic glutamate receptor mGluR5 subcellular distribution and developmental expression in hypothalamus. *J.Comp.Neurol.* **362**:134-150.

VAN DEN POL, A.N. and TSUJIMOTO, K.L. (1985). Neurotransmitters of the hypothalamic suprachiasmatic nucleus: immunocytochemical analysis of 25 neuronal antigens. *Neurosci.* **15**: 1049-1086.

VAN REETH, O. and TUREK, F.W. (1989). Stimulated activity mediates phase shifts in the hamster circadian clock induced by dark pulses or benzodiazepines. *Nature* **339**:49-51.

VILLAR, M.J., VITALE, M.L., PARISI, M.N. (1987). Dorsal raphe serotonergic projection to the retina. A combined peroxidase tracing-neurochemical / high-performance liquid chromatography study in the rat. *Neurosci.* **22**:681-686.

WANG, H. and MORRIS, J.F. (1996). Presence of neuronal nitric oxide synthase in the suprchiasmatic nuclei of mouse and rat. *Neurosci.* **74**:1059-1068.

WATANABE, A., HAMADA, T., SHIBATA, S., WATANABE, S. (1994). Effects of nitric oxide inhibitors on N-methyl-D-aspartate-induced phase delay of circadian rhythm of neuronal activity in the rat suprachiasmatic nucleus in vitro. *Brain Res.* **646**: 161-164.

WATANABE, A., ONO, M., SHIBATA, S., WATANABE, S. (1995). Effect of a nitric oxide synthase inhibitor, N-nitro-L-arginine methylester, on light-induced phase delay of circadian rhythm of wheel-running activity in golden hamsters. *Neurosci. Lett.* **192**: 25-28.

WATTS, A.G. and SWANSON, L.W. (1987). Efferent projections of the suprachiasmatic nucleus: II. studies using retrograde transport of fluorescent dyes and simultaneous peptide immunohistochemistry in the rat. *J. Comp. Neurol.* **258:** 230-252.

WATTS, A.G., SWANSON, L.W., SANCHEZ-WATTS, G. (1987). Efferent projections of the suprachiasmatic nucleus: I. studies using anterograde transport of *Phaseolus vulgaris* leucoagglutinin in the rat. *J. Comp. Neurol.* **258:** 204-229.

WEBER, E.T., GANNON, R.L., MICHEL, A.M., GILLETTE, M.U., REA, M.A. (1995a). Nitric oxide synthase inhibitor blocks light-induced phase shifts of the circadian activity rhythm, but not c-*fos* expressionin the suprachiasmatic nucleus of the Syrian hamster. *Brain Res.* **692**: 137-142.

WEBER, E.T., GANNON, R.L., REA, M.A. (1995b). cGMP-dependent protein kinase inhibitor blocks light-induced phase advances of circadian rhythms in vivo. *Neurosci. Letts.* **197**:227-230.

WHITTON, P.S., RICHARDS, D.A., BIGGS, C.S., FOWLER, L.J. (1994). *N*-methyl-D-aspartate receptors modulate extracellular 5-hydroxytryptamine concentration in rat hippocampus and striatum in vivo. *Neurosci. Letts.* **169**:215-218.

WICKLAND, C. and TUREK, F.W. (1994). Lesions of the thalamic intergeniculate leaflet block activity-induced phase shifts in the circadian activity rhythm of the golden hamster. *Brain Res.* **660**:293-300.

WILLNER, P. (1985). Antidepressants and serotonergic neurotransmission: an integrative review. *Psychopharmacol.* **85**:387-404.

WIRZ-JUSTICE, A., KRAUCHI, K., MORIMASA, T., WILLENER, R., FEER, H. (1983). Circadian rhythm of [^{3}H] imipramine binding in the rat suprachiasmatic nucleus. *Eur. J. Physiol.* **87**: 331-333.

WOOTTON, R. and HAZELWOOD, R. (1990). 8-OH-DPAT labels two sites in the raphe nucleus area of rat brains. *Brit. J. Pharmacol. (Suppl.)* **26**:236P.

YAMAZAKI, S., MARUYAMA, M., CAGAMPANG, F.R.A., INOUYE, S.-I.,T. (1994). Circadian fluctuations of cAMP content in the suprachiasmatic nucleus and the anterior hypothalamus of the rat. *Brain Res.* **651**:329-331.

YING, S-W and RUSAK, B. (1994). Effects of serotonergic agonists on firing rates of photically responsive cells in the hamster suprachiasmatic nucleus. *Brain Res.* **651**:37-46.

ZOELLER, R.T., BROYLES, B., EARLEY, J., ANDERSON, E.R., ALBERS, H.E. (1991). Cellular levels of messenger ribonucleic acids encoding vasoactive intestinal peptide and gastrin-releasing peptide in neurons of the suprachiasmatic nucleus exhibit distinct 24-hour rhythms. *J.Neuroendocrinol.* **4**:119-124.

APPENDIX

RT-PCR

The following solutions were supplied with the Dynabeads® mRNA DIRECT kit (DYNAL®, Norway):

Lysis/binding buffer: 100 mM Tris-HCl, pH 8.0, 500 nM LiCl, 10 mM EDTA, pH 8.0, 1 % LiDS, 5 mM dithiothreitol

Washing buffer with LiDS: 10 mM Tris-HCl, ph 8.0, 0.15 M LiCl, 1 mM EDTA, 0.1 % LiDS

Washing buffer: 10 mMTris-HCl, pH 8.0, 0.15 M LiCl, 1 mM EDTA

Elution solution: 10 mM Tris-HCl, pH8.0

IMMUNOCYTOCHEMISTRY

Gelatin coated slides: Into 100 ml distilled water add 1 g gelatin (Sigma). Heat and stir. Once the solution has cleared add 100 mg chromic potassium sulphate (Sigma). Allow to cool. Coat slides generously and allow to aire dry.

Phosphate buffered saline (PBS): Available in tablet form from Sigma. One tablet is dissolved into 200 ml distilled water to yield a 0.01 M sodium and potassium phosphate buffer, pH 7.4 containing 0.0027 M potassium chloride and 0.137 M sodium chloride.

4 % paraformaldehyde: 40 g per litre of PBS. Heat the PBS to 70°C in a fume hood. Add the paraformaldehyde (sigma) and wait for it to dissolve. Allow to cool, filter and pH to 7.4-7.6.

ABC comple/HRP: 45 µl reagent A and 45 µl reagent B are added to 5 ml PBS and vortexed. The solution is left at 4°C for 30 min prior to use.

DAB peroxidase substrate tablet set: Each SIGMA FAST DAB tablet set contains 0.7 mg/ml DAB, 1.6 mg/ml urea hydrogen peroxide in 0.06 M Tris buffer when dissolved in 1 nl distilled water.

WESTERN BLOTTING

Constituent	10% Running gel*	5% Stacking gel*
MilliQ water	4.35 ml	6.0 ml
1M Tris-HCl pH 6.8	-	1.25 ml
1M Tris-HCL pH 8.8	5.6 ml	-
Acrylamide	5.0 ml	1.67 ml
10% SDS (w/v)	0.25 ml	0.15 ml
10% APS	50 µl	50 µl
TEMED	20 µl	20 µl

*Volumes sufficient for 4 gels

SDS-PAGE running buffer: 25 mM Tris base, 192 mM glycine, 0.1% (w/v) SDS, pH 8.3.

5x SDS sample buffer: 5% SDS, 50% glycerol, 200 mM Tris-HCL pH 6.8, bromophenol blue.

Semi-dry transfer buffer: 39 mM glycine, 48 mM Tris base, 0.0375% SDS, 20% (v/v) methanol.

Tris buffered saline (TBS): 20 mM Tris-HCL pH 7.5, 150 mM NaCl.